Design and Synthesis of Donor-Acceptor Low Band Gap Copolymers for Photoconductive and Non-linear Optical Applications

Thesis submitted to

Cochin University of Science and Technology

in partial fulfilment of the requirements

for the award of the degree of

Doctor of Philosophy

under the Faculty of Technology

by

Sona Narayanan

Department of Polymer Science and Rubber Technology

Cochin University of Science and Technology

Kochi- 682 022, Kerala, India

February 2015

Design and Synthesis of Donor-Acceptor Low Band Gap Copolymers for Photoconductive and Non-linear Optical Applications

Ph. D. Thesis

Author

Sona Narayanan
Department of Polymer Science and Rubber Technology
Cochin University of Science and Technology
Kochi - 682 022, Kerala, India
sonachalil@gmail.com, sonasreejesh@gmail.com

Supervising teachers

Prof. Rani Joseph
Emeritus Professor
Department of Polymer Science and Rubber Technology
Cochin University of Science and Technology
Kochi-682022, Kerala, India
ranigeorge2011@gmail.com, rani@cusat.ac.in

Prof. K. Sreekumar
Department of Applied Chemistry
Cochin University of Science and Technology
Cochin-682022, Kerala, India
ksk@cusat.ac.in, drksreekumar@gmail.com

Prof. C. Sudha Kartha
Department of Physics
Cochin University of Science and Technology
Cochin-682022, Kerala, India
csk@cusat.ac.in

Department of Polymer Science and Rubber Technology
Cochin University of Science and Technology
Kochi- 682 022, Kerala, India

Certificate

Certified that the work presented in the thesis entitled "**Design and Synthesis of Donor-Acceptor Low Band Gap Copolymers for Photoconductive and Non-linear Optical Applications"** is the bonafide record of research work done by Ms. Sona Narayanan under our guidance at the Department of Polymer Science and Rubber Technology, Department of Applied Chemistry, Department of Physics, Cochin, India-682 022, and that it has not been included in any other thesis submitted previously for the award of any other degree/diploma. All the relevant corrections and modifications suggested by the audience and recommended by the doctoral committee of the candidate during the presynopsis seminar have been incorporated in the thesis.

Dr. Rani Joseph
(Supervising Guide)

Dr. K. Sreekumar
(Co- Supervising Guide)

Dr. C. Sudha Kartha
(Co- Supervising Guide)

Kochi-682022
February, 2015

Declaration

I hereby declare that the work presented in the thesis entitled **"Design and Synthesis of Donor-Acceptor Low Band Gap Copolymers for Photoconductive and Non-linear Optical Applications"** is my own unaided work under the guidance of Prof. Rani Joseph (Emeritus professor, Department of Polymer Science and Rubber Technology), Prof. K. Sreekumar (Department of Applied Chemistry) and Prof. C. Sudha Kartha (Department of Physics), Cochin University of Science and Technology, Cochin-682022, Kerala, India, and the same has not been submitted elsewhere for the award of any other degree.

Kochi-682022 **Sona Narayanan**
February, 2015

Acknowledgements

First and foremost, I would like to thank my supervising guide, Prof. Rani Joseph for the guidance and constant support during the course of the research work. I am so grateful to her for the valuable suggestions, inspirations, love and care during the period of research. Also my heartfelt thanks to the co-supervisors, Prof. K. Sreekumar, Department of Applied Chemistry and Prof. C. Sudha Kartha, Department of Physics for their timely help, encouragement, excellent supervision, valuable advice and support rendered to me.

I record my sincere thanks to Prof. Sunil K. Narayanankutty, Head, Department of PS & RT, for his encouragement and whole-hearted support. I would like to thank Prof. Eby Thomas Thachil and Prof. Thomas Kurian, Former HODs, Department of PS & RT for their support during my research. I am also grateful to my research committee member, Dr. K. E. George, Department of PS &RT. I would like to thank Dr. Jayalatha and Dr. Philip Kurian for their constant support. I would also like to extend my sincere thanks to all the office and technical staff of PS & RT for their support.

I wish to express my sincere thanks to Prof. P. Radhakrishnan and Dr. Sheenu Thomas, International School of Photonics for extending NLO characterisation facilities in their lab. I whole heartedly thank Prof. K. Girish Kumar, Department of Applied Chemistry for the electrochemical characterisation facilities provided in his lab.

I am so grateful to my co-workers, Anshad A. (Department of Physics), Mathew S. (International School of Photonics) and Sreeroop S. (Iqbal College Peringammala) for the stimulating discussions and constant help.

I acknowledge University Grants Commission (UGC) & Cochin University of Science and Technology (CUSAT) for providing the financial assistance.

Special thanks to Dr. Aby C. P. for his ever loving friendship and support. I am so grateful to my dearest friend Dr. Nisha for being my helping hand in my difficulties and for her motivating friendship. I am so thankful to Renju chechi, Sinu chettan and Resmi for their sincere friendship right from the beginning of my work. I extend sincere thanks to my seniors, Dr. Sinto Jacob, Dr. Bipinbal, Abilash chettan, Murali chettan,

Dhanya chechi, Jeneesh chettan, Julie chechi, Newly chechi, Dr. Anna, Dr. Nimmi, Dr. Vidya G., Dr. Vidya Francis, Rajesh chettan (cs), Poornima chechi, Rajesh Mon, Rajesh Menon, Anoop chettan, Geetha chechi for their encouragement and support during my initial days at CUSAT.

I am very thankful to Dr. Mahesh Kumar who made me familiar with theoretical methods for designing suitable polymers and for valuable help during crucial stages of my research work.

My heartfelt thanks to Anuja, Divya chechi and Unni for their valuable time spent in the electrochemical measurements of the polymers.

I am also thankful to Jabin teacher, Prameela teacher, Jolly Sir, Preetha teacher, Denny teacher, Neena chechi, Parameswaran Sir, Zeena teacher, Bindu teacher, Suma teacher, Vijayalakshmi chechi, Anjana teacher, Manoj Sir and Jasmine teacher for their timely advices and for beautiful memories. I express my sincere thanks to Asha, Aiswarya, Ajilesh, Shadiya, Jayesh, Neena, Neethu, Soumya, Remya, Bhagesh, Nishad, Anju, Teena, Abitha, Sona, Dhanya, Divya, Renjitha, Swapna and all my friends in PS & RT. I extend my special thanks to Anjali, Jabiya, Jibi, Soumya, Anjaly, Jisha, Sinija, Smitha chechi, Sherly teacher, Jithin, Bhavya, Reshma, Sandya chechi, Suma, Cisy, Mothi, Rakesh, for their valuable friendship and love. Also I would like to thank Jisha, Aswathy, Deepu, Sreejith, Santhosh, Geethu, Jisa, Jincy, Tittu, for their constant support. I thank all of them individually for their love, support and cooperation.

I am indebted to my loving parents, Pappa, Achan, Sobha Amma, Viji Amma for their unconditional support, inspiration, love and prayers. Without their love, dream of mine would not have been ripened into a reality.

I was extremely fortune in having a brother like you who was always there to help and support me anytime. I take this opportunity to express my love to my dear Manu.

Last but not the least, to my loving Sreejesh who is the word of true friendship and he never let me feel that I am away from my parents. I express my sincere thanks to him for being a constant source of inspiration.

Sona Narayanan

Preface

In recent years, π-conjugated polymers have been subjected to extensive study as regards their potential applications in transistors, photovoltaic devices, polymer light-emitting diodes, photorefractive devices and in non-linear optical devices. Conjugated polymers continue to fascinate many scientists due to their several advantages such as low cost, processability, high optical contrast, high stability etc. The major goal of the present investigation was to synthesize low band gap polymers possessing both photoconducting and non-linear optical property. Four major objectives of the present study are listed here under:

- Design of donor-acceptor low band gap conjugated polymers for photoconductive and non-linear optical application using Density Functional Theory in the Periodic Boundary Condition (PBC) formalism.
- Synthesis of the copolymers using direct arylation and Suzuki coupling methods.
- Explore the application of conjugated polymers as active layer in photoconducting devices.
- Explore the application of conjugated copolymers in non-linear optical devices.

The thesis is comprised of **seven chapters**.

The **first chapter** consists of a concise introduction to some fundamental principles of photoconducting and non-linear optical (NLO) polymers. The first section begins with the tool box for band gap engineering to produce low band gap conjugated polymers, followed by different polymerization methods for obtaining the D-A copolymers. In the next section, the use of quantum chemical tools for designing the active layer polymers is

explained. This chapter concludes with scope and aim of the work presented in the thesis.

Chapter 2 deals with theoretical and experimental investigations on the photoconductivity and non-linear optical properties of 3,4-ethylenedioxythiophene (EDOT)-fluorene copolymer. EDOT-fluorene copolymer was synthesized via a simple and facile method, direct arylation polycondensation reaction. Structure of the copolymer was confirmed by FT-IR, ^{1}H NMR and XPS. Electronic structure and properties were investigated by DFT theory using periodic boundary condition formalism. Photophysical, electrochemical and thermal properties are also included. Optical limiting property is presented.

Chapter 3 deals with design, synthesis and third-order non-linear optical properties of 3,4-ethylenedioxythiophene-chalcogenadiazole donor-acceptor copolymers via direct arylation method. Copolymers of EDOT with benzothiadiazole and benzoselenadiazole are investigated by theoretical and experimental (optical and electrochemical) methods. Non-linear absorption and non-linear refraction properties were determined by open aperture and closed aperture z-scan technique, respectively. In addition, suitability of the copolymers for optical limiting application is studied.

Chapter 4 includes synthesis and third-order NLO properties of low band gap 3,4-ethylenedioxythiophene-quinoxaline copolymers. The effect of structural changes of quinoxaline derivatives on the band gap of EDOT-quinoxaline copolymers are investigated by theoretical calculation (DFT theory) and experimental methods like UV-Visible absorption spectroscopy and electrochemical methods. Third-order NLO properties were evaluated by z-scan technique and are included in this chapter. The optical limiting properties of EDOT-quinoxaline copolymers are also discussed.

Chapter 5 discusses electronic structure calculation, synthesis and third-order NLO properties of EDOT-thiophene copolymers. Copolymers were

synthesized by direct arylation polycondensation reaction. Structure of the synthesized copolymer was confirmed by FT-IR, ^{1}H NMR, and XPS. Thermal properties of the copolymer were studied using TG and DSC analysis. Optical studies were done by using UV-Visible absorption spectra and photolumniscence spectra. Third-order NLO properties were determined using z-scan technique and the optical limiting properties are also presented.

Chapter 6 focusses on the electronic structure, synthesis and third-order NLO properties of novel phenothiazine-triazine copolymer. Copolymer was synthesized via standard Suzuki coupling reaction of phenothiazine with piperidine substituted triazine. The theoretically determined frontier energy levels and energy gap of copolymer agreed with experimentally determined optical and electrochemical results. The third-order NLO properties and optical limiting behaviour of the polymer was also investigated.

The conclusions drawn from each part of the work and references are given at the end of each chapter. The summary and outlook of the work done are presented as the final chapter.

Contents

.....ꕥ.....

Chapter 1
Introduction

1.1. Introduction

In twenty-first century, conducting polymers have emerged as one of the vital materials owing to their useful optical, electronic, energy storage and mechanical properties. Initially, organic polymers have been considered as insulators. The importance of this class of materials was realized by the world scientific community when A. J. Heeger, H. Shirakawa and A. G. MacDiarmid won the Nobel Prize in Chemistry in 2000 for their research in halogen doped polyacetylene.[1] This was the real breakthrough in the evolution of organic conducting polymers. After their pioneering work, a number of conjugated polymers were developed including polythiophene, polypyrrole, poly(paraphenylene), polyaniline, poly(phenylene vinylene), polyfluorene etc.[2] These polymers exhibited unusual electronic properties like good conductivity, low ionization potentials, high electron affinities and low energy optical transitions, due to the delocalization of the π electrons over the conjugated backbone. Band theory reasonably explains the electronic structure of materials.[3,4] The electronic properties of conducting polymers cannot be described well by the standard band theory, because, they are unusual and they don't transport electrons via the same mechanism that are used to define classical semiconductors. In a conducting polymer,

mobile carriers introduced into the π conjugated backbone via doping results in electrical conductivity. This electronic phenomenon can be explained by the existence of soliton, poloron or bipoloron formation.[5] Now a days, polymeric non-linear optical (NLO) materials have attracted considerable research interest and have been the subject of intensive investigations. Polymeric NLO materials possess large second and third-order NLO properties, transparency over a broad wavelength range, ultrafast response time, high optical damage threshold, and capability to be easily processed into good optical quality thin films, offer significant advantages over the traditional inorganic materials.[6,7] These properties enable them for applications in fabricating integrated optical devices, such as waveguides, electro-optic (EO) modulators and optical frequency doublers, optical signal processing devices and in holography.[8-13] The thesis presents the synthesis of donor-acceptor copolymers and the experimental investigations on the photoconductivity and third-order NLO properties of the synthesized polymers.

This introductory chapter describes some fundamental principles of photoconducting polymers and NLO polymers. This chapter includes six sections. The first section, illustrates the tool box for band gap engineering to produce low band gap conjugated polymers. In the next section, different polymerization methods for obtaining the D-A copolymers are included. In the third section, the use of quantum chemical tools for designing the active layer polymers is described. Special emphasis is given to the use of Density Functional Theory. In the fourth section, fundamental principles of photoconducting polymers are included. In the fifth section, NLO effects in molecular systems are described. In the final section, aim and scope of the thesis is explained.

1.2. Band-Gap Tailoring: 'the Tool Box' for Low Band Gap Polymers

The considerable development of research on solar cells,[14-19] light-emitting devices[20-22] and organic field-effect transistors (OFETs),[23-26] paved the way for the development of π-conjugated polymers with tailored optical properties. The crucial challenge in developing an ideal p-type material is to design a conjugated polymer with requisite properties. The design should be in such a way that, the polymer should possess suitable HOMO-LUMO (highest occupied molecular orbital-lowest unoccupied molecular orbital) energy levels, high hole mobility, strong absorption ability and good film forming properties simultaneously.[27] Band gap is the most important property as far as the other properties are concerned. For a linear π-conjugated system, band gap (E_g) can be expressed as the sum of five contributions[28] (equation (1)):

$$E_g = E_{BLA} + E_{Res} + E_{Sub} + E_{\Theta} + E_{Int} \quad \text{..... (1)}$$

Bond length alternation (BLA), resonance effect (Res), introduction of electron-withdrawing or electron-releasing substituents (Sub), mean dihedral angle (Θ) between consecutive units and intermolecular interactions (Int) are the factors offering major contribution to the magnitude of band gap (Fig. 1.1).

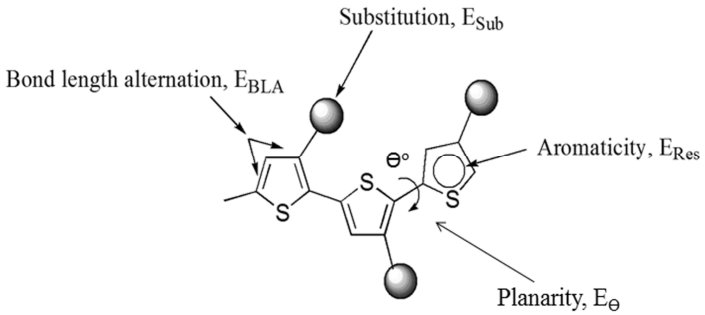

Fig. 1.1: Structural factors that determine the band gap of materials in linear π-conjugated systems.[28]

1.2.1. Structural Factors and Band Gap

Synthetic approaches by structural modifications (Fig. 1.2) can be expected to produce a polymer with reduced HOMO-LUMO gap. In a simple polyene system, BLA offers a major contribution, E_{BLA}, to the magnitude of band gap. The combined effects of electron-electron correlation and electron-phonon coupling results in the delocalization of π electrons that can lead to a low band gap of ~ 1.50 eV. Therefore, a decreased BLA can lead to a reduction in HOMO-LUMO gap, i.e., rigidification of the conjugated system resulting in a fully planar conjugated structure with significantly lowered band gap values in comparison with the parent open chain system.[29]

The energy required for switching of aromatic form to the quinoid form is called aromatic stabilization or resonance energy. This resonance effect traps the π electrons within the aromatic unit preventing them from delocalizing through the entire conjugated polymer backbone.[30] This effect can be represented by a quantity, E_{Res}. For example, the insertion of double bonds into the polymeric backbone reduces the overall aromaticity of the material resulting in the reduction of band gap.[31] A mean dihedral angle, 'Θ' between consecutive units limits the delocalization of π electrons through the conjugated polymeric backbone, leading to a high band gap. This effect can be represented by a quantity, E_{Θ}. The insertion of electron-donating (donor) or electron-withdrawing (acceptor) substituents is the simple way to control the HOMO and LUMO gap of a π conjugated system.[28] This can be represented by a term, E_{Sub}. In the case of thiophene unit, the insertion of acceptor groups like cyano, carboxy or nitro at the 3-position of the thiophene unit results in an increased oxidation potential.[32] In addition, the insertion of electron releasing groups to a conjugated system also yields

a higher energy HOMO level with reduction in band gap. It was reported that the inductive effect of simple alkyl groups lowered the oxidation potential of the thiophene ring by ~ 0.20 V.[33] The Fifth contribution (E_{Int}) to band gap involves intermolecular interactions, which have great impact on the magnitude of band gap. For example, intramolecular sulphur-oxygen interactions in EDOT-thiophene conjugated system, lead to a self-rigidification of the conjugated structure and thereby a low band gap.[34]

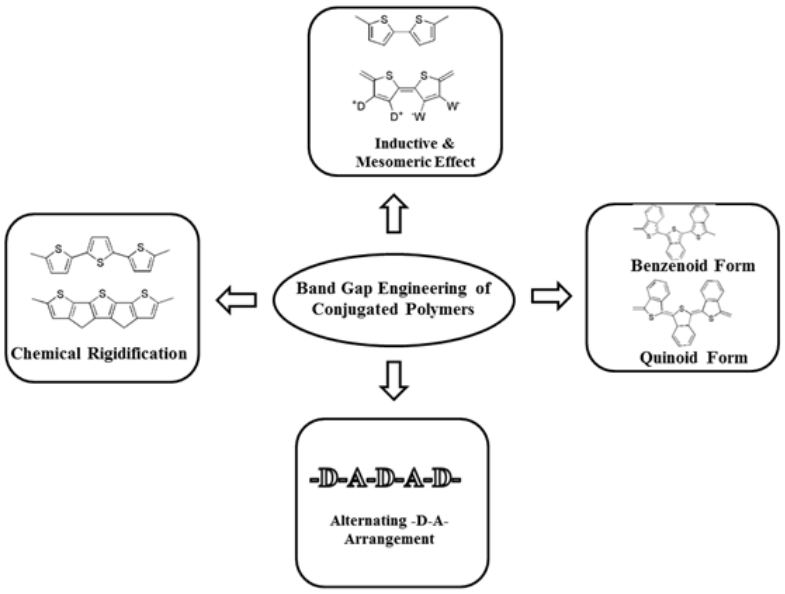

Fig. 1.2: Band gap engineering strategies in conjugated polymers.

1.2.2. Alternating Donor-Acceptor (D-A) Groups

The D-A concept was first introduced by E. E. Havinga *et al*., in 1992.[35] A regularly alternating donor-acceptor patterns in conjugated polymer results in broadening of the valence and conduction bands and hence reduction in band gap. Very low optical band gaps (~ 0.5 eV) have been reported for combinations of different donor groups with different

acceptors like croconic or squaric acid.[36] For a given conjugated polymer, the HOMO, LUMO energy levels and band gap have a major role in determining the electrical and optical properties. Lowering of band gap is possible either by increasing the HOMO level or decreasing the LUMO level of the polymer or by compressing the two levels closer together simultaneously. The reduction in the band gap in D-A copolymer is explained by the hybridization concept,[37] i.e., the HOMO level of the donor will interact with the HOMO level of the acceptor unit and the LUMO level of the donor will interact with LUMO level of the acceptor to yield two new HOMOs and two new LUMOs. The electrons rearrange themselves from their original non interacting orbitals in to the new set of hybridized orbitals of the polymer, i.e., a high lying HOMO level and a low lying LUMO level (Fig. 1.3). This results in lowering of the band gap in a D-A copolymer.[27]

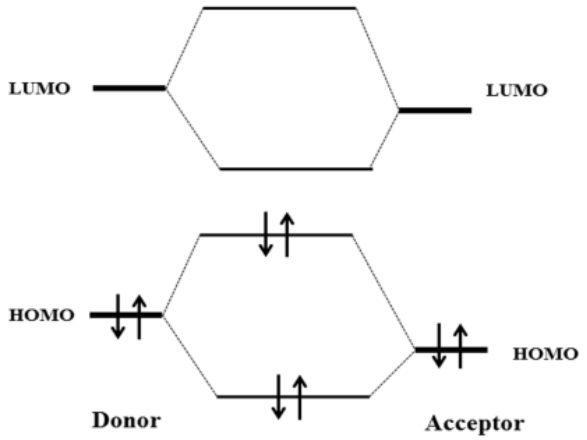

Fig. 1.3: Orbital interactions of donor and acceptor units in D-A copolymer.[27]

1.3. Polymerization methods for D-A copolymers

A good choice of the D-A combination permits the fine tuning of band gap to the desired magnitude.[27] Now a days, several synthetic strategies are

available for the preparation of conjugated copolymers. Most used polymerization techniques include chemical oxidative polymerization, electrochemical polymerization, Suzuki polymerization and Stille polymerization. Among the different techniques, transition metal-catalyzed cross-coupling reactions have been used as powerful synthetic strategy in copolymer synthesis. The most generally used transition-metal catalysts are palladium or nickel based complexes. The organometallic nucleophiles supported reactions are Stille (stannyl),[38] Kumada-Corriu (grignard reagents),[39] Suzuki-Miyaura (boron reagents)[40] or Sonogashira (copper).[41] Catalytic cycle of transition-metal catalyzed reactions is shown in Fig. 1.4. The first step is the formation of organo palladium species by the oxidative addition of palladium to the halide. Second step is the formation of an intermediate via transmetallation reaction with the organometallic nucleophiles. Final step is the reductive elimination of the desired product which restores the original palladium catalyst and completes the catalytic cycle.[42] These polymerization mechanisms normally follow a step-growth mechanism, and are still the most suitable choice for the synthesis of alternating copolymers.

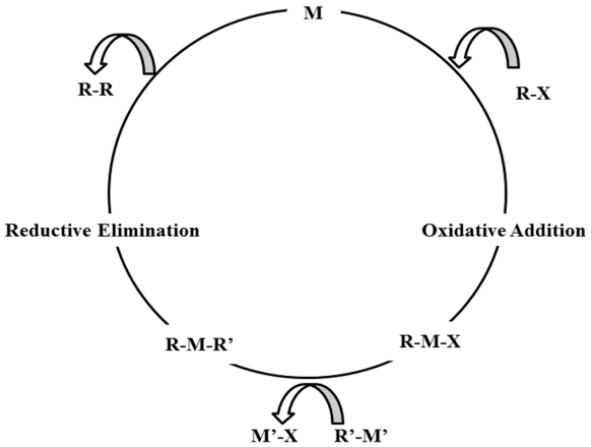

Fig. 1.4: Catalytic cycle of transition-metal catalysed reaction.

1.3.1. Kumada-Corriu reaction

Most of the D-A polymers are synthesized through metal-catalyzed polycondensation reactions based on Suzuki, Kumada or Stille coupling reactions. These polymers usually possess broad molecular weight distribution, in which all the end groups of the monomers and oligomers in the reaction mixture react equally with one another.[43] To attain better properties of the polymers, synthesis of polymers with controlled molecular weight and low polydispersity is very important. Compared to step-growth method, the catalyst-transfer Kumada coupling polymerization[39] can often be used to afford polymers with high molecular weight and narrow molecular weight distribution under relatively undemanding conditions.

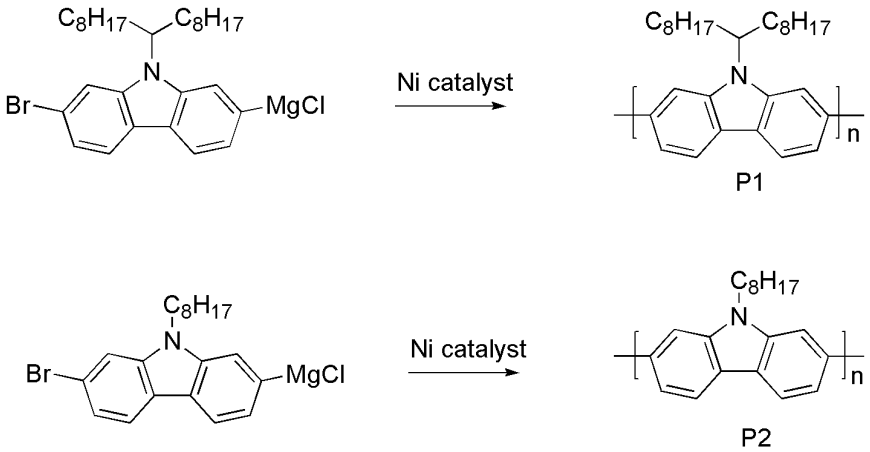

Scheme 1: Synthesis of polycarbazoles (P1 & P2) by catalyst transfer Kumada coupling.[44]

Recently, H. Wen *et al*., have prepared well-defined polycarbazoles with moderate molecular weight and low polydispersitiy index of 1.18 via catalyst-transfer Kumada coupling polymerization (Scheme 1).[44]

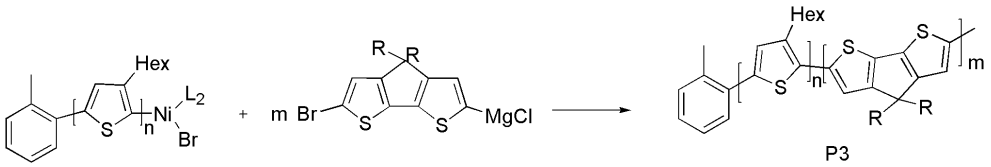

Scheme 2: Synthesis of P3HT-b-PCPDT block copolymer (P3) by catalyst transfer Kumada coupling.[45]

Also, a one-pot synthesis of P3HT-b-PCPDT (P3) block copolymer by Kumada catalyst transfer polymerization was reported by P. Willot *et al*., (Scheme 2).[45] F. Pammer have synthesized poly(4-alkylthiazole), highly head-to-tail regioregular material with a number average molecular weight significantly greater than 3.0 kDa via Kumada-coupling polycondensation of reversed monomers (Scheme 3).[46]

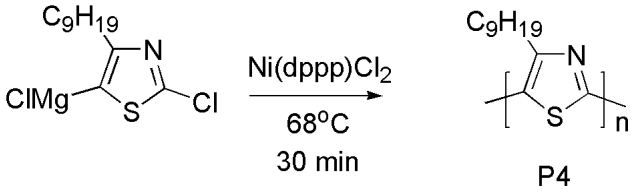

Scheme 3: Synthesis of poly(4-alkylthiazole) (P4) by Kumada-coupling polycondensation.[46]

1.3.2. Suzuki-Miyaura Coupling Reaction

Suzuki reaction is a C-C coupling reaction where the coupling partners are a boronic acid with a halide catalyzed by a palladium (0) complex.[47-49] It was first reported in 1979 by Akira Suzuki and he shared the Nobel Prize in Chemistry in 2010 with R. F. Heck and Ei-ichi Negishi for their efforts for the discovery and development of palladium-catalyzed cross-coupling reactions in organic synthesis.[50]

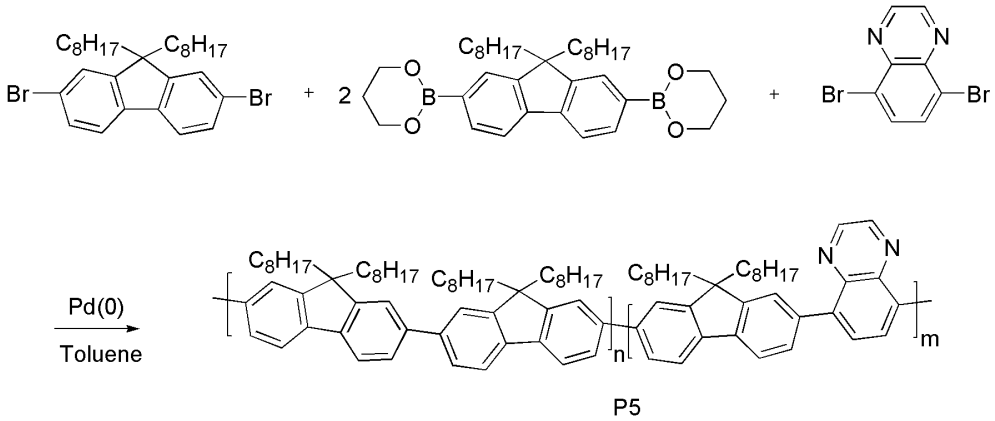

Scheme 4: Synthesis of poly(fluorene-co-quinoxaline) by Suzuki coupling.[51]

Recently, S. Jo *et al.,* have reported the preparation of poly(fluorene-co-quinoxaline), via conventional Suzuki cross-coupling polymerization as shown in Scheme 4.[51] S. Song *et al.,* have synthesized new conjugated polymers with 1,4-diphenylpyrrolo[3,2-b]pyrrole-2,5-dione, thiophene and carbazole using Suzuki polymerization (Scheme 5). A photovoltaic device was fabricated using a blend of these polymers with PCBM and showed 1.42 % efficiency.[52]

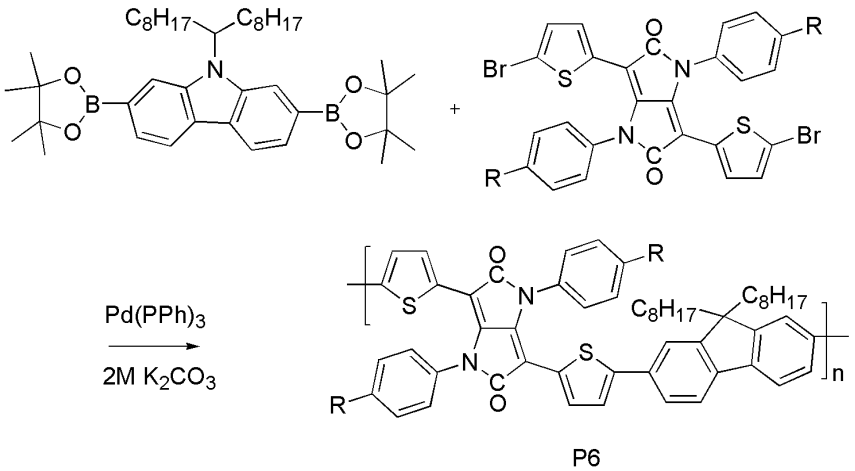

Scheme 5: Synthesis of copolymer with 1,4-diphenylpyrrolo[3,2-b]pyrrole-2,5-dione, thiophene and carbazole.[52]

Also, S. M. Park *et al*., have synthesized low band gap polymers with dithienylquinoxaline moieties and 6H-phenanthro[1,10,9,8-cdefg]carbazole via the Suzuki coupling reaction (Scheme 6).[53]

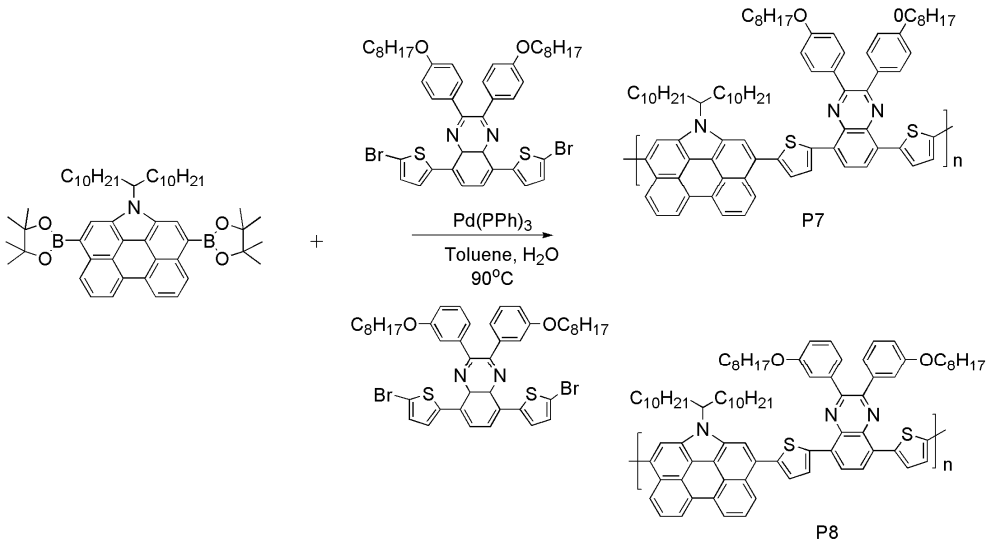

Scheme 6: Synthesis of dithienylquinoxaline-phenanthro[1,10,9,8-cdefg]carbazole copolymer using Suzuki coupling.[53]

1.3.3. Stille Cross-coupling Reaction

The Stille coupling is a versatile C-C coupling reaction between stannanes and halides or pseudohalides in organic synthesis. Recently, W. Cheng *et al*., have reported new low band gap conjugated copolymers bearing benzo[1,2-b:4,5-b']dithiophene as donor moiety and tetrazine as acceptor by Stille cross-coupling polymerization (Scheme 7).[54]

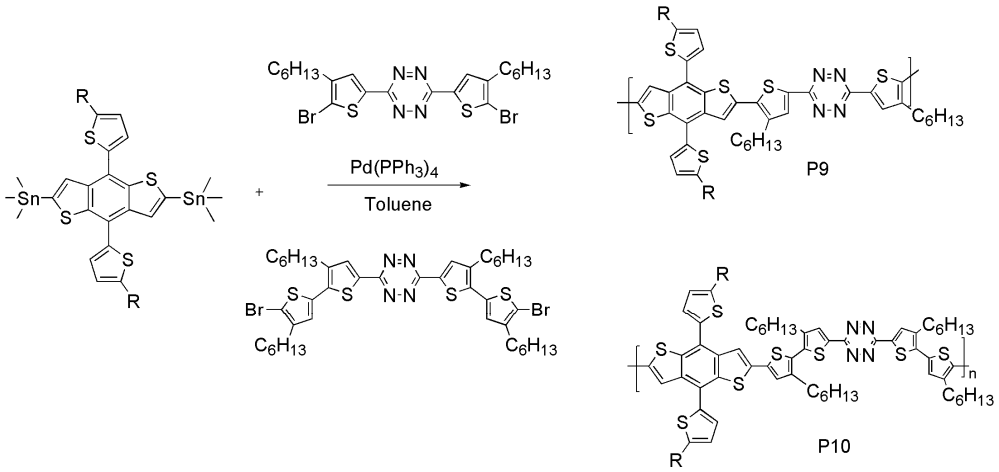

Scheme 7: Synthesis of benzo[1,2-b:4,5-b']dithiophene-tetrazine donor-acceptor copolymers by Stille coupling.[54]

Similarly, T. -L. Wang *et al*., have used Stille coupling reaction to copolymerize dithienothiophene and fluorenone (Scheme 8).[55]

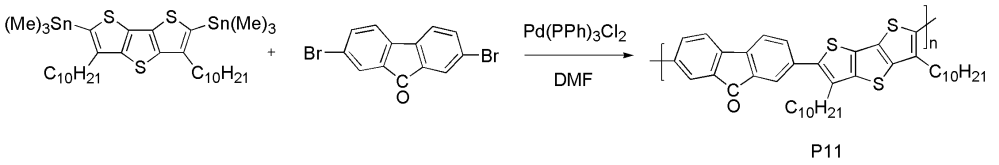

Scheme 8: Synthesis of dithienothiophene-fluorenone copolymer by Stille coupling.[55]

1.3.4. Sonogashira Reaction

The Sonogashira coupling reaction is one of the most widely used methods for the cross-coupling of vinyl or aryl halides with terminal alkynes. The Sonogashira cross-coupling reaction was first reported by K. Sonogashira, Y. Tohda, and N. Hagihara in 1975.[56]

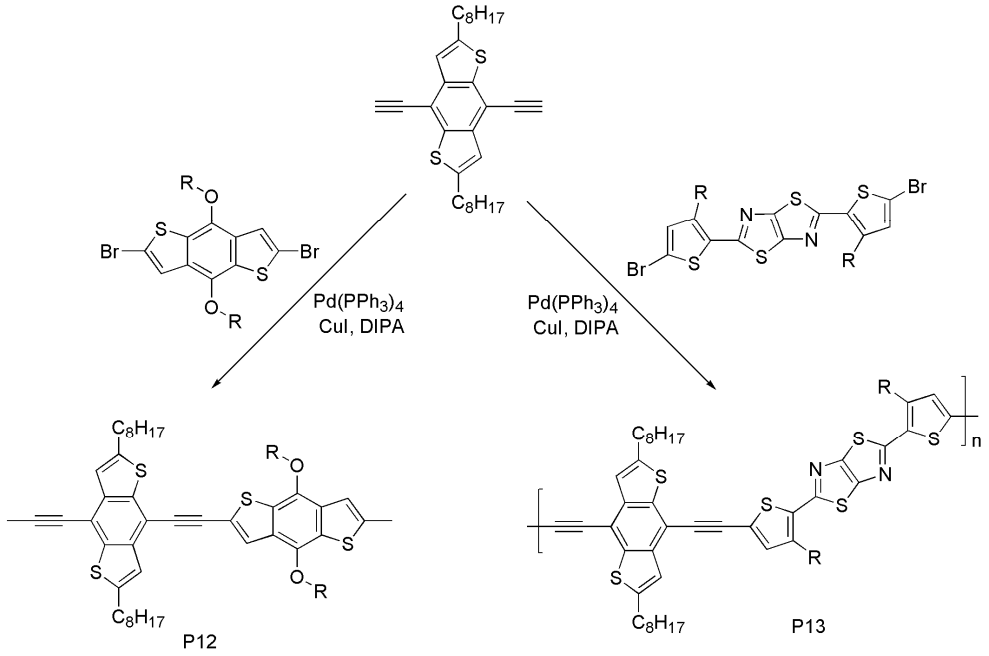

Scheme 9: Synthesis of benzodithiophene based poly(aryleneethynylene)s by Pd-catalyzed Sonogashira coupling reaction.[57]

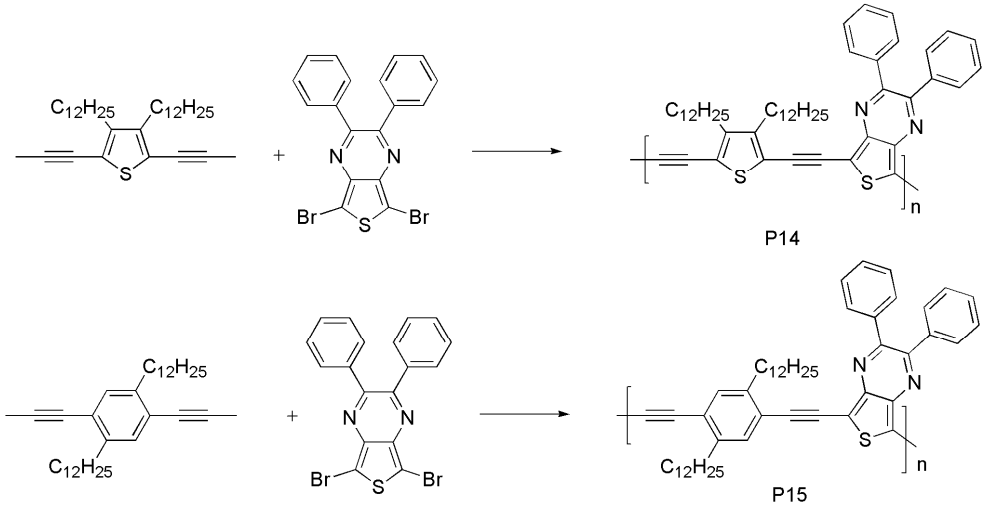

Scheme 10: Synthesis of thienopyrazine based poly(heteroaryleneethynylene)s by palladium catalysed Sonogashira reaction.[58]

Recently, S. Wen *et al*., have synthesized benzodithiophene-based poly(aryleneethynylene)s via Pd-catalyzed Sonogashira coupling reaction (Scheme 9). Bulk heterojunction solar cell with PCBM showed power conversion efficiency of 0.85 and 2.40 %.[57] R. S. Ashraf *et al*., have also reported thienopyrazine based low band gap poly(heteroaryleneethynylene)s, synthesized via palladium catalysed Sonogashira reaction (Scheme 10). The polymers showed about 2 % efficiency under illumination.[58]

1.3.5. Heck Coupling Reaction

The palladium-catalysed Mizoroki-Heck reaction is one of the most successful routes for the vinylation of aryl/vinyl halides. The first intermolecular Heck reaction was reported by Heck in 1972.[59] S. J. Chen *et al*., synthesized alternating copolymers of electron-rich 1,4-divinyl-2,5-dioctyloxybenzene and electron-deficient 5,8-(2,3-dipyridyl)-quinoxaline through Heck reaction (Scheme 11).[60]

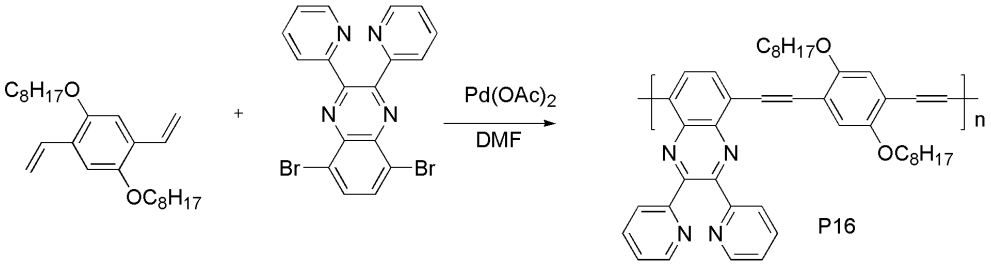

Scheme 11: Synthesis of alternating copolymers of 1,4-divinyl-2,5-dioctyloxybenzene and 5,8-(2,3-dipyridyl)-quinoxaline through Heck reaction.[60]

Also, L. Huo *et al*., have reported the synthesis and photovoltaic properties of alternating copolymers of electron-rich arylamine/dialkoxyphenylene and electron-deficient 2,1,3-benzothiadiazole using palladium acetate as catalyst by Heck reaction (Scheme 12).[61]

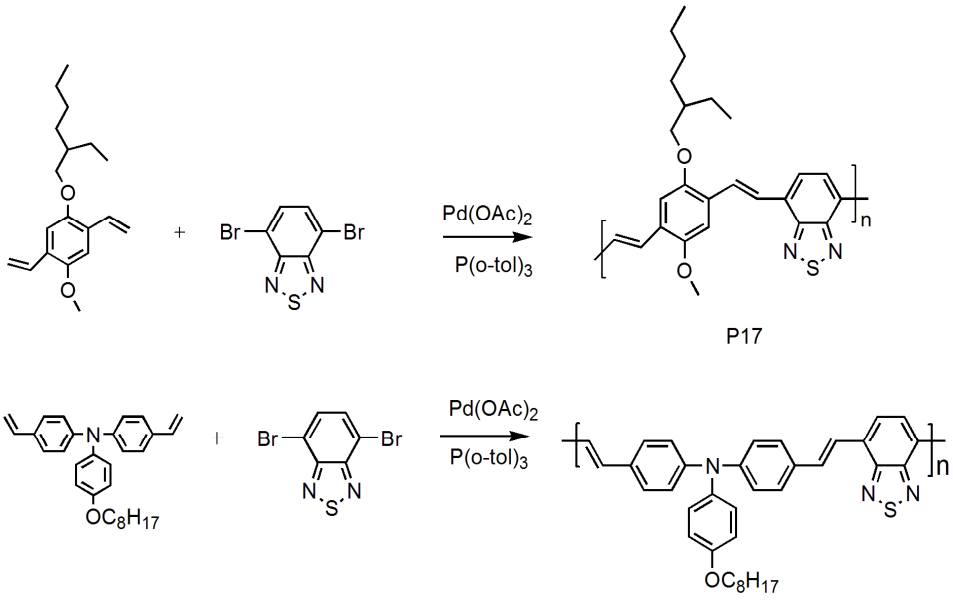

Scheme 12: Synthesis of alternating copolymers of arylamine/dialkoxyphenylene and 2,1,3-benzothiadiazole by Heck reaction.[61]

1.3.6. Direct Arylation Reaction

Generally, reductive polymerization via GRIM (grignard metathesis) is more expensive method compared to oxidative polymerization. It requires stringent polymerization conditions; it is irreversible and sensitive to functional groups. Although the reductive polymerization is having major disadvantages compared to oxidative polymerization, it yields better quality materials in terms of their electrochemical properties. Recently, A. Kumar *et al*., have reported a new single step reductive polymerization method via direct C–H arylation which uses less stringent polymerization conditions, inert to the presence of functional groups and is economically viable. They have reported single step reductive polymerization of ProDOT derivatives which is amenable for scale-up and is compatible with functional side chains (Scheme 13).[62]

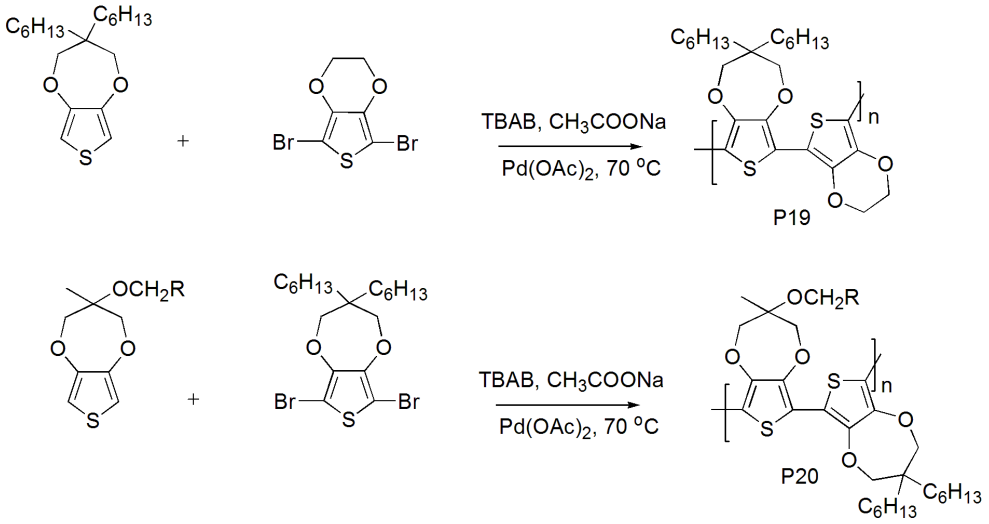

Scheme 13: Synthesis of of ProDOT copolymers using direct arylation.[62]

More recently, M. Wakioka *et al*., have introduced another highly efficient catalyst for the synthesis of alternating copolymers with thieno[3,4-c]pyrrole-4,6-dione units via direct arylation polymerization method (Scheme 14).[63]

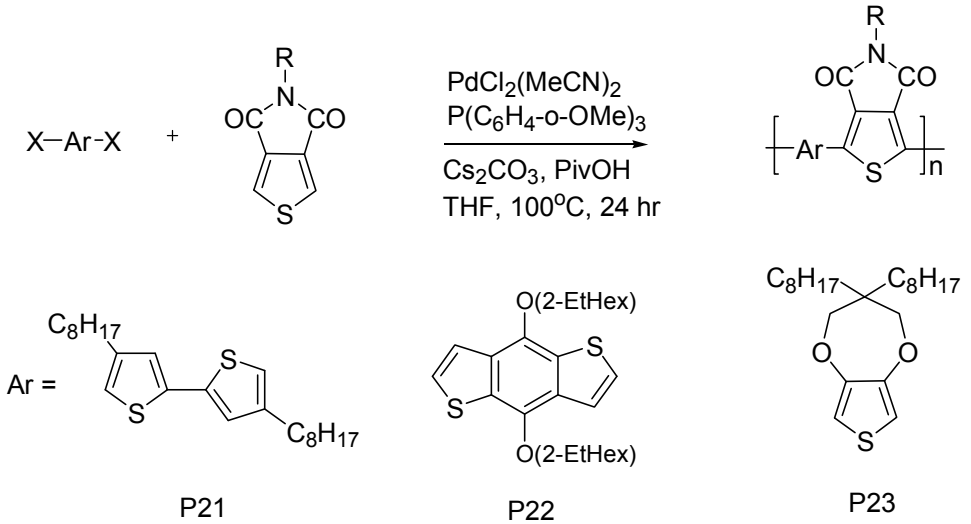

Scheme 14: Synthesis of alternating copolymers with thieno[3,4-c]pyrrole-4, 6-dione and thiophene copolymers.[63]

S. J. Choi *et al*., have reported microwave-assisted polycondensation via direct arylation of 3,4-ethylenedioxythiophene with 9,9-dioctyl-2, 7-dibromofluorene (Scheme15).[64]

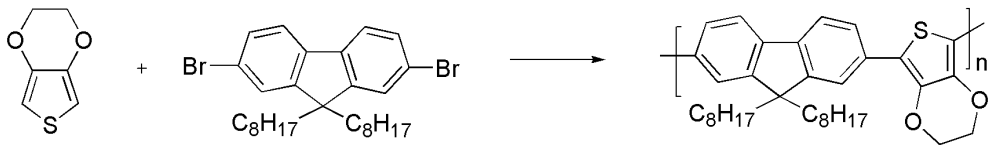

P24

Scheme 15: Synthesis of EDOT-fluorene copolymer using direct arylation.[64]

Merits of direct arylation

This method has several advantages,[62] some of which are

1) Avoids the use of tributyl tin and boronate esters
2) Economically viable
3) No need of dry solvent
4) Relatively high yield
5) Inert to the presence of fuctional groups
6) Less stringent polymerization conditions

1.4. Quantum-chemical calculation of electronic structure of conjugated polymers

The most important task of conjugated polymer research is to find a suitable low band gap polymer which possesses optimal property for device applications. Normally, polymers are synthesized and their properties are measured. This procedure is obviously very expensive. Economically viable and safe procedure is to calculate the electronic structure with a good approximation using quantum chemistry tools and eliminate unsuitable

molecules before synthesis.[65] However, such calculations require large CPU time; they are certainly much cheaper than the conventional experimental research. Theoretical studies will help to establish the structure-property relationship of conjugated polymers. Hence it plays a major role in better understanding of the structure dependent variables and helps to identify the strategies for effective band gap control. Two kinds of theoretical approaches are available to calculate the electronic structure and properties of a conjugated polymer. The first approach is called the oligomer approach. Several researchers have used this oligomer approach to find band gaps of conjugated polymers. The important feature of this method is to assess the physical properties of the oligomers as a function of progressively increasing size, until convergence is reached.[66-70] The second one is based on the standard solid state methods using Born–Karman PBC (periodic boundary condition), bloch functions, and translational symmetry called periodic boundary condition approach.[71] The PBC-DFT method was implemented in the Gaussian 03[72] and Gaussian 09[73] quantum chemical codes. In order to get good agreement with experimental data, hybrid exchange correlation functional is widely used in the PBC/DFT formalism. Commonly employed hybrid DFT methods include Becke's three parameter hybrid functional using the Lee-Yang-Parr (LYP)[74,75] correlation functional (B3LYP). Recently, B. G. Janesko *et al*., have reported good agreement between B3LYP and experimental band gaps for semiconducting polymers in the theoretical study of organic polymers.[76] More Recently, C. -K. Tai *et al*., have demonstrated the use of PBC-DFT method to determine geometric and electronic structures and the corresponding energies of polythiophene (PTH) and its derivative systems (PTs).[77] They used B3LYP functional, and the

6-31G(d) basis set in their studies and the results showed good agreement with experimental data. T. M. Pappenfus *et al*., have performed DFT calculations on a series of D-A copolymers using the oligomer approach and periodic boundary conditions.[78] They have demonstrated that the two methods agree well with one another and correlated with experimental data in a nearly identical manner. Recently, Heyd-Scuseria-Ernzerhof (HSE06) functional[79] incorporating a screened Hartree-Fock interaction has been introduced which is more computationally effective than traditional hybrid functional, B3LYP. In the present work, we have used Local Spin Density Approximation (LSDA),[80,81] B3LYP and HSE06 in combination with 6-31G basis set for calculating the properties of the D-A conjugated polymers.

1.5. Photoconductivity

An increase in electrical conductivity when a material is irradiated with electromagnetic radiation of appropriate energy is termed as photoconductivity. Photogeneration of carriers in polymers is carried out by a multi-step process. The initial process is the absorption of photon and this absorbed energy leads to the formation of excited state, which is stable for a specific life time. The excited state has high electric dipole moment due to charge separation; this is called charge transfer (CT) state. If undisturbed, the excited species may relax back to initial state together with the release of absorbed energy as photon of light. It can also undergo a non-radiative relaxation as thermal energy dissipation within the material.[82,83] The bound pair can be either separated by thermal environment or by an applied electric field.[83] The Goliber and Perlstein model described the creation of the CT state through the generation and diffusion of exciton.[84] An exciton

can also be considered as a species with absorption spectrum different from the molecule in the ground state and show fluorescence and stimulated emission.[85] The exciton dissociates at interfaces, impurity sites with asymmetric ionization potentials or it can be dissociated by application of strong electric field.[82,83]

The second requirement for photoconductivity is the transport of generated charge carriers through the medium. In organic semiconductors, charge transport proceeds via hopping within a positional disorder and energetic disorder system of localized states.[86] The terms positional and energetic disorder implies that the distance between hopping sites and the energy required to hop from one localized state to the other, vary significantly. Usually the carrier mobility is low and is in the range 10^{-2} to 10^{-8} cm^2/Vs and carrier mobility in polymers can be determined using the time of flight (TOF) technique. According to Gill's model, the temperature and field dependence of mobility must be $\log \mu \alpha 1/T$ and $\log \mu \alpha E^{1/2}$. Whereas, according to Bassler model, the temperature dependence has the form $\log \mu \alpha 1/T^2$ and field dependence $\log \mu \alpha E$.[87] In polymers, addition of molecules with low ionization potential than the polymer host will lead to hole trapping. Holes will remain trapped at these locations until an electron from a neighbouring electron rich unit gains sufficient energy and move to following trap. At moderate number densities of sensitizers, such trap states can form alternate transport levels.[88]

In photoconductors, electrons and holes are produced by the irradiation of light, which can be separated under an electric field of required magnitude and permit transport towards the appropriate electrode.

In most amorphous organic media, hole transport is most significant. A hole (an electron vacancy) can move through the material while the negative charge remains trapped and bound to the site of creation, which is therefore an anion. When a photoconductor is irradiated with suitable radiation, carrier generation and recombination will take place. After reaching equilibrium, the resultant photoconductivity is given by equation (2):[89]

$$\sigma_{ph} = G\tau e\mu \quad \text{..... (2)}$$

where, 'G' is the rate at which carriers are photogenerated within the photoconductor, 'τ' is the average time between generation and recombination of a carrier (recombination time), 'e' is the electronic charge and 'μ' is the mobility, the velocity of the carrier in unit electric field. Thus, the steady state photocurrent density is given by equation (3):[89]

$$J_{ph} = \sigma_{ph} E = G\,\tau e\mu E \quad \text{..... (3)}$$

where, 'E' is the electric field applied to the photoconductor.

Photoconductive sensitivity, change in conductivity per incident light intensity is given by equation (4):[90]

$$S = \frac{i_{ph} L}{P_0 A V} \quad \text{..... (4)}$$

where, 'i_{ph}' is the photocurrent, 'L' is the thickness of the sample, 'P_0' is the light power density, 'A' is the illuminated area and 'V' is the applied voltage. Mostly used photoconducting polymers absorb only in the ultraviolet region and thus suitable sensitizers are required to extend their spectral sensitivity to the desired region.

1.5.1. Role of Sensitizer

Most of the polymers do not absorb strongly near the operating wavelength region owing to their wide band gap. A wide gap between HOMO and LUMO energy levels leads to optical absorption near the ultraviolet region of the spectrum. So in polymers, charge generation at the wavelength of interest is brought about by the addition of small concentrations of molecules with appropriate HOMO and LUMO levels compared to the host polymer. Lower HOMO and LUMO levels than the host matrix are chosen for this purpose. Sensitizer molecules are used to extend the photocurrent generation ability of a given polymer to longer wavelengths. Generally used sensitizers include azo dyes, perylene dyes, squaraines, phthalocyanines, and thiapyrylium salts.[91,92] The charge-transfer (CT) complexes formed between a donor like polymer and an acceptor like sensitizer leads to longer wavelength absorption. The well-known complex, PVK:TNF[93,94] is shown in Fig. 1.5.

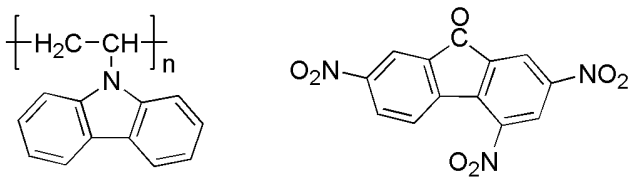

PVK TNF

Fig. 1.5: The most well-known charge transfer complex, PVK:TNF system.

The commonly employed electron acceptors are summarized in Fig. 1.6. Among the different electron acceptor molecules, the most important and soluble sensitizer, $PC_{61}BM$ ([6,6]-phenyl C_{61}-butyric acid methyl ester) has been subjected to intense studies. The HOMO and LUMO energy level

values of $PC_{61}BM$ are -3.7 and -6.1 eV, respectively. Different optoelectronic devices have been demonstrated based on $PC_{61}BM$-semiconducting polymer heterojunctions together with better device performance.[95-102]

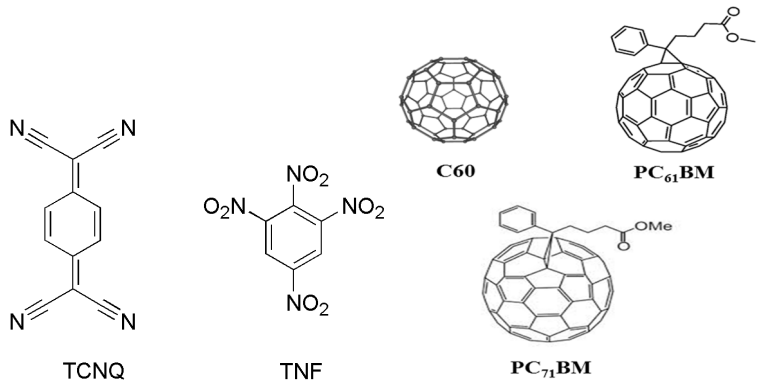

Fig. 1.6: Commonly employed electron acceptor molecules.

1.5.2. Steady state photocurrent measurement

Steady state photocurrent measurement involves measuring the steady state direct current (DC) developed within sandwich cell in the presence of light and in the dark. In this, a Keithley 236 Source Measure Unit is used. A DC voltage is applied to the sandwich cell placed in the dark and the current is measured with respect to time. After the stabilization of dark current developed in the cell, light is allowed to fall on the ITO surface. As a result of photoinduced change in conductivity, the current rises suddenly and approaches a steady state. After reaching the steady state, light is cut off and the measurement of current is continued. If I_D and I_L are the steady state current values, before and after illumination, respectively, the photosensitivity of the device can be calculated using the equation (5):

$$I_{ph} = \left(I_L - I_D\right) \Big/ I_D \quad \text{..... (5)}$$

The experimental arrangement is shown schematically in Fig. 1.7.

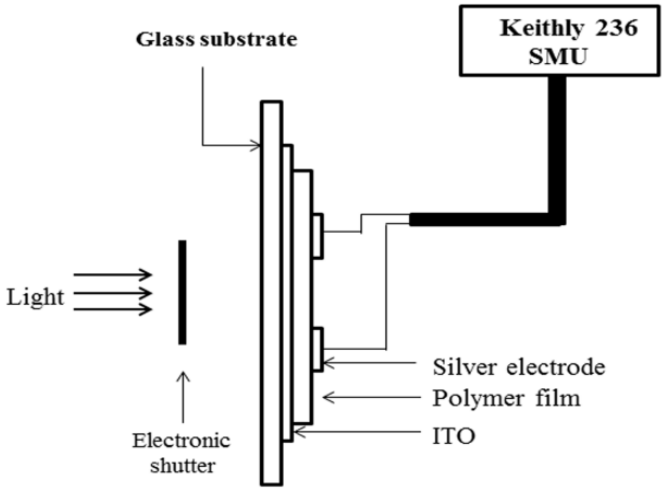

Fig. 1.7: The experimental setup for steady state photocurrent measurement.

1.6. Non-linear Optical Effects

Non-linear optical (NLO) processes in π-conjugated molecular systems have attracted considerable research interest because of their wide applications in opto-electronic devices. As the field progressed towards technological applications, research started to focus on developing high-performance materials that comply with device applications. Davydov *et al*., have first reported the second harmonic generation (SHG) in organic molecules in 1970.[103] This discovery led to a new concept of molecular engineering, i.e., to synthesize new organic materials for NLO studies. NLO research is mainly focused on the second and third-order properties. Of which third-order NLO property of donor-acceptor conjugated copolymer is the current area of interest. An ideal NLO material should have fast optical response time, wide phase matchable angle, large non-linear figure of merit, flexibility for molecular design and morphology, processability into crystals or thin films, ease of

fabrication, nontoxicity, optical transparency, good environmental stability and high mechanical and thermal stability.[104] Organic NLO materials can fulfil many of these primary requirements in comparison with inorganic materials. Third-order NLO effects in organic molecules is mainly due to strong donor-acceptor intramolecular interaction, i.e., strong delocalization produces NLO properties.[105] The optical non-linearities of organic materials are governed by the nature of π-bonding sequence and the conjugation length.[106] The non-linear response of a material when the material interacts with the electric field of light is termed as NLO effect. In the presence of intense light such as laser, the charge distribution in a medium gets modified under the influence of strong electric field, and the medium gets polarized.[107] At the microscopic level, dipole moment dependence on the electric field (E) is given by equation (6):

$$\mu_i = \mu_i(0) + \alpha_{ij} E_j + \beta_{ijk} E_j E_k + \gamma_{ijkl} E_j E_k E_l + \ldots\ldots\ldots \quad (6)$$

where, 'α', 'β' and 'γ' are the polarizability, first hyperpolarizability and second hyperpolarizability respectively, which determines the strength of the NLO effects in molecular systems.

Organic materials possessing a large third-order NLO response have attracted significant attention for the past two decades, because of their potential applications in optical switching,[108,109] optical limiting,[110-115] three-dimensional (3D) lithographic microfabrication,[116,117] 3D fluorescence imaging[118] and 3D optical data storage.[119] In 1989, M. S. Bahae *et al*.,[120,121] have introduced z-scan method to determine third-order non-linear optical coefficients of materials. Here, the transmittance of the material is measured as the material is moved along the propagation path of a Gaussian beam in

z-direction using an aperture or without an aperture.[120] In this method, sign as well as magnitude of non-linear coefficient can be easily deduced from transmittance curve. This technique can be used for measuring both non-linear absorption and non-linear refraction coefficients.[120]

1.6.1. Non-linear Absorption

Here the absorption process involves the change in absorption of a material as a function of input fluence.[122] At higher intensities, the probability of absorption of more than a single photon before relaxing down to the ground state can be increased. Non-linear absorption can be due to two phenomena; firstly, the reverse saturable absorption (RSA), which leads to increase in absorption of the material with increase in laser intensity and secondly, the saturable absorption (SA); which leads to decrease in absorption of a material, as the laser intensity increases.[123,124] SA is observed when excited state absorption is lower than the ground state absorption, which leads to an increase in the transmission through the material as the input intensity is increased. While, RSA is observed when excited state absorption is greater than the ground state absorption, which leads to a decrease in the transmission through the material as the input intensity is increased.[125] RSA generally represents positive absorption induced either by excited state absorption (ESA) or by a two photon absorption (TPA) process, which requires intensity of the order of $\sim 10^8$ W/cm^2.[106]

1.6.1.1. *Two Photon Absorption*

This phenomenon refers to the transition of electrons from the ground state to excited state by simultaneously absorbing two photons from the

incident radiation. Here, the non-linear absorption is directly proportional to the square of the intensity of the incident radiation (I) and is shown in equation (7):[122]

$$\frac{dI}{dz} = -\alpha I - \beta I^2 \quad \text{..... (7)}$$

here, 'α' and 'β' are the linear absorption coefficient, two photon absorption coefficient, respectively.

1.6.1.2. *Multiphoton Absorption*

Multiphoton absorption process involves the simultaneous absorption of 'n' photons from the incident beam. The absorption of (n+1) photons from a single optical beam can be written as equation (8):[122]

$$\frac{dI}{dz} = -\left(\alpha + \gamma^{(n+1)} I^n\right) I \quad \text{..... (8)}$$

where, '$\gamma^{(n+1)}$' stands for (n+1) photon absorption coefficient.

1.6.1.3. *Excited State Absorption*

Semiconductors and polyatomic molecules possess a high density state near to their excited states.[122] Therefore, before the photon relaxes to the ground state, it absorbs more number of photons and gets promoted to excited state. This process is referred to as excited state absorption.[122]

1.6.2. Optical Limiting

Optical limiters are those devices which are transparent to light at low input fluences, but become opaque at higher input intensities. This device finds application in optical pulse compression, pulse shaping and protection of eyes and sensitive optical devices from laser induced damages.[126,127] The

criteria required for a material to act as a promising optical limiter is: high linear transmittance throughout the sensor band width, low optical limiting threshold, stability, etc.[128] An ideal limiter should exhibit a linear transmission upto input threshold fluence called optical limiting threshold, which varies from material to material. Optical limiting threshold mainly depends on non-linear absorption coefficient (β) of a material.

1.6.3. Non-linear refraction

Non-linear refraction (NLR) is the change in refractive index of a medium when a material is exposed to electromagnetic radiation of suitable frequency. This property has been utilized in various applications like optical switching, logic gates, communication systems, data processing, non-linear spectroscopy and optical limiting devices. The dependence of NLR on intensity of illumination (I) is given by equation (9):[122]

$$n = n_0 + n_2 I \quad \text{..... (9)}$$

where, 'n_0' is the linear refractive index and 'n_2' is non-linear refraction coefficient. The NLR property of a material could be due to Raman induced Kerr effect, electronic polarization, thermal contributions, molecular orientation effects and photorefractive effects.[122]

1.6.4. z-scan technique

This is a simple single beam technique designed and developed by M. S. Bahae *et al.*,[120,121] to measure the sign as well as magnitude of non-linear absorption and non-linear refraction. Principle used in this technique is spatial beam distortion. It offers high sensitivity and simplicity than non-

linear interferometry, degenerate four wave mixing, ellipse rotation and beam distortion measurements. It allows to determine the third-order NLO properties of solids, liquids as well as liquid crystals. If transmitted light is measured through a finite aperture placed in the far field as the sample is moved in z-direction, is referred to as closed aperture (CA) z-scan technique. However, if the transmitted light is measured without an aperture, then it is referred to as open aperture (OA) z-scan technique. Here the output is sensitive only to non-linear absorption of a material. CA and OA z-scan methods yield the real and imaginary parts of non-linear susceptibility, respectively.[120,121]

The experimental setup for single beam z-scan is given in Fig. 1.8.

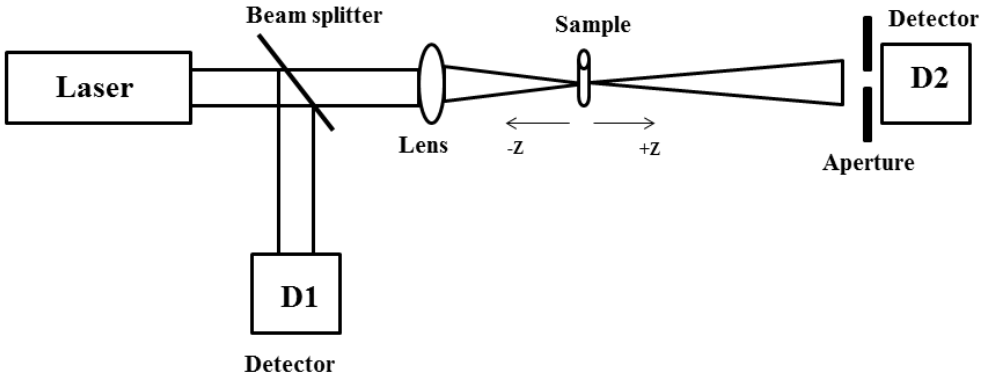

Fig. 1.8: Schematic representation of the experimental setup for z-scan technique.

1.6.4.1. *Open Aperture (OA) z-scan*

In this method, non-linear absorption of a material is measured. If the material is exhibiting NLO absorption like two photon absorption, the material can behave as either reverse saturable absorber (transmission is

minimum at focal point) or saturable absorber (transmission is maximum at the focal region).[120]

1.6.4.2. *Closed Aperture (CA) z-scan*

The basis of CA z-scan is the self phase modulation and self refraction effects. In CA z-scan technique, sample bahaves like thin lens of variable focal length due to change in refractive index at each position ($n = n_0 + n_2 I$).[122] If the material with negative non-linear refractive index is brought closer to focus, the beam irradiance enhances, which lead to self-lensing in the sample. A negative self-lensing prior to focus will tend to collimate the beam, resulting in beam narrowing at the aperture which causes an increase in transmission (peak). As the sample passes the focal plane to the right in z-direction, the same self-defocusing enhances the beam divergence causing a beam broadening at the aperture, and thus a decreased transmission (valley). A peak in the transmittance curve followed by valley in the transmittance curve reveals the negative non-linearity of a material. Whereas, positive non-linear refraction gives valley-peak configuration.[120]

Advantages and disadvantages of z-scan technique:[120]

This technique has several advantages, like:

a) Simplicity and ease of interpretation.

b) Possibility of isolating the refractive and absorptive parts of non-linearity.

c) Similarity between z-scan and optical limiting geometry.

d) Sign and magnitude of non-linearity can be measured simultaneously.

e) Can resolve a phase distortion of λ/300 indicating a high degree of sensitivity.

Disadvantages are,

a) Stringent requirement of high quality Gaussian TEM_{00} beam for absolute measurements.

b) Determination of the non-linear coefficients is entirly dependent on energy content, spatial and temporal profiles, and laser source stability.

1.7. Aim and Scope of the Thesis

1) Design of donor-acceptor low band gap conjugated polymers for photoconductive and non-linear optical application using Density Functional Theory in the Periodic Boundary Condition (PBC) formalism.

2) Synthesis of the copolymers using direct arylation and Suzuki coupling methods.

3) Explore the application of conjugated polymers as active layer in photoconducting devices.

4) Explore the application of conjugated copolymers in non-linear optical devices.

References

[1] H. Shirakawa, E. J. Louis, A. G. MacDiarmid, C. K. Chiang, A. J. Heeger, *J. Chem. Soc. Chem. Commun.*, 1977, 474, 578.

[2] T. A. Skotheim, J. R. Reynolds, Handbook of Conducting Polymers, 2nd ed., CRC Press, Boca Raton, Florida, 2007.

[3] D. Neamen, An Introduction to Semiconductor Devices, 1st ed., McGraw-Hill Science/Engineering/Math, USA, 2006.

[4] C. E. Housecroft, A. G. Sharpe, Inorganic Chemistry, 3rd ed., Pearson Education Limited, 2008.

[5] M. S. Freud, B. Deore, Self-Doped Conducting Polymers, John Wiley & Sons Ltd, 2007.

[6] P. N. Prasad, D. J. Williams, Introduction to nonlinear optical effects in molecules and polymers, Wiley, New York, 1992.

[7] H. S. Nalwa, S. Miyata, Nonlinear optics of organic molecules and polymers, CRC Press, Boca Raton, Florida, 1996.

[8] C. Q. Tang, Q. D. Zheng, H. M. Zhu, L. X. Wang, S. C. Chen, E. Ma, X. Y. Chen, *J. Mater. Chem. C,* 2013, 1, 1771.

[9] J. M. Hales, S. Zheng, S. Barlow, S. R. Marder, J. W. Perry, *J. Am. Chem. Soc.,* 2006, 128, 11362.

[10] R. Zieba, C. Desroches, F. Chaput, M. Carlsson, B. Eliasson, C. Lopes, M. Lindgren, S. Parola, *Adv. Funct. Mater.,* 2009, 19, 235.

[11] T. C. Lin, Y. F. Chen, C. L. Hu, C. S. Hsu, *J. Mater. Chem.,* 2009, 19, 7075.

[12] T. C. Lin, G. S. He, Q. D. Zheng, P. N. Prasad, *J. Mater. Chem.,* 2006, 16, 2490.

[13] T. C. Lin, G. S. He, P. N. Prasad, L. S. Tan, *J. Mater. Chem*., 2004, 14, 982.

[14] S. Liu, C. Zhong, S. Dong, J. Zhang, X. Huang, C. Zhou, J. Lu, L. Ying, L. Wang, F. Huang, Y. Cao, *Organic Electronics*, 2014, 15, 850.

[15] J. Liua, X. Suna, Z. Lib, B. Jina, G. Laib, H. Lic, C. Wanga, Y. Shena, J. Huaa, *J. Photochem. Photobiol. A*, 2014, 294, 54.

[16] N. Wang, X. Bao, Y. Yan, D. Ouyang, M. Sun, V. A. L. Roy, C. S. Lee, R. Yang, *J. Polym. Sci., Part A: Polym. Chem.*, 2014, 52, 3198.

[17] E. H. Jung, S. Bae, T. W. Yoo, W. H. Jo, *Polym. Chem*., 2014, 5, 6545.

[18] J. -S. Wu, J. -F. Jheng, J. -Y. Chang, Y. -Y. Lai, K. -Y. Wu, C. -L. Wang, C. -S. Hsu, *Polym. Chem.,* 2014, 5, 6472.

[19] S. Venkatesan, N. Obadja, T. -W. Chang, L. -T. Chen, Y. -L. Lee, *J. Power Sources*, 2014, 268, 77.

[20] S. H. Yoon, J. Shin, H. A. Um, T. W. Lee, M. J. Cho, Y. J. Kim, Y. H. Son, J. H. Yang, G. Chae, J. H. Kwon, D. H. Choi, *J. Polym. Sci., Part A: Polym. Chem.*, 2014, 52, 707.

[21] M. D. Ho, D. Kim, N. Kim, S. M. Cho, H. Chae, *Appl. Mater. Interfaces*, 2013, 5, 12369.

[22] Y. Yang, L. Yu, Y. Xue, Q. Zou, B. Zhang, L. Ying, W. Yang, J. Peng, Y. Cao, *Polymer*, 2014, 55, 1698.

[23] C. Wang, Y. Zang, Y. Qin, Q. Zhang, Y. Sun, C. Di, W. Xu, D. Zhu, *Chem. Eur. J.*, 2014, 20, 13755.

[24] S. Hunter, J. Chen, T. D. Anthopoulos, *Adv. Funct. Mater.,* 2014, 24, 5969.

[25] J. -W. Ha, Y. Kim, J. Roh, F. Xu, J. Il Park, J. Kwak, C. Lee, D. -H. Hwang, *J. Polym. Sci., Part A: Polym. Chem.*, 2014, 52, 3260.

[26] G. Zhang, M. Zhu, J. Guo, J. Ma, X. Wang, H. Lu, L. Qiu, *Organic Electronics*, 2014, 15, 2608.

[27] Y. -J. Cheng, S. -H. Yang, C. -S. Hsu, *Chem. Rev*., 2009, 109, 5868.

[28] J. Roncali, *Macromol. Rapid Commun*., 2007, 28, 1761.

[29] H. Koezuka, A. Tsumura, T. Ando, *Synth. Met.,* 1987, 18, 699.

[30] J. -L. Bredas, *J. Chem. Phys.,* 1985, 82, 3808.

[31] A. C. Grimsdale, K. L Chan, R. E. Martin, P. G. Jokisz, A. B. Holmes, *Chem. Rev.* 2009, 109, 89.

[32] R. J. Waltman, J. Bargon, A. F. Diaz, *J. Phys. Chem.,* 1983, 87, 1459.

[33] J. Roncali, R. Garreau, A. Yassar, P. Marque, F. Garnier, M. Lemaire, *J. Phys. Chem*., 1987, 91, 6706.

[34] J. Roncali, P. Blanchard, P. Frere, *J. Mater. Chem*. 2005, 15, 1589.

[35] E. E. Havinga, W. Hoeve, H. Wynberg, *Polym. Bull*., 1992, 29, 119.

[36] E. E. Havinga, W. Hoeve, H. Wynberg, *Synth. Met.,* 1993, 299, 55.

[37] G. Brocks, A. Tol, *J. Phys. Chem*., 1996, 100, 1838.

[38] J. K. Stille, *Angew. Chem., Int. Ed*., 1986, 25, 508.

[39] K. Tamao, M. J. Kumada, *J. Am. Chem. Soc.,* 1972, 94, 4374.

[40] N. Miyaura, A. Suzuki, *Chem. Rev*., 1995, 95, 2457.

[41] K. J. Sonogashira, *Organomet. Chem.,* 2002, 653, 46.

[42] R. Bates, Organic Synthesis Using Transition Metals, 2nd ed., John Wiley & Sons Ltd., 2012.

[43] T. Yamamoto, *Macromol. Rapid Commun.,* 2002, 23, 583.

[44] H. Wen, Z. Ge, Y. Liu, T. Yokozawa, L. Lu, X. Ouyang, Z. Tan, *Eur. Polym. J.,* 2013*,* 49, 3740.

[45] P. Willot, S. Govaerts, G. Koeckelberghs, *Macromolecules*, 2013, 46, 8888.

[46] F. Pammer, U. Passlack, *Macro Lett.,* 2014, 3, 170.

[47] M. Norio, Y. Kinji, S. Akira, *Tetrahedron Lett.,* 1979*,* 20, 3437.

[48] M. Norio, S. Akira, *Chem. Commun.,* 1979, 19, 866.

[49] M. Norio, S. Akira, *Chem. Rev.*, 1995, 95, 2457.

[50] Nobelprize.org., The Nobel Prize in Chemistry 2010. Nobel Prize Foundation. Retrieved 2013-10-25.

[51] S. Jo, D. Kim, S. -H. Son, Y. Kim, T. S. Lee, *Appl. Mater. Interfaces*, 2014, 6, 1330.

[52] S. Song, S. -J. Ko, H. Shin, Y. Jin, I. Kim, J. Y. Kim, H. Suh, *Bull. Korean Chem. Soc.,* 2013, 34, 3399.

[53] S. M. Park, Y. Yoon, C. W. Jeon, H. Kim, M. J. Ko, D. -K. Lee, J. Y. Kim, H. J. Son, S. -K. Kwon, Y. -H. Kim, B. S. Kim, *J. Polym. Sci., Part A: Polym. Chem.*, 2014, 52, 796.

[54] W. Cheng, Z. Wub, S. Wenc, B. Xu, H. Li, F. Zhu, W. Tian, *Organic Electronics,* 2013*,* 14, 2124.

[55] T. -L. Wang, Y. -T. Shieh, C. -H. Yang, Y. -Y. Chen, T. -H. Ho, C. -H. Chen, *J. Polym. Res*., 2013, 20, 213.

[56] K. Sonogashira, Y. Tohda, N. Hagihara, *Tetrahedron Lett.,* 1975, 16, 4467.

[57] S. Wen, X. Bao, W. Shen, C. Gu, Z. Du, L. Han, D. Zhu, R. Yang, *J. Polym. Sci., Part A: Polym. Chem.,* 2014, 52, 208.

[58] R. S. Ashraf, M. Shahid, E. Klemm, M. Al-Ibrahim, S. Sensfuss, *Macromol. Rapid Commun.,* 2006, 27, 1454.

[59] J. P. Nolley, R. F. Heck, *Tetrahedron*, 1972, 37, 2320.

[60] S. J. Chen, Q. Y. Zhang, J. W. Gu, M. L. Ma, L. Zhang, J. Zhou, Y. Y. Zhou, *Polymer Letters,* 2012, 6, 454.

[61] L. Huo, C. He, M. Han, E. Zhou, Y. Li, *J. Polym. Sci. Part A: Poly. Chem*., 2007, 45, 3861.

[62] A. Kumar, A. Kumar, *Polym. Chem.,* 2010, 1, 286.

[63] M. Wakioka, N. Ichihara, Y. Kitano, F. Ozawa, *Macromolecules*, 2014, 47, 626.

[64] S. J. Choi, J. Kuwabara, T. Kanbara, *Chem. Eng.,* 2013, 1, 878.

[65] J. J. Ladik, *Physics Reports*, 1999, 313, 171.

[66] S. M. Cassemiro, C. Zanlorenzi, T. D. Z. Atvars, G. Santos, F. J. Fonseca, L. Akcelrud, *J. Lumin.*, 2013, 134, 670.

[67] S. S. Zade, N. Zamoshchik, M. Bendikov, *Acc. Chem. Res*., 2011, 44, 14.

[68] L. Zhang, Q. Zhang, H. Ren, H. Yan, J. Zhang, H. Zhang, J. Gu, *Sol. Energy Mater. Sol. Cells*, 2008, 92, 581.

[69] C. S. Ra, S. Yim, G. Park, *Bull. Korean Chem. Soc*., 2008, 29, 891.

[70] U. Salzner, J. B. Lagowski, P. G. Pickup, R. A. Poirier, *Synth. Met.* 1998, 96, 177.

[71] T. E. Cheatham, J. H. Miller, T. Fox, P. A. Darden, P. A. Kollman, *J. Am. Chem. Soc*., 1995, 117, 4193.

[72] M. J. Frisch, G. W. Trucks, H. B. Schlegel, G. E. Scuseria, M. A. Robb, J. R. Cheeseman, J. A. Montgomery, Jr. T. Vreven, K. N. Kudin, J. C. Burant, J. M. Millam, S. Iyengar, J. Tomasi, V. Barone, B. Mennucci, M. Cossi, G. Scalmani, N. Rega, G. A. Petersson, H. Nakatsuji, M. Hada, M. Ehara, K. Toyota, R. Fukuda, J. Hasegawa, M. Ishida, T. Nakajima, Y. Honda, O. Kitao, H. Nakai, M. Klene, X. Li, J. E. Knox, H. P. Hratchian, J. B. Cross, V. Bakken, C. Adamo, J. Jaramillo, R. Gomperts, R. E. Stratmann, O. Yazyev, A. J. Austin, R. Cammi, C. Pomelli, J. W. Ochterski, P. Y. Ayala, K. Morokuma, G. A. Voth, P. Salvador, J. J. Dannenberg, V. G. Zakrzewski, S. Dapprich, A. D. Daniels, M. C. Strain, O. Farkas, D. K. Malick, A. D. Rabuck, K. Raghavachari, J. B. Foresman, J. V. Ortiz, Q. Cui, A. G. Baboul, S. Clifford, J. Cioslowski, B. B. Stefanov, G. Liu, A. Liashenko, P. Piskorz, I. Komaromi, R. L. Martin, D. J. Fox, T. Keith, M. A. Al-Laham, C. Y. Peng, A. Nanayakkara, M. Challacombe, P. M. W. Gill, B. Johnson, W. Chen, M. W. Wong, C. Gonzalez, J. A. Pople, Gaussian 03, Revision C.02, Gaussian, Inc., Wallingford CT, 2004.

[73] Gaussian 09, Revision B02, M. J. Frisch, G. W. Trucks, H. B. Schlegel, G. E. Scuseria, M. A. Robb, J. R. Cheeseman, G. Scalmani, V. Barone, B. Mennucci, G. A. Petersson, H. Nakatsuji, M. Caricato, X. Li, H. P. Hratchian, A. F. Izmaylov, J. Bloino, G. Zheng, J. L. Sonnenberg, M. Hada, M. Ehara, K. Toyota, R. Fukuda, J. Hasegawa, M. Ishida, T. Nakajima, Y. Honda, O. Kitao, H. Nakai, T. Vreven, Jr. J. A. Montgomery, J. E. Peralta, F. Ogliaro, M. Bearpark, J. J. Heyd, E. Brothers, K. N. Kudin, V. N. Staroverov, R. Kobayashi, J. Normand, K. Raghavachari, A. Rendell, J. C. Burant, S. S. Iyengar, J. Tomasi, M. Cossi, N. Rega, N. J. Millam, M. Klene, J. E. Knox, J. B. Cross, V. Bakken, C. Adamo, J. Jaramillo, R. Gomperts, R. E. Stratmann, O. Yazyev, A. J. Austin, R. Cammi, C. Pomelli, J. W. Ochterski, R. L. Martin, K. Morokuma, V. G. Zakrzewski, G. A. Voth, P. Salvador, J. J. Dannenberg, S. Dapprich, A. D. Daniels, Ö. Farkas, J. B. Foresman, J. V. Ortiz, J. Cioslowski, D. J. Fox, Gaussian, Inc., Wallingford CT, 2009.

[74] C. Lee, W. Yang, R. G. Parr, *Phys. Rev. B.,* 1988, 37, 785.

[75] K. Burke, J. P. Perdew, Y. Wang, J. F. Dobson, G. Vignale, M. P. Das, (Eds.), Electronic Density Functional Theory: Recent Progress and New Directions, Plenum Press, New York, 1998.

[76] B. G. Janesko, *J. Chem. Phys.,* 2011, 134, 184105.

[77] C. -K. Tai, P. -L. Yeh, C. -C. Chang, W. -H. Chen, R. -H. Wu, Y. -M. Chou, B. -C. Wang, *Res Chem Intermed.,* 2014, 40, 2355.

[78] T. M. Pappenfus, J. A. Schmidt, R. E. Koehn, J. D. Alia, *Macromolecules,* 2011, 44, 2354.

[79] J. Heyd, G. E. Scuseria, M. J. Ernzerhof, *Chem. Phys*., 2006, 124, 219906.

[80] S. H. Vosko, L. Wilk, M. Nusair, *Can. J. Phys.*, 1980, 58, 1200.

[81] U. Salzner, J. B. Lagowski, P. G. Pickup, R. A. Poirier, *J. Comp. Chem.,* 1997, 18, 1943.

[82] V. I. Arkhipov, H. BÄassler, M. Deussen, E. O. GÄobel, R. Kersting, H. Kurz, U. Lemmer, R. F. Mahrt, *Phys. Rev. B.,* 1995, 52, 4932.

[83] V. I. Arkhipov, H. BÄassler, *Phys. Stat. Sol.,* 2004, 201, 1152.

[84] D. West, D. J. Binks, Physics of Photorefraction in Polymers, No. 6 in Advances in Nonlinear Optics, CRC press, New York, 2005.

[85] V. Gulbinas, Y. Zaushitsyn, H. BÄassler, A. Yartsev, V. SundstrÄom, *Phys. Rev. B*, 2004, 70, 035215.

[86] C. Brabec, H. Johannson, F. Padinger, H. Neugebauer, J. Hummelen, N. Sariciftci, *Sol. Energy Mater. Sol. Cells,* 2000, 61, 19.

[87] T. K. DÄaubler, R. Bittner, K. Meerholz, V. Cimrov, D. Neher, *Phys. Rev. B.,* 2000, 61, 13515.

[88] G. G. Malliaras, V. V. Krasnikov, H. J. Bolink, G. Hadziioannou, *Appl. Phys. Lett.,* 1995, 66, 1038.

[89] M. Stolka, Photoconductive Polymers, In Special Polymers for Electronics and Optoelectronics, (J. A. Chilton and M. T. Goosey, eds.), Chapman & Hall, London, pp. 284-285, 1995.

[90] S. -H. Park, K. Ogino, H. Sato, *Synth. Met.,* 2000, 113, 135.

[91] K. -Y. Law, *Chem. Rev.,* 1993, 93, 449.

[92] E. Hendrickx, B. Kippelen, S. Thayumanavan, S. R. Marder, A. Persoons, N. Peyghambarian, *J. Chem. Phys.,* 2000, 112, 9557.

[93] T. K. DÄaubler, R. Bittner, K. Meerholz, V. Cimrov, D. Neher, *Phys. Rev. B*., 2000, 61, 13515.

[94] K. -Y. Law, *Chem. Rev*., 1993, 93, 449.

[95] J. Wang, H. Ye, H. Li, C. Mei, J. Ling, W. Li, Z. Shen, *Chin. J. Chem.,* 2013, 31, 1367.

[96] S. Chen, C. Tang, Z. Yin, Y. Ma, D. Cai, D. Ganeshan, Q. Zheng, *Chin. J. Chem.,* 2013, 31, 1409.

[97] S. Li, Z. Yuan, J. Yuan, P. Deng, Q. Zhang, B. Sun, *J. Mater. Chem. A*, 2014, 2, 5427.

[98] Y. Huang, M. Zhang, H. Chen, F. Wu, Z. Cao, L. Zhang, S. Tan, *J. Mater. Chem. A*, 2014, 2, 5218.

[99] K. Li, P. P. Khlyabich, L. Li, B. Burkhart, B. C. Thompson, J. C. Campbell, *J. Phys. Chem. C*, 2013, 117, 6940.

[100] Z. Deng, L. Chen, F. Wu, Y. Chen, *J. Phys. Chem. C*, 2014, 118, 6038.

[101] C. S. Ponseca, Jr. H. Nemec, N. Vukmirovic, S. Fusco, E. Wang, M. R. Andersson, P. Chabera, A. Yartsev, V. Sundstrom, *J. Phys. Chem. Lett*., 2012, 3, 2442.

[102] W. Zhuang, M. Bolognesi, M. Seri, P. Henriksson, D. Gedefaw, R. Kroon, M. Jarvid, A. Lundin, E. Wang, M. Muccini, M. R. Andersson, *Macromolecules,* 2013, 46, 8488.

[103] B. L. Davydov, L. D. Derkacheva, V. V. Dunina, M. E. Zhabolinski, V. F. Zolin, L. G. Coreneva, M. A. Samokhina, *JETP Lett.,* 12, 16.

[104] Y. Zhang, J. Etxebarria, Ferroelectric Liquid Crystals for Nonlinear Optical Applications, in Liquid Crystals Beyond Displays: Chemistry, Physics, and Applications (ed Q. Li), John Wiley & Sons, Inc., Hoboken, NJ, USA, 2012.

[105] K. B. Sophy, S. V. Shedge, S. Pal, *J. Phys. Chem. A*, 2008, 112, 11266.

[106] G. Sreekumar, P. G. L. Frobel, C. I. Muneera, K. Sathiyamoorthy, C. Vijayan, C. Mukherjee, *J. Opt. A: Pure Appl. Opt.,* 2009, 11, 125204.

[107] P. Yeh, Introduction to Photorefractive Nonlinear Optics, 1st ed., John Wiley & Sons, Inc., New York, 1993.

[108] S. Sun, L. R. Dalton, Introduction to Organic Electronic and Optoelectronic Materials and Devices, CRC Press, Taylor & Francis Group, Boca Raton, FL, 2008.

[109] L. V. Interrante, M. J. Hampden-Smith, Chemistry of Advanced Materials: An Overview, Wiley-VCH, New York, 1998.

[110] C. Q. Tang, Q. D. Zheng, H. M. Zhu, L. X. Wang, S. C. Chen, E. Ma, X. Y. Chen, *J. Mater. Chem. C,* 2013, 1, 1771.

[111] J. M. Hales, S. Zheng, S. Barlow, S. R. Marder, J. W. Perry, *J. Am. Chem. Soc.,* 2006, 128, 11362.

[112] R. Zieba, C. Desroches, F. Chaput, M. Carlsson, B. Eliasson, C. Lopes, M. Lindgren, S. Parola, *Adv. Funct. Mater*., 2009, 19, 235.

[113] T. C. Lin, Y. F. Chen, C. L. Hu, C. S. Hsu, *J. Mater. Chem*., 2009, 19, 7075.

[114] T. C. Lin, G. S. He, Q. D. Zheng, P. N. Prasad, *J. Mater. Chem.,* 2006, 16, 2490.

[115] L. Kamath, K. B. Manjunatha, S. Shettigar, G. Umesh, B. Narayana, S. Samshuddin, B. K. Sarojini, *Opt. Laser Technol.*, 2014, 56, 425.

[116] L. D. Zarzar, B. S. Swartzentruber, J. C. Harper, D. R. Dunphy, C. J. Brinker, J. Aizenberg, B. Kaehr, *J. Am. Chem. Soc*., 2012, 134, 4007.

[117] B. H. Cumpston, S. P. Ananthavel, S. Barlow, *Nature*, 1991, 398, 51.

[118] W. Denk, J. H. Strickler, W. W. Webb, *Science,* 1990, 248, 73.

[119] C. C. Corredor, Z. L. Huang, K. D. Belfield, A. R. Morales, M. V. Bondar, *Chem. Mater*., 2007, 19, 5165.

[120] M. S. Bahae, A. A. Said, T. -H Wei, D. J. Hagan, E. W. Van Stryland, *IEEE Journal of Quantum Electronics*, 1990, 26, 760.

[121] M. S. Bahae, A. A. Said, E. W. Van Stryland, *Opt. Lett*., 1989, 14, 955.

[122] R. L. Sutherland, Hand book of nonlinear optics, 2nd ed., Eastern Hemisphere Distribution, Marcel Dekker. Inc., USA, 2003.

[123] N. K. M. N. Srinivas, S. V. Rao, D. N. Rao, *J. Opt. Soc. Am. B: Opt. Phys.,* 2003, 20, 2470.

[124] U. Kurum, M. Yuksek, H. G. Yagliolu, A. Elmali, A. Ates, M. Karabutlut, G. M. Mamedov, *J. Appl. Phys.*, 2010, 108, 063102.

[125] M. D. Zidan, Z. Ajji, *Opt. Laser Technol*, 2011, 43, 934.

[126] C. Zhang, Y. L. Song, Y. Xu, H. K. Fun, G. Y. Fang, Y. X. Wang, X. Q. Xin, *J. Chem. Soc. Dalton Trans*., 2823, 2000.

[127] E. I. Stiefel, K. Matsumoto, Transition Metal Sulfur Chemistry: Biological and Industrial Significance, American Chemical Society, Washington, DC, 1996.

[128] R. Tong, H. Wuc, B. Lia, R. Zhua, G. Youa, S. H. Qian, *Physica B*, 2005, 366, 192.

.....ൠ.....

Chapter 2

Theoretical and Experimental Investigations on the Photoconductivity and Non-linear Optical Properties of Donor-Acceptor π Conjugated Copolymer, Poly(2,5-(3,4-ethylenedioxythiophene)-alt-2,7-(9,9-dioctylfluorene))*

Abstract

Donor-acceptor (D-A) π conjugated copolymer, poly(2,5-(3,4-ethylenedioxythiophene)-alt-2,7-(9,9-dioctylfluorene)) (P(EDOT-FL)), a photoconductive and non-linear optical polymer was synthesized via, direct arylation method using palladium acetate as catalyst and characterized. Theoretical studies along with photophysical and electrochemical studies confirmed that the copolymer exhibited relatively low band gap (2.29 eV) than that of polyfluorene. The photoconductivity properties of the P(EDOT-FL)-$PC_{61}BM$ films under various illumination wavelengths were studied and high photosensitivity was observed at 488 nm. Field dependence of photoconductivity in P(EDOT-FL)/$PC_{61}BM$ blend films showed that the films could withstand upto 75 V/μm and the photosensitivity at higher electric fields was even greater than two lakh (at 75 V/μm, the photosensitivity was 2,89,742). At higher electric fields, the photocurrent entered into micro ampere ranges. The intensity dependence on photocurrent in these films was also investigated. Third-order non-linear optical properties of P(EDOT-FL) under nanosecond laser excitation at 532 nm was studied by z-scan technique. Polymer exhibited high non-linear absorption and refraction coefficient. The polymer also showed good optical limiting response at 532 nm. These results provide an avenue for application of P(EDOT-FL) in photoconducting and non-linear optical devices.

* Theoretical and experimental investigations on the photoconductivity and non-linear optical properties of donor–acceptor π conjugated copolymer, poly(2,5-(3,4-ethylenedioxythiophene)-alt-2,7-(9,9-dioctylfluorene)), Sona Narayanan, Anshad Abbas, Sreejesh Poikavila Raghunathan, Krishnapillai Sreekumar, Cheranellore Sudha Kartha, Rani Joseph, RSC Adv., 2015, 5, 8657, DOI: 10.1039/c4ra13024c.

2.1. Introduction

Over the last three decades, conducting polymers have attracted a great deal of research interest owing to their electrical, electrochemical and optical properties. Nowadays, with the advent of better design and fabrication technology, a wide variety of conductive polymers are available in optoelectronic device applications. They are promising candidates for commercial application in photovoltaics,[1-4] lightnon-linear-emitting diodes,[5-7] field-effect transistors,[8-12] sensors,[13] and electrochromic devices.[14-17] Synthesis of D-A copolymers appears to be a general strategy to achieve enhanced efficiency than that of the parent homopolymers due to a combination of efficiency and versatility by allowing multiple possibilities of combination of D and A building blocks.[18-20] Conjugated polymers based on 3, 4-ethylenedioxythiophene (EDOT) have been widely investigated owing to their relatively low ionization potential, high conductivity when doped, and good stability.[21,22] These properties enable them to be ideally fit in various applications such as hole transport layer in light emitting devices, design and fabrication of chemical and biological sensors, antistatic coatings, transparent electrodes, and electrochromic displays etc.[23-28] Polyfluorenes (PFs) have been widely studied for polymer light-emitting diodes (PLED) because of their processability, high photoluminescence efficiency, high hole mobility and good photostability.[29-33] However, its large band gap (in the range of 2.95 eV to 3.68 eV)[34,35] combined with poor electron-transport properties results in a large electron-injection barrier and imbalance of charge carrier transport. Copolymerization of fluorene with EDOT moieties was investigated to rectify the shortcomings.

Generally, EDOT-Fluorene copolymer with alternating D-A structures were synthesized via, Stille[36,37] or Suzuki[38-40] coupling reactions or electrochemical polymerization.[41-43] In fact, they demand stringent reaction conditions and polymers with high purity results only on substantial product purification. Recently, Anil Kumar *et al*.,[44] have developed a new reductive polymerization method for the synthesis of polymers which is economically viable, inert to the presence of functional groups and uses less stringent polymerization conditions. This method was adopted for the preparation of P(EDOT-FL) for utilising the desirable properties of the two monomeric species, EDOT and fluorene. Currently, there are two reports on direct arylation polycondensation for the synthesis of P(EDOT-FL) and high OPV performance with a power conversion efficiency of 4 %.[45,46] P. Blondin *et al.,* have reported the synthesis of such copolymer via palladium-catalyzed Suzuki coupling and have attracted great attention due to their thermochromic and solvatochromic properties.[39] Also, S. M. Cassemiro *et al.,*[38] have synthesized an alternating copolymer of EDOT and fluorene, ((poly(2,5-(3,4-ethylenedioxythiophene)-alt-2,7-(9,9-dihexylfluorene)) by Suzuki coupling reaction and their investigation revealed the light emitting mechanism in the polymer. EDOT-Fluorene copolymers have wide research interest due to their unique electro-optic properties. As a result, these copolymers are potential candidates in electrochromic devices,[37,43] organic polymer light emitting diodes,[36,38,40] and organic lasers.[42] Photoconductivity refers to the increase in electrical conductivity when a material is exposed to electromagnetic radiation of suitable energy. Charge-transfer (CT) complexes are well-known solid-state organic functional materials which are composed of electron-rich molecules/polymers as donor (D) and electron-deficient

molecules as acceptor (A). Hence a blend of narrow-band gap donor (P (EDOT-FL) and $PC_{61}BM$ ([6,6]-Phenyl C_{61}butyric acid methyl ester) have been investigated in this study, thus forming a novel photoconductive material.

Third-order non-linear optical materials have attracted a great deal of research interest because of their potential applications in optical devices.[47-49] Among the wide range of non-linear optical (NLO) materials, π conjugated organic materials are promising because of their inherent large third-order susceptibilities, fast response time, processability and good mechanical properties. In organic NLO materials, non-linearity originates due to strong donor-acceptor intermolecular interaction and delocalized π electrons.[50] Therefore, non-linear optical properties can be tuned by adopting suitable synthetic strategies such as copolymerization. Since P(EDOT-FL) is D-A alternate copolymer, it can induce a strong intramolecular charge transfer transition. In this chapter, the design, synthetic procedure and properties (electrochemical and photophysical) of the conjugated polymer, P(EDOT-FL) is reported together with photoconductivity studies of P(EDOT-FL)/$PC_{61}BM$ blends. Wavelength, intensity and electric field dependence of photocurrent have been studied. The third-order non-linear optical properties of the P(EDOT-FL) in solution and as film has also been discussed in detail. This work presents a correlation between the theoretical and experimental results aiming to add further information about photorefractive properties of this material.

2.2. Results and Discussion

2.2.1. Theoretical Calculation

Quantum mechanical calculation at the density functional theory (DFT)[51] level has been carried out to examine the interaction between EDOT and FL units when they are directly linked in copolymer chain. In the present work, we have used B3LYP (Becke, three parameter, Lee-Yang-Parr),[52-54] HSE06 (Heyd-Scuseria-Ernzerhof functional)[55,56] and LSDA (Local Spin Density Approximation)[57,58] combined with 6-31G basis set to calculate the electronic properties of P(EDOT-FL) copolymer. Here, periodic boundary condition (PBC) calculation was used to study the electronic properties of the P(EDOT-FL), because, it is more computationally cost effective than oligomer approach. In PBC calculation, polymer molecule of infinite chain length is optimized using translational symmetry. The energy levels of the HOMO (highest occupied molecular orbital) and LUMO (lowest unoccupied molecular orbital) were determined from the maximum point of the highest occupied crystal orbital and the minimum point of the lowest unoccupied crystal orbital, respectively. The band gap corresponded to the lowest energy difference between the HOMO and LUMO energy levels at a constant k.

Recently, S.M. Cassemiro *et al.*[38] have demonstrated the use of oligomer approach in poly(2,5-(3,4-ethylenedioxythiophene)-alt-(9,9'-dihexyl-2,7-fluorene)) to generate the band gap of 2.62 eV and 2.46 eV, showing good agreement with that obtained experimentally (2.5 eV). Error of about 4.6 % and 1.0 %, respectively resulted. Electronic properties of vinylene-linked heterocyclic conducting polymers were calculated using DFT method in periodic boundary condition approach.[59-62] Newly introduced HSE06

functional incorporates a screened Hartree-Fock interaction, more computationally efficient than traditional hybrid functionals like B3LYP. The obtained HOMO and LUMO values are summarized in Table 2.1. For the sake of comparison, PBC calculation of poly(dioctylfluorene) (P(FL)) was also carried out. It can be seen from Fig. 2.1 that lowest band gap occur at Γ point (k=0), suggesting that the copolymer was a direct band gap polymer.

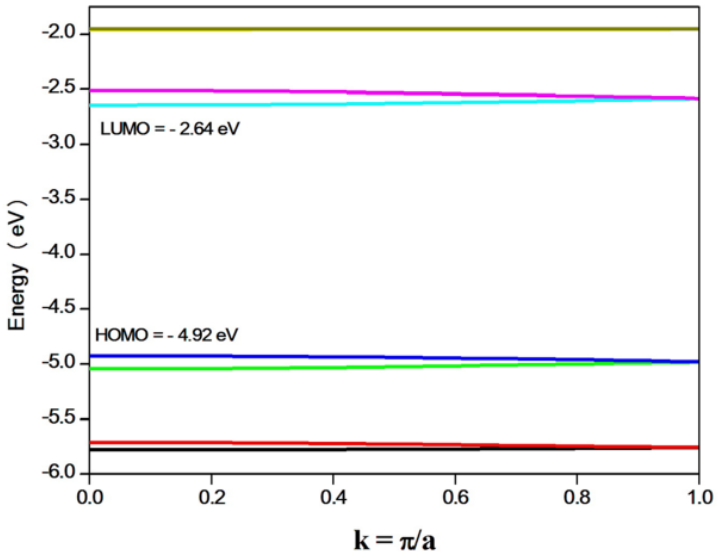

Fig. 2.1: Band structure of P(EDOT-FL) obtained from DFT/LSDA/6-31G calculation.

From the theoretical results it was found that band gap from LSDA was more comparable to experimental values than B3LYP and HSE06. The HOMO and LUMO values obtained for P(EDOT-FL) were -4.92 eV and -2.64 eV, respectively. Meanwhile, HOMO and LUMO values for P(FL) were -5.24 eV and -1.30 eV respectively. As seen from band structure, it can be seen that the introduction of EDOT unit increased the energy of HOMO

level of P(FL) by a factor of 0.3 eV, while LUMO level is decreased by a factor of 1.34 eV and we get P(EDOT-FL) with a reduced band gap of 2.28 eV.

Table 2.1: Band structure data of P(EDOT-FL).

Sample	HOMO (eV)	LUMO (eV)	Band gap(eV)
P(EDOT-FL)	-4.95[a]	-1.44[a]	3.51[a]
	-4.82[b]	-1.70[b]	3.12[b]
	-4.92[c]	-2.64[c]	2.28[c]
P(FL)	-5.24[a]	-1.30[a]	3.94[a]

[a]Estimated from DFT/B3LYP/6-31G calculation. [b]Estimated from DFT/HSE06/6-31G calculation. [c]Estimated from DFT/LSDA/6-31G calculation.

2.2.2. Polymer Synthesis

P(EDOT-FL) have been synthesized via direct arylation of EDOT with 2,7-dibromo-9,9-dioctylfluorene in dry DMAc and 0.01 mol% palladium acetate served as catalyst. Polymer was obtained in moderate yield (61%). To increase the solubility of targeted copolymer, two bulky octyl chains were introduced to the fluorene building unit. Hence P(EDOT-FL) exhibited good solubility in organic solvents such as CH_2Cl_2, $CHCl_3$, THF and dichlorobenzene. This provides the processability required for electronic device applications. The molecular weight of the P(EDOT-FL) was evaluated by gel permeation chromatography in THF referring to polystyrene standards. Copolymer exhibited number average molecular weight (Mn) of 6994 and weight average molecular weight (Mw) of 7106 with polydispersity index (PDI) of 1.01. Scheme 1 illustrates the synthesis route used for the preparation of P(EDOT-FL).

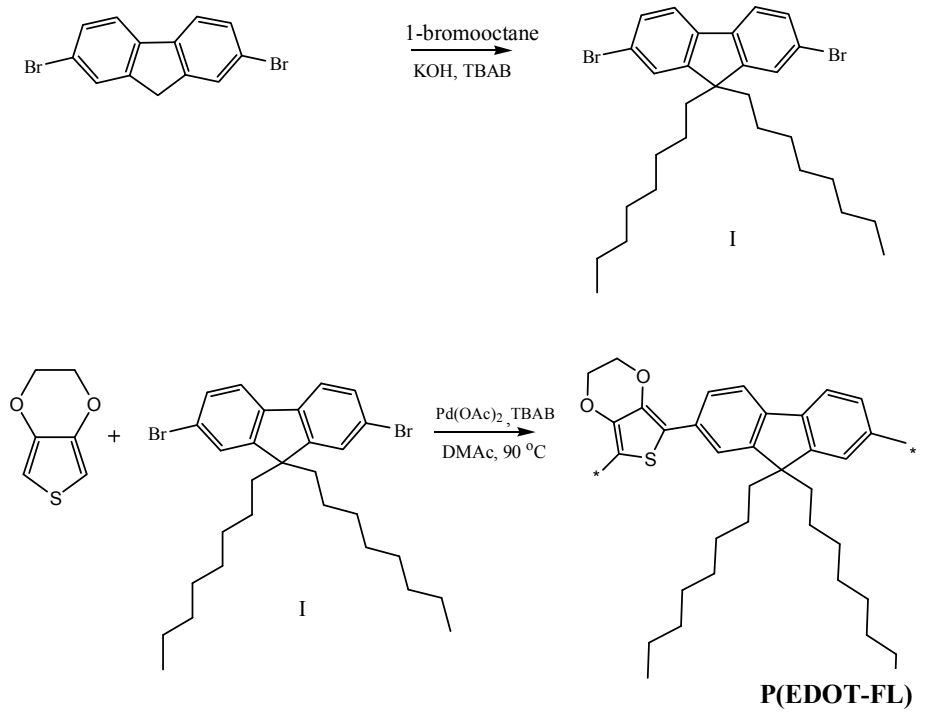

P(EDOT-FL)

Scheme 1: Synthesis of P(EDOT-FL) by direct arylation.

2.2.2.1. *Structural Characterization*

P(EDOT-FL) copolymer was characterized by FT-IR (Fig. 2.2), ^{1}H NMR (Fig. 2.3) and XPS. FT-IR spectrum of the P(EDOT-FL) showed intense peaks at 2918 and 1364 cm^{-1} characteristic of aliphatic C-H stretching and bending vibration of fluorene (FL) unit, respectively. The C-O-C stretching vibration arising from bridged C-O in the ethylenedioxy group of EDOT was revealed at 1086 and 1050 cm^{-1} and ethylenedioxy ring deformation mode at 920 cm^{-1}.[63,64] The broad band observed at 1667 cm^{-1} proved polyconjugation in the copolymer.[65] Bands at 814, 845 and 943 cm^{-1} are assigned to the C-H out-of-plane vibration of the phenyl ring of FL unit and the peak at 1060 cm^{-1} was due to C-H in-plane vibration of the phenyl ring of FL unit.[66]

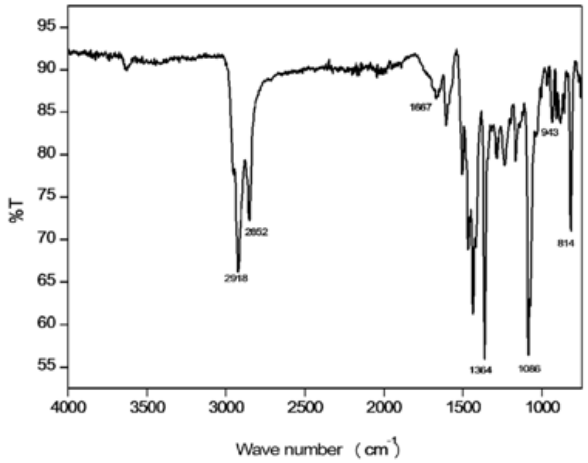

Fig. 2.2: FT-IR spectrum of P(EDOT-FL).

The intense peaks at 2918 and 1086 cm^{-1} were attributed to the incorporation of EDOT-FL units into the polymer structure during copolymerization. From the results of FT-IR analysis, the successful achievement of copolymerization was revealed.

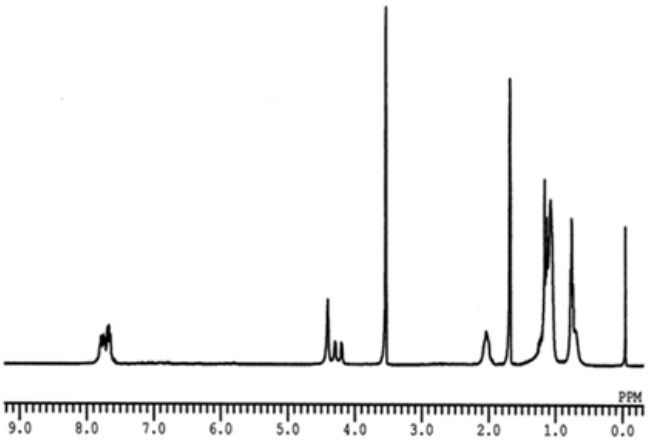

Fig. 2.3: ^{1}H NMR spectrum of P(EDOT-FL).

The structure of the polymer was further confirmed with ^{1}H NMR spectrum. P(EDOT-FL) showed multiplets at δ 0.8-2 ppm region due to alkyl protons. Resonance peaks corresponding to -O-CH_2- protons of EDOT units were observed at δ 4.2-4.5 ppm as multiplet. The broad peak corresponding to aromatic protons observed at δ 6.9-7.8 ppm were confirmed to be the part of FL units. The characteristic signals at δ 0.8-2 and 6.9-7.8 ppm were attributed to FL units and δ 4.2-4.5 ppm are related to EDOT units. They are in good agreement with the FT-IR results. In order to get more insight into the polymer structure XPS investigation was also carried out. The XPS survey scan is given in Fig. 2.4.

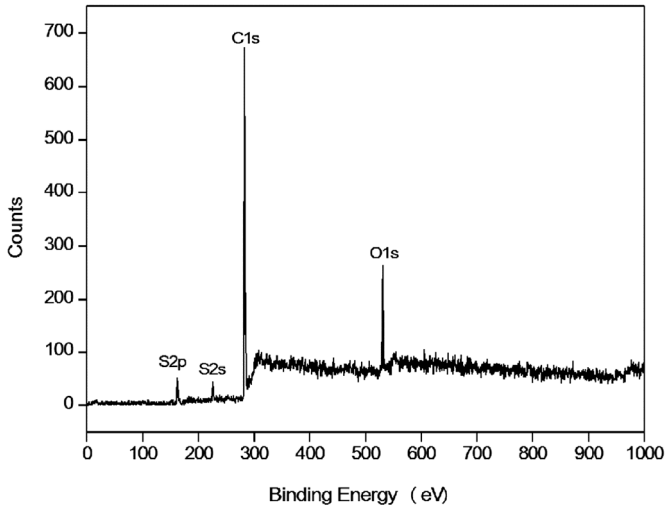

Fig. 2.4: XPS survey scan of P(EDOT-FL).

XPS survey scans of the copolymer revealed the presence of C, O, S as the characteristic elements of the co-monomers. As seen from the Fig. 2.5, the C-C and C-H functional groups are centered at 282.51 eV and C-S and C-O bonds of EDOT moiety were revealed at 284.09 and 285.0 eV,

respectively.[67] The results obtained from XPS of P(EDOT-FL) are in good agreement with those corresponding to FT-IR and ^{1}H NMR.

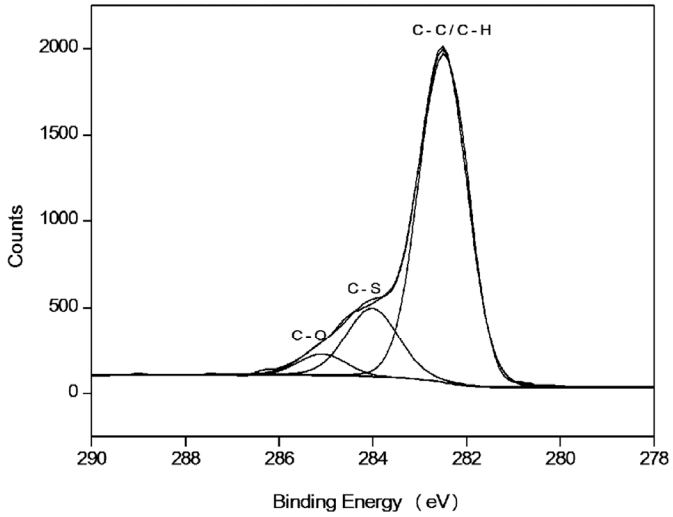

Fig. 2.5: XPS C1s high- resolution spectra of P(EDOT-FL).

2.2.3. Thermal Properties of P(EDOT-FL)

Thermal properties of the copolymer P(EDOT-FL) was investigated by both TG and DSC analysis. Fig. 2.6 shows the TG, DTG and DSC (insert figure) traces of (PEDOT-FL). In TGA of the copolymer there is an exotherm coincident with mass loss due to decomposition under nitrogen atmosphere. Decomposition onset was defined as a mass loss of 5 %. The peak decomposition temperature was defined as the first inflection point in the thermogravimetric curve, corresponding to peak in the derivative of TG data. On the basis of TGA exotherm, the onset of degradation and degradation temperature were 354 and 430 ^{o}C, respectively.

As revealed by TGA, the polymer exhibited excellent thermal stability, which is higher than that of polyfluorene degradation temperature

(400 ^{o}C) implying that the polyfluorene backbone has become more rigid upon the incorporation of EDOT units in the copolymer.[68] This is possibly because of the fact that EDOT groups encourage stronger inter chain vander Waals bonding. The glass transition temperature (T_g) estimated from DSC trace was 123 ^{o}C, which is higher than that of polyfluorene with 67 ^{o}C.[68] These results allow for the use of high temperature sealing procedures in device fabrication.

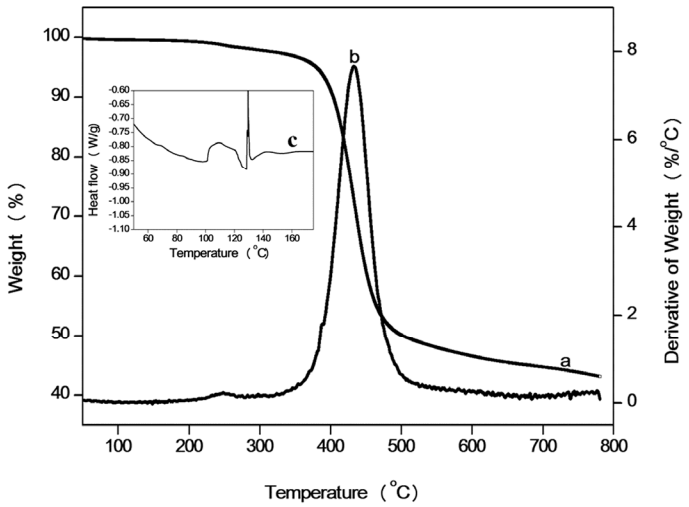

Fig. 2.6: (a) TG, (b) DTG, and (c) DSC (insert figure) traces of P(EDOT-FL).

2.2.4. Optical and electrochemical properties and band gap evaluation

Absorption spectra of the copolymer P(EDOT-FL) in THF and in spin coated films are shown in Fig. 2.7. In the absorption spectrum, the band with absorption maximum below 350 nm is due to π-π* transition of the backbone and the peak at longest wavelength is attributed to the intermolecular charge transfer (ICT) band. As seen from the Fig. 2.7, the optical absorption edges of the copolymer P(EDOT-FL) in solution was 540 nm from which the optical band gap (E_g^{opt}) was calculated to be 2.29 eV (from the onset of low

energy transition). Meanwhile, the absorption edges of the polymer in thin film form was 586 nm for P(EDOT-FL), from which E_g^{opt} was calculated to be 2.12 eV. Thus ICT band edge is red shifted by 46 nm compared to P(EDOT-FL) in solution. Significant red shift of the ICT band in the film state than in the solution indicates the presence of strong dipole-dipole interactions of this polymer in solid state. This is attributable to small permanent dipole moment in the film, which does a major role in solid-state packing in the polymer. As expected, P(EDOT-FL) exhibited low band gap compared to polyfluorene.[34,35] This difference reflects the strong donor property of the EDOT moieties, which raises the HOMO level and decreases the LUMO level, leading to low band gap. This finding is also consistent with previous reports.[40] This E_g^{opt} values agree well with theoretical values obtained by DFT/LSDA/6-31G than those obtained by DFT/B3LYP/6-31G and DFT/HSE06/6-31G calculation. To improve the efficiency of P(EDOT-FL) devices, the concept of bulk heterojunction was introduced, in which the interfacial area between the donor and acceptor was increased. Here an n-type material having high electron affinity, $PC_{61}BM$ was used as strong acceptor. Optical properties of P(EDOT-FL):$PC_{61}BM$ (1:1) blend was studied both in solution and in the solid state. P(EDOT-FL) exhibits similar absorption spectral features both in pristine films and in blend films, but a red shift towards longer wavelength (at 605 nm) was revealed due to polaron formation or inter molecular charge transition between P(EDOT-FL) and $PC_{61}BM$. This reveals that the molecular organization of P(EDOT-FL) was kept unchanged in the blend films. The λ_{max} of P(EDOT-FL) in blend with $PC_{61}BM$ was also improved for 1:1 ratio, i.e., an increase from 444 nm to 455 nm. The presence of EDOT units led to

more structured material through S-O interaction, which permits to obtain more planar chains and thus more structured materials even in the presence of $PC_{61}BM$.

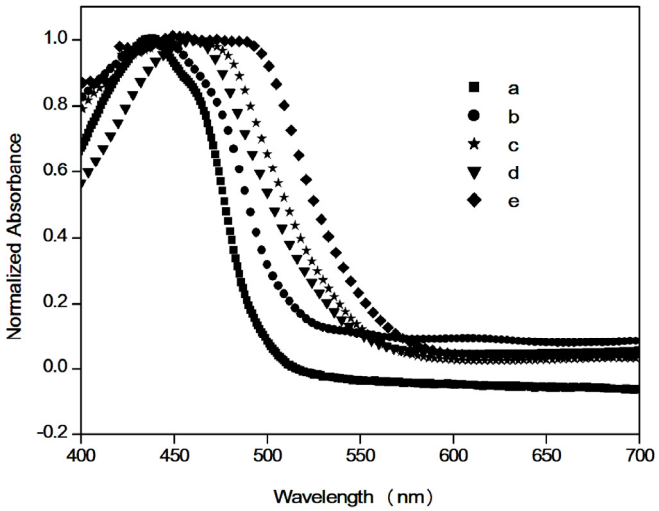

Fig. 2.7: Absorption spectra of (a) P(EDOT-FL) in solution, (b) P(EDOT-FL) as film, c) P(EDOT-FL):$PC_{61}BM$ (1:1) as film, (d) P(EDOT-FL):$PC_{61}BM$ (1:2) in solution, and (e) P(EDOT-FL):$PC_{61}BM$ (1:2) as film.

Electrochemical methods provide an excellent means of establishing HOMO and LUMO energies. Electrochemical properties of the P(EDOT-FL) was investigated by cyclic voltammetry (CV) and differential pulse voltammetry (DPV) (Fig. 2.8). CV and DPV were performed in a solution of Bu_4NPF_6 (0.1 M) in dry acetonitrile at 100 mV/s under nitrogen atmosphere. The setup was a three-electrode configuration with a Ag/Ag^+ reference electrode, a platinum button electrode (0.08 cm^2) coated with the thin copolymer film as working electrode, and a platinum wire as counter electrode.

HOMO level of the P(EDOT-FL) was calculated using the formula, HOMO = - $(4.4+E_{ox}^{onset})$ eV and LUMO level was estimated using the

optical band gap. The values are -5.19 eV and -2.9 eV, respectively. Moreover, from DPV, HOMO and LUMO was calculated to be -5.14 eV and -2.86 eV, respectively. The DPV estimated HOMO-LUMO levels were found to be lower than those determined by CV.

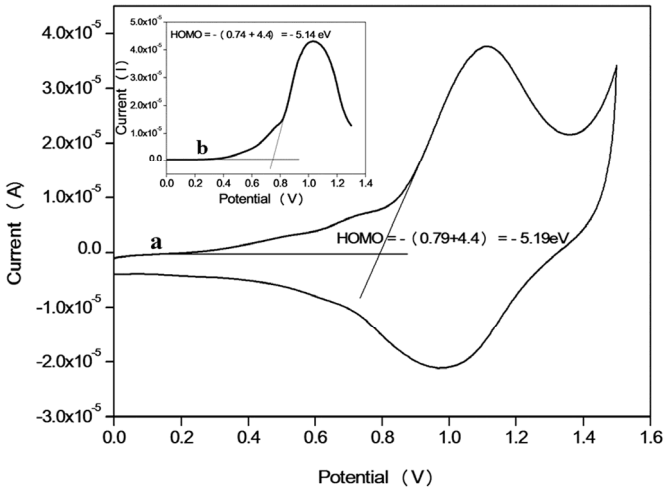

Fig. 2.8: CV (a) and DPV (insert picture) (b) curves of P(EDOT-FL) film on Pt electrode in 0.1 M Bu_4NPF_6 solution in acetonitrile at a scan rate of 100 mV/sec.

This may be due to reduced background current in DPV and sharper redox onset compared to the CV. In conclusion, incorporation of EDOT unit to the P(EDOT-FL) chain effectively increases the HOMO level and reduces the LUMO level of the polymer, because of more planar structure and conjugation.

2.2.5. Photoluminescence properties

The photoluminescence spectrum (PL) of the P(EDOT-FL) in dilute solution and as solid film ($PC_{61}BM$ blend) is shown in Fig. 2.9. The wavelength corresponding to the absorption maximum of each polymer was used as

excitation wavelength. The emission maximum of the P(EDOT-FL) occur at 514 nm. Before testing the photoconductivity of P(EDOT-FL) in blend with $PC_{61}BM$ in devices, fluorescence measurements were performed to examine the charge transfer efficiency from the copolymer (donor) to $PC_{61}BM$ (acceptor). There is a drastic decrease in PL emission of P(EDOT-FL) after the incorporation of $PC_{61}BM$. Poor PL efficiency could be attributed to the increase in intermolecular charge transfer between the polymer matrix and $PC_{61}BM$ units. The significant fluorescence quenching is a strong evidence to the efficient charge transfer from the photoexcited P(EDOT-FL) conjugated backbone to $PC_{61}BM$ and thus this system can be used in photoconductive applications.

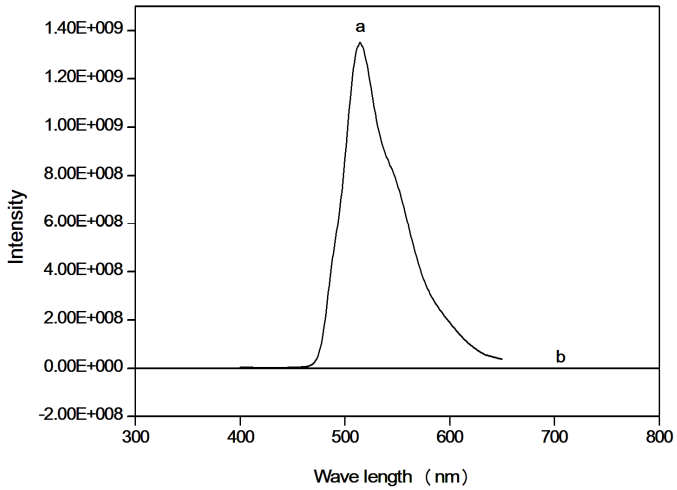

Fig. 2.9: PL spectra of the polymer (a) P(EDOT-FL) in solution (1:0) and (b) P(EDOT-FL):$PC_{61}BM$ (1:1) as blend film.

2.2.6. Photoconductivity

Heterojunction photoconductive device was fabricated using the P(EDOT-FL) as the electron donor and $PC_{61}BM$ as the electron acceptor.

The energy diagram presented in Fig. 2.10 shows the potential of P(EDOT-FL) to serve as appropriate host for $PC_{61}BM$ and hence efficient charge transfer and better photoconductivity. In this device, the donor and acceptor materials are mixed together and excitons can easily access the donor-acceptor interface and dissociate to free charge carriers.[69,70] From the theoretical as well as experimental data, it was found that the polymer P(EDOT-FL) has narrow band gap which is very much suitable for photoconductive application. Hence devices were fabricated with a typical sandwich structure of glass/ITO/(PEDOT-FL):$PC_{61}BM$/Ag and the steady state photocurrent measurements were performed using Keithly-236 Source Measure Unit.

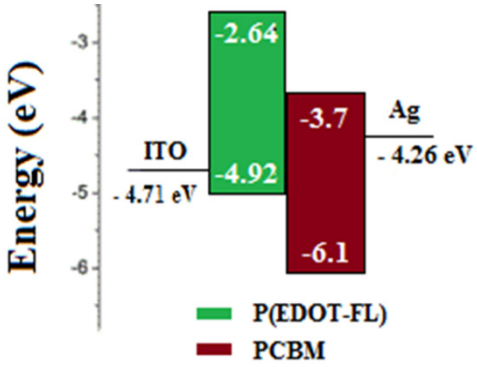

Fig. 2.10: Energy level diagram of P(EDOT-FL) and $PC_{61}BM$ blend in comparison with work functions of common electrodes used in the device.

Photocurrent measurement in the steady state involves measuring the steady state DC current through the sandwich cell with and without light. For this, DC voltage was applied to the sandwich cell which was kept in the dark and the resulting current was measured with respect to time. After the dark current through the cell was stabilized, light was allowed to fall on the ITO surface. Due to the photoinduced change in conductivity, the current increased suddenly and reached a steady state. If 'I_D' and 'I_L' are the steady

state current values, prior to illumination and after illumination respectively, the photosensitivity of the polymer device can be written as,

$$I_{ph} = \frac{(I_L - I_D)}{I_D} \quad \text{..... (1)}$$

Under dark conditions, the P(EDOT-FL):$PC_{61}BM$ device produced a very low current (10^{-11} A), meaning an "off" state with a very low concentration of charge carriers. But after the exposure to a pulsed light, the charge transfer process from the donor to acceptor led to high photoconductivity in P(EDOT-FL):$PC_{61}BM$ without any thermal treatment and photosensitivity obtained was found to be 415 at an applied field of 3.75 V/μm and laser power density of 10 mW/cm^2. Indeed, the alternative D-A arrangement ensures a stable CT and avoids phase separation and resulting in good photoconductivity. On further increasing the $PC_{61}BM$ content (1:2) in the polymer blends led to significant decrease of film quality and thereby photosensitivity.

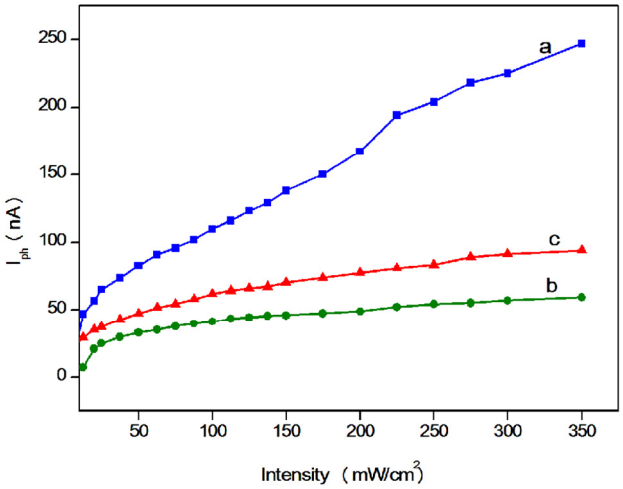

Fig. 2.11: Intensity dependence of photocurrent of P(EDOT-FL) blend at 3 photon energy values (a) 488 nm, (b) 532 nm, and (c) 632 nm (at an applied field of 3.75 V/μm).

Dependence of photocurrent on intensity of illumination was studied at three different photon energies in blend film and is shown in Fig. 2.11. The intensity of the laser beam was varied using a polarizer. The sample exhibited a good photo response at 488 nm. Electric field dependence of photoconductivity at 488 nm was also investigated (Fig. 2.12).

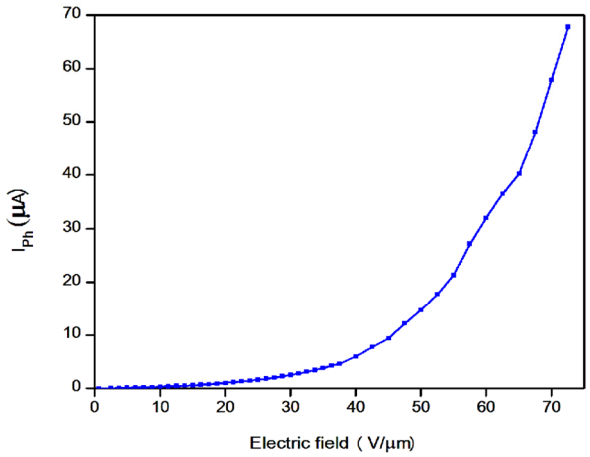

Fig. 2.12: Electric field dependence of photocurrent of blend film at 5 mW/cm^2.

Generally, in organic semiconductors, photoconductivity is not through a direct generation of carriers, but through the formation and subsequent dissociation of an exciton. The exciton can dissociate at impurity sites, interfaces with asymmetric ionization potentials or it can be dissociated by a strong electric field.[71,72] The photogenerated carrier move within the transporting medium in the general direction of the applied electric field. Field dependences of photogeneration quantum yields of charge carriers in films of amorphous molecular semiconductors at high external electric field strengths cannot be always explained in terms of the Onsager or the Poole-Frenkel model. It is expected that an external electric field shifts the electron

density in molecules from its equilibrium distribution, thus altering the probability of electronic transitions resulting in changes not only in intermolecular electronic transitions but also in probabilities of intramolecular transitions.[73] As seen in Fig. 2.12, it is observed that the films can withstand upto an electric field of 75 V/μm and the photosensitivity at higher electric fields was even greater than two lakh (at 75 V/μm, the photosensitivity is 2,89,742). At higher electric fields, the photocurrent was of the order of micro ampere range and showed a steep increase in the current with respect to field. The photogeneration efficiency for carrier generation is strongly dependent on applied field, since; polymers have a low dielectric constant.[74] The sensitivity of the polymer to light, expressed as photoconductive sensitivity, i.e., the photoconductivity per unit light intensity, can be calculated as,

$$\sigma/I = \frac{i_{ph}\, d}{PV} \quad \text{..... (2)}$$

where, 'σ' is the photoconductivity, 'I' is the light intensity, 'i_{ph}' is the photocurrent, 'P' is the laser power, 'd' is the thickness and 'V' is the applied voltage. At 10 V/μm, for 488 nm, the photoconductive sensitivity was calculated to be 7.6×10^{-10} $ScmW^{-1}$, which is significantly higher than other polymer systems such as polybenzoxazine-C_{60}[75] and PVK:TNF:DANS.[76] This photoconductive sensitivity is sufficiently high for photorefractive effect.

2.2.7. Non-linear optical properties

The third-order NLO properties of P(EDOT-FL) was investigated using z-scan technique,[77] which was distinguished for its simplicity and

sensitivity. The open-aperture (OA) z-scan trace of P(EDOT-FL) in dilute $CHCl_3$ (a) and as thin film (b) is shown in Fig. 2.13.

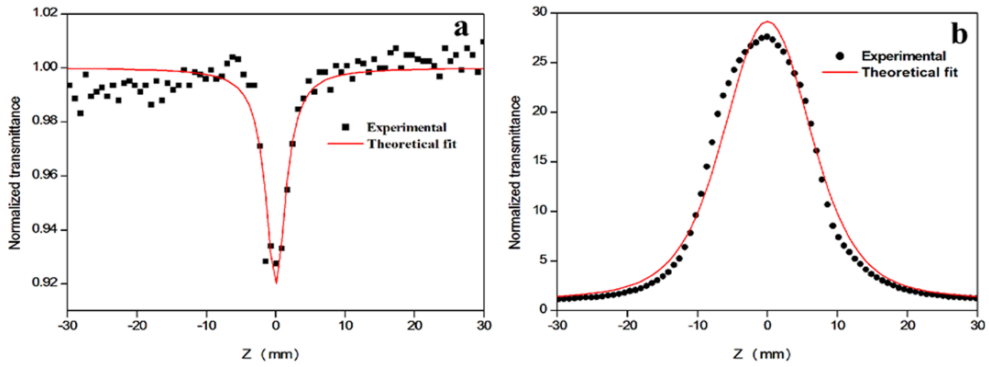

Fig. 2.13: Open aperture z-scan traces of P(EDOT-FL) (a) in solution and (b) as film at 112 µJ.

In solution phase, the P(EDOT-FL) shows a normalized valley, indicating that polymer is behaving as reverse saturation absorber (RSA) with a positive NLO absorption coefficient. However, in film phase the copolymer is behaving as a saturation absorber (SA). This is due to ground state band bleaching in film phase,[78] i.e., the excited state absorption and free carrier absorption leading to ground state band bleaching in the polymer. The non-linear absorption of the copolymer was fitting well by two photon absorption (TPA). The non-linear absorption coefficient, β is obtained by fitting the experimental scan plot of the OA measurement to equation (3):[77]

$$T(z)=\frac{C}{q_0\sqrt{\pi}}\int_{-\infty}^{\infty}\ln(1+q_0\,e^{-t^2})\,dt \quad \text{..... (3)}$$

where, $q_{0(z,r,t)}=\beta I_0(t)L_{eff}$ and $L_{eff}=\left(1-e^{-\alpha l}\right)/\alpha$ is the effective thickness with linear absorption coefficient α, and 'I'_0 is the irradiance at focus. The

solid curves in Fig. 2.13 are the theoretical fit to the experimental data. The imaginary part of the third-order susceptibility is given by equation (4):[77]

$$I_m \chi^{(3)} = \frac{n_0^2 c^2 \beta}{(240\pi^2 \omega)} \quad \text{..... (4)}$$

where, $n_0 = 1.45$ is the linear refractive index of the polymer solution, 'c' is the velocity of light in vacuum, 'ω' is the angular frequency of radiation used.

In order to determine the sign and magnitude of non-linear refraction (NLR) property of P(EDOT-FL), closed-aperture (CA) z-scan technique was performed by placing an aperture in front of the detector. The NLR z-scan curve after excluding non-linear absorption effects was assessed from the ratio of CA normalized z-scan data to the corresponding normalized OA data. The normalized transmittance, T(z) for NLR is given by equation (5):[77]

$$T(z) = 1 - \frac{4x\Delta\Phi_0}{(x^2+9)(x^2+1)} \quad \text{..... (5)}$$

where, 'T(z)' is the normalized transmittance for the pure refractive non-linearity at different z, 'Φ_0' is on-axis non-linear phase shift and 'x' is given by z/z_0. The CA trace of P(EDOT-FL) is shown in Fig. 2.14. The polymer exhibits peak-valley characteristics, indicating the negative NLR index due to self-defocusing. The non-linear refractive index (n_2), the real parts of $\chi^{(3)}$ (Re $\chi^{(3)}$) and third-order non-linear susceptibility ($\chi^{(3)}$) are calculated by the following equations (6)-(8):[77]

$$n_2\,(esu) = \frac{cn_0}{40\pi}\gamma \quad \text{..... (6)}$$

$$\mathrm{Re}\,\chi^{(3)} = \frac{n_0\, n_2}{3\pi}(esu) \quad \text{..... (7)}$$

$$\chi^{(3)} = \mathrm{Re}\,\chi^{(3)} + i\,\mathrm{Im}\,\chi^{(3)} \quad \text{..... (8)}$$

where, 'γ' is the molecular cubic hyperpolarizability of the polymer which can be estimated through the following equations $\gamma = \frac{\Delta n_0}{I_0}$ and $\Delta n_0 = \frac{\Delta \Phi_0}{k\, L_{eff}}$ where, 'k' is wave vector.

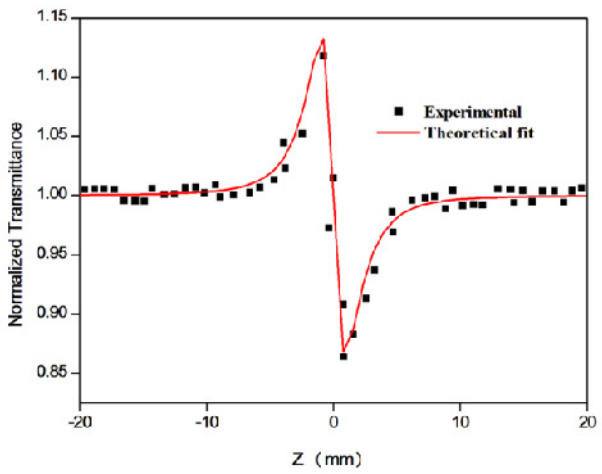

Fig. 2.14: Closed aperture z-scan trace of P(EDOT-FL) at 112 µJ.

The calculated values of non-linear absorption coefficient (β, m/W), the non-linear refraction coefficient (n_2, esu) and the third-order non-linear susceptibility ($\chi^{(3)}$, esu) are given in Table 2.2. The β value of P(EDOT-FL) is obtained to be 3.19×10^{-10} m/W. Furthermore, the $\chi^{(3)}$ value is found to be 1.25×10^{-11} esu. As expected, P(EDOT-FL) show large optical non-linearity, due to donor-acceptor scheme. Here, non-linearity is mainly due to the charge transfer from donor to acceptor unit, i.e., due to strong delocalization of π electrons.

Table 2.2: Calculated values of non-linear absorption, non-linear refraction, and non-linear susceptibility of P(EDOT-FL).

Copolymer	Non-linear absorption coefficient (β, m/W)	Non-linear refractive index (n_2, esu)	Imaginary part of non-linear susceptibility (Im $\chi^{(3)}$, esu)	Real part of non-linear susceptibility (Re $\chi^{(3)}$, esu)	Non-linear susceptibility ($\chi^{(3)}$, esu)
P(EDOT-FL)	3.19×10^{-10}	-0.68×10^{-10}	0.07×10^{-10}	-1.04×10^{-11}	1.25×10^{-11}

2.2.8. Optical power limiting

Optical limiters are materials in which they are transparent at low input fluences, but become opaque at high inputs,[79] due to enhanced absorption from the excited state or multiphoton absorption or both.[80] Such materials can be used for the protection of eyes and sensitive optical devices from laser induced damage. The criteria required for a good optical limiter are low limiting threshold, high linear transmittance throughout the sensor band width, stability etc. Optical limiting experiment was performed at 532 nm using OA z-scan technique. The optical limiting process has different origins, such as TPA, free carrier absorption, RSA, self-focusing, self-defocusing and induced scattering.[81] Fig. 2.15 shows the transmitted energy of P(EDOT-FL) as a function of input fluence. From the figure, it could be seen that, at low input fluence, the output varies linearly with input power. The deviation from linearity is noted as optical limiting threshold. Optical limiting threshold of P(EDOT-FL) is determined to be 0.47 GW/cm^2. The P(EDOT-FL) exhibits low limiting threshold due to the presence of donor-acceptor units in the polymer, i.e., due to the large variation in excited state dipole moment.

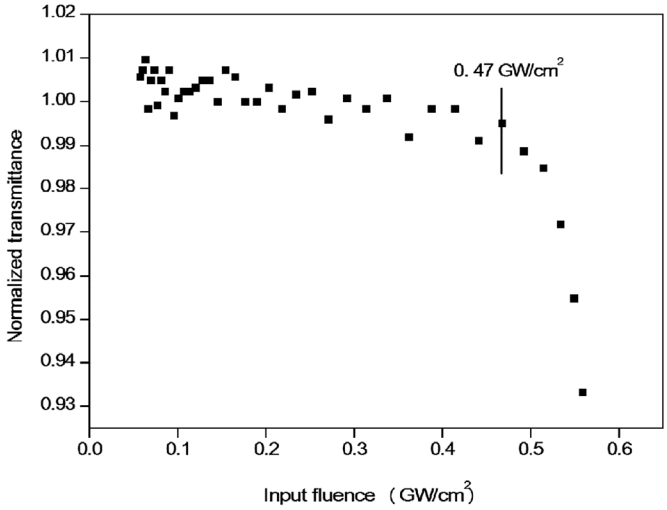

Fig. 2.15: Optical limiting curve of P(EDOT-FL).

2.3. Experimental Section

2.3.1. Materials

3,4-Ethylenedioxythiophene (EDOT, Aldrich, 98 %), 2,7-dibromofluorene (Aldrich, 97 %), magnesium sulphate (anhydrous) ($MgSO_4$, Spectrochem Pvt. Ltd.), tetrabutyl ammoniumbromide (TBAB, Avra Synthesis Pvt. Ltd., 98 %), sodium acetate (anhydrous) (Spectrochem Pvt. Ltd.), $PC_{61}BM$ (Solenne BV, >99 %), potassium hydroxide (KOH, Spectrochem Pvt. Ltd.), palladium (II) acetate ($Pd(OAc)_2$, Aldrich, 99.98%), tetrabutylammonium hexafluorophosphate (Bu_4NPF_6, Aldrich, > 99 %), and 1-bromooctane (Avra Synthesis Pvt. Ltd., 98 %) were used as received. Acetonitrile HPLC grade (Aldrich), dimethyl acetamide (anhydrous) (DMAc, Spectrochem Pvt. Ltd.), chloroform ($CHCl_3$, Spectrochem Pvt. Ltd.), dimethyl sulphoxide (DMSO, Spectrochem Pvt. Ltd.), dicholoromethane (DCM, Spectrochem Pvt. Ltd.), tetrahydrofuran HPLC grade (THF, Spectrochem Pvt. Ltd.), dichlorobenzene (Spectrochem Pvt. Ltd.) and methanol (anhydrous) (MeOH, Spectrochem Pvt. Ltd.) were dried and distilled when necessary according to standard procedures.

2.3.2. Synthesis Methods

2.3.2.1. *Synthesis of 2,7-dibromo-9,9-dioctylfluorene (I)*

In a three necked round bottom flask, KOH (8.0 g) was dissolved in 100 mL DMSO and degassed under N_2. After degassing, 2,7-dibromofluorene (1.03 g, 6.77 mmol) and TBAB (1.0 g, 3.08 mmol) were added to the stirred solution and kept for 30 min. 1-bromooctane was added in small portions under stirring and, the reaction was allowed to proceed for 24 h at 80 ^oC. The solution was cooled and poured into distilled water. The organic layer was extracted with DCM and solvent was removed under vacuum by rotary evaporation. Finally it was purified twice using chloroform and activated charcoal and washed with cold MeOH until pale yellow powder was obtained with 80 % yield.

M.P	:	62 ^oC (from chloroform)
^1H NMR (400 MHz, $CDCl_3$, δ)	:	0.40-0.60 (m, 4H), 0.70-0.92 (t, 6H), 1.02-1.25 (m, 20H), 1.85-1.91 (m, 4H), 7.41-7.48 (3d, 6H).

2.3.2.2. *Synthesis of Poly(2,5-(3,4-ethylenedioxythiophene)-alt-2,7-(9,9-dioctylfluorene))*

To a stirred solution of EDOT (0.024 g, 0.17 mmol) in 10 mL DMAc was added TBAB (0.05 g, 0.17 mmol) and sodium acetate (0.05 g, 0.68 mmol). The reaction mixture was stirred at room temperature for 30 min followed by addition of 2,7-dibromo-9,9-dioctylfluorene (0.1 g, 0.17 mmol) and 10 % palladium acetate (0.003 g). The reaction mixture was stirred at 90 ^oC for 48 h. The mixture was cooled to room temperature and poured in to methanol (20 mL). The precipitate was filtered and washed with methanol. The polymer was purified by soxhlet extraction using hexane and methanol

for 24 h. The residue was dissolved in minimum amount of $CHCl_3$ and precipitated using methanol and dried under vacuum.

Yield	:	61 %.
FT-IR (ν_{max}/cm^{-1})	:	2918s and 2852s (CH), 1086s and 1050w (CO), 1667br (conjugation).
^1H NMR (400 MHz, d8-THF, δ)	:	0.7-0.8 (m, 10H), 1.1-1.3 (m, 20H), 2.06 (br, 4H), 4.2-4.5 (m, 4H), 6.9-7.8 (m, 6H).

2.3.3. Instrumentation

^1H Nuclear magnetic resonance (^1H NMR) spectrum was recorded on JEOL, JNM-EX400, FT-NMR SYSTEM operating at 400 MHz and chemical shifts were quoted down field of TMS. Fourier transform Infra-Red (FT-IR) analysis was obtained from Perkin Elmer Spectrum 100, FT-IR Spectrometer. The copolymer was characterized by X-ray Photoelectron Spectroscopy (XPS) measurements (Kratos Analytical XPS), which was carried out using a monochromatic Al anode at energy of 40 eV. Gel permeation chromatography (GPC) was carried out with Waters GPC with THF as the eluent. All the electrochemical experiments were performed in dry acetonitrile with Bu_4NPF_6 (the supporting electrolyte) using BAS Epsilon Electrochemical analyser with quiet time of 2 sec and scan rate of 100 mV/s. Absorption spectra were recorded with Thermo Scientific, Evolution 201, Ultraviolet-Visible (UV–Visible) spectrophotometer. Fluorescence spectra were recorded with DT 1000CE, Fluorescence spectrophotometer and were corrected for the spectral response of the machine. Thermogravimetric measurements (TG and DTG) were performed on a TA Instrument Q 50

Thermogravimetric analyzer with a continuous nitrogen flow and a heating rate of 10 °C/min. Differential scanning calorimetry (DSC) was carried out on TA Instrument Q 100 with a continuous nitrogen flow and a heating rate of 2 °C/min. The steady state photocurrent measurements were done using Keithly-236 Source Measure Unit. He-Ne Laser (632.8 nm, Melles Griot), Diode Pumped Solid State Laser (532 nm, Coherent), and Optically Pumped Semiconductor Laser (488 nm, Coherent) were used as different laser sources.

2.3.4. Computation methods

To determine the lowest energy structure of the P(EDOT-FL) copolymer, a sequence of steps were followed involving quantum mechanical calculations, based on DFT methods. Initially, the ground state geometries of oligomers were optimized by means of the DFT at the B3LYP level of theory using 6-31G basis set. In order to correlate the experimental data with theory, DFT calculations at three different energy levels were carried out using B3LYP, HSE06 and LSDA on 6-31G basis set as implemented in Gaussian 09 package.[82] The periodic boundary condition was used to study the electronic properties of P(EDOT-FL) copolymer. The starting unit cell geometries for the PBC calculation was taken from the central portion of the optimized oligomer and optimized inside a given lattice length on the constraints of PBC by assuming that the unit cell is repeated identically an infinite number of times along the translation vector. In the main chain of the polymer, long alkyl groups have been replaced by methyl group to reduce the time of calculation and to avoid the frequently encountered convergence problems. It has been assumed that the presence of alkyl groups does not significantly affect the equilibrium geometry, and hence, the opto-electronic properties. Band structure in the positive region of the

first Brillouin zone (between k=0 and k=π/a) was plotted, i.e., the lowest 4 unoccupied and highest 4 occupied bands in the positive region of the first Brillouin zone were plotted.

2.3.5. Preparation of sandwich cells

For photoconductivity measurements, a device configuration consisting of glass/ITO/P(EDOT-FL):$PC_{61}BM$/Ag was used. The samples were prepared by spin coating of 5 wt% polymer solution (at 1:1 ratio) in dried spectroscopic grade chloroform onto ITO coated glass plates. The ITO layer had a thickness of 200 nm. The solution was filtered using a 0.45 μm PTFE filter prior to spin coating. After drying at room temperature for 12 h, the samples were transferred to a vacuum desiccator and kept for complete solvent removal. Thicknesses of the films were determined using a Dektak 6M Stylus profiler. The prepared films had a thickness of 800 nm. Finally, silver electrodes of area 2x2 mm^2 were vacuum deposited on to the films to complete the sandwich structure. The silver electrode had a thickness of 50 nm.

2.3.6. NLO Measurements

NLO measurements were performed by the single beam z-scan technique with nanosecond laser performed with a Q-switched Nd:YAG laser system (Spectra Physics LAB-1760) with pulse width of 7 ns at 10 Hz repetition rate and 532 nm wavelength. The sample was moved in the direction of light propagation near the focal spot of the lens with focal length of 200 mm. The radius of the beam waist was calculated to be 42.56 μm. The Rayleigh length, $Z_0 = \pi\omega_o^2/\lambda$, was calculated to be 10.69 mm, which was greater than the thickness of the sample cuvette (1 mm), an essential requirement for z-scan experiments. The z-scan system was calibrated using

CS_2 as the standard. The transmitted beam energy, reference beam energy and their ratios were measured simultaneously by an energy ratiometer (REj7620, Laser Probe Corp.) having two identical pyroelectric detector heads (Rjp 735). The effect of fluctuations of laser beam was eliminated by dividing the transmitted power by the power obtained at the reference detector; both being measured using identical photo detectors. The data were analysed according to the procedure described by Bahae *et al.*,[77] and the non-linear coefficients were obtained by fitting the experimental z-scan plot with the theoretical plots.

2.4. Conclusions

In summary, this chapter describes the synthesis and characterization of a copolymer containing fluorene and EDOT monomer units. The copolymer has been synthesized via direct arylation method. The optical, electrochemical, photoluminescence, photoconductive and third-order non-linear optical properties were evaluated. The copolymer revealed good thermal stability and amenable solubility. DFT computations have been performed for analysing the electronic properties and the band gap (E_g) of the P(EDOT-FL) was found to be 2.28 eV, using LSDA/6-31G level. The band gap of the copolymer was obtained to be 2.29 eV from the electronic absorption spectrum of copolymer which is in good agreement with theoretical band gap. Theoretical and experimental studies revealed that the copolymer film exhibited better properties than that of P(FL). Photocurrent measurements were done in the sandwich cell configuration as blend with $PC_{61}BM$ (1:1). Photoluminescence quenching and moderate photoconductive sensitivity (7.6×10^{-10} $ScmW^{-1}$) confirmed the suitability of the copolymer for fabricating

photoconductive devices. The third-order non-linear optical properties of P(EDOT-FL) was investigated by z-scan technique. The polymer showed negative non-linear refraction and switch over from RSA to SA behaviour was observed as the sample changed from the solution to the thin film. The non-linear absorption coefficient (β), the non-linear refraction coefficient (n_2), the third-order non-linear susceptibility ($\chi^{(3)}$) and the optical limiting threshold of the polymer were determined to be 3.19×10^{-10} m/W, -0.68×10^{-10} esu, 1.25×10^{-11} esu and 0.47 GW/cm^2, respectively.

References

[1] P. Dutta, H. Park, W. H. Lee, I. N. Kang, S. H. Lee, *Polym. Chem.,* 2014, 5, 132.

[2] C. -W. Ge, C. -Y. Mei, J. Ling, J. -T. Wang, F. -G. Zhao, L. Liang, H. -J. Li, Y. -S. Xie, W. -S. Li, *J. Polym. Sci., Part A: Polym. Chem.,* 2014, 52, 2356.

[3] W. Zhuang, M. Bolognesi, M. Seri, P. Henriksson, D. Gedefaw, R. Kroon, M. Jarvid, A. Lundin, E. Wang, M. Muccini, M. R. Andersson, *Macromolecules,* 2013, 46, 8488.

[4] J. Y. Ma, H. -J. Yun, S. -O. Kim, G. B. Lee, H. Cha, C. E. Park, S. -K. Kwon, Y. -H. Kim, *J. Polym. Sci., Part A: Polym. Chem.,* 2014, 52, 1306.

[5] A. Kraft, A. C. Grimsdale, A. B. Holmes, *Angew. Chem. Intl. Ed.,* 1998, 37, 402.

[6] N. R. Evans, L. S. Devi, C. S. K. Mak, S. E. Watkins, S. I. Pascu, A. Kohler, R. H. Friend, C. K. Williams, A. B. Holmes, *J. Am. Chem Soc.,* 2006, 128, 6647.

[7] Q. Huang, G. A. Evmenenko, P. Dutta, P. Lee, N. R. Armstrong, T. J. Marks, *J. Am. Chem. Soc*., 2005, 127, 10227.

[8] H. H. Fong, V. A. Pozdin, A. Amassian, G. G. Malliaras, D. M. Smilgies, M. He, S. Gasper, F. Zhang, M. Sorensen, *J. Am. Chem. Soc.,* 2008, 130, 13202.

[9] M. H. Hoang, M. J. Cho, D. C. Kim, K. H. Kim, J. W. Shin, M. Y. Cho, J. Joo, D. H. Choi, *Org. Electron.,* 2009, 10, 607.

[10] P. M. Beaujuge, W. Pisula, H. N. Tsao, S. Ellinger, K. Mullen, J. R. Reynolds, *J. Am. Chem. Soc*., 2009, 131, 7514.

[11] S. Pang, H. N. Tsao, X. Feng, K. Mullen, *Adv. Mater*., 2009, 21, 3488.

[12] H. H. Chang, C. E. Tsai, Y. Y. Lai, W. W. Liang, S. L. Hsu, C. S. Hsu, Y. J. Cheng, *Macromolecules,* 2013, 46, 7715.

[13] D. T. McQuade, A. E. Pullen, T. M. Swager, *Chem. Rev.,* 2000, 100, 2537.

[14] P. M. Beaujuge, C. M. Amb, J. R. Reynolds, *Acc. Chem. Res.,* 2010, 43, 1396.

[15] P. M. Beaujuge, J. R. Reynolds, *Chem. Rev.,* 2010, 110, 268.

[16] P. Shi, C. M. Amb, A. L. Dyer, J. R. Reynolds, *Appl. Mater. Interfaces,* 2012, 4, 6512.

[17] E. Kaya, A. Balan, D. Baran, A. Cirpan, *Org. Electron.,* 2011, 12, 202.

[18] P. Leriche, P. Frère, A. Cravino, O. Aleveque, J. Roncali, *J. Org. Chem.,* 2007, 72, 8332.

[19] M. Melucci, P. Frère, M. Allain, E. Levillain, G. Barbarella, J. Roncali, *Tetrahedron,* 2007, 63, 9774.

[20] J. Y. Balandier, F. Quist, C. Amato, S. Bouzakraoui, J. Cornil, S. Sergeyev, Y. Geerts, *Tetrahedron,* 2010, 66, 9560.

[21] L. B. Groenendaal, F. Jonas, D. Freitag, H. Pielartzik, J. R. Reynolds, *Adv. Mater.,* 2000, 12, 481.

[22] L. B. Groenedaal, G. Zotti, P. H. Aubert, S. M. Waybright, J. R. Reynolds, *Adv. Mater*., 2003, 15, 855.

[23] J. Roncali, P. Blanchard, P. Frere, *J. Mater. Chem.,* 2005, 15, 1589.

[24] C. B. Nielsen, A. Angerhofer, K. A. Abboud, J. R. Reynolds, *J. Am. Chem. Soc.,* 2008, 130, 9734.

[25] I. Schwendeman, C. L. Gaupp, J. M. Hancock, L. Groenendaal, J. R. Reynolds*, Adv. Funct. Mater.,* 2003, 13, 541.

[26] K. Krishnamoorthy, R. S. Gokhale, A. Q. Contractor, A. Kumar, *Chem. Commun*., 2004, 820.

[27] R. B. Bazaco, R. Gomez, C. Seoane, P. Baeuerle, J. L. Segura, *Tetrahedron Lett.,* 2009, 50, 4154.

[28] B. Winther-Jensen, O. Winther-Jensen, M. Forsyth, D. Macfarlane, *Science,* 2008, 321, 671.

[29] F. I. Wu, P. I. Shih, C. F. Shu, Y. L. Tung, Y. Chi, *Macromolecules,* 2005, 38, 9028.

[30] Y. Yang, Q. Pei, *J. Appl. Phys.,* 1997, 81, 3294.

[31] B. Liu, W. L. Yu, Y. H. Lai, W. Huang, *Chem. Mater.,* 2001, 13, 1984.

[32] O. Stephan, F. Tran-Van, C. Chevrot, *Synth. Met.,* 2002, 131, 31.

[33] L. Akcelrud, *Prog. Polym. Sci.,* 2003, 28, 875.

[34] W. C. Wu, C. L. Liu, W. C. Chen, *Polymer,* 2006, 47, 527.

[35] E. Bundgaard, F. C. Krebs, *Sol. Energy Mater. Sol. Cells.,* 2007, 91, 954.

[36] A. Cuendias, M. Urien, S. Lecommandoux, G. Wantz, E. Cloutet, H. Cramail, *Org. Electron*., 2006, 7, 576.

[37] C. B. Bezgin, A. Kivrak, M. A. Onal, *Electrochim. Acta,* 2011, 58, 223.

[38] S. M. Cassemiro, C. Zanlorenzi, T. D. Z. Atvars, G. Santos, F. J. Fonseca, L. Akcelrud, *J. Lumin*., 2013, 134, 670.

[39] P. Blondin, J. Bouchard, S. Beaupr, M. Bellete, G. Durocher, M. Leclerc, *Macromolecules,* 2000, 33, 5874.

[40] P. H. Aubert, M. Knipper, L. Groenendaal, L. Lutsen, J. Manca, D. Vanderzande, *Macromolecule*s, 2004, 37, 4087.

[41] B. Bezgin, A. Yagan, A. M. Onal, *J. Electroanal. Chem.,* 2009, 632, 143.

[42] B. Bezgin, A. M. Onal, *Electrochim. Acta,* 2010, 55, 779.

[43] G. Nie, H. Yang, J. Chen, Z. Bai*, Org. Electron*., 2012, 13, 2167.

[44] A. Kumar, A. Kumar, *Polym. Chem.,* 2010, 1, 286.

[45] K. Yamazaki, J. Kuwabara, T. Kanbara, *Macromol. Rapid Commun.,* 2013*,* 34*,* 69.

[46] J. Kuwabara, T. Yasuda, S. J. Choi, W. Lu, K. Yamazaki, S. Kagaya, L. Han T. Kanbara, *Adv. Funct. Mater*., 2014, DOI: 10.1002/adfm.201302851.

[47] Z. B. Liu, Y. F. Xu, X. Y. Zhang, X. L. Zhang, Y. S. Chen, J. G. Tian, *J. Phys. Chem. B*., 2009, 113, 9681.

[48] K. Yoneda, M. Nakano, R. Kishi, H. Takahashi, A. Shimizu, T. Kubo, K. Kamada, K. Ohta, B. Champagne, E. Botek, *Chem. Phys. Lett.*, 2009, 480, 278.

[49] E. Hendry, P. Hale, J. Moger, A. Savchenko, S. A. Mikhailov, *Phys. Rev. Lett.,* 2010, 105, 97401.

[50] L. Kamath, K. B. Manjunatha, S. Shettigar, G. Umesh, B. Narayana, S. Samshuddin, B. K. Sarojini, *Optics & Laser Technology*, 2014, 56, 425.

[51] R. G. Parr, W. Yang, Density-Functional Theory of Atoms and Molecules, Oxford University Press, New York, 1989.

[52] A. D. Becke, *J. Chem. Phys*.,1993, 98, 5648.

[53] C. Lee, W. Yang, R. G. Parr, *Phys. Rev. B.,* 1994, 37, 785.

[54] K. Burke, J. P. Perdew, Y. Wang, J. F. Dobson, G. Vignale, M. P. Das*,* Electronic Density Functional Theory: Recent Progress and New Directions, Plenum Press, New York, 1998.

[55] J. Heyd, G. E. Scuseria, M. Ernzerhof, *J. Chem. Phys.,* 2003, 118, 8207.

[56] A. V. Krukau, O. A. Vydrov, A. F. Izmaylov, G. E. Scuseria, *J. Chem. Phys*., 2006, 125, 224106.

[57] S. H. Vosko, L. Wilk, M. Nusair, *Can. J. Phys*., 1980, 58, 1200.

[58] U. Salzner, J. B. Lagowski, P. G. Pickup, R. A. Poirier, *J. Comp. Chem.,* 1997, 18, 1943.

[59] P. Feibelman, *J. Phys. Rev. B*., 1987, 35, 2626.

[60] J. E. Jaffe, A. C. Hess, *J. Chem. Phys*., 1996, 105, 10983.

[61] S. Hirata, S. Iwata, *J. Chem. Phys*., 1997, 107, 10075.

[62] J. Q. Sun, R. J. Bartlett, *J. Chem. Phys.,* 1998, 109, 4209.

[63] S. G. Im, K. K. Gleason, E. A. Olivetti, *Appl. Phys. Lett.,* 2007, 90, 152112.

[64] C. Kvarnstrom, H. Neugebauer, S. Blomquist, H. J. Ahonen, J. Kankare, A. Ivaska, *Electrochim. Acta,* 1999, 44, 2739.

[65] A. Yildirima, S. Tarkuc, M. Ak, L. Toppare, *Electrochim. Acta,* 2008, 53, 4875.

[66] G. Nie, H. Yang, J. Chen, Z. Bai, *Org. Electron.,* 2012, 13, 2167.

[67] D. Bhattacharyya, K. K. Gleason, *Chem. Mater.,* 2011, 23, 2600.

[68] W. C. Wu, C. L. Liu, W. C. Chen, *Polymer,* 2006, 47, 527.

[69] M. Hiramoto, H. Fujiwara, M. Yokoyama, *J. Appl. Phys.,* 1992, 72, 3781.

[70] T. Taima, M. Chikamatsu, Y. Yoshida, K. Saito, K. Yase, *Appl. Phys. Lett*., 2004, 85, 6412.

[71] V. I. Arkhipov, H. BÄassler, M. Deussen, E. O. GÄobel, R. Kersting, H. Kurz, U. Lemmer, R. F. Mahrt, *Phys. Rev. B*., 1995, 52, 4932.

[72] V. I. Arkhipov, H. BÄassler, *Phys. Stat. Sol*., 2004, 201, 1152.

[73] N. A. Davidenko, M. A. Zabolotny, A. A. Ishchenko, N. G. Kuvshinskii, N. P. Borolina, *High Energ. Chem.,* 2004, 38, 13.

[74] L. Onsagar, *Phys. Rev*., 1938, 54, 554.

[75] V. C. Kishore, Ph. D. thesis, Cochin University of Science and Technology (India), 2008.

[76] D. Shuo-xing, Z. Jia-zen, Ye-Pei-xian, H. Hai-ping, Y. Cheng, *Acta Physica*, 1995, 4, 663.

[77] M. S. -bahae, A. A. Said, T. -H Wei, D. J. Hagan, E. W. Van Stryland, *IEEE Journal of Quantum Electronics*, 1990, 26, 760.

[78] A. Thankappan, S. Thomas, V. P. N. Nampoori, *Optics & Laser Technology*, 2014, 58, 63.

[79] G. S. He, G. C. Xu, P. N. Prasad, B. A. Reinhardt, J. C. Bhatt, A. G. Dillard, *Opt. Lett*., 1995, 20, 35.

[80] N. K. M. N. Srinivas, S. V. Rao, D. N. Rao, *J. Opt. Soc. Am.* B, 2003, 20, 2470.

[81] R. L. Sutherland, Handbook of non-linear optics, New York, Dekker, 1996.

[82] Gaussian 09, Revision B02, M. J. Frisch, G. W. Trucks, H. B. Schlegel, G. E. Scuseria, M. A. Robb, J. R. Cheeseman, G. Scalmani, V. Barone, B. Mennucci, G. A. Petersson, H. Nakatsuji, M. Caricato, X. Li, H. P. Hratchian, A. F. Izmaylov, J. Bloino, G. Zheng, J. L. Sonnenberg, M. Hada, M. Ehara, K. Toyota, R. Fukuda, J. Hasegawa, M. Ishida, T. Nakajima, Y. Honda, O. Kitao, H. Nakai, T. Vreven, Jr. J. A. Montgomery, J. E. Peralta, F. Ogliaro, M. Bearpark, J. J. Heyd, E. Brothers, K. N. Kudin, V. N. Staroverov, R. Kobayashi, J. Normand, K. Raghavachari, A. Rendell, J. C. Burant, S. S. Iyengar, J. Tomasi, M. Cossi, N. Rega, N. J. Millam, M. Klene, J. E. Knox, J. B. Cross, V. Bakken, C. Adamo, J. Jaramillo, R. Gomperts, R. E. Stratmann, O. Yazyev, A. J. Austin, R. Cammi, C. Pomelli, J. W. Ochterski, R. L. Martin, K. Morokuma, V. G. Zakrzewski, G. A. Voth, P. Salvador, J. J. Dannenberg, S. Dapprich, A. D. Daniels, Ö. Farkas, J. B. Foresman, J. V. Ortiz, J. Cioslowski, D. J. Fox, Gaussian, Inc., Wallingford CT, 2009.

.....ooo.....

Chapter 3

Design, Synthesis and Third-order Non-linear Optical Properties of EDOT-Chalcogenadiazole Donor-Acceptor Copolymers via Direct Arylation Method*

Abstract

Two 3,4-ethylenedioxythiophene (EDOT) based low band gap donor-acceptor (D-A) conjugated copolymers were designed and synthesized via direct arylation, in which the HOMO-LUMO gaps were fine-tuned by the regular insertion of electron deficient units, 2,1,3-benzothiadiazole (BTZ) and 2,1,3-benzoselenadiazole (BTSe), respectively. Structural characterization was performed by FT-IR, ^1H NMR and XPS. In order to investigate the variation in energy band structure of the copolymers, quantum-chemical calculation using DFT theory was carried out. The alternating insertion of chalcogenadiazole unit in the PEDOT (poly(3,4-ethylenedioxythiophene)) lowers the HOMO and LUMO energy levels. As a result, polymers with low band gap compared to that of the homopolymer, PEDOT was obtained. Present experimental results correlate with HSE06 level theoretical calculations than those with B3LYP level. z-scan experiments reveal that the copolymers exhibit strong non-linear absorption coefficient and non-linear refraction coefficient of the order 10^{-10} esu and the third-order non-linear susceptibility is of the order of 10^{-11} esu. These findings indicated that the EDOT-chalcogenadiazole copolymers can be developed into excellent third-order non-linear optical material.

* Third-order non-linear optical properties of 3,4-ethylenedioxythiophene copolymers with chalcogenadiazole acceptors, Sona Narayanan, Sreejesh Poikavila Raghunathan, Aby Cheruvathoor Poulose, Sebastian Mathew, Krishnapillai Sreekumar, Cheranellore Sudha Kartha, Rani Joseph, New Journal of Chemistry, 2015, DOI: 10.1039/c4nj01899k.

3.1. Introduction

Conjugated polymers with donor-acceptor architecture have been widely investigated in photovoltaic devices,[1-5] electrochromic devices,[6-8] and in light emitting diodes (LEDs),[9-10] owing to their better electron-hole affinities and intramolecular charge transfer properties. Till date, one of the best strategies to design narrow band gap polymers is the synthesis of an alternating polymer containing electron rich (donor) and electron deficient (acceptor) unit in the polyconjugated backbone there by allowing intramolecular charge transfer. Among the conjugated polymers, EDOT based polymers continue to fascinate many researchers due to their several advantages such as low ionization potential, high conductivity and good environmental stability.[11,12] EDOT is a good electron donor as it shows relatively high energy HOMO levels and small steric interaction between the repeating units. By copolymerizing with different electron acceptors it gives low band gap polymers with good conductivity and high stability. EDOT based low band gap conjugated polymers with alternate donor-acceptor structures in the main chain have been intensively studied in several reports.[13-16] Besides, there are several reports on polycondensation of EDOT via direct arylation.[17-21] Here we have focused on the alternate donor-acceptor copolymers bearing EDOT, as their electronic properties can be tuned efficiently by varying the acceptor moieties and a broadening of absorption spectrum can be resulted. The interaction between the electron donor (D) and acceptor (A) moieties in an alternating D-A copolymer can lead to the hybridization of the high-lying HOMO energy level of the donor and low-lying energy level of the acceptor, leading to a relatively small band gap polymer with novel electronic structure and ambipolar charge transport properties.[22]

Recently, π conjugated polymers bearing the benzothiadiazole (BTZ) unit have received great deal of interest because of their potential applications in optoelectronic devices.[23] The BTZ moiety ensures strong electron injection or transporting properties and wide visible light absorption in copolymers. Within the chalcogenadiazole family of charge transfer materials, replacement of sulphur atom by selenium raises the dimensionality and conductivity of the materials, because of strong intermolecular interaction between Se atoms and greater stabilization effect towards radical cations.[24,25] Based on this idea, we have investigated the effect of introduction of two chalcogenadiazoles, 2,1,3-benzothiadiazole and 2,1,3-benzoselenadiazole (BTSe) in to the PEDOT backbone, keeping in mind the higher acceptor strength of the BTSe unit than the BTZ unit. In this chapter, the electronic properties of EDOT based D-A π conjugated polymers containing BTZ and BTSe moieties have been investigated, both theoretically and experimentally. BTZ and BTSe units can serve as electron accepting units, owing to the presence of two electron withdrawing imine (C=N) nitrogens. Here, we discuss the effect of BTZ and BTSe units as electron accepting moieties and the influence of replacement of sulphur atom in the BTZ unit with selenium by comparing the HOMO and LUMO energy levels. In recent years, organic photonic materials possessing large non-linear optical (NLO) properties are the subject of current research interest, owing to their potential applications in a wide variety of optoelectronic and photonic devices.[26,27] Conjugated structures with donor-acceptor groups have been studied by several researchers.[28-32] However, there have been only a few reports on the third-order non-linear properties of the polymers.[33-35] Nevertheless, the organic NLO materials possess large third order susceptibility, fast response time and processability.[36,37]

This in turn attracted our interest in investigating non-linear optical properties of donor-acceptor copolymers. Therefore, third-order non-linearity of the EDOT-chalcogenadiazole copolymers has been investigated using z-scan method. This is for the first time a synthesis via direct arylation is being discussed; followed by electrochemistry, optical, thermal and third-order non-linear optical properties.

3.2. Results & Discussion

3.2.1. Theoretical calculation of electronic structure of conjugated polymers

To understand the electronic structure of P(EDOT-BTZ) and P(EDOT-BTSe) copolymers, theoretical calculations were performed by hybrid density functional theory (DFT)[38] using B3LYP (Becke, three parameter, Lee-Yang-Parr)[39-41]/6-31G level and HSE06 (Heyd-Scuseria-Ernzerhof functional)[42]/6-31G level.

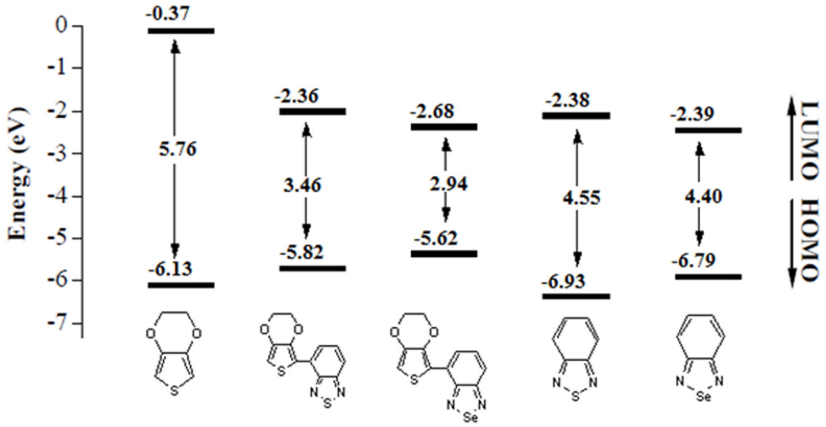

Fig. 3.1: Energy levels of EDOT, EDOT-BTZ, EDOT-BTSe, BTZ and BTSe.

These are computationally cost effective procedures to calculate the electronic structure with a good approximation and enable elimination of

unsuitable materials before synthesis Before proceeding to evaluate the electronic structure of the polymers, the ground state geometries of oligomers were optimized by means of DFT at the B3LYP level of theory using 6-31G basis set and the results are summarized in Fig. 3.1.

The relative ordering of occupied and virtual orbitals provides reasonable qualitative information regarding the excitation properties[43] and ability of electron/hole transport. The HOMO/LUMO energy levels describes electron or hole transporting capacity. As EDOT is copolymerized with chalcogenadiazole moieties, HOMOs are elevated, and the LUMOs are lowered, which facilitates electron and hole transport. The electron density isocontours of HOMO and LUMO of the model compounds in P(EDOT-BTZ) and P(EDOT-BTSe) by B3LYP/6-31G levels are plotted in Fig. 3.2.

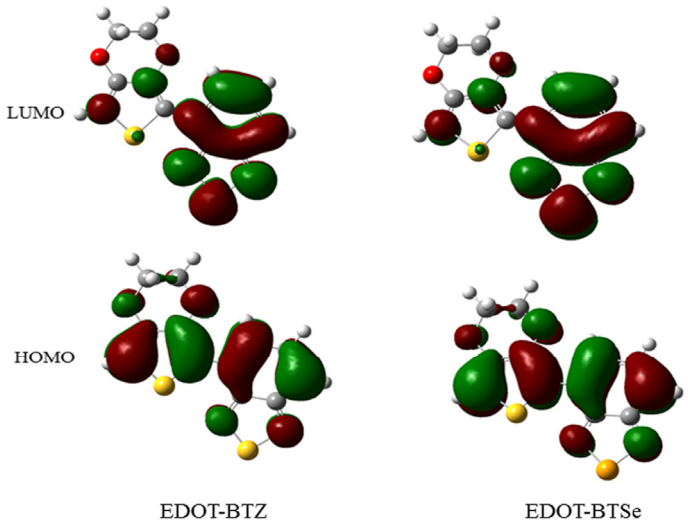

Fig. 3.2: Frontier molecular orbital distribution of monomeric units of P(EDOT-BTZ) and P(EDOT-BTSe) by B3LYP/6-31G method.

Here, the LUMO isocountours indicate more planar configuration in the singlet excited state, leading to the efficient excitation of an electron from the HOMO to the LUMO level. Since electrical and optical activity of materials relies on the ability of a material to transport electrical charges through their structures, it could be concluded that EDOT-chalcogenadiazole copolymers consisting of BTZ and BTSe are good candidates for application as donor-acceptor copolymers. Hence periodic boundary condition (PBC) calculation, which is computationally economic than the oligomer approach was used to solve the electronic structure of the copolymers at two levels of theory (B3LYP/6-31G and HSE06/6-31G) and the evolved band structures with HSE06/6-31G levels are depicted in Fig. 3.3.

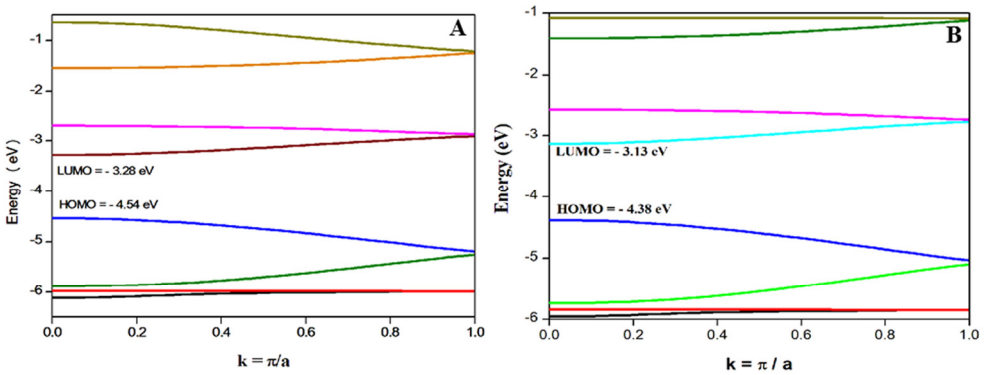

Fig. 3.3: Band structure of (A) P(EDOT-BTZ) and (B) P(EDOT-BTSe) by HSE06/6-31G method.

From the band structures, it is revealed that, by the introduction of chalcogenadiazole unit, energy of HOMO level of PEDOT is lowered by a factor of 0.92 eV and 0.76 eV, while LUMO level is lowered by a factor of 1.29 eV and 1.14 eV and we get P(EDOT-BTZ) and P(EDOT-BTSe) with a reduced band gap of 1.26 eV and 1.25 eV, respectively. The intramolecular charge transfer induced a quinoid character in the polymer backbone which

caused reduction in band gap. Here the electronic properties of the copolymers did not vary systematically with the model compounds due to the change in geometry from model compound to polymer. It could be seen from the band structure that all the polymers are direct band gap polymers, because the lowest band gap occurs at k=0. There is no significant decrease in the band gap on the introduction of BTSe unit instead of BTZ. This may be due to the slight increase in the dihedral angle between the adjacent EDOT and BTSe than the BTZ unit. Band structure data (HOMO, LUMO and HOMO-LUMO gap), ionization potential (IP) and electron affinity (EA) of PEDOT and copolymers are compiled in Table 3.1.

Table 3.1: Computational data of P(EDOT-BTZ) and P(EDOT-BTSe) with DFT/B3LYP/6-31G and DFT/HSE06/6-31G methods.

Polymer	HOMO (eV)	IP (eV)	LUMO (eV)	EA (eV)	E_g (eV)
PEDOT	-3.62[a]	3.62[a]	-1.99[a]	1.99[a]	1.64[a]
P(EDOT-BTZ)	-4.71[b]	4.71[b]	-2.99[b]	2.99[b]	1.72[b]
	-4.54[c]	4.54[c]	-3.28[c]	3.28[c]	1.26[c]
P(EDOT-BTSe)	-4.51[b]	4.51[b]	-2.85[b]	2.85[b]	1.66[b]
	-4.38[c]	4.38[c]	-3.13[c]	3.13[c]	1.25[c]

[a]Reproduced from ref. 22, [b]Obtained by the DFT/B3LYP/6-31G method, [c]Obtained by the DFT/HSE06/6-31G method.

The balanced transport of both injected electrons and holes are important as far as device performance is considered. The enhancement in well-defined properties such as IP and EA (negative of HOMO and LUMO energy, respectively) indicates an efficient electron accepting/transporting ability in the copolymers.

3.2.2. Polymer Synthesis

Donor-acceptor EDOT-chalcogenadiazole copolymers were synthesized via a simple, new and facile route, i.e., direct arylation method. Usually

EDOT-chalcogenadiazole copolymers were synthesized through electrochemical polymerization.[44] However, direct arylation method confirms the regular alternation of donor and acceptor in the polyconjugated backbone. The synthesis of key monomers and copolymers are summarized in Scheme 1. 2,1,3-benzothiadiazole (2) was prepared from o-phenylenediamine (1) and $SOCl_2$ in DCM, 4,7-dibromo-2,1,3-benzothiadiazole (3) was prepared by bromination of 2,1,3-benzothiadiazole (2) in 47 % HBr. To obtain 4,7-dibromo-2,1,3-benzoselenadiazole (5), 4,7-dibromo-2,1,3-benzothiadiazole (3) was reduced by $NaBH_4$ in absolute ethanol to give 2,3-diamino-1, 4-dibromobenzene (4). The 2,3-diamino-1,4-dibromobenzene was (4) reacted with selenium dioxide to give 4,7-dibromo-2,1,3-benzoselenadiazole (5). All the reactions were performed according to standard procedures.[45]

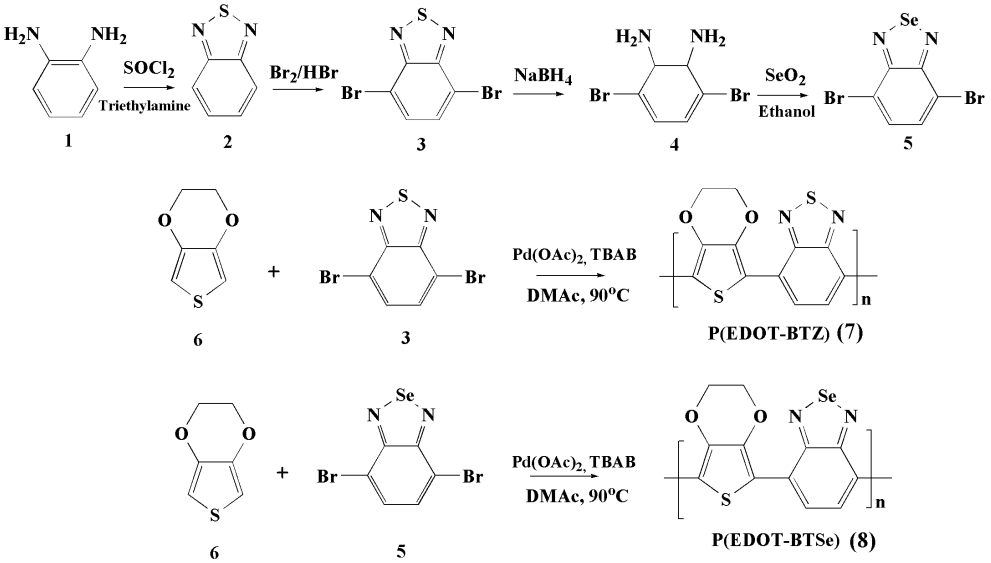

Scheme 1: Synthesis of P(EDOT-BTZ) (7) and P(EDOT-BTSe) (8).

The resulting copolymers were collected by precipitation to cold methanol followed by filtration and the crude polymer was further purified by soxhlet extraction using methanol and hexane to remove the oligomers. The

molecular weights of the polymers were obtained from gel permeation chromatography in THF referring to polystyrene standards. The isolated yield and molecular weight of both the polymers are summarized in Table 3.2. The copolymers were readily soluble in common organic solvents such as THF and chlorobenzene (50 mg/mL), hence can be easily processed in to thin films.

Table 3.2: Results of polymerization of copolymers.

Copolymer	Mn[a]	Mw[a]	PDI[a]	Yield (%)
P(EDOT-BTZ)	3237	4549	1.82	58
P(EDOT-BTSe)	3580	4928	1.66	55

[a]Determined by GPC in THF based on polystyrene standards.

3.2.3. Structural characterization

The copolymers, P(EDOT-BTZ) and P(EDOT-BTSe) were characterized by FT-IR (Fig. 3.4), ^{1}H NMR and XPS. FT-IR spectrum of the P(EDOT-BTZ) showed the characteristic peaks at 1080 and 1062 cm^{-1}, which were assigned to the stretching vibration of bridged C-O in the ethylenedioxy unit and the peak at 905 cm^{-1} is due to the ethylenedioxy ring deformation mode, which signifies the existence of EDOT moieties in the copolymer.[46,47]

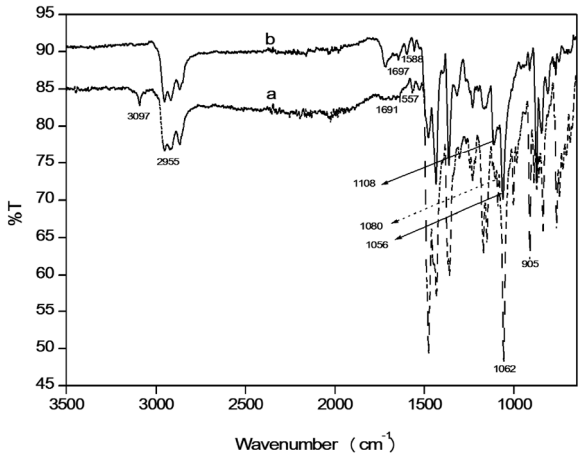

Fig. 3.4: FT-IR spectra of (a) P(EDOT-BTZ) and (b) P(EDOT-BTSe).

Furthermore, the vibration peaks at 3097 cm^{-1} (aromatic C-H stretching) and 1691 cm^{-1} (imine C=N stretching) were attributed to the incorporation of BTZ unit in the polymer, P(EDOT-BTZ).[48] P(EDOT-BTSe) also showed the vibration peaks at 1108 and 1056 cm^{-1} (stretching vibration of bridged C–O in the ethylenedioxy unit) and the peak at 905 cm^{-1} (ethylenedioxy ring deformation mode). The broad peak at 1697 cm^{-1} is a marker for BTSe moieties in the copolymer, P(EDOT-BTSe). The broad band observed at 1557 and 1588 cm^{-1} for P(EDOT-BTZ) and P(EDOT-BTSe), respectively proves the polyconjugation in the copolymers.[49] The results of these FT-IR analyses clearly indicated that copolymerization was successfully achieved.

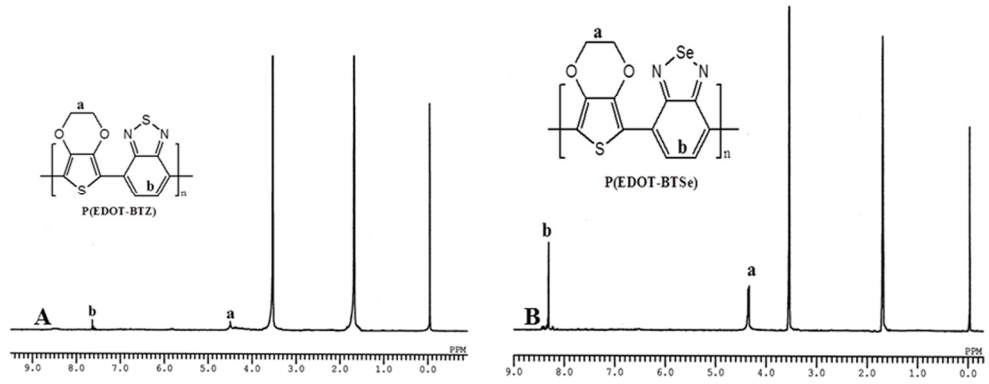

Fig. 3.5: ^{1}H NMR spectra of (A) P(EDOT-BTZ) and (B) P(EDOT-BTSe)

In order to get more insight into the polymer structure ^{1}H NMR (Fig. 3.5) was used for analysis. The P(EDOT-BTZ) revealed resonance peaks at δ 7.6 ppm and 4.5 ppm because of the aromatic protons of the BTZ units and -O-CH_2- protons of EDOT units, respectively. P(EDOT-BTSe) also exhibited broad resonance peak at δ 8.4 ppm and 4.2 ppm corresponding to aromatic protons of BTSe units and -O-CH_2- protons of EDOT units, is in well agreement with FT-IR results.

The copolymers were further investigated by XPS measurements. XPS survey scans are summarized in Fig. 3.6. The signals related to C1s are observed at 284 eV, which are mainly due to the aromatic carbon atoms of the polymeric conjugated backbone.[50] The N1s signals appeared at 397 eV and 398 eV, respectively for P(EDOT-BTZ) and P(EDOT-BTSe) due to the nitrogen atoms of the imine units of BTZ and BTSe moieties, which are attributed to the C=N bonding.[51,52] In addition, the O1s signals are observed at 531 eV, as expected. For both copolymers, the signal related to the 2p core levels of the S atom is observed at 163 eV, proved the presence of EDOT units. Whereas, P(EDOT-BTSe) showed an additional signal at 56 eV which is attributed to the presence of Se atom. Furthermore, the spectra of copolymers confirmed the lack of contaminates. Noticeable peaks were absent at 334 and 340 eV indicating complete removal of catalyst (palladium) in the copolymers.

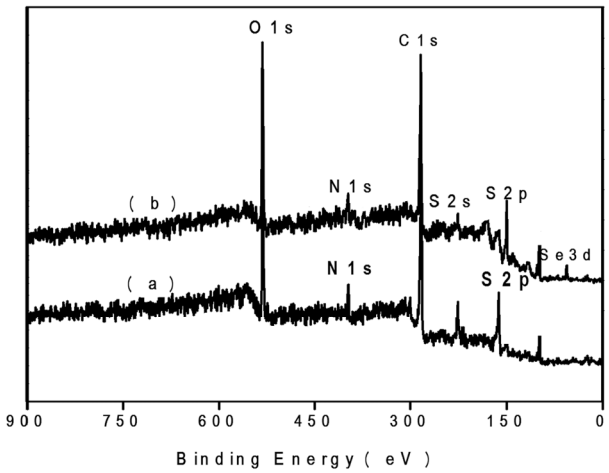

Fig. 3.6: XPS survey scans of (a) P(EDOT-BTZ) and (b) P(EDOT-BTSe).

Fig. 3.7 represents the high resolution core-electron C1s spectra of P(EDOT-BTZ) and P(EDOT-BTSe) copolymers. In the C1s core-electron

spectra of P(EDOT-BTZ), the peak centered at 283 eV is assigned to C-C and C-H bonds, where carbon is non-bonded to any hetero atoms such as oxygen, nitrogen, sulphur etc. While the peak centered at 284 eV is attributed to C-S bonds in the copolymer and the peak centered at 286 eV is due to the combination of C-O and C-N bonds present in the copolymer.[53] In conclusion, the results obtained from XPS spectra of copolymers are in good agreement with those corresponding to FT-IR and ^{1}H NMR.

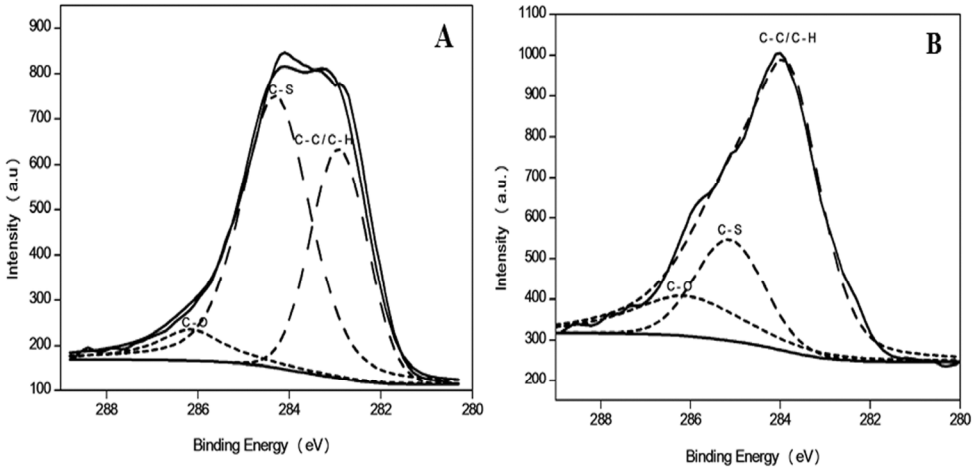

Fig. 3.7: High resolution core-electron C1s spectra of (A) P(EDOT-BTZ) and (B) P(EDOT-BTSe).

3.2.4. Electrochemical properties

Electrochemical measurements were performed to determine the HOMO and LUMO energy levels of P(EDOT-BTZ) and P(EDOT-BTSe). Cyclic voltammetry (CV), differential pulse voltammetry (DPV) and square wave voltammetry (SWV) were performed on these copolymers to analyse the electrochemical behaviour of the polymers in detail.

Table 3.3: Redox properties of P(EDOT-BTZ) and P(EDOT-BTSe).

Polymer	Onset of oxidation (V)	HOMO (eV)	Onset of reduction (V)	LUMO (eV)	Band Gap (eV)
P(EDOT-BTZ)	0.32[a]	-4.72[a]	-0.87[a]	-3.53[a]	1.19[a]
	0.26[b]	-4.66[b]	-0.80[b]	-3.6[b]	1.06[b]
	0.25[c]	-4.65[c]	-0.80[c]	-3.6[c]	1.05[c]
P(EDOT-BTSe)	0.30[a]	-4.70[a]	-0.81[a]	-3.59[a]	1.11[a]
	0.23[b]	-4.63[b]	-0.80[b]	-3.6[b]	1.03[b]
	0.26[c]	4.66[c]	-0.80[c]	3.6[c]	1.06[c]
P(EDOT)[d]		-3.62		-1.99	1.64
P(BTZ-EDOT-BTZ)[e]					1.19
P(BTSe-EDOT-BTSe)[e]					1.05

[a]Determined by CV, [b]Determined by DPV, [c]Determined by SWV, [d]Reproduced from ref. 22, [e]Reproduced from ref. 54.

In order to get a clear comparison, the electrochemical data is summarized in Table 3.3, revealing that all the methods showed a good agreement with theoretical calculation. From the onset of oxidation, the HOMO levels of P(EDOT-BTZ) and P(EDOT-BTSe) were calculated to be -4.66 eV and -4.63 eV (DPV), respectively based on the equation, HOMO = - ($4.4+E_{ox}^{onset}$). The SCE energy level of -4.4 eV below the vacuum level is used. While the LUMO energy levels (from the onset of reduction potential) of P(EDOT-BTZ) and P(EDOT-BTSe) are calculated to be -3.6 eV and -3.6 eV, respectively. In both the polymers, the HOMO and LUMO energies were lowered on copolymerization, indicating enhanced electron accepting/ transporting properties in conjugated backbone. The results are in good agreement with DFT/PBC calculation, though some deviation still exists. This is due to, the fact that the predicted band gaps are for the isolated gas-phase chains and also, the solid state effects such as polarization effects and intermolecular packing forces are neglected.[55,56] Electrochemical

measurements, DPV and SWV yielded close values for both copolymers. Thus, through copolymerization electron injection and transportation are expected to be enhanced.

3.2.5. Optical Properties

A regular alternation of conjugated donor and acceptor moieties increases the double bond character which leads to broadening of valence and conductance band. The normalized absorption spectra of pristine polymers in THF solution and as thin films are reported in Fig. 3.8. The absorption spectra of P(EDOT-BTZ) and P(EDOT-BTSe) were characterized with strong and broad absorption peaks at 532 and 537 nm (λ_{max}), respectively with onset at 725 and 768 nm, respectively. This can be assigned to the intramolecular charge transfer (ICT) transition between the donor unit (EDOT) and acceptor unit (chalcogenadiazole). The copolymers also display a characteristic peak at lowered wavelength due to high energy transition such as π-π^* transition of the conjugated backbone. The thin film absorption of both copolymers has much broad absorption range than solution absorption spectra. The optical band gaps (E_g^{opt}) derived from the absorption edge of a polymer thin film for P(EDOT-BTZ) and P(EDOT-BTSe) are 1.04 and 1.04 eV respectively, differing by 0.67 and 0.57 eV respectively, from the solution optical band gap values. As expected, both P(EDOT-BTZ) and P(EDOT-BTSe) copolymers exhibit low band gap compared to PEDOT (1.6 eV), reflecting the enhanced acceptor property of the BTZ and BTSe unit, which lowers the LUMO levels, leading to low band gap.

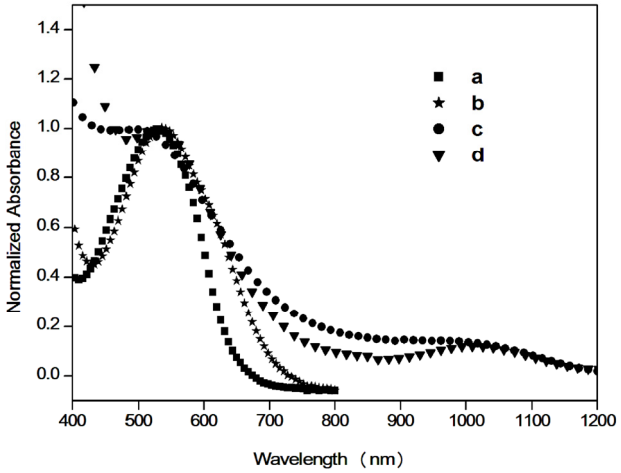

Fig. 3.8: UV-Visible spectra of the copolymers in THF solution (a) P(EDOT-BTZ) (b) P(EDOT-BTSe) and in thin film (c) P(EDOT-BTZ), (d) P(EDOT-BTSe). The polymer films were spin coated from $CHCl_3$ solution on to glass substrate.

Compared with solution absorption, the film sample prepared by spin coating showed pronounced peak broadening and a remarkable red shift of approximately above 470 nm of the absorption edge. This significant red shift is attributed to the planarization of aryl rings and the presence of inter chain interactions in the solid state. These E_g^{opt} values agree closely with theoretical results, obtained by HSE06/6-31G method than the B3LYP/6-31G method.

3.2.6. Photoluminescence properties

The photoluminescence spectra of the polymers in THF solution are shown in Fig. 3.9. The wavelengths corresponding to the absorption maxima of the polymers are used as the excitation wavelength. P(EDOT-BTZ) and P(EDOT-BTSe) exhibit fluorescence in THF with an emission maximum at 689 and 667 nm, respectively, regardless of excitation. The PL emission spectrum was red shifted for P(EDOT-BTZ) relative to those of P(EDOT-

BTSe) and this suggests the high energy transfer of EDOT (donor) unit to BTZ (acceptor) unit.

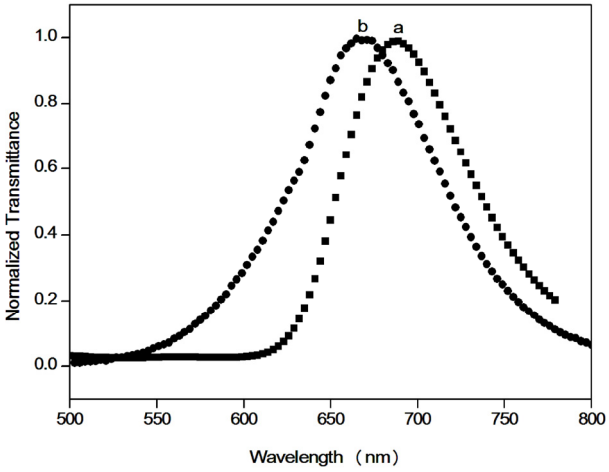

Fig. 3.9: PL spectra of the polymers (a) P(EDOT-BTZ) and (b) P(EDOT-BTSe) in THF solution.

3.2.7. Thermal properties

The thermal characteristics of the polymers were investigated by DSC and TG. The TG traces are shown in Fig. 3.10. DSC showed no characteristic thermal transition between 40 and 200 °C. This suggests that the polymers were in an amorphous glassy state, probably due to the rigid backbone in the copolymer, making it suitable for device applications. From the TG traces, it was found that the copolymers exhibit step wise degradation and the decomposition exotherms are broad with multiple peaks. The first exotherm can be assigned to elimination of imine (C=N) nitrogen which is more susceptible to degradation. TG traces of P(EDOT-BTZ) showed degradation temperature of 160 and 426 ^{o}C and onset degradation temperature of 103 and 344 ^{o}C, choosing 5 wt% loss as the onset loss point. While P(EDOT-BTSe) has onset degradation temperature of 203 and 371 ^{o}C and

degradation temperature of 335 and 399 ^{o}C, which is an indication of excellent thermal stability than PEDOT. The DTG peaks show exotherms at this temperature which is indicative of degradation rather than vaporization. Kiebooms *et al*., have reported that PEDOT films are stable upto 150 °C and complete decomposition occurs above 390 °C.[57] The P(EDOT-BTSe) exhibits higher onset and peak degradation temperatures than P(EDOT-BTZ) and PEDOT. This is probably due to intermolecular van der Waals bonding between the Se units, which result in self rigidification in the polymer chain.

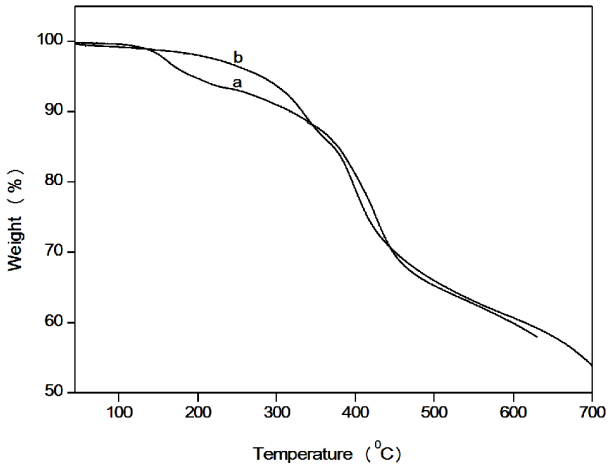

Fig. 3.10: TG traces of polymers (a) P(EDOT-BTZ) and (b) P(EDOT-BTSe).

3.2.8. Non-linear optical properties

The non-linear optical transmission of D-A copolymers was investigated at 532 nm using z-scan technique, which is known for simplicity and sensitivity. The NLO absorption coefficients were evaluated by z-scan technique under an open aperture configuration. Fig. 3.11 presents the open aperture (OA) z-scan traces of copolymers in dilute $CHCl_3$ solution (A) and

as thin film (B). The solid curves in the figure are the theoretical fit to the experimental data.

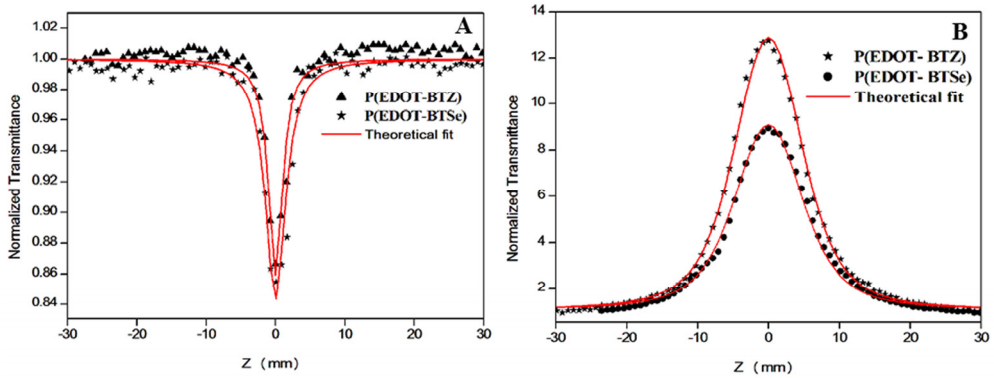

Fig. 3.11: Open aperture z-scan traces of P(EDOT-BTZ) and P(EDOT-BTSe) (A) in solution and (B) as film.

In solution phase, the open-aperture curve shows a normalized valley, indicating the presence of reverse saturation absorption (RSA) with a positive coefficient. However, the copolymer films exhibit different optical response. The polymers show saturation absorption (SA) in film phase. The polymers show complete switch over behaviour from RSA to SA in thin film. This could be due to ground state band bleaching,[58] i.e., the excited state absorption and free carrier absorption result in ground state band bleaching. From the figure it could be seen that the experimental curve is fitted well with two photon absorption (TPA) theory. This infers that TPA is the basic mechanism involved in the non-linear absorption process. The non-linear absorption coefficient, β is obtained by fitting the experimental scan plot of the OA measurement to equation (1) (equation (3), given in section 2.2.7).

The non-linear refractive (NLR) property of the copolymers was investigated by closed aperture (CA) z-scan configuration. The pure NLR z-scan curves after excluding non-linear absorption effects can be obtained by dividing the CA z-scan data by the corresponding open aperture data (Fig. 3.12). Here, the normalized transmittance T(z) is given by equation (2) (equation (5), described in section 2.2.7). All the spectra display peak-valley pattern, indicating a negative NLR index due to self-defocusing. The non-linear refractive index (n_2), the real parts of $\chi^{(3)}$ (Re $\chi^{(3)}$) and third-order non-linear susceptibility ($\chi^{(3)}$) are calculated by using equations (3)-(5) (equation (6)-(8), given in section 2.2.7).

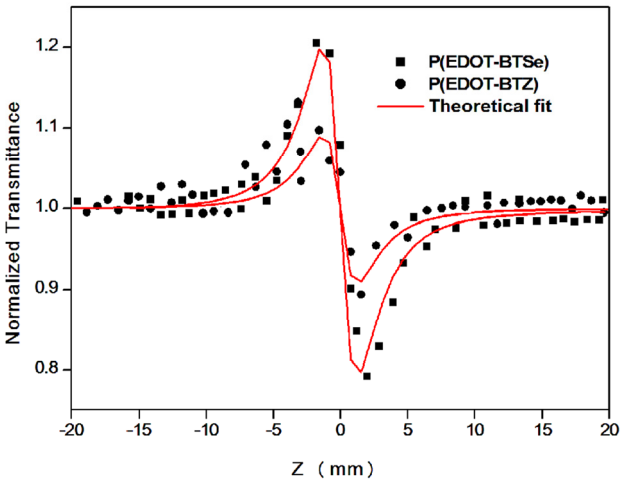

Fig. 3.12: Closed aperture z-scan traces of P(EDOT-BTZ) and P(EDOT-BTSe).

The non-linear absorption coefficient (β, m/W), the non-linear refraction coefficient (n_2, esu), and the third-order non-linear susceptibility ($\chi^{(3)}$, esu) at 532 nm are calculated and listed in Table 3.4. The β is obtained to be 0.8×10^{-10} and 2.08×10^{-10} m/W for P(EDOT-BTZ) and P(EDOT-BTSe), respectively. In addition, the $\chi^{(3)}$ value is also found to be

increased for P(EDOT-BTSe). As given in table, it is found that the P(EDOT-BTSe) show large optical non-linearity than P(EDOT-BTZ), as expected. This is due to the more acceptor strength of BTSe than the BTZ unit. The magnitude of the non-linear refractive index is directly related to the polarizability of polymers. In D-A compounds, non-linearity is mainly due to the charge transfer from donor to acceptor unit, i.e., the non-linearity due to strong delocalization of π electrons or in other words, due to charge asymmetry.

Table 3.4: Calculated values of non-linear absorption, non-linear refraction, and non-linear susceptibility of copolymers at 532 nm.

Copolymer	Non-linear absorption coefficient (β, m/W)	Non-linear refractive index (n_2, esu)	Imaginary part of non-linear susceptibility (Im $\chi^{(3)}$, esu)	Real part of non-linear susceptibility (Re $\chi^{(3)}$, esu)	Non-linear susceptibility ($\chi^{(3)}$, esu)
P(EDOT-BTZ)	0.8×10^{-10}	-0.46×10^{-10}	0.02×10^{-10}	-0.71×10^{-11}	0.74×10^{-11}
P(EDOT-BTSe)	2.08×10^{-10}	-1.29×10^{-10}	0.05×10^{-10}	-1.98×10^{-11}	2.04×10^{-11}
PABAzo[a]	3.33×10^{-10}	-0.81×10^{-11}	0.11×10^{-10}	-1.84×10^{-11}	2.15×10^{-11}
P-NPAPA-5[b]	1.07×10^{-10}				
PANI/SiO2[c]	2.17×10^{-12}				
PMMA-M3[d]					2.29×10^{-12}

[a]Reproduced from ref. 59, [b]Reproduced from ref. 60, [c]Reproduced from ref. 61, [d]Reproduced from ref. 62.

3.2.9. Optical power limiting

The non-linear optical process in which the transmittance of a material decreases as the input light intensity increases is called optical limiting process. This occurs mostly due to non-linear absorption. Optical limiters are devices which are transparent at low input fluences, but become opaque at high inputs, used for the protection of eyes and sensitive

optical devices from laser induced damage. The optical limiting property of the copolymers was investigated at 532 nm by OA z-scan technique. Fig. 3.13 shows the transmitted energy of copolymers as a function of input fluence.

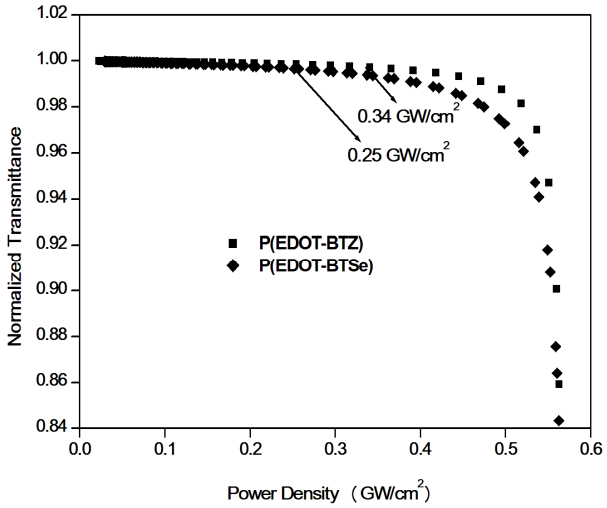

Fig. 3.13: Optical limiting curves of P(EDOT-BTZ) and P(EDOT-BTSe).

At lower fluence, polymers obey Beer's law very well. When the input energy reaches optical limiting threshold, the transmitted energy starts to deviate and exhibit a typical optical limiting effect. Optical limiting threshold is determined to be 0.34 and 0.25 GW/cm^2 for P(EDOT-BTZ) and P(EDOT-BTSe), respectively. The lower the optical limiting threshold the better is the optical limiting material. The P(EDOT-BTSe) showed good optical limiting response than P(EDOT-BTZ). This is due to the large variation of the dipole moment of the polymer in the excited electronic state.[63,64]

3.3. Experimental

3.3.1. Materials

3,4-Ethylenedioxythiophene (EDOT, Aldrich, 98 %), o-phenylenediamine (Merck, 98%), tetrabutyl ammonium bromide (TBAB, Avra Synthesis Pvt. Ltd., 98%), sodium acetate (anhydrous) (Spectrochem Pvt. Ltd.), triethyl amine (Spectrochem Pvt. Ltd.), palladium (II) acetate ($Pd(OAc)_2$, Aldrich, 99.98%), tetrabutylammonium hexafluorophosphate (Bu_4NPF_6, Aldrich, >99%), thionyl chloride ($SOCl_2$, Merck, 97%), hydrobromic acid (HBr, Spectrochem Pvt. Ltd., 47%), bromine (Merck), sodium borohydride ($NaBH_4$, Merck, 98%), ethanol absolute (Merck), diethyl ether (Spectrochem Pvt. Ltd.), magnesium sulphate (anhydrous) ($MgSO_4$, Spectrochem Pvt. Ltd.) and selenium dioxide (SeO_2, Aldrich, 98%) were used as received. Acetonitrile HPLC grade (CH_3CN, Aldrich), dimethyl acetamide (anhydrous) (DMAc, Spectrochem Pvt. Ltd.), chloroform ($CHCl_3$, Spectrochem Pvt. Ltd.), dicholoromethane (CH_2Cl_2, Spectrochem Pvt. Ltd.), tetrahydrofuran HPLC grade (THF, Spectrochem Pvt. Ltd.), n-hexane (Spectrochem Pvt. Ltd.) and methanol (anhydrous) (MeOH, Spectrochem Pvt. Ltd.) were dried and distilled when necessary according to the standard procedures.

3.3.2. Computation methods

Theoretical calculations were done using computation methods, which has been described in section 2.3.4.

3.3.3. Chemical procedures

3.3.3.1. *2,1,3-Benzothiadiazole (2):*

1,2-phenylenediamine (1) (5.42 g, 50 mmol), triethylamine (30 mL) and dichloromethane (150 mL) were stirred under nitrogen with drop wise

addition of thionyl chloride (9.5 mL) in dichloromethane (30 mL). After the addition was complete, the reaction mixture was heated at reflux for 30 min. The mixture was filtered; the solid residue was washed with dichloromethane and discarded. The filtrate was evaporated under vacuum to give a yellowish red residue. The residue was recrystallized from hexane to give 2,1,3-benzothiadiazole (2) as yellow needles.

Yield	:	54 % (3.7 g).
M.P.	:	43-45 ^{o}C.
^{1}H NMR (400 MHz, $CDCl_3$)	:	δ 7.52 (s, 2H), 7.94 (s, 2H).

3.3.3.2. ***4,7-Dibromo-2,1,3-benzothiadiazole (3):***

A mixture of 6.8 g (0.5 mol) of 2,1,3-benzothiadiazole (2) in 15 mL of 47 % HBr was heated under reflux with stirring while 24 g (0.15 mol, 15.3 mL) of bromine was added slowly. After completion of the bromine addition, the reaction mixture became a suspension of solid in HBr and 7.5 mL of HBr was added, and the reaction mixture was heated under reflux for another 2.5 h. The mixture was filtered, washed well with water, recrystallized from chloroform, and dried to give white needle crystals.

Yield	:	93 % (13.65 g)
M. P.	:	187-188 °C.
^{1}H NMR (400 MHz, $CDCl_3$)	:	δ 7.73 (s, 2H).

3.3.3.3. ***3,6-Dibromo-1,2-phenylenediamine (4):***

To a suspension of 4,7-dibromo-2,1,3-benzothiadiazole (3) (5.88 g, 0.02 mol) in ethanol (190 mL), sodium borohydride (14 g, 0.37 mol) was added in three portions at 0 °C, and the mixture was stirred for 20 h at room

temperature. After evaporation of the solvent, 200 mL of water was added, and the mixture was extracted with ether. The extract was washed with brine and dried over anhydrous sodium sulfate. Evaporation of the solvent gave 3,6-dibromo-1,2-phenylenediamine (4) as a pale yellow solid.

Yield	:	85 % (4.52 g)
M. P.	:	100 ^{o}C
^{1}H NMR (400 MHz, $CDCl_3$)	:	δ 3.90 (s, 4 H), 6.85 (s, 2H).

3.3.3.4. ***4,7-Dibromo-2,1,3-benzoselenadiazole (5):***

To a solution of 3,6-dibromo-1,2-phenylenediamine (4) (2.7 g, 10 mmol) in refluxing ethanol (55 mL), was added a solution of selenium dioxide (1.17 g, 10.5 mmol) in hot water (22 mL). The reaction mixture was heated under reflux for 2 h. Filtration of the yellow precipitate and recrystallization from ethyl acetate gave 4,7-dibromo-2,1,3-benzoselenadiazole (5) as golden yellow needles.

Yield	:	73 % (2.5 g)
M. P.	:	285-287 °C
^{1}H NMR (400 MHz, $CDCl_3$)	:	δ 7.63 (s, 2H).

3.3.3.5. ***Synthesis of P(EDOT-BTZ) (7)***

To a stirred solution of EDOT (6) (0.024 g, 0.17 mmol) in 10 mL DMAc was added TBAB (0.055 g, 0.17 mmol) and sodium acetate (0.055 g, 0.68 mmol). The reaction mixture was stirred at room temperature for 30 min followed by addition of 4,7-dibromo-2,1,3-benzothiadiazole (3) (0.05 g, 0.17 mmol) and 10 % palladium acetate. The reaction mixture was stirred at 90 ^{o}C for 48 h. The reaction mixture

was cooled to room temperature and poured in to methanol (20 mL). The precipitate was filtered and washed with methanol. The polymer was purified by soxhlet extraction using hexane and methanol for 24 h. The residue was dissolved in minimum amount of $CHCl_3$ and precipitated using methanol and dried under vacuum.

Yield	: 58 %
FT-IR (ν_{max}/cm^{-1})	: 2956s and 2874s (C-H), 1080w, 1062s and 905w (C-O), 1557br (conjugation), 3097br (C-H ar), 1691(C=N).
^{1}H NMR (400 MHz, d8-THF): δ (ppm)	: 4.5 (m, 4H), 7.6 (m, 2H).

3.3.3.6. *Synthesis of P(EDOT-BTSe) (8)*

To a stirred solution of EDOT (6) (0.024 g, 0.17 mmol) in 10 mL DMAc was added TBAB (0.055 g, 0.17 mmol) and sodium acetate (0.055 g, 0.68 mmol). The reaction mixture was stirred at room temperature for 30 min followed by addition of 4,7-dibromo-2,1,3-benzoselenadiazole (5) (0.06 g, 0.17 mmol) and 10 % palladium acetate. The reaction mixture was stirred at 90 ^oC for 48 h. The reaction mixture was cooled to room temperature and poured in to methanol (20 mL). The precipitate was filtered and washed with methanol. The polymer was purified by soxhlet extraction using hexane and methanol for 24 h. The residue was dissolved in minimum amount of $CHCl_3$ and precipitated using methanol and dried under vacuum.

Yield	: 55 %
FT-IR (ν_{max}/cm^{-1})	: 2956s and 2874s (C-H), 1094w, 1056s and 905w (C-O), 1588br (conjugation), 1697(C=N);
^1H NMR (400 MHz, d8-THF): δ (ppm)	: 4.2 (m, 4H), 8.4 (m, 2H).

3.3.4. Instrumentation

Copolymers were characterized by instrumentation methods which have been described in section 2.3.3.

3.3.5. NLO Measurements

NLO properties were determined by methods which have been described in section 2.3.6.

3.4. Conclusion

Two promising low band gap D-A EDOT based alternate copolymers have been designed and successfully synthesized via direct arylation reaction using palladium acetate as catalyst. Electronic properties of the two polymers based on 3,4-ethylenedioxythiophene and 2,1,3-chalcogenadiazole were calculated using density functional theory under periodic boundary condition. Theoretical calculation revealed the HOMO and LUMO levels of the P(EDOT-BTZ) at -4.54 and -3.28 eV respectively, and showed a band gap of 1.26 eV. The HOMO and LUMO levels of the P(EDOT-BTSe) were revealed at -4.38 eV and -3.13 eV respectively, and hence had a band gap of 1.25 eV. The polymer exhibited good thermal and chemical stability, as evidenced by TG and CV. Polymers exhibited broad absorption band and

the band gaps were estimated to be 1.04 eV for both P(EDOT-BTZ) and P(EDOT-BTSe). The band gap and energy levels of the polymers were determined using both optical and electrochemical methods. The results showed good agreement with the theoretical prediction obtained by HSE06/6-31G method compared to the B3LYP/6-31G method. The z-scan results indicated that the copolymers exhibited negative non-linear refractive index which was of the order of 10^{-10} esu. The non-linear absorption coefficient (β, m/W) and third-order non-linear susceptibility ($\chi^{(3)}$, esu) of polymers are in the order of 10^{-10} and 10^{-11}, respectively. The polymers exhibited good optical power limiting behaviour at 532 nm. Hence the polymers investigated seem to be promising candidates for future photonic applications.

References

[1] P. Dutta, H. Park, W. -H. Lee, I. N. Kang, S. -H. Lee, *Polym. Chem.,* 2014, 5, 132.

[2] Q. Hou, J. Liu, T. Jia, S. Luo, G. Shi, *J. Appl. Polym. Sci.,* 2013, 130, 3276.

[3] W. Zhuang, M. Bolognesi, M. Seri, P. Henriksson, D. Gedefaw, R. Kroon, M. Jarvid, A. Lundin, E. Wang, M. Muccini, M. R. Andersson, *Macromolecules*, 2013, 46, 8488.

[4] E. Zhou, J. Cong, K. Hashimoto, K. Tajima, *Macromolecules*, 2013, 46, 763.

[5] L. Dou, C. -C. Chen, K. Yoshimura, K. Ohya, W. -H. Chang, J. Gao, Y. Liu, E. Richard, Y. Yang, *Macromolecules*, 2013, 46, 3384.

[6] P. M. Beaujuge, J. R. Reynolds, *Chem. Rev.,* 2010, 110, 268.

[7] P. Shi, C. M. Amb, A. L. Dyer, J. R. Reynolds, *Appl. Mater. Interfaces*, 2012, 4, 6512.

[8] E. Kaya, A. Balan, D. Baran, A. Cirpan, *Organic Electronics*, 2011, 12, 202.

[9] N. R. Evans, L. S. Devi, C. S. K. Mak, S. E. Watkins, S. I. Pascu, A. Kohler, R. H. Friend, C. K. Williams, A. B. Holmes*, J. Am. Chem. Soc.,* 2006, 128, 6647.

[10] Q. Huang, G. A. Evmenenko, P. Dutta, P. Lee, N. R. Armstrong, T. J. Marks, *J. Am. Chem. Soc*., 2005, 127, 10227.

[11] L. Groenendaal, F. Jonas, D. Freitag, H. Pielartzik, J. R. Reynolds, *Adv. Mater.,* 2000, 12, 481.

[12] L. Groenendaal, G. Zotti, P. -H. Aubert, S. M. Waybright, J. R. Reynolds*, Adv. Mater*., 2003, 15, 855.

[13] H. Huang, P. G. Pickup, *Chem. Mater.,* 1998, 10, 2212.

[14] J. Rault-Berthelot, E. Raoult, *Adv. Mat. Opt. Electr.,* 2000, 10, 267.

[15] J. Rault-Berthelot, E. Raoult, F. L. Floch, *J. Electroanal. Chem*., 2003, 546, 29.

[16] S. Akoudad, J. Roncali, *Chem. Commun.,* 1998, 2081.

[17] K. Yamazaki, J. Kuwabara, T. Kanbara, *Macromol. Rapid Commun.,* 2013*,* 34*,* 69.

[18] J. Kuwabara, T. Yasuda, S. J. Choi, W. Lu, K. Yamazaki, S. Kagaya, L. Han T. Kanbara, *Adv. Funct. Mater*., 2014, 24, 3226.

[19] Y. Nohara, J. Kuwabara, T. Yasuda, L. Han, T. Kanbara, *J. Polym. Sci. A Polym. Chem*., 2014, 52, 1401.

[20] E. Rudenko, B. C. Thompson, *J. Polym. Sci. A Polym. Chem*., 2014, DOI: 10.1002/pola.27279.

[21] M. K. Poduval, P. M. Burrezo, J. Casado, J. T. L. Navarrete, R. P. Ortiz, T. -H. Kim, *Macromolecules*, 2013, 46, 9220.

[22] C. -L. Pai, C. -L. Liu, W. -C. Chen, S. A. Jenekhec, *Polymer*, 2006, 47, 699.

[23] S. Ellinger, K. R. Graham, P. Shi, R. T. Farley, T. T. Steckler, R. N. Brookins, P. Taranekar, J. Mei, L. A. Padilha, T. R. Ensley, H. Hu, S. Webster, D. J. Hagan, E. W. V. Stryland, K. S. Schanze, J. R. Reynolds, *Chem. Mater*., 2011, 23, 3805.

[24] D. Cowan, A. Kini, The Chemistry of Organic Selenium and Tellurium Compounds: Wiley: Chichester, U. K, Vol. 2, 1987.

[25] M. R. Bryce, *J. Mater. Chem.,* 1995, 5, 1481.

[26] M. Bass, J. M. Enoch, E. W. Van Stryland, W. L. Wolfe, Handbook of optics IV, Fiber optics and non-linear optics: New York, McGraw-Hill, 2nded, 2001.

[27] Y. Guo , C. K. Kao, E. H. Li, K. S. Chiang, Nonlinear photonics: Berlin, Springer., 2002.

[28] S. Webster, J. Fu, L. A. Padilha, O. V. Przhonska, D. J. Hagan, E. W. Van Stryland, M. V. Bondar, Y. L. Slominsky, A. D. Kachkovski, *Chem. Phys.,* 2008, 348, 143.

[29] M. Charlot, N. Izard, O. Mongin, D. Riehl, M. Blanchard-Desce, *Chem. Phys. Lett.,* 2006, 417, 297.

[30] L. A. Padilha, S. Webster, O. V. Przhonska, H. Hu, D. Peceli, J. L. Rosch, M. V. Bondar, A. O. Gerasov, Y. P. Kovtun, M. P. Shandura, A. D. Kachkovski, D. J. Hagan, E. W. Van Stryland, *J. Mater. Chem.,* 2009, 19, 7503.

[31] Y. Jiang, Y. Wang, J. Hua, S. Qu, S. Qian, H. Tian, *J. Polym. Sci. A Polym. Chem*., 2009, 47, 4400.

[32] B. Li, R. Tong, R. Zhu, F. Meng, H. Tian, S. Qian, *J. Phys. Chem. B*, 2005, 109, 10705.

[33] R. Sun, Y. -T. Lu, B. -L. Yan, J. -M. Lu, X. -Z. Wu, Y. -L. Song, J. -F. Ge, *Thin Solid Films*, 2014, 551, 153.

[34] C. Cabanetos, E. Blart, Y. Pellegrin, V. Montembault, L. Fontaine, F. Adamietz, V. Rodriguez, F. Odobel, *Eur. Polym. J.,* 2012, 48, 116.

[35] J. Britton, M. Durmus, V. Chauke, T. Nyokong, *J. Mol. Struct*., 2013, 209, 1054.

[36] P. N. Prasad, D. J. Williams, Introduction to nonlinear optical effects in molecules and polymers: New York, Wiley, 1992.

[37] H. S. Nalwa, S. Miyata, Nonlinear optics of organic molecules and polymers: USA, CRC Press, 1997.

[38] R. G. Parr, W. Yang, Density-Functional Theory of Atoms and Molecules: Oxford University Press, New York, 1989.

[39] A. D. Becke, *J. Chem. Phys.,* 1993, 98, 5648.

[40] C. Lee, W. Yang, R. G. Parr, *Phys. Rev. B*., 1994, 37, 785.

[41] P. J. Stephens, F. J. Devlin, C. F. Chabalowski, M. J. Frisch*, J. Phys. Chem.,* 1994, 98, 11623.

[42] J. Heyd, G. E. Scuseria, M. Ernzerhof, *J. Chem. Phys.,* 2003, 118, 8207.

[43] M. A. D. Oliveira, H. A. Duarte, J. -M. Pernaut, W. B. D. Almeida, *J. Phys. Chem. A*, 2000, 104, 8256.

[44] M. Sendur, A. Balan, D. Baran, B. Karabay, L. Toppare, *Organic Electronics*, 2010, 11, 1877.

[45] I. Yamaguchi, B. -J. Choi, T. -A. Koizumi, K. Kubota, T. Yamamoto, *Macromolecules*, 2007, 40, 438.

[46] S. G. Im, K. K. Gleason, E. A. Olivetti, *Appl. Phys. Lett.* 2007, 90, 152112.

[47] C. Varnstrom, H. Neugebauer, S. Blomquist, H. J. Ahonen, J. Kankare, A. Ivaska, *Electrochim. Acta*, 1999, 44, 2739.

[48] I. Kaya, M. Yildirim, M. Kamaci, *Eur. Polym. J.,* 2009, 45, 1586.

[49] S. G. Im, K. K. Gleason, *Macromolecules,* 2007, 40, 6552.

[50] I. Venditti, I. Fratoddi, C. Palazzesi, P. Prosposito, M. Casalboni, C. Cametti, C. Battocchio, G. Polzonetti, M. V. Russo, *J. Colloid. Interf. Sci.,* 2010, 348, 424.

[51] A. S. Sarac, S. A. M. Tofail, M. Serantoni, J. Henry, V. J. Cunnane, J. B. McMonagle, *Appl. Surf. Sci.,* 2004, 222, 148.

[52] M. Yildirim, I. Kaya, A. Aydin, *React. Funct. Polym.,* 2013, 73, 1167.

[53] D. Bhattacharyya, K. K. Gleason, *Chem. Mater.,* 2011, 23, 2600.

[54] A. Cihaner, F. Algi, *Adv. Funct. Mater.,* 2008, 18, 3583.

[55] P. Puschnig, C. Ambrosch-Draxl, G. Heimel, E. Zojer, R. Resel, G. Leising, M. Kriechbaum, W. Graupner, *Synthetic Met.,* 2001, 116, 327.

[56] V. J. Eaton, D. Steele, *J. Chem. Soc., Faraday Trans.,* 1973, 2, 1601.

[57] R. Kiebooms, A. Aleshin, K. Hutchison, F. Wudl, A. Heeger, *Synthetic Met.,* 1999, 101, 436.

[58] A. Thankappan, S. Thomas, V. P. N. Nampoori, *Opt. Laser Technol.,* 2014, 58, 63.

[59] N. Li, J. Lu, X. Xia, Q. Xu, L. Wang, *Polymer*, 2009, 50, 428.

[60] N. Li, Q. Xu, J. Lu, X. Xia, L. Wang, *Macromol. Chem. Phys.,* 2007, 208, 399.

[61] Y. D. Zhang, L. Ma, C. B. Yang, P. Yuan, *Journal of Physics: Conference Series*, 2009, 188, 012030.

[62] F. A. Jerca, V. V. Jerca, F. Kajzar, A. M. Manea, I. Rauc, D. M. Vuluga, *Phys. Chem. Chem. Phys.,* 2013, 15, 7060.

[63] J. L. Oudar, D. S. Chemla, *J. Chem. Phys*., 1977, 66, 2664.

[64] H. H. Jaffe, M. Orchin, Theory and application of ultraviolet spectroscopy: New York, Wiley, 1962.

.....ꕥ.....

Chapter 4

Synthesis and Third-order Non-linear Optical Properties of Low Band Gap 3,4-ethylenedioxythiophene-quinoxaline Copolymers*

Abstract

A series of low band gap 3,4-ethylenedioxythiophene (EDOT) and quinoxaline donor-acceptor (D-A) copolymers were designed and their electronic structure and properties were investigated by employing density functional theory (DFT) in the periodic boundary condition using HSE06 exchange correlation functional and 6-31G basis set. The acceptors investigated were acenaphthylene, phenyl and phenanthrene substituted quinoxaline units. DFT calculations have been performed for both monomers and model oligomers to analyse their electronic properties. The designed copolymers have been synthesized through a simple and facile method, i.e., direct arylation reaction. The photophysical and electrochemical properties of EDOT-quinoxaline copolymers were investigated. The copolymers, P(EDOT-ACEQX), P(EDOT-BZQX), and P(EDOT-PHQX) exhibited theoretical band gap of 1.81, 1.76 and 1.63 eV, respectively using the DFT/HSE06/6-31G calculation and the optical band gap of 1.80, 1.75, and 1.66 eV, respectively, according to the onset edge of lower energy peak of the polymers in solution. Electrochemical studies demonstrated that quinoxaline moieties elevated the HOMO (highest occupied molecular orbital) level and lowered the LUMO (lowest unoccupied molecular orbital) level of the PEDOT (Poly(3,4-ethylenedioxythiophene)) backbone. The theoretical and experimental evaluations revealed the regular alternation of quinoxaline moieties. The band gap of the copolymers was well correlated with the acceptor strength. The experimental results supported the theoretical predictions. The third-order non-linear optical (NLO) properties of D-A EDOT-quinoxaline copolymers, evaluated by z-scan method with nanosecond laser beam at 532 nm, are reported. Polymers possess strong refractive effect with non-linear refraction coefficient of -0.47×10^{-10}, -0.95×10^{-10} and -0.64×10^{-10} esu, respectively. Effective third-order non-linear susceptibilities were calculated to be 0.82×10^{-11}, 1.46×10^{-11} and 1.17×10^{-11} esu, respectively. Polymers showed good optical limiting behaviour due to two photon absorption (TPA). The results suggest that EDOT-quinoxaline copolymers are promising materials for third-order non-linear optical applications.

* Synthesis and third-order non-linear optical properties of low band gap 3,4-ethylenedioxythiophene–quinoxaline copolymers, Sona Narayanan, Sreejesh Poikavila Raghunathan, Sebastian Mathew, M.V. Mahesh Kumar, Anshad Abbas, Krishnapillai Sreekumar, Cheranellore Sudha Kartha, Rani Joseph, Eur. Polym. J., 2015, 64, 157. http://dx.doi.org/10.1016/j.eurpolymj.2015.01.002.

4.1. Introduction

Organic conjugated polymers are widely used in electronic devices owing to their good opto-electronic properties. Conjugated polymers with D-A architecture have attracted considerable research interest, since they permit fine tuning of band gap and thereby improved electron or hole affinities. Electronic properties of a polymer can be fine-tuned by structural modification via increasing quinanoid character by alternating electron donor and electron acceptor along the conjugated backbone.[1] Band structure engineering by alternating donor and acceptor groups has become significant in the field of material science, where the mixing of monomer segments with high HOMO and low LUMOs is effective in producing low band gap polymers through efficient inter-chain charge transfer.[2] The D-A copolymers have found a variety of advanced technological applications in the field of light emitting diodes (LEDs),[3,4] photovoltaic[5-9] and elecrochromic[10-12] devices, owing to their tunable opto-electronic properties. EDOT based D-A copolymers have been widely studied in several opto-electronic devices, due to strong electron donor effect of ethylenedioxy group.[13-17] The regular insertion of EDOT unit can serve to raise the HOMO level of the copolymer through self rigidification of conjugated chain by intramolecular sulphur-oxygen interactions.[18] Quinoxaline moieties have proved to be promising acceptors in LEDs,[19-21] photovoltaic devices[22-28] and electrochromic devices,[29-32] owing to their high electron affinity due to the presence of two symmetric unsaturated nitrogen atoms in quinoxaline ring. Here, we have investigated the acceptor strength of quinoxaline units in PEDOT chain by keeping in mind the fact that, both the acceptor strength and the stable geometry govern the optoelectronic properties of D-A copolymers. The

effect of structural changes in the quinoxaline unit on the band gap and energy levels of alternating copolymers of EDOT with acenaphthylene (ACEQX), phenyl (BZQX) and phenanthrene (PHQX) substituted quinoxalines are investigated. In order to get deep insight into the structure-property relationship, the electronic properties were calculated using density functional theory (DFT) adopting two levels of theory. Generally, the quinoxaline copolymers were reported to be synthesized either through Stille,[22,27,28,33] Suzuki polycondensation[23-26] or electrochemical reaction,[29,31,34-37] which make the synthesis tedious and costly. We have attempted to synthesize EDOT-quinoxaline polymers through a simple and facile route, direct arylation reaction.[38] The results of the investigation of third-order NLO and optical limiting properties of EDOT-quinoxaline copolymers through z-scan technique under nanosecond laser excitation at 532 nm are reported.

4.2. Results and discussion

4.2.1. Electronic structure of model compounds

To investigate the effect of structural change of the quinoxaline derivatives on the band gap of EDOT-quinoxaline copolymers, a sequence of steps were followed involving quantum chemical calculations, based on DFT[39] at B3LYP[40-42] and HSE06[43,44] level of theory using 6-31G basis set. B3LYP/6-31G method was employed to predict the ground state geometries of the model compounds and the relevant electronic structure data of monomers obtained are summarized in Fig. 4.1.

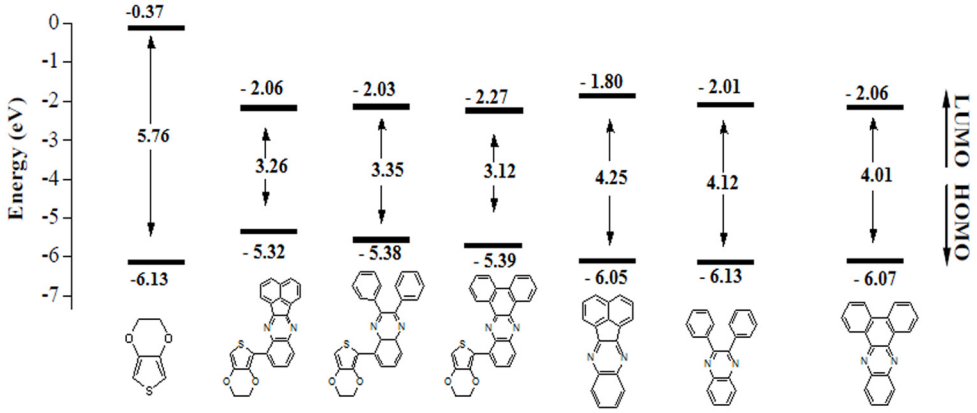

Fig. 4.1: Energy levels of EDOT, EDOT-ACEQX, EDOT-BZQX, EDOT-PHQX, ACEQX, BZQX and PHQX.

The LUMO levels of ACEQX, BZQX, and PHQX moieties obtained are -1.80, -2.01 and -2.06 eV, respectively. The lower the LUMO energy level, the higher is the acceptor strength. Hence, the quinoxaline acceptor strength follows the order, PHQX > BZQX > ACEQX. As revealed from the energy level diagram, the LUMO level of EDOT-ACEQX, EDOT-BZQX and EDOT-PHQX were calculated to be -2.06, -2.03 and -2.27 eV, respectively, i.e., during coupling, the HOMO levels were elevated and the LUMO levels lowered. The energy gap of the model compounds, EDOT-ACEQX, EDOT-BZQX and EDOT-PHQX followed the order, EDOT-BZQX > EDOT-ACEQX > EDOT-PHQX, which revealed that both the geometry and acceptor strength has played a major role in band gap reduction. This band gap reduction in the D-A monomer is mainly due to the charge transfer between donor, EDOT and acceptor, quinoxaline ring, i.e., the intramolecular charge transfer significantly improves the π-electron delocalization and thus decreases the bond length alteration (BLA) of EDOT-quinoxaline monomers.[45] This can be visualized from the frontier orbital

distribution of the model compounds (Fig. 4.2). The wave functions of HOMO and LUMO are localized on the EDOT and quinoxaline unit, respectively.

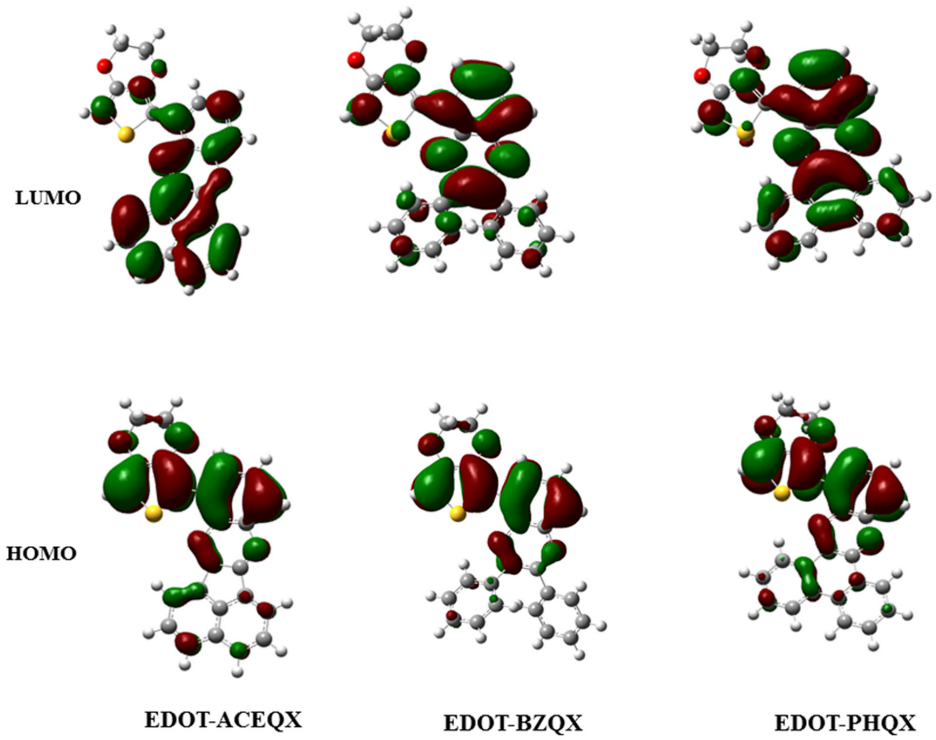

Fig. 4.2: Frontier molecular orbital distribution of monomeric units of P(EDOT-ACEQX), P(EDOT-BZQX), and P(EDOT-PHQX) by B3LYP/6-31G method.

4.2.2. Band structure of copolymers

The electronic structure and properties of the copolymers were well studied at the DFT level of theory as implemented in Gaussion 09[46] software package. In order to account for the reliability of the theoretical results with the experimental results, DFT calculations at two different levels (at B3LYP and HSE06) were carried out. The band structure of the copolymers, P(EDOT-ACEQX), P(EDOT-BZQX) and P(EDOT-PHQX) calculated through HSE06/6-31G level is as shown in Fig. 4.3.

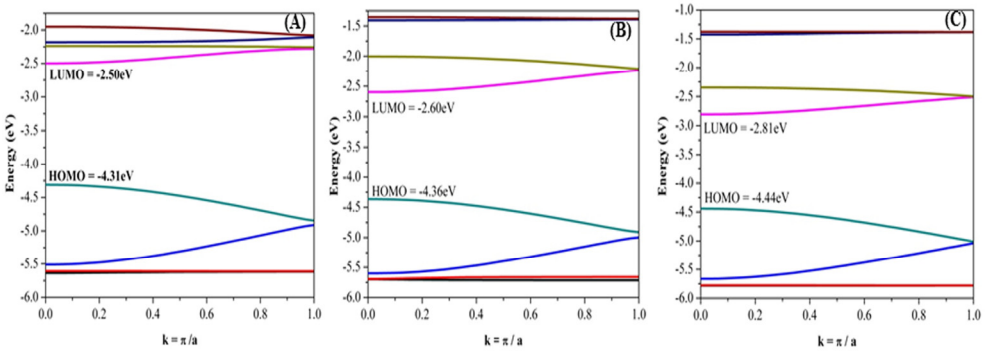

Fig. 4.3: Band structure of (A) P(EDOT-ACEQX), (B) P(EDOT-BZQX), and (C) P(EDOT-PHQX) by HSE06/6-31G method.

As expected, the regular insertion of quinoxaline unit lowers the LUMO level of PEDOT. From the Fig. 4.3, it could be seen that the band gaps for P(EDOT-ACEQX), P(EDOT-BZQX) and P(EDOT-PHQX) are 1.81, 1.76 and 1.63 eV, respectively, which are in the order of acceptor strength. The band structure data of the copolymers are summarized in Table 4.1. The LUMO level of PEDOT is reduced by a factor of 0.51, 0.61 and 0.82 eV, respectively, by introducing ACEQX, BZQX and PHQX units into the PEDOT backbone. The band gap of P(EDOT-PHQX) is much lower than that of both P(EDOT-BZQX) and P(EDOT-ACEQX).

Table 4.1: Computational data of P(EDOT-ACEQX), P(EDOT-BZQX) and P(EDOT-PHQX) with DFT/B3LYP/6-31G and DFT/HSE06/6-31G methods.

Copolymer	HOMO (eV)	LUMO (eV)	E_g (eV)
PEDOT	-3.62[a]	-1.99[a]	1.64[a]
P(EDOT-ACEQX)	-4.47[b]	-2.20[b]	2.27[b]
	-4.31[c]	-2.50[c]	1.81[c]
P(EDOT-BZQX)	-4.36[b]	-2.27[b]	2.09[b]
	-4.36[c]	-2.60[c]	1.76[c]
P(EDOT-PHQX)	-4.57[b]	-2.50[b]	2.07[b]
	-4.44[c]	-2.81[c]	1.63[c]

[a]Reproduced from Ref. 47, [b]Obtained by the DFT/B3LYP/6-31G method, [c]Obtained by the DFT/HSE06/6-31G method.

Significant difference is observed between the values of band gap obtained by the HSE06 and B3LYP methods. The difference between the DFT/B3LYP and HSE06 methods is that HSE06 exchange correlation functional uses an error function screened coulomb potential to calculate the exchange portion of the energy in order to improve computational efficiency.[43] N. Marom *et al*., have reported that screened-hybrid functionals such as the HSE approach reduce self-interaction errors in systems possessing both localized and delocalized orbitals and could be applied to both finite and extended systems.[48]

4.2.3. Monomer synthesis

Scheme 1 summarizes the synthesis of key monomers. 2,1,3-Benzothiadiazole (2) was prepared from o-phenylene diamine (1) and $SOCl_2$ in DCM. 4,7-Dibromo-2,1,3-benzothiadiazole (3) was prepared by bromination of 2,1,3-benzothiadiazole (2) in 47 % HBr. To obtain 2,3-diamino-1, 4-dibromobenzene (4), 4,7-dibromo-2,1,3-benzothiadiazole (3) was reduced by $NaBH_4$ in absolute ethanol. 5,8-Dibromoacenaphthylquinoxaline (8), 5, 8-dibromo-2,3-diphenylquinoxaline (9), 10,13-dibromodibenzo[a,c]phenazine (10) were synthesized through condensation reaction of 2,3-diamino-1, 4-dibromobenzene (4) with 1,2-acenaphthaquinone (5), benzil (6) and 9, 10-phenanthrenequinone (7) in ethanol/acetic acid mixture, in 70 %, 60 % and 72 % yields. The compounds were characterized using ^1H NMR and melting point measurement. All the reactions were performed according to standard procedures.[49]

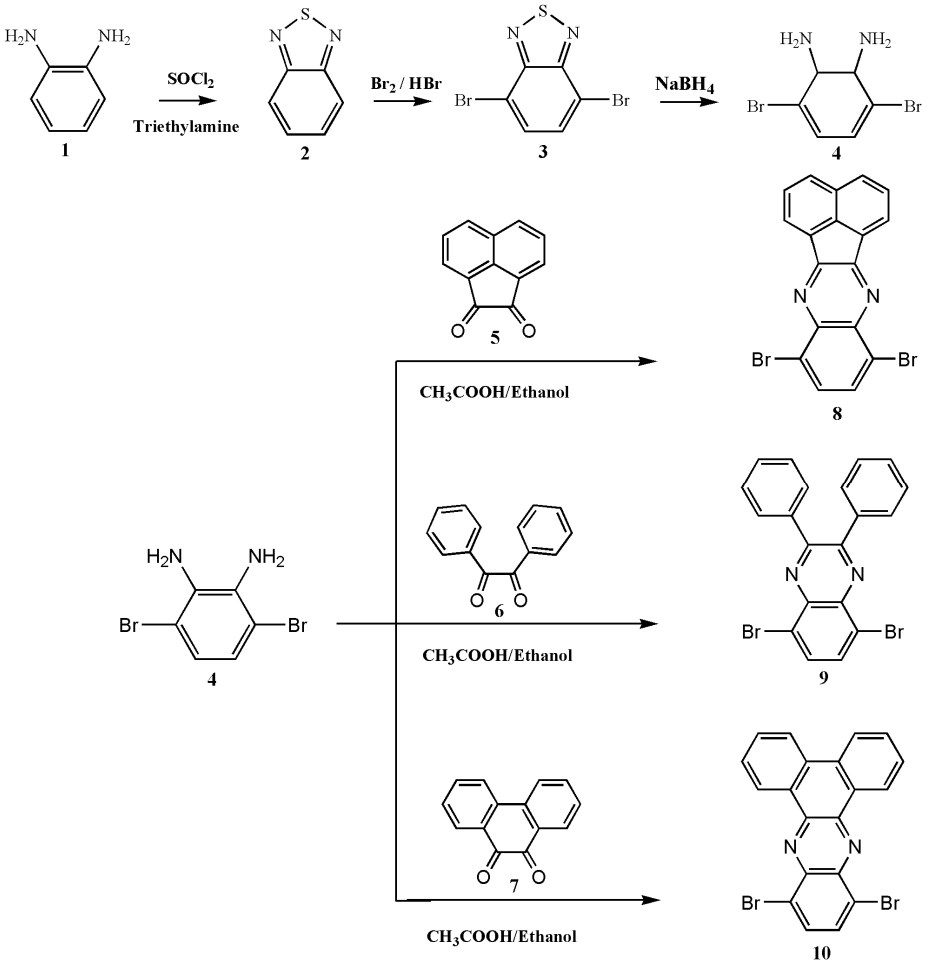

Scheme 1: Synthesis of quinoxaline monomers.

4.2.4. Polymer synthesis

The synthetic route toward the EDOT-quinoxaline copolymers is depicted in Scheme 2. The designed copolymers were synthesized by simple and economic method, direct arylation reaction using palladium acetate as catalyst.[38] It eliminates tedious steps involved in Stille and Suzuki polymerization reactions. The crude polymers were purified by precipitating in methanol followed by Soxhlet extraction using methanol and hexane. The

polymers were soluble in common organic solvents (50 mg/mL) such as chloroform, chlorobenzene and THF. Table 4.2 summarizes the polymerization results including molecular weight, polydispersity index (PDI) and yield of the copolymers. Only low molecular weight polymers were obtained by the polymerization method adopted. The reaction did not proceed to high yield, probably because of the steric hindrance offered by the quinoxaline ring.

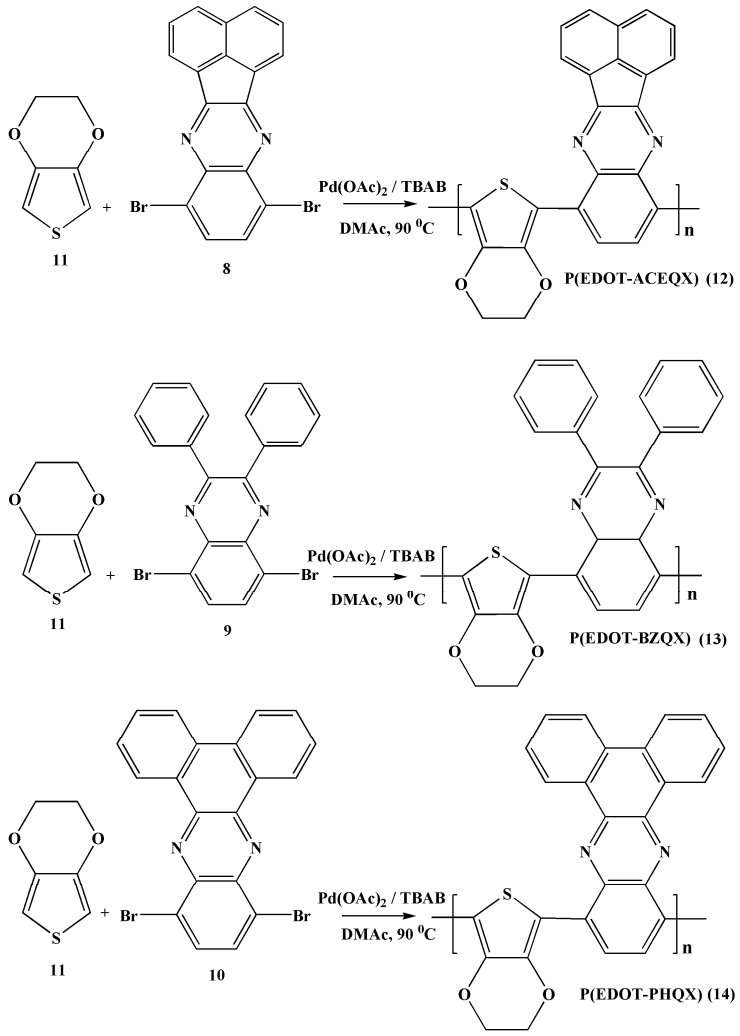

Scheme 2: Synthesis of P(EDOT-ACEQX), P(EDOT-BZQX) and P(EDOT-PHQX).

Table 4.2: Results of polymerization reaction.

Polymer	Mn[a]	Mw[a]	PDI[a]	Yield (%)
P(EDOT-ACEQX)	3789	6595	1.74	40
P(EDOT-BZQX)	3207	6300	1.96	45
P(EDOT-PHQX)	4556	6048	1.90	35

[a]Determined by GPC in THF based on polystyrene standards.

4.2.5. Structural characterization

The EDOT-quinoxaline copolymers were characterized by FT-IR (Fig. 4.4), ^{1}H NMR and XPS. FT-IR spectra of the P(EDOT-ACEQX) showed the following peaks: 3055 cm^{-1} (aromatic C-H stretching), 2949 cm^{-1} (aliphatic C-H stretching of ethylenedioxy group), 1551 cm^{-1} (aromatic C-C and C=N stretching of quinoxaline unit), 1062 cm^{-1} (C-O-C stretching vibration of ethylenedioxy group). The broad band around 1659 cm^{-1} was attributed to the polyconjugation in P(EDOT-ACEQX). Both P(EDOT-BZQX) and P(EDOT-PHQX) had consistent number of peaks as in P(EDOT-ACEQX). The results of FT-IR studies clearly indicated that the copolymerization was successfully achieved.

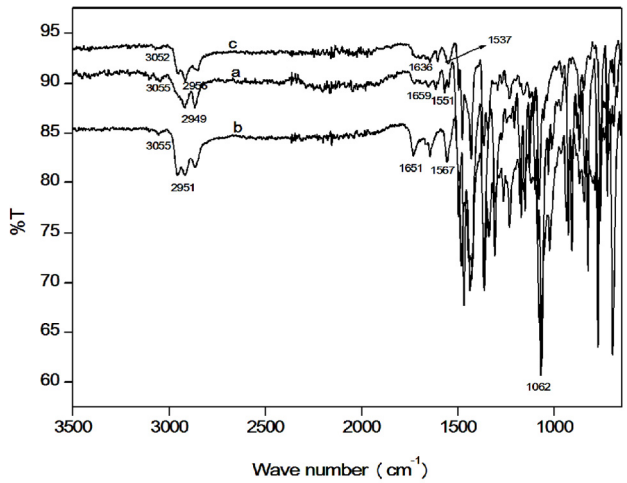

Fig. 4.4: FT-IR spectra of (a) P(EDOT-ACEQX), (b) P(EDOT-BZQX) and (c) P(EDOT-PHQX).

The ^{1}H NMR spectra (Fig. 4.5) of P(EDOT-ACEQX), P(EDOT-BZQX) and P(EDOT-PHQX) showed the resonance signals around 4.5 ppm which corresponded to the protons in ethylenedioxy ring of EDOT moieties in the copolymers. Additionally, P(EDOT-ACEQX), P(EDOT-BZQX) and P(EDOT-PHQX) revealed the multiple peaks at 7.8-8.8, 7.2-7.8 and 7.2-7.8 ppm, respectively which were attributed to aromatic protons of acenaphthylene, phenyl and phenanthrene substituted quinoxaline moieties in the copolymers. All the detected peaks are consistent with the proposed structure.

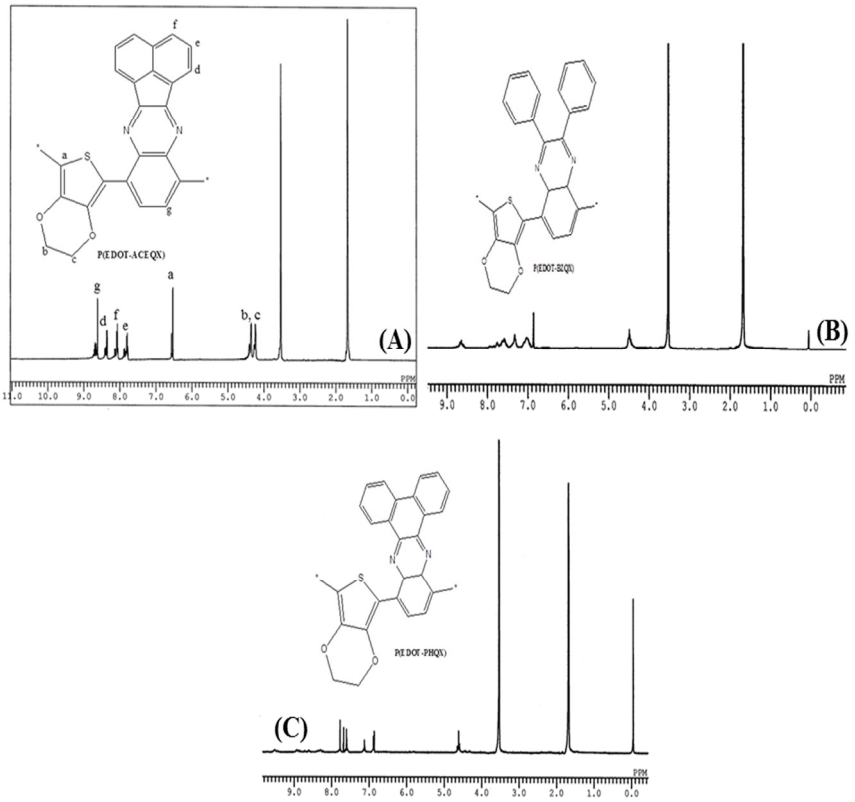

Fig. 4.5: ^{1}H NMR spectra of (A) P(EDOT-ACEQX), (B) P(EDOT-BZQX) and (C) P(EDOT-PHQX).

In order to evaluate the core level composition of the quinoxaline copolymers, XPS investigation was carried out. XPS survey scans of copolymers are depicted in Fig. 4.6. As seen in figure, The C1s signal observed at 283 eV, corresponded to the C-C bonding which was irrespective of the type of hybridization in the polymeric conjugated backbone. The N1s signal of copolymers observed at 396 eV, was mainly due to the nitrogen atoms in the quinoxaline moiety, and indicated the presence of C=N bonding. Moreover, the signals at 531 eV was attributed to the presence of O1s in the copolymers, and refers to the presence of C-O bonding in the copolymers. S2s and S2p core levels have signals at 226 and 163 eV, respectively.[50] XPS results of copolymers are in agreement with the FT-IR and ^{1}H NMR results. However, weak signals at 100 and 150 eV are seen in spectrum 'c', due to the presence of Si2p and Si2s which are originated from the silicon substrate.

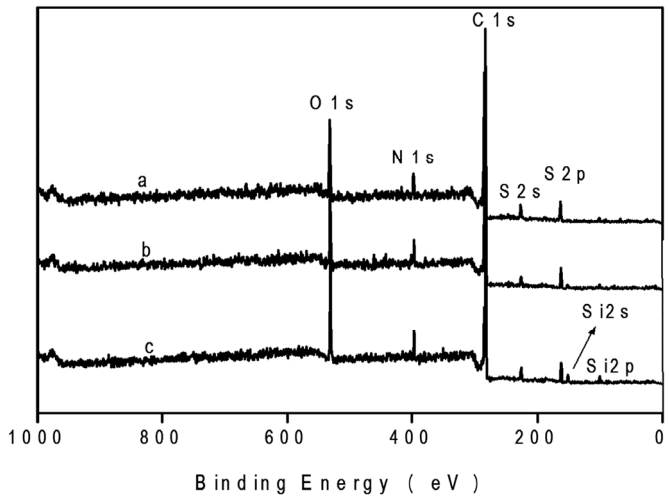

Fig. 4.6: XPS survey scans of (a) P(EDOT-ACEQX), (b) P(EDOT-BZQX) and (c) P(EDOT-PHQX).

4.2.6. Optical properties

To probe the spectral response of polymers, UV-Visible spectra were monitored both in THF solution and as thin film. The normalized optical absorption spectra of the three quinoxaline copolymers are depicted in Fig. 4.7. All the three quinoxaline polymers revealed two absorption maxima (λ_{max}), the first one in the shorter wavelength ranging from 300-450 nm, owing to π-π^* transition, whereas the second at the longer wavelength region, which refers to intramolecular charge transfer transitions from the donor, EDOT units to the acceptor, quinoxaline moieties. As shown in the figure, the P(EDOT-ACEQX) showed a broad absorption peak at 507 nm with an onset at 687 nm, whereas the P(EDOT-BZQX) and P(EDOT-PHQX) had peaks at 561 and 575 nm with an onset at 707 and 748 nm, respectively. The absorption maximum of P(EDOT-BZQX) and P(EDOT-PHQX) were red shifted by 54 and 68 nm, respectively compared to that of P(EDOT-ACEQX).

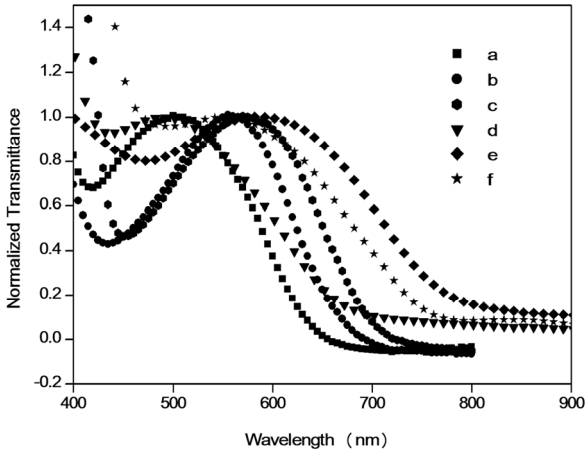

Fig. 4.7: UV-Visible spectra of the copolymers in THF solution (a) P(EDOT-ACEQX) (b) P(EDOT-BZQX), (c) P(EDOT-PHQX) and as thin film (d) P(EDOT-ACEQX), (e) P(EDOT-BZQX), (f) P(EDOT-PHQX). The polymer films were spin coated from $CHCl_3$ solution on to glass substrate.

The band gap of the copolymers, P(EDOT-ACEQX), P(EDOT-BZQX) and P(EDOT-PHQX) were calculated to be 1.80, 1.75 and 1.66 eV, respectively according to the onset edge of the lower energy peak of polymer in solution. As expected, the optical band gap varies as the function of the acceptor strength of the quinoxaline units. This could be because 'greater the acceptor strength of the quinoxaline, greater will be the donor-acceptor interaction', which leads to greater reduction in the band gap.[45] Thus, the reduction in the band gap is mainly due to the charge transfer from EDOT unit to the quinoxaline unit. These E_g^{opt} values could be correlated with the theoretical prediction that is obtained by HSE06/6-31G than the B3LYP/6-31G method. Despite the agreement, some deviations still exist due to the negligence of solid state effects such as polarization effects and intermolecular packing forces in the periodic boundary condition calculation.[51]

The thin film of polymers showed more broad absorption spectra than in solution phase. The λ_{max} of P(EDOT-BZQX) film was red shifted by 21 nm from the corresponding polymer in solution phase. While considering the P(EDOT-ACEQX) and P(EDOT-PHQX), the λ_{max} values are quite similar. The onset of absorption of P(EDOT-ACEQX), P(EDOT-BZQX) and P(EDOT-PHQX) were red shifted by 37, 103, and 34 nm, respectively. The band gap of P(EDOT-ACEQX), P(EDOT-BZQX), and P(EDOT-PHQX) obtained are 1.71, 1.53, and 1.58 eV, respectively. The significant redshift in band gap suggests reduction in conformational freedom, less solvent interaction, and aggregation/ordered arrangement in the solid state. Here, the band gap did not vary systematically with acceptor strength of quinoxaline unit. This could be due to the influence of polymer geometry. The geometry of the donor-acceptor material was significantly affected by

the ring size and intramolecular charge transfer;[45] i.e., the lower band gap of P(EDOT-BZQX) could be attributed to the structural planarity compared to the P(EDOT-ACEQX) and P(EDOT-PHQX), owing to the π-π interaction between the polymer chains.

4.2.7. Electrochemical studies

The electrochemical behaviour of the copolymers was investigated by cyclic voltammetry (CV). Electrochemical methods provide a means of establishing the HOMO and LUMO energies of conjugated polymers. The redox behaviour of polymer was measured using polymer coated platinum (Pt) electrode as working electrode, Pt wire as the counter, and Ag/Ag^+ as the reference electrodes in 0.1 M Bu_4NPF_6-acetonitrile solution. The electrochemical data of the polymers are summarized in Table 4.3. The HOMO and LUMO were estimated from the onset of oxidation and reduction potential according to the equation proposed by Bredas.[52]

The HOMO levels of P(EDOT-ACEQX), P(EDOT-BZQX) and P(EDOT-PHQX) are obtained to be -2.72, -2.65, and -2.66 eV, respectively. The LUMO levels were calculated to be -3.77, -3.65, and -3.65 eV, for P(EDOT-ACEQX), P(EDOT-BZQX) and P(EDOT-PHQX), respectively. The band gap of the copolymers were calculated to be 1.05, 1.0, and 0.99 eV, respectively, for P(EDOT-ACEQX), P(EDOT-BZQX) and P(EDOT-PHQX). The band gap of copolymers followed the order, P(EDOT-ACEQX) > P(EDOT-BZQX) > P(EDOT-PHQX), in the order of acceptor strength. The copolymers have relatively low LUMO energy compared to PEDOT, indicating better electron accepting/transporting property.[51] The electrochemical band gap showed deviations of the order of 0.6-0.75 eV

from the optical band gap. This could be due to the difference in the mechanism of optical excitation and electrochemical oxidation/reduction processes. In the former process, excitation creates excitons (bound electrons and hole pair) and the latter process creates ions. The low energy of excitons, compared to the ions and solvation of the ions during electrochemical experiment was reflected in the observed electrochemical band gap.

Table 4.3: Electrochemical data of P(EDOT), P(EDOT-ACEQX), P(EDOT-BZQX), P(EDOT-PHQX), P(EDOT-ACEQX-EDOT) and P(EDOT-BZQX-EDOT).

Polymer	Onset oxdn (V)	HOMO (eV)	Onset Redn(V)	LUMO (eV)	$E_g^{(el)}$ (eV)
P(EDOT)[a]		-3.62		-1.99	1.64
P(EDOT-ACEQX)[b]	-1.68	-2.72	-0.63	-3.77	1.05
P(EDOT-BZQX)[b]	-1.75	-2.65	-0.75	-3.65	1.0
P(EDOT-PHQX)[b]	-1.74	-2.66	-0.75	-3.65	0.99
P(EDOT-ACEQX-EDOT)[c]	-1.14		-0.51		0.93
P(EDOT-BZQX-EDOT)[d]					1.01

[a]Reproduced from Ref. 45, [b]Determined by CV, [c]Reproduced from Ref. 35, [d]Reproduced from Ref. 37.

4.2.8. Photoluminescence (PL) properties

The PL emission spectra of copolymers in THF and as film are shown in Fig. 4.8. In solution, copolymers exhibited distinct emission at 653, 672 and 731 nm for P(EDOT-ACEQX), P(EDOT-BZQX) and P(EDOT-PHQX), respectively. The red shift in emission maximum is observed for P(EDOT-BZQX) and P(EDOT-PHQX) compared to that of P(EDOT-ACEQX). The polymers exhibited emission max in the order of P(EDOT-PHQX) > P(EDOT-BZQX) > P(EDOT-ACEQX), which are in the order of acceptor strength of quinoxaline units.

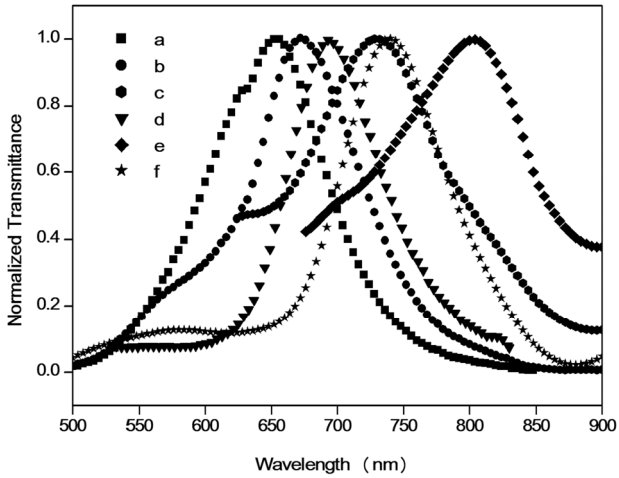

Fig. 4.8: PL spectra of the polymers (a) P(EDOT-ACEQX), (b) P(EDOT-BZQX), and (c) P(EDOT-PHQX) in THF solution, (d) P(EDOT-ACEQX), (e) P(EDOT-BZQX), and (f) P(EDOT-PHQX) as thin film.

To get insight into the intramolecular charge transfer process, PL spectra of thin films have been investigated. In thin film, all the copolymers revealed broad and red shifted emission with a tail extending to lower energy side of the spectrum, which indicated the efficient intramolecular charge transfer in copolymers. The emission peaks of P(EDOT-ACEQX), P(EDOT-BZQX) and P(EDOT-PHQX) in thin films are red shifted to around 692, 803 and 740 nm, respectively. This can be attributed to the reduced torsion angles between the adjacent units and hence the energy levels are affected in various degrees.[53] In thin film, polymers exhibited emission maximum in the order of P(EDOT-BZQX) > P(EDOT-PHQX) > P(EDOT-ACEQX). The red shift of emission of these alternating copolymers is not in consistence with the increasing order of acceptor strength of quinoxaline units. The variation in emission maximum of P(EDOT-BZQX) could be due to better delocalization and thus better intramolecular charge transition.

The most reliable method for determining the quantum yield is the comparative method proposed by Willams *et al*.,[54] which involve the use of well-known studied samples with known quantum yield (Φ) values. The absolute PL quantum yield of the polymers in solution was estimated by plotting the magnitude of the integrated fluorescence intensity against solution absorbance. Absolute values were calculated using the standard sample, rhodamine 6G (Φ_{std} = 0.75 in chloroform),[55] according to the following equation (1),

$$\phi_p = \frac{Grad_p}{Grad_{std}} \times \phi_{std} \quad \text{..... (1)}$$

where, the subscripts 'p' and 'std' denote polymer and standard, respectively and 'Grad' is the gradient from the plot of integrated fluorescence intensity vs. absorbance. The quantum yield of P(EDOT-ACEQX), P(EDOT-BZQX) and P(EDOT-PHQX), was obtained to be 0.21, 0.20 and 0.29, respectively. No systematic variation in the PL quantum yield with acceptor strength of quinoxaline units was observed.

4.2.9. Thermal properties

The thermal stability of the copolymers was investigated by both TGA and DSC. The TG traces of copolymers are depicted in Fig. 4.9. As shown in the figure, the copolymers reveal step wise degradation. DSC is devoid of any characteristic peak in the temperature range of 40 and 200 ^{o}C. This confirms the suitability in device applications. On the basis of TGA exotherm, the thermal decomposition temperature for P(EDOT-ACEQX), P(EDOT-BZQX) and P(EDOT-PHQX) were determined to be 146, 328 and 140 ^{o}C, respectively, choosing 5% weight loss at the onset loss point. The

P(EDOT-ACEQX) copolymer showed the degradation temperature at 173, 402 and 440^{o}C. While P(EDOT-BZQX) showed the degradation temperature of 406 and 435 ^{o}C. Whereas the copolymer P(EDOT-PHQX) showed the significant weight losses at 170, 250, 390 and 440 ^{o}C. The lower thermal stability of quinoxaline copolymers could be attributed to the presence of azomethine bonds which are highly prone to degradation. The copolymer, P(EDOT-BZQX) displayed more thermal stability than P(EDOT-ACEQX) and P(EDOT-PHQX), owing to the lack of ring strain in phenyl substituted quinoxaline when compared to the others.

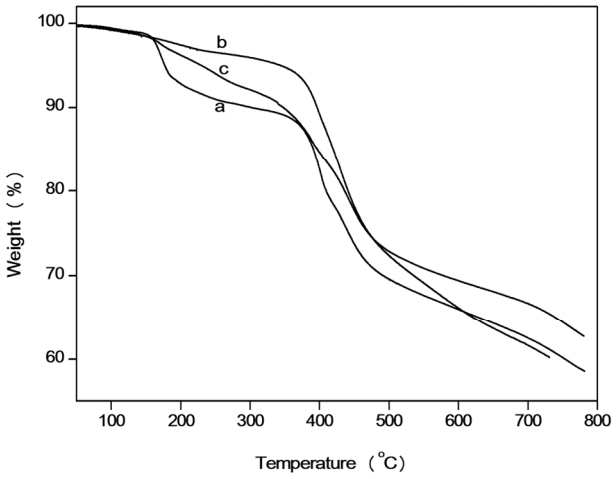

Fig. 4.9: TG traces of polymers (a) P(EDOT-ACEQX), (b) P(EDOT-BZQX) and (c) P(EDOT-PHQX).

4.2.10. Non-linear optical properties

The third-order NLO parameters of EDOT-quinoxaline copolymers were investigated using z-scan technique. To study the non-linear optical absorption of polymers, the open aperture (OA) z-scan technique was conducted at 532 nm. The OA trace of quinoxaline copolymers in dilute $CHCl_3$ (A) and as thin film (B) is shown in Fig. 4.10.

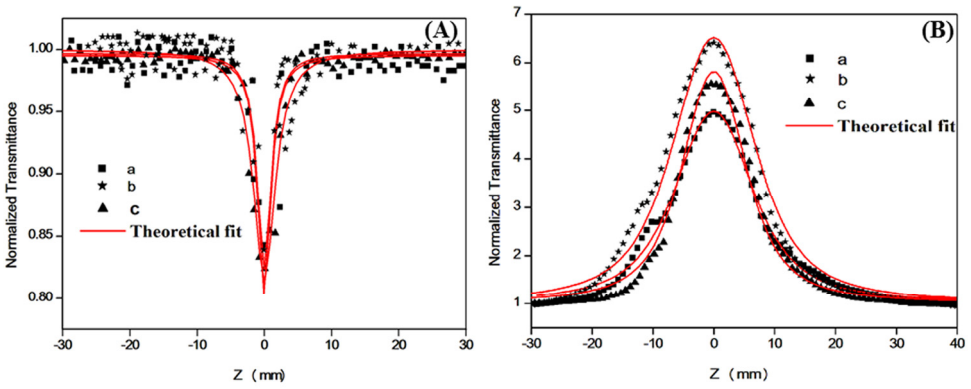

Fig. 4.10: Open aperture z-scan traces of (a) P(EDOT-ACEQX), (b) P(EDOT-BZQX) and (c) P(EDOT-PHQX), in solution (A) and as film (B) at 112 µJ.

In solution phase, copolymers depict a normalized transmittance valley, indicating the reverse saturation (RSA) type of absorption with a positive NLO absorption coefficient. However, the z-scan data of copolymer film show enhanced transmittance at the focus, indicating saturation absorption (SA) type behaviour with a negative NLO absorption coefficient. The switch over from RSA to SA could be attributed to ground state band bleaching of polymers in film phase.[56] The normalized transmittance for the standard OA z-scan[57] is expressed by the equation (2) (equation (3), given in section 2.2.7.). The theoretical curves obtained with the equation (2) (equation (3), given in section 2.2.7.) were fitted with the experimental data for SA and RSA and the effective non-linear absorption coefficients, β for the copolymers were calculated. Also the imaginary part of the third-order susceptibility ($\mathrm{Im}\,\chi^{(3)}$)[57] of copolymers is determined by equation (3) (equation (4), given in section 2.2.7.).

Closed aperture (CA)[57] z-scan measurements with aperture in front of the detector were performed to study the non-linear refractive index of the

polymers in $CHCl_3$. Fig. 4.11 shows the CA traces of EDOT-quinoxaline copolymers in $CHCl_3$. The CA traces show the transmittance maximum (peak) followed by transmittance minimum (valley) pattern for all the solutions. Thus, all the copolymers exhibited strong self-defocusing behaviour and negative non-linear refraction coefficient, n_2 as revealed in the peak-valley patterns. Since the CA transmittance is affected by both non-linear refraction and non-linear absorption, it is necessary to eliminate the effect of non-linear absorption from that of non-linear refraction. This could be achieved by dividing the CA z-scan data by the corresponding OA data. The normalized transmittance, T(z) for non-linear refraction[57] is given by the relation (4) (equation (5), given in section 2.2.7.). The non-linear refractive index (n_2), the real parts of $\chi^{(3)}$ (Re $\chi^{(3)}$) and third-order non-linear susceptibility ($\chi^{(3)}$) of EDOT-quinoxaline copolymers is calculated by the following equations (5)-(7)[57] (equations (6)-(8), given in section 2.2.7.).

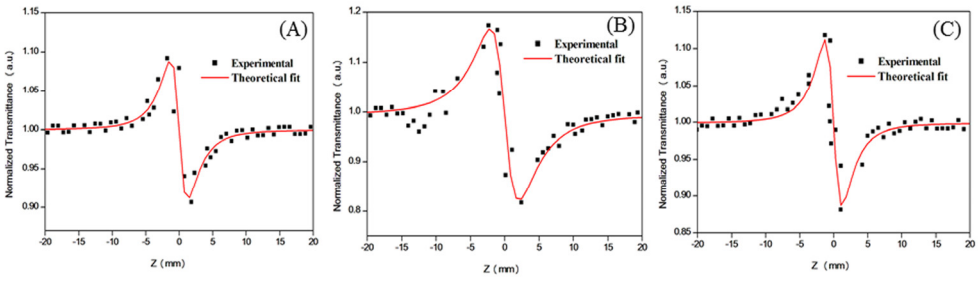

Fig. 4.11: Closed aperture z-scan traces of (A) P(EDOT-ACEQX), (B) P(EDOT-BZQX) and (C) P(EDOT-PHQX) at 112 µJ.

The calculated values of non-linear absorption coefficient (β, m/W), the non-linear refraction coefficient (n_2, esu) and the third-order non-linear susceptibility ($\chi^{(3)}$, esu) at 112 µJ are given in Table 4.4. The β value of P(EDOT-ACEQX), P(EDOT-BZQX) and P(EDOT-PHQX) is obtained to

be 1.58×10^{-10}, 0.4×10^{-10} and 2.54×10^{-10} m/W, respectively. Furthermore, the $\chi^{(3)}$ value is found to be 0.82×10^{-11}, 1.46×10^{-11} and 1.17×10^{-11} esu, respectively. Copolymers show strong optical non-linearity, due to donor-acceptor scheme. Here, non-linearity is mainly due to the charge transfer from donor to acceptor unit, i.e., due to strong delocalization of π electrons. The results also indicate that the structure of the copolymers have great impact on NLO properties. In film, saturation intensity (Is) was calculated using the equation $Is = -\alpha_o/ 2\beta$ and it was found to be 1.3×10^5, 1.6×10^5 and 1.47×10^5 W/m^2 for P(EDOT-ACEQX), P(EDOT-BZQX) and P(EDOT-PHQX), respectively, that too not in the order of acceptor strength.

Table 4.4: Values of non-linear absorption, non-linear refraction, and non-linear susceptibility of P(EDOT-ACEQX), P(EDOT-BZQX) and P(EDOT-PHQX) at 112 μJ intensity.

Copolymer	Non-linear absorption coefficient (β, m/W)	Non-linear refractive index (n_2, esu)	Imaginary part of non-linear susceptibility (Im $\chi^{(3)}$, esu)	Real part of non-linear susceptibility (Re $\chi^{(3)}$, esu)	Non-linear susceptibility ($\chi^{(3)}$, esu)
P(EDOT-ACEQX)	1.58×10^{-10}	-0.47×10^{-10}	0.04×10^{-10}	-0.72×10^{-11}	0.82×10^{-11}
P(EDOT-BZQX)	2.4×10^{-10}	-0.95×10^{-10}	0.01×10^{-10}	-1.42×10^{-11}	1.46×10^{-11}
P(EDOT-PHQX)	2.54×10^{-10}	-0.64×10^{-10}	0.06×10^{-10}	-1.0×10^{-11}	1.17×10^{-11}
P3[a]					1.57×10^{-12}
P2[b]	9.4×10^{-11}				2.7×10^{-11}
TPD-PFE[c]					5.7×10^{-14}
P[d]	3.0×10^{-11}				6.25×10^{-12}
P1[e]	1.3×10^{-11}				
HMePc[f]	5.7×10^{-12}		3.6×10^{-13}	1.9×10^{-13}	4.07×10^{-13}

[a]Reproduced from ref. 58, [b]Reproduced from ref. 59, [c]Reproduced from ref. 60, [d]Reproduced from ref. 61, [e]Reproduced from ref. 62, [f]Reproduced from ref. 63.

The results revealed that the copolymers investigated in the present study have a good non-linear optical response and are comparable to or even

better than the D-A copolymers reported in the literature (given in Table 4.4), and hence could be chosen as ideal candidates with potential applications for non-linear optics.

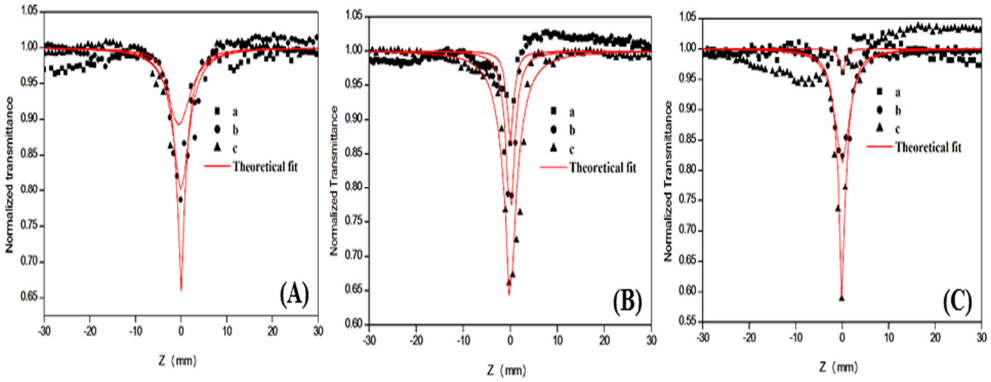

Fig. 4.12: The open-aperture z-scan traces of (A) P(EDOT-ACEQX), (B) P(EDOT-BZQX) and (C) P(EDOT-PHQX) at (a) 55, (b) 112 and (c) 141 µJ input fluences.

Fig. 4.12 shows variation of non-linear transmission of copolymers at different input fluences (55, 112 and 141 µJ). The calculated values of β at different fluences are gathered in Table 4.5. From the results it is clear that there is considerable variation in the non-linear absorption with input fluences.

Table 4.5: Calculated values of non-linear absorption coefficient of P(EDOT-ACEQX), P(EDOT-BZQX) and P(EDOT-PHQX) at 55, 112 and 141 µJ intensity.

Polymer	β (m/W) at 55 µJ	β (m/W) at 112 µJ	β (m/W) at 141 µJ
P(EDOT-ACEQX)	1.38×10^{-10}	1.58×10^{-10}	2.12×10^{-10}
P(EDOT-BZQX)	0.62×10^{-10}	2.4×10^{-10}	3.6×10^{-10}
P(EDOT-PHQX)	1.76×10^{-10}	2.54×10^{-10}	5.27×10^{-10}

4.2.11. Optical power limiting

To investigate the optical limiting property of the polymers, the non-linear transmission is measured as a function of input fluence. A material which transmits light at low input intensities and become opaque at high inputs is called optical limiter. Optical limiting property of a material is mainly due to absorptive non-linearity, which corresponds to the imaginary part of third-order susceptibility,[64] i.e., it could be due to TPA, free carrier absorption, RSA, self-focusing, self-defocusing or induced scattering. Thus, the optical limiting property of EDOT-quinoxaline copolymers was studied by a standard OA z-scan technique at 532 nm. As shown in Fig. 4.13, the approximate fluence at which the normalized transmission begins to deviate from linearity corresponds to optical limiting threshold and it is found to be 0.41, 0.35 and 0.41 GW/cm^2 for P(EDOT-ACEQX), P(EDOT-BZQX) and P(EDOT-PHQX), respectively, which are not in the order of acceptor strength of quinoxaline unit. In conjugated polymeric materials, electrons can move in the molecular orbitals, which results from the linear superposition of the carbon p_z atomic orbitals. This leads to high optical non-linearity, which increases with conjugation length.[65] On the other hand, non-linearity is the result of an optimum combination of various factors such as π-delocalization length, donor-acceptor groups, dimensionality, conformation, and orientation for a given molecular structure.[66-68] The results indicate that these polymers can be used for optical power limiting at high laser fluences.

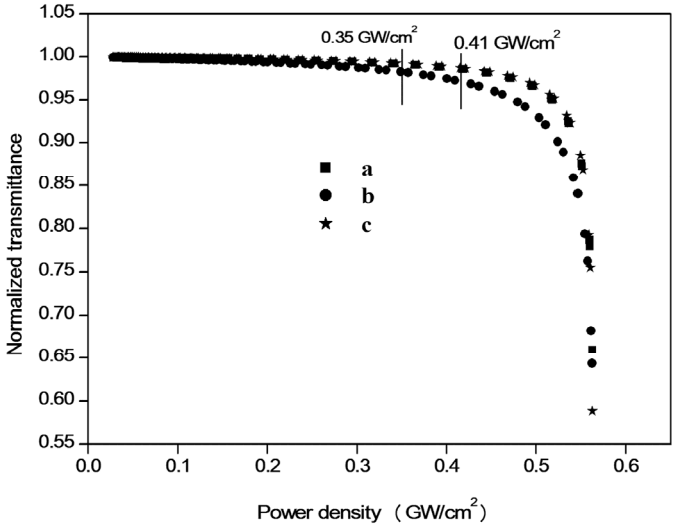

Fig. 4.13: Optical limiting curves of (a) P(EDOT-ACEQX), (b) P(EDOT-BZQX) and (c) P(EDOT-PHQX).

4.3. Materials and methods

4.3.1. Materials

3,4-Ethylenedioxythiophene (EDOT, Aldrich, 98 %), o-phenylene diamine (Merck, 98 %), tetrabutyl ammonium bromide (TBAB, Avra synthesis Pvt. Ltd., 98 %), sodium acetate (anhydrous) (Spectrochem Pvt. Ltd.), triethyl amine (Spectrochem Pvt. Ltd.), palladium (II) acetate (Aldrich, 99.98 %), tetrabutylammonium hexafluorophosphate (Bu_4NPF_6, Aldrich, >99 %), thionyl chloride ($SOCl_2$, Merck, 97 %), hydrobromic acid (HBr, Spectrochem Pvt. Ltd., 47 %), bromine (Merck), sodium borohydride ($NaBH_4$, Merck, 98%), ethanol absolute (Merck), diethyl ether (Spectrochem Pvt. Ltd.), magnesium sulphate (anhydrous) ($MgSO_4$, Spectrochem Pvt. Ltd.), acenaphthenequinone (Aldrich), benzil (Aldrich, 98 %), phenanthrene-9,10-dione (Aldrich, 95 %) and glacial acetic acid were used as received. Acetonitrile HPLC grade (CH_3CN, Aldrich), dimethyl acetamide (anhydrous)

(DMAc, Spectrochem Pvt. Ltd), chloroform ($CHCl_3$, Spectrochem Pvt. Ltd.), dicholoromethane (CH_2Cl_2, Spectrochem Pvt. Ltd.), tetrahydrofuran HPLC grade (THF, Spectrochem Pvt. Ltd.), hexane (Spectrochem Pvt. Ltd.) and methanol (anhydrous) (MeOH, Spectrochem Pvt. Ltd.) were dried and distilled when necessary according to the standard procedures.

4.3.2. Computation methods

Theoretical calculations were done using computational methods, which has been described in section 2.3.4.

4.3.3. Chemical procedures

4.3.3.1. *Synthesis of 5,8-dibromoacenaphthyl quinoxaline (ACEQX) (8):*

A solution of 2,3-diamino-1,4-dibromobenzene (4) (0.15 g, 0.56 mmol) (section 3.3.3.3) and acenaphthenequinone (5) (0.10 g, 0.55 mmol) in ethanol (20 mL) and few drops of glacial acetic acid was heated to reflux for 1h, and cooled to 0 ^{o}C. The precipitate formed was separated by filtration and washed with ethanol to afford 5,8-dibromoacenaphthyl quinoxaline (8) as light yellow solid.

Yield	:	70 %
^{1}H NMR (400 MHz, $CDCl_3$)	:	δ 8.54 (d, 2H), 8.15 (d, 2H), 7.92 (s, 2H), 7.89-7.86 (m, 2H).

4.3.3.2. *Synthesis of 5,8-dibromo-2,3-diphenyl quinoxaline (BZQX) (9):*

A solution of 2,3-diamino-1,4-dibromobenzene (4) (1.0 g, 3.8 mmol) (section 3.3.3.3) and benzil (6) (0.80 g, 3.8 mmol) in ethanol (40 mL) and few drops of glacial acetic acid was heated to reflux for 1h, and cooled to

0 ^{o}C. The precipitate formed was isolated by filtration and washed with ethanol to afford 5,8-dibromo-2,3-diphenyl quinoxaline (9) as light yellow solid.

Yield : 60 %

M. P. : 221 ^{o}C.

^{1}H NMR (400 MHz, $CDCl_3$) : δ 7.92 (s, 2H), 7.64 (m, 4H), 7.37 (m, 6 H).

4.3.3.3. *Synthesis of 10,13-dibromodibenzo[a,c]phenazine (PHQX) (10):*

A solution of 2,3-diamino-1,4-dibromobenzene (4) (1.03 g, 3.9 mmol) (section 3.3.3.3) and phenanthrene-9,10-dione (7) (0.81 g, 3.9 mmol) in 42 mL ethanol/acetic acid (20:1) was heated to reflux for 2 h, and cooled to 0 ^{o}C. The precipitate formed was isolated by filtration and washed with ethanol to afford 10,13-dibromodibenzo[a,c]phenazine (10) as yellow solid.

Yield : 72 %.

M.P. : 317 ^{o}C

^{1}H NMR (400 MHz, $CDCl_3$) : δ 9.48 (dd, J1=8 Hz, J2=1.2 Hz, 2 H), 8.57 (dd, J1=8 Hz, J2=0.8 Hz, 2 H), 8.04 (s, 2H), 7.87-7.83 (dt, J1=15.2 Hz, J2=1.6 Hz, 2 H), 7.81-7.77 (dt, J1=13.2 Hz, J2=1.2 Hz, 2 H).

4.3.3.4. *Synthesis of P(EDOT-ACEQX) (12):*

To a stirred solution of EDOT (11) (0.024 g, 0.17 mmol) in 10 mL DMAc was added TBAB (0.05 g, 0.17 mmol) and sodium acetate (0.05 g, 0.68 mmol). The reaction mixture was stirred at room temperature for 30 min followed by addition of 5,8-dibromoacenaphthyl quinoxaline (8)

(0.07 g, 0.17 mmol) and 10 % palladium acetate (0.003 g). The reaction mixture was stirred at 90 ^{o}C for 48 h. The reaction mixture was cooled to room temperature and poured in to methanol (20 mL). The precipitate was filtered and washed with methanol. The polymer was purified by soxhlet extraction using hexane and methanol for 24 h. The residue was dissolved in minimum amount of $CHCl_3$ and precipitated using methanol and dried under vacuum.

Yield	: 40%
FT-IR (ν_{max}/cm^{-1})	: 3055br (C-H ar), 2949s (C-H), 1551w (C-C/C=N), 1062s and 905w (C-O), 1659br (conjugation).
^{1}H NMR (400 MHz, d8-THF)	: δ (ppm): 4.3 (m, 2H), 4.5 (m, 2H), 7.6 (s, 1H), 7.8 (m, 2H), 8.1 (m, 2H), 8.4 (m, 2H), 8.7 (m, 2H).

4.3.3.5. *Synthesis of P(EDOT-BZQX) (13):*

To a stirred solution of EDOT (11) (0.024 g, 0.17 mmol) in 10 mL DMAc was added TBAB (0.05 g, 0.17 mmol) and sodium acetate (0.05 g, 0.68 mmol). The reaction mixture was stirred at room temperature for 30 min followed by addition of 5,8-dibromo-2,3-diphenylquinoxaline (9) (0.074 g, 0.17 mmol) and 10% palladium acetate (0.003 g). The reaction mixture was stirred at 90 ^{o}C for 48 h. The reaction mixture was cooled to room temperature and poured in to methanol. The precipitate was filtered and washed with methanol. The polymer was purified by soxhlet extraction using hexane and methanol for 24 h. The residue was dissolved in minimum amount of $CHCl_3$ and precipitated using methanol and dried under vacuum.

Yield : 45 %.

FT-IR (ν_{max}/cm^{-1}) : 3055br (C-H ar), 2951s (C-H), 1567w (C-C/C=N), 1062s and 905w (C-O), 1651br (conjugation).

^{1}H NMR (400 MHz, d8-THF): δ (ppm): 4.5 (m, 4H), 6.9 (s, 1H), 7.0 (m, 2H), 7.4 (m, 2H), 7.6 (m, 2H), 8.7 (m, 2H).

4.3.3.6. *Synthesis of P(EDOT-PHQX) (14):*

To a stirred solution of EDOT (11) (0.024 g, 0.17 mmol) in 10 mL DMAc was added TBAB (0.05 g, 0.17 mmol) and sodium acetate (0.05 g, 0.68 mmol). The reaction mixture was stirred at room temperature for 30 min followed by addition of 10,13-dibromodibenzo[a,c]phenazine (10) (0.074 g, 0.17 mmol) and 10% palladium acetate (0.003 g). The reaction mixture was stirred at 90 ^oC for 48 h. The reaction mixture was cooled to room temperature and poured in to methanol. The precipitate was filtered and washed with methanol (20 mL). The polymer was purified by soxhlet extraction using hexane and methanol for 24 h. The residue was dissolved in minimum amount of $CHCl_3$ and precipitated using methanol and dried under vacuum.

Yield : 35 %.

FT-IR (ν_{max}/cm^{-1}) : 3052br (C-H ar), 2956s (C-H), 1537w (C-C/C=N), 1062s and 905w (C-O), 1636br (conjugation).

^{1}H NMR (400 MHz, d8-THF): δ (ppm): 4.7 (m, 4H), 6.9 (s, 1H), 7.1 (m, 2H), 7.6 (m, 2H), 7.7 (m, 2H), 7.8 (m, 2H).

4.3.4. Instrumentation

EDOT-quinoxaline copolymers were characterized by instrumentation methods which have been described in section 2.3.3.

4.3.5. NLO Measurements

NLO properties were measured by methods which have been described in section 2.3.6.

4.4. Conclusions

Three alternating D-A EDOT-quinoxaline copolymers were designed and have been synthesized by an economic method, direct arylation from the corresponding EDOT and quinoxaline monomers. The electronic structure of copolymers were calculated using HSE06/6-31G and B3LYP/6-31G method. Theoretically predicted values are in good agreement with the optical band gap. The copolymers, P(EDOT-ACEQX), P(EDOT-BZQX), and P(EDOT-PHQX) exhibited electrochemical band gap of 1.05, 1.0 and 0.99 eV, respectively. The reduction in band gap is the function of the acceptor strength of the quinoxaline unit. Third-order non-linear optical parameters of EDOT-quinoxaline copolymers were studied by z-scan technique. The z-scan results imply that the copolymers exhibited negative non-linear absorption and the β value was obtained to in the order of 10^{-10} m/W. The non-linear refractive index of copolymers was found to be negative and it was in the order of 10^{-11} esu.

References

[1] J. Roncali, *Macromol. Rapid Commun*., 2007, 28, 1761.

[2] E. E. Havinga, W. T Hoeve, H. Wynberg, *Polym. Bull*., 1992, 29, 119.

[3] N. R. Evans, L. S. Devi, C. S. K. Mak, S. E. Watkins, S. I. Pascu, A. Kohler, R. H. Friend, C. K. Williams, A. B. Holmes, *J. Am. Chem. Soc.,* 2006, 128, 6647.

[4] Q. Huang, G. A. Evmenenko, P. Dutta, P. Lee, N. R. Armstrong, T. J. Marks, *J. Am. Chem. Soc*., 2005, 127, 10227.

[5] P. Dutta, H. Park, W. -H. Lee, I. N. Kang, S. -H. Lee, *Polym. Chem*., 2014, 5, 132.

[6] Q. Hou, J. Liu, T. Jia, S. Luo, G. Shi, *J. Appl. Polym. Sci.,* 2013, 130, 3276.

[7] W. Zhuang, M. Bolognesi, M. Seri, P. Henriksson, D. Gedefaw, R. Kroon, M. Jarvid, A. Lundin, E. Wang, M. Muccini, M. R. Andersson, *Macromolecules*, 2013, 46, 8488.

[8] E. Zhou, J. Cong, K. Hashimoto, K. Tajima, *Macromolecules*, 2013, 46, 763.

[9] L. Dou, C. -C. Chen, K. Yoshimura, K. Ohya, W. -H. Chang, J. Gao, Y. Liu, E. Richard, Y. Yang, *Macromolecules*, 2013, 46, 3384.

[10] P. M. Beaujuge, J. R. Reynolds, *Chem. Rev*., 2010, 110, 268.

[11] P. Shi, C. M. Amb, A. L. Dyer, J. R. Reynolds, *Appl. Mater. Interfaces*, 2012, 4, 6512.

[12] E. Kaya, A. Balan, D. Baran, A. Cirpan, *Organic Electronics*, 2011, 12, 202.

[13] K. Yamazaki, J. Kuwabara, T. Kanbara, *Macromol. Rapid Commun.,* 2013, 34, 69.

[14] J. Kuwabara, T. Yasuda, S. J. Choi, W. Lu, K. Yamazaki, S. Kagaya, L. Han, T. Kanbara, *Adv. Funct. Mater*., 2014, 24, 3226.

[15] Y. Nohara, J. Kuwabara, T. Yasuda, L. Han, T. Kanbara, *J. Polym. Sci., Part A: Polym. Chem.*, 2014, 52, 1401.

[16] A. E. Rudenko, B. C. Thompson, *J. Polym. Sci., Part A: Polym. Chem.*, 2015, 53, 135.

[17] M. K. Poduval, P. M. Burrezo, J. Casado, J. T. L. Navarrete, R. P. Ortiz, T. -H. Kim, *Macromolecules*, 2013, 46, 9220.

[18] M. Melucci, P. Frere, M. Allain, E. Levillain, G. Barbarella, J. Roncali, *Tetrahedron*, 2007, 63, 9774.

[19] P. Karastatiris, J. A. Mikroyannidis, I. K. Spiliopoulos, *Macromolecules,* 2004, 37, 7867.

[20] E. Xu, H. Zhong, H. Lai, D. Zeng, J. Zhang, W. Zhu, Q. Fang, *Macromol. Chem. Phys*., 2010, 211, 651.

[21] P. -I. Lee, S. L. -C. Hsu, P. Lin, *Macromolecules*, 2010, 43, 8051.

[22] G. Zhang, Y. Fu, Q. Zhang, Z. Xie, *Polymer*, 2010, 51, 2313.

[23] H. Yi, R. G. Johnson, A. Iraqi, D. Mohamad, R. Royce, D. G. Lidzey, *Macromol. Rapid Commun*., 2008, 29, 1804.

[24] D. Kitazawa, N. Watanabe, S. Yamamoto, J. Tsukamoto, *Appl. Phys. Lett*., 2009, 95, 053701.

[25] H. J. Song, J. Y. Lee, E. J. Lee, D. K. Moon, *Eur. Polym. J.,* 2013, 49, 3261.

[26] H. J. Song, T. H. Lee, M. H. Han, J. Y. Lee, D. K. Moon, *Polymer*, 2013, 54, 1072.

[27] Y. Lee, T. P. Russell, W. H. Jo, *Organic Electronics*, 2010, 11, 846.

[28] H. Tan, X. Deng, J. Yu, J. Chen, K. Nie, Y. Huang, Y. Liu, Y. Wang, M. Zhu, W. Zhu, *J. Polym. Sci., Part A: Polym. Chem.*, 2013, 51, 1051.

[29] S. Özdemir, A. Balan, D. Baran, Ö. Dogan, L. Toppare, *React. Funct. Polym.,* 2011, 71, 168.

[30] S. Celebi, D. Baran, A. Balan, L. Toppare, *Electrochim. Acta*, 2010, 55, 2373.

[31] S. Tarkuc, Y. A. Udum, L. Toppare, *Thin Solid Films*, 2012, 520, 2960.

[32] R. Matsidik, X. Mamtimin, H. Y. Mi, I. Nurulla*, J. Appl. Polym. Sci*., 2010, 118, 74.

[33] A. T. Taskina, A. Balana, B. Epika, E. Yildiz, Y. A. Udumb, L. Topparea, *Electrochim. Acta*, 2009, 54, 5449.

[34] G. Gunbas, A. Durmus, L. Toppare, *Adv. Funct. Mater*., 2008, 18, 2026.

[35] X. Mamtimin, R. Matsidik, A. Obulda, S. Sidik, I. Nurulla, *Fibers and Polymers*, 2013, 14, 1066.

[36] F. Algi, A. Cihaner, *Organic electronics*, 2009, 10, 704.

[37] A. Durmus, G. E. Gunbas, L. Toppare, *Adv. Mater.,* 2008, 20, 691.

[38] A. Kumar, A. Kumar, *Polym. Chem.,* 2010, 1, 286.

[39] R. G. Parr, W. Yang, Density-Functional Theory of Atoms and Molecules, Oxford University Press, New York, 1989.

[40] A. D. Becke, *J. Chem. Phys*., 1993, 98, 5648.

[41] C. Lee, W. Yang, R. G. Parr, *Phys. Rev. B*., 1994, 37, 785.

[42] K. Burke, J. P. Perdew, Y. Wang, J. F. Dobson, G. Vignale, M. P. Das, Electronic Density Functional Theory: Recent Progress and New Directions, Plenum Press, New York, 1998.

[43] J. Heyd, G. E. Scuseria, M. Ernzerhof, *J. Chem. Phys*., 2003, 118, 8207.

[44] A. V. Krukau, O. A. Vydrov, A. F. Izmaylov, G. E. Scuseria, *J. Chem. Phys*., 2006, 125, 224106.

[45] C. -L. Pai, C. -L. Liu, W. -C. Chen, S. A. Jenekhe, *Polymer*, 2006, 47, 699.

[46] Gaussian 09, Revision B02, M. J. Frisch, G. W. Trucks, H. B. Schlegel, G. E. Scuseria, M. A. Robb, J. R. Cheeseman, G. Scalmani, V. Barone, B. Mennucci, G. A. Petersson, H. Nakatsuji, M. Caricato, X. Li, H. P. Hratchian, A. F. Izmaylov, J. Bloino, G. Zheng, J. L. Sonnenberg, M. Hada, M. Ehara, K. Toyota, R. Fukuda, J. Hasegawa, M. Ishida, T. Nakajima, Y. Honda, O. Kitao, H. Nakai, T. Vreven, Jr. J. A. Montgomery, J. E. Peralta, F. Ogliaro, M. Bearpark, J. J. Heyd, E. Brothers, K. N. Kudin, V. N. Staroverov, R. Kobayashi, J. Normand, K. Raghavachari, A. Rendell, J. C. Burant, S. S. Iyengar, J. Tomasi, M. Cossi, N. Rega, N. J. Millam, M. Klene, J. E. Knox, J. B. Cross, V. Bakken, C. Adamo, J. Jaramillo, R. Gomperts, R. E. Stratmann, O. Yazyev, A. J. Austin, R. Cammi, C. Pomelli, J. W. Ochterski, R. L. Martin, K. Morokuma, V. G. Zakrzewski, G. A.Voth, P. Salvador, J. J. Dannenberg, S. Dapprich, A. D. Daniels, Ö. Farkas, J. B. Foresman, J. V. Ortiz, J. Cioslowski, D. J. Fox, Gaussian, Inc., Wallingford CT, 2009.

[47] C. -L. Pai, C. -L. Liu, W. -C. Chen, S. A. Jenekhe, *Polymer*, 2006, 47, 699.

[48] N. Marom, A. Tkatchenko, M. Rossi, V. V. Gobre, O. Hod, M. Scheffler, L. Kronik, *J. Chem. Theory Comput.*, 2011, 7, 3944.

[49] M. Younus, A. Kohler, S. Cron, N. Chhawdary, M. R. A. Al-Mandhary, M. S. Khan, J. Lewis, N. J. Long, R. H. Friend, P. R. Raithby, *Angew. Chem. Int. Ed.,* 1998, 37, 3036.

[50] M. Yildirim, I. Kaya, A. Aydin, *React. Funct. Polym.,* 2013, 73, 1167.

[51] L. Yang, J. -K. Feng, A. -M. Ren, J. -Z. Sun, *Polymer*, 2006, 47, 1397.

[52] J. L. Bredas, R. Silbey, D. X. Boudreux, R. R. Chance, *J. Am. Chem. Soc*., 1983, 105, 6555.

[53] S. M. Cassemiro, C. Zanlorenzi, T. D. Z. Atvars, G. Santos, F. J. Fonseca, L. Akcelruf, *J. Lumin.*, 2013, 134, 670.

[54] A. T. R. Williams, S. A. Winfield, J. N. Miller, *Analyst*, 1983, 108, 1067.

[55] R. Reisfeld, R. Zusman, Y. Cohen, M. Eyal, *Chem. Phys. Lett.,* 1988, 147, 142.

[56] A. Thankappan, S. Thomas, V. P. N. Nampoori, *Opt. Laser Technol.,* 2014, 58, 63.

[57] M. S. -Bahae, A. A. Said, T. -H. Wei, D. J. Hagan, E. W. VanStryland, *IEEE Journal of Quantum Electronics*, 1990, 26, 760.

[58] P. K. Hegde, A. V. Adhikari, M. G. Manjunatha, C. S. S. Sandeep, R. Philip, *J. Appl. Polym. Sci.*, 2010, 117, 2641.

[59] M. S. Sunitha, A. V. Adhikari, K. A. Vishnumurthy, K. Safakath, R. Philip, *Int. J. Polymer. Mater.*, 2012, 61, 483.

[60] X. Zhan, Y. Liu, D. Zhu, W. Huang, Q. Gong, *Chem. Mater.,* 2001, 13, 1540.

[61] K. A. Vishnumurthy, A. V. Adhikari, M. S. Sunitha, K. A. A. Mary, R. Philip, *Synth. Met.,* 2011, 161, 1699.

[62] P. K. Hegde, A. V. Adhikari, M. G. Manjunatha, C. S. Sundeep, R. Philip, *Synth. Met*., 2010, 160, 1712.

[63] X. Chen, J. Zhang, W. Wei, Z. Jiang, Y. Zhang, *Eur. Polym. J*., 2014, 53, 58.

[64] S. Mathew, A. D. Saran, S. A. Joseph, B. S. Bhardwaj, D. Punj, P. Radhakrishnan, V. P. N. Nampoori, C. P. G. Vallabhan, J. R. Bellare, *J Mater Sci: Mater Electron*, 2012, 23, 739.

[65] S. Q. Zheng, H. Guang, L. Changgui, P. N. Prasad, *J. Mat. Chem*., 2005, 15, 3488.

[66] J. L. Bredas, C. Adant, P. Tackx, A. Persoons, M. Pierce, *Chem. Rev.,* 1994, 94, 243.

[67] P. N. Prasad, D. J. Williams, Introduction to nonlinear optical effects in molecules and polymers, John Wiley, 1991.

[68] P. Audebert, K. Kamada, K. Matsunaga, K. Ohta, *Chem. Phys. Lett*., 2003, 367, 62.

.....ഇ൦ര.....

Chapter 5

Third-order Non-linear Optical Properties of EDOT-Thiophene Copolymers*

Abstract

Alternate copolymers of thiophene (TH) and 3-methyl thiophene (MeTH) with EDOT (3,4-ethylenedioxythiophene) were synthesized via a simple and facile route, i.e., direct arylation and their electronic and third-order non-linear optical properties were investigated. The resultant copolymers, P(EDOT-TH) and P(EDOT-MeTH) were characterized by FT-IR, ^1H NMR and XPS. The photophysical, thermal and electrochemical characterizations were performed to highlight the structural attributes to the electronic properties of the copolymers. The band structure of the homopolymers and copolymers have been investigated by quantum mechanical calculation using density functional theory (DFT) at B3LYP/6-31G level. The copolymers revealed low band gap and better electronic properties as compared to the homopolymers. The introduction of EDOT unit in the polythiophene leads to decreased HOMO-LUMO energy levels, and the absorption spectra was red shifted when compared with that of the parent compound. The third-order optical non-linearities of EDOT-thiophene copolymers were studied by z-scan method under nanosecond excitation. The non-linear absorption and non-linear refraction coefficient of copolymers have been investigated at 532 nm. The optical limiting properties of copolymers have also been measured. The copolymers exhibited strong optical non-linearity owing to the presence of alternate donor-π-acceptor scheme in the polymers.

* Third-order Non-linear Optical Properties of EDOT-thiophene Copolymers, Sona Narayanan, Sreejesh Poikavila Raghunathan, Sebastian Mathew, Krishnapillai Sreekumar, Cheranellore Sudha Kartha, Rani Joseph, Polymer International. (Under Review)

5.1. Introduction

A great deal of attention was focused on donor-acceptor polymers owing to the broad spectrum range and commercial applications in photovoltaics,[1-4] light emitting diodes (LEDs),[5] and electrochromic devices.[6-8] EDOT bearing copolymers have received a great deal of research interest because of their potential application in opto-electronic devices.[9-11] Several synthetic strategies have been described for the modification of polymer backbone. Structural modifications can be done by altering the planarity of backbone as a function of steric hindrance, increasing the conjugation length by means of fused heterocyclic rings, the attachment of electron-donating and/or electron-accepting group to the repeating unit or by copolymerization of different monomers. Band structure engineering by copolymerization is ideally suited to develop narrow band gap polymers with broad band spectrum. This strategy enables the fine-tuning of band gap and leads to an interesting combination of properties. The copolymerization of EDOT and thiophene has been studied in several reports.[12-14] Herein, the copolymerization of thiophene and 3-methyl thiophene by direct arylation is described with a view to improve the electronic properties of the copolymers. The opto-electronic properties of the conjugated polymers mainly depend on the HOMO and LUMO energy levels. In this chapter, it was aimed to investigate the effects of EDOT units on the band structure of thiophene and 3-methyl thiophene homopolymers. The structural characterization was carried out with various spectral techniques. Electronic structure and properties of resultant copolymers were investigated through DFT calculation at B3LYP/6-31G level of theory.

Materials possessing large third-order non-linear optical (NLO) coefficients have been subjected to extensive study as regards their potential applications in optical switching,[15,16] three dimensional (3D) fluorescence imaging,[17] 3D optical data storage,[18] 3D lithographic micro fabrication,[19,20] and optical power limiting.[21-25] Among the wide range of NLO materials, π conjugated organic molecules appear as most promising because of their potentially large third-order susceptibility, fast response time and processablity.[26,27] Several design strategies available for getting large optical non-linearity in organic molecules are donor-acceptor-donor (D-A-D), donor-π-donor (D-π-D), donor-π-acceptor (D-π-A) and acceptor-donor-acceptor (A-D-A) arrangements.[28,29] This in turn intrigued our research interest in third-order NLO properties of EDOT/thiophene copolymers. The values of the effective non-linear optical absorption, refraction coefficients and the third-order non-linear susceptibility of P(EDOT-TH) and P(EDOT-MeTH), determined using z-scan technique, are reported here.

5.2. Results and Discussion

5.2.1. Electronic structure of model compounds

Theoretical calculation based on DFT[30] was employed to investigate the electronic properties of model compounds. To gain more insight into the structural dependence on the energy band gap of the oligomers, the geometry optimizations were carried out at B3LYP[31-33]/6-31G level of theory as implemented in Gaussian 09 package.[34] Fig. 5.1 compares the highest occupied molecular orbital (HOMO), lowest unoccupied molecular orbital (LUMO) energy levels and band gap of model compounds and the monomer units.

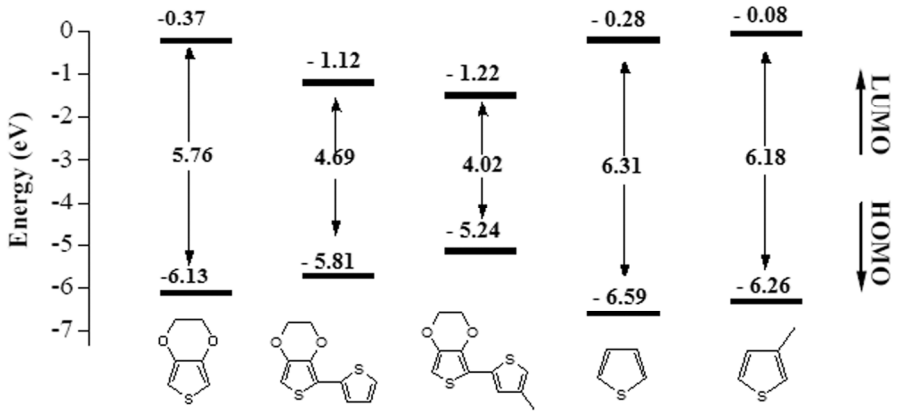

Fig. 5.1: Energy levels of EDOT, EDOT-TH, EDOT-MeTH, TH and MeTH units.

As expected, the introduction of electron donating EDOT unit and thereafter the more planar conformation lift the HOMO energy level and lower the LUMO energy level of thiophene and 3-methyl thiophene. The HOMO level of EDOT-TH and EDOT-MeTH is elevated by a factor of 0.78 and 1.02 eV, respectively, than with TH and MeTH unit. The LUMO level is lowered by a factor of 0.84 and 1.14 eV, respectively. This effect is much pronounced in the case of 3-methyl thiophene than with thiophene unit. Thus, the introduction of EDOT unit, leads to lowering of band gap. The electron donating moiety; EDOT enhances the extended conjugation over the whole molecule by decreasing the dihedral angle between the two neighbouring units and thus stabilizes the LUMOs. This facilitates the overlap between the levels and enhanced absorption occurs at the lowest optical transition. This can be visualized in Fig. 5.2. Here, the electron density isocountours of EDOT-TH and EDOT-MeTH indicated that HOMO and LUMO wave function is distributed over both EDOT and thiophene units. Indeed, the insertion of EDOT unit leads to delocalization of the electron density distribution and therefore, a lowering of band gap is an indication of superior charge transfer properties of monomers.

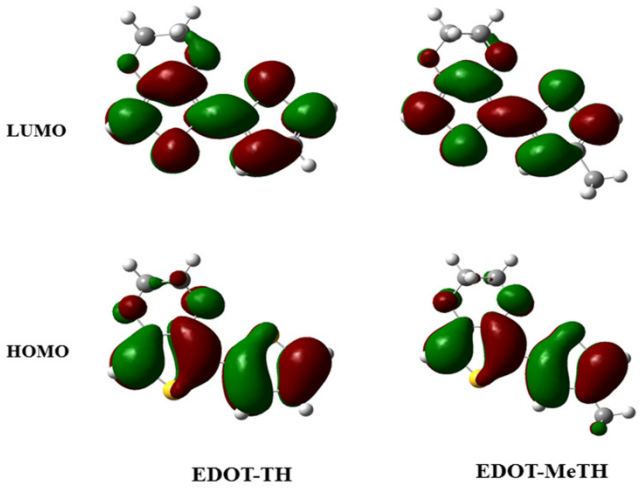

Fig. 5.2: Frontier molecular orbital distribution of monomeric units of P(EDOT-TH) and P(EDOT-MeTH) by B3LYP/6-31G method.

5.2.2. Band structure of copolymers

In order to analyse the electronic properties of copolymers in detail, theoretical calculations have been performed using DFT and PBC calculation at the B3LYP/6-31G level. Here, the effects of EDOT units in the poly(thiophene) (PTH) and poly(3-methyl thiophene) (PMeTH) have been investigated. The evolved band structure of the copolymers is depicted in Fig. 5.3.

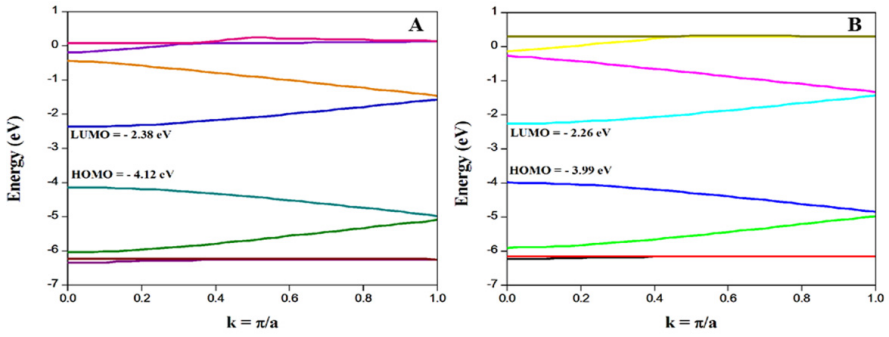

Fig. 5.3: Band structure of (A) P(EDOT-TH) and (B) P(EDOT-MeTH) by B3LYP/6-31G method.

To correlate the electronic properties (HOMO/LUMO energy levels and band gap) of copolymers and homopolymers, the results are gathered in Table 5.1. The Ionization potential (negative of HOMO energy) and the electron affinity (negative of LUMO energy) are also calculated at the B3LYP/6-31G level and summarized in Table 5.1.

Table 5.1: Computational data of P(EDOT-TH) and P(EDOT-MeTH) estimated by B3LYP/6-31G method.

Polymer	HOMO (eV)	LUMO (eV)	BG (eV)	IP (eV)	EA (eV)
P(EDOT-TH)	-4.12	-2.38	1.74	4.12	2.38
P(EDOT-MeTH)	-3.98	-2.26	1.72	3.98	2.26
PTH	-4.73	-2.87	1.86	4.73	2.87
PMeTH	-4.40	-2.60	1.80	4.4	2.6

The HOMO energy level of P(EDOT-TH) and P(EDOT-MeTH) are -4.12 and -3.98 eV, differed by 0.61 and 0.42 eV and the LUMOs are -2.38 and -2.26 eV, differed by 0.49 and 0.34 eV, respectively as far as the energy levels of homopolymers are concerned. As expected, the copolymers revealed low band gap (1.74 and 1.72 eV) than the homopolymers, poly(thiophene) (1.86 eV) and poly(3-methyl thiophene) (1.80 eV). The higher the HOMO level, the better the hole injection and transportation in the material. The ionization potential, the energy required to create a hole in the polymers, P(EDOT-TH) and P(EDOT-MeTH) are 4.12 and 3.98 eV, respectively, which are lower to that in PTH (4.73 eV) and PMeTH (4.4 eV). Hence, the hole injection and transportation in EDOT-thiophene copolymers are expected to be bettter than the homopolymers.

5.2.3. Polymer Synthesis

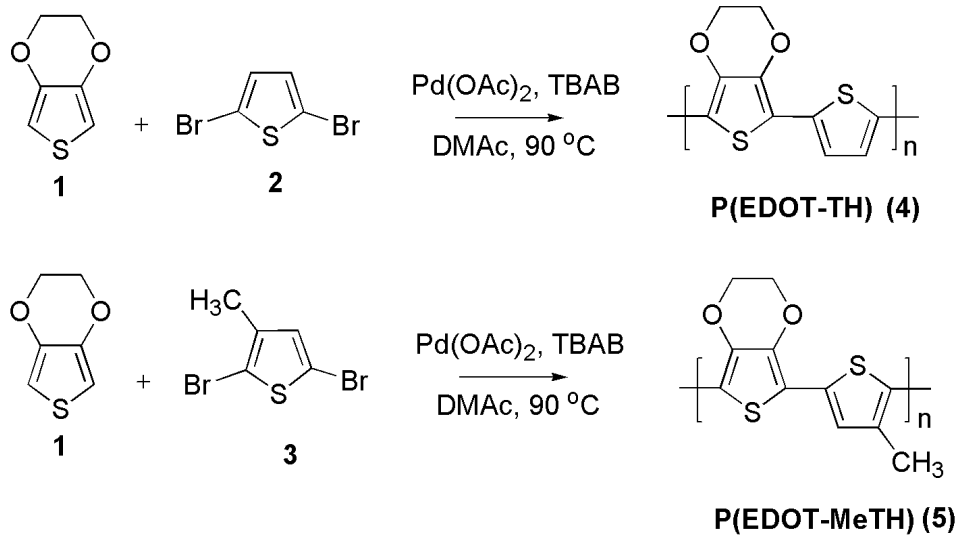

Scheme 1: Synthesis of P(EDOT-TH) and P(EDOT-MeTH).

The copolymers, P(EDOT-TH) and P(EDOT-MeTH) were synthesized via, economic and facile route, direct arylation method. The synthesis routes are shown in Scheme 1. The copolymers were purified by soxhlet extraction and characterized using FT-IR, ^{1}H NMR, XPS and GPC analysis. The GPC data and the polymerization results are summarized in Table 5.2. The copolymers show amenable solubility in solvents such as THF, chlorobenzene and 1, 2-dichlorobenzene (50 mg/mL).

Table 5.2: Results of polymerization of EDOT with TH and MeTH.

Copolymer	Mn	Mw	PDI	Yield (%)
P(EDOT-TH)	4500	7115	1.58	62
P(EDOT-MeTH)	5800	16847	2.05	65

[a]Determined by GPC in THF based on polystyrene standards.

5.2.4. Structural characterization

FT-IR spectra of the copolymers are depicted in Fig. 5.4. As shown in the FT-IR spectra of P(EDOT-TH) and P(EDOT-MeTH) copolymers, aliphatic C-H stretching bands of ethylenedioxy group were observed at 2966 and 2955 cm^{-1}, respectively. The FT-IR spectrum of P(EDOT-TH) showed bands at 1082 and 768 cm^{-1}, characteristic of C-O and C-S stretching vibrations, respectively. Whereas, P(EDOT-MeTH) showed the C-O and C-S stretching vibration at 1077 and 774 cm^{-1}, respectively. The coupled C-C stretching of P(EDOT-TH) and P(EDOT-MeTH) appear at 1231 and 1227 cm^{-1}, respectively. The broad bands observed at 1649 and 1638 cm^{-1} attest the polyconjugation in the thiophene copolymers.

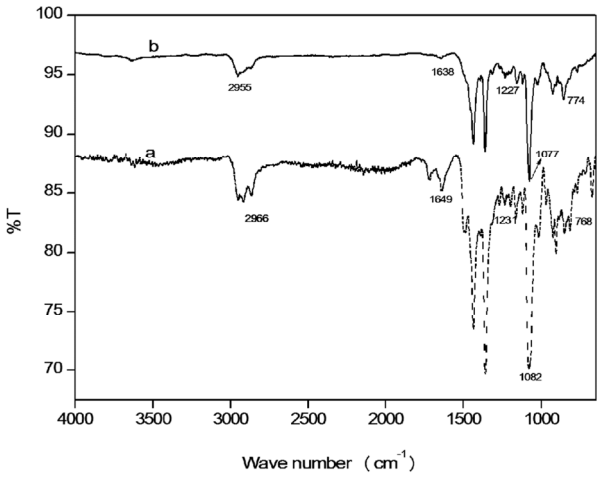

Fig. 5.4: FT-IR spectra of (a) P(EDOT-TH) and (b) P(EDOT-MeTH).

The ^1H NMR spectra of P(EDOT-TH) and P(EDOT-MeTH) are shown in Fig. 5.5. From the spectra, it could be seen that the polymers showed a broad peak in the region δ 4.2-4.4 ppm, which is due to $-OCH_2-$ protons of EDOT unit. Also, P(EDOT-TH) and P(EDOT-MeTH) exhibited

multiple peaks in the region δ 6.9-7.1 ppm, which are due to the aromatic protons of thiophene units.

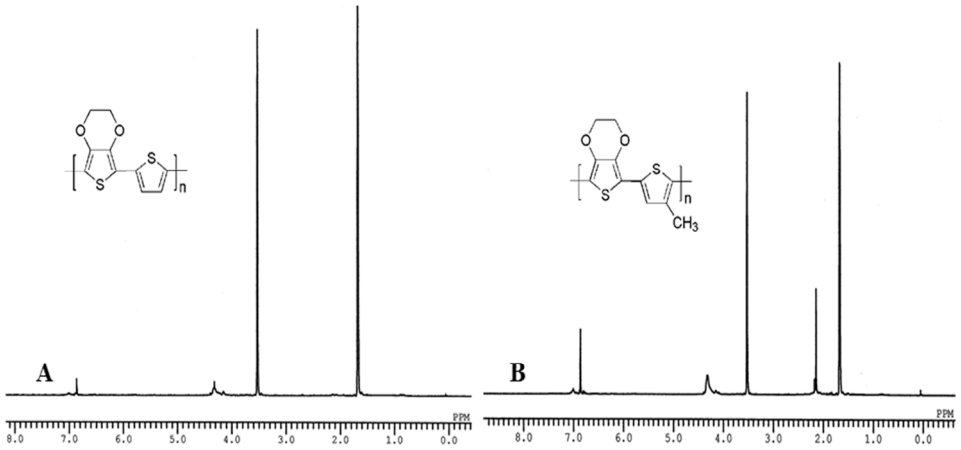

Fig. 5.5: ^{1}H NMR spectra of (A) P(EDOT-TH) and (B) P(EDOT-MeTH).

P(EDOT-MeTH) showed an added peak at δ 2.1-2.2 ppm which is characteristic of methyl group of 3-methyl thiophene moiety. XPS investigations were performed to evaluate the surface composition of copolymers in detail. As seen in XPS results (Fig. 5.6), the signals observed at 285 eV, is due to the carbon atoms belonging to aromatic carbon elements of the polymeric conjugated backbone. The O1s signals were observed at 532 eV, assigned to C-O bonding in the copolymers. The 2p and 2s core levels of S atom of polymers have the signals at 167 and 228 eV, respectively.[35] As observed from the XPS spectra, there is no contaminants at the expected area (334 and 349 eV), which confirms the complete removal of palladium catalyst. The results of FT-IR, ^{1}H NMR and XPS studies clearly indicated that the copolymerization was successfully achieved.

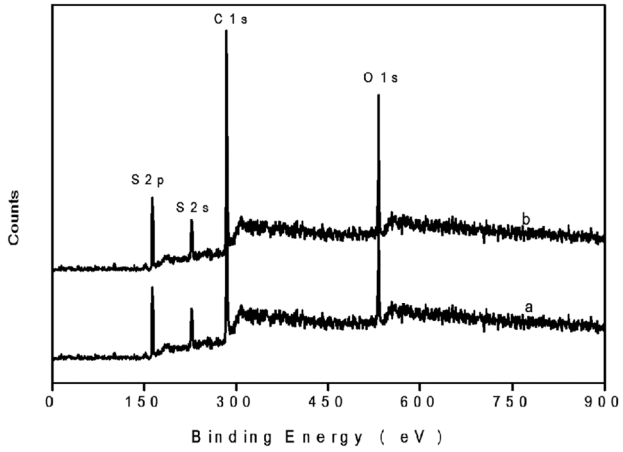

Fig. 5.6: XPS survey scans of (a) P(EDOT-TH) and (b) P(EDOT-MeTH).

5.2.5. Photophysical properties

Absorption spectra of copolymers in THF solution and as thin films are shown in Fig. 5.7.

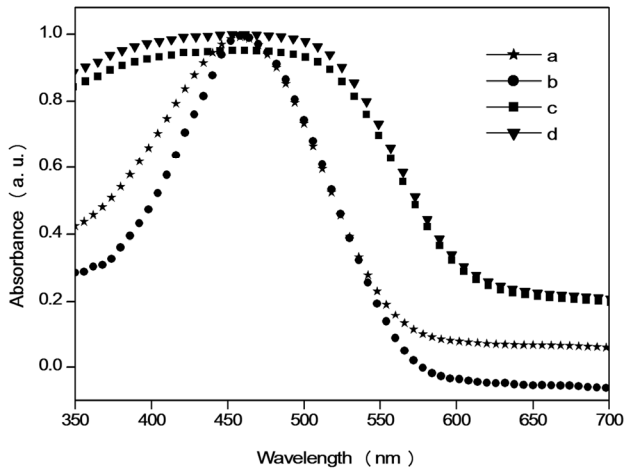

Fig. 5.7: Absorption spectra of copolymers in solution, (a) P(EDOT-TH) and (b) P(EDOT-MeTH) and as film, (c) P(EDOT-TH) and (d) P(EDOT-MeTH).

Both copolymers, P(EDOT-TH) and P(EDOT-MeTH) showed a broad ICT transition maxima centered around 453 nm with the optical band gap of 2.10

and 2.06 eV, respectively, determined from the onset of absorption in solution. To gain more insight into the self-assembly and morphology of copolymers in the solid state, absorption spectra were measured using thin films.

The copolymers showed intramolecular charge transfer band centered around 463 nm with band edge at 678 nm (1.82 eV), which is lower than PTH (2.1 eV)[36] and PMeTh (2.0 eV).[37] The magnitude of the optical band gap primarily reflects the extent of intramolecular π electron conjugation and the presence of well-defined band structure. The red shift in absorption indicated the enhanced molecular order along the conjugated backbone. The optical band gaps are in good agreement with the theoretical prediction. Thus, introduction of EDOT unit into the PTH backbone causes reduction in band gap as well as yielded better electronic properties. Fluorescence emission of copolymers in THF solution is shown in Fig. 5.8. The copolymers, P(EDOT-TH) and P(EDOT-MeTH) showed distinct emission at 564 and 586 nm, respectively.

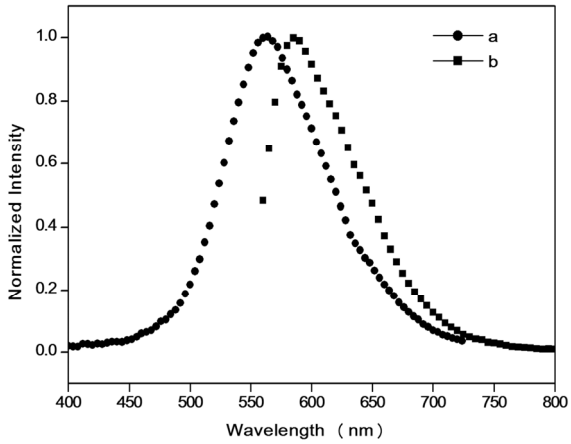

Fig. 5.8: PL spectra of (a) P(EDOT-TH) (b) P(EDOT-MeTH).

5.2.6. Electrochemical studies

The electrochemical behaviour of the copolymers was investigated using cyclic voltammetry (CV), differential pulse voltammetry (DPV), and square wave voltammetry (SWV) methods and the results are summarized in Table 5.3. The HOMO energy level of P(EDOT-TH) and P(EDOT-MeTH) were calculated to be -4.83 eV (DPV). The LUMO energy levels were observed at -3.40 and -3.41 eV, respectively. Thus, the electrochemical band gap of P(EDOT-TH) and P(EDOT-MeTH) are determined to be 1.42 and 1.40 eV, respectively. From the table, it could be seen that HOMO levels of copolymers were elevated and LUMO levels were lowered by the addition of EDOT unit to polythiophene backbone. This implies that the introduction of EDOT unit significantly affects the electron distribution and hence the electronic properties. The DPV and SWV estimated band gaps were found to be smaller than those determined by CV, due to reduced back ground current and sharper redox onset. The obtained electrochemical band gaps are not in good agreement with the optical band gap as well as the predicted band gap. The predicted band gaps are actually obtained for the isolated gas phase chains and the difference in the mechanism of optical excitation and electrochemical oxidation/reduction processes in the system under study leads to this mismatch.

Table 5.3. Electrochemical data of P(EDOT-TH) and P(EDOT-MeTH).

Polymer	Oxidation onset (V)	HOMO (eV)	Reduction onset (V)	LUMO (eV)	BG (eV)
P(EDOT-TH)	0.50[a]	-4.90[a]	-1.12[a]	-3.28[a]	1.62[a]
	0.43[b]	-4.83[b]	-0.99[b]	-3.40[b]	1.42[b]
	0.57[c]	-4.97[c]	-0.88[c]	-3.52[c]	1.45[c]
P(EDOT-MeTH)	0.48[a]	-4.88[a]	-1.09[a]	-3.31[a]	1.57[a]
	0.43[b]	-4.83[b]	-1.0[b]	-3.41[b]	1.40[b]
	0.57[c]	-4.97[c]	-0.81[c]	-3.59[c]	1.38[c]
PTH	0.50[d]	-4.90[d]	-1.6[d]	-2.8[d]	2.1[d]

[a]determined by CV, [b]determined by DPV, [c]determined by SWV, [d]Reproduced from ref. 38.

5.2.7. Thermal properties

The thermal properties of the copolymers were investigated using DSC and TGA. DSC is devoid of any characteristic peak in the temperature range of 40 and 200 ^{o}C. The TG traces are shown in Fig. 5.9. As observed in the figure, the copolymer underwent step wise degradation. The decomposition temperatures (defined as 5 wt% loss) were determined at 303 and 223 ^{o}C for P(EDOT-TH) and P(EDOT-MeTH), respectively, which is higher than PEDOT. TG traces display that P(EDOT-TH) possess higher thermal stability than P(EDOT-MeTH). Both the copolymers were found to be moderately stable to thermal changes or degradation.

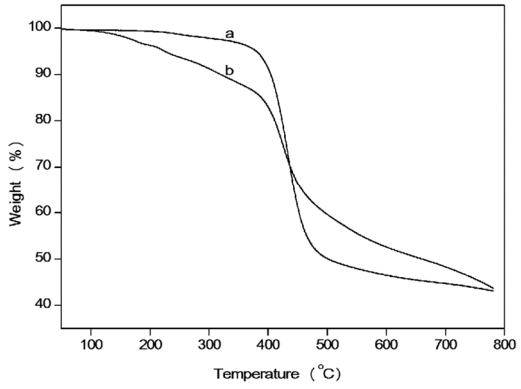

Fig. 5.9: TG traces of (a) P(EDOT-TH) and (b) P(EDOT-MeTH).

5.2.8. Non-linear optical properties

The third-order NLO properties of EDOT/thiophene copolymers were investigated using z-scan technique. The non-linear transmission of polymers without aperture (open aperture, OA) was measured in the far field as the sample was moved through the focal point at 532 nm. The OA traces of EDOT/thiophene copolymers in dilute $CHCl_3$ (a) and as thin film (b) are presented in Fig. 5.10.

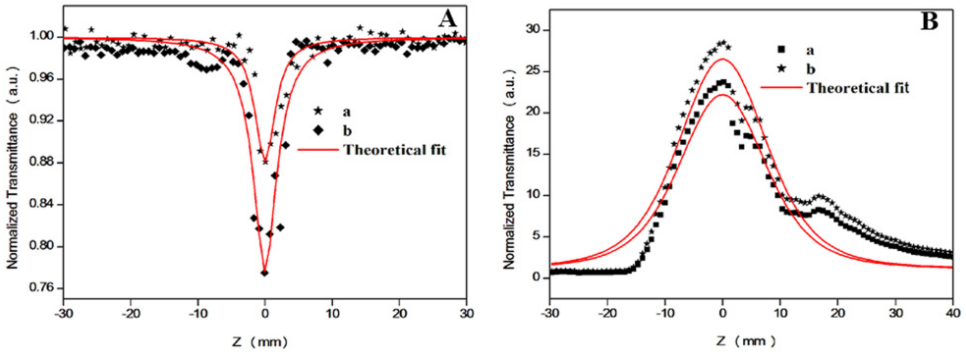

Fig. 5.10: Open aperture z-scan traces of (a) P(EDOT-TH) and (b) P(EDOT-MeTH) in solution (A) and as film (B) at 112 µJ.

As seen in the figure, the two polymers showed a normalized transmittance valley of light. From the OA traces, it can be concluded that polymers are reverse saturation absorbers (RSA) with positive NLO absorption coefficient, whereas, the copolymer film showed enhanced transmission of light at the focus, indicating saturation absorption (SA) with negative NLO absorption coefficient. Polymers showed complete switchover from RSA to SA in film phase due to ground state band bleaching. z-scan data were analysed by using the procedure described by M. S. Bahae *et al.*,[39] and the non-linear coefficients were obtained by fitting the experimental z-scan plot with the theoretical plots. The non-linear absorption coefficient, β of the copolymer sample is obtained by fitting the experimental data using equation (1) (equation (3), given in section 2.2.7). The imaginary part of the third-order susceptibility (Im $\chi^{(3)}$) of copolymers is determined by equation (2) (equation (4), given in section 2.2.7).

The non-linear refractive (NLR) property of EDOT/thiophene copolymers was evaluated by dividing the normalized z-scan data obtained under closed aperture configuration by the normalized z-scan data obtained

under open aperture configuration, shown in Fig. 5.11. The peak to valley configuration of the traces indicates that the refractive index change of copolymers is negative, signifying self-defocusing effect of polymer samples. The normalized transmittance, T(z) for NLR is given by relation (3) (equation (5), given in section 2.2.7). The effective non-linear refractive index (n_2), the real parts of $\chi^{(3)}$ (Re $\chi^{(3)}$) and third-order non-linear susceptibility ($\chi^{(3)}$) of EDOT/ thiophene copolymers are calculated by following the equation (4)-(6) (equations (6)-(8), given in section 2.2.7).

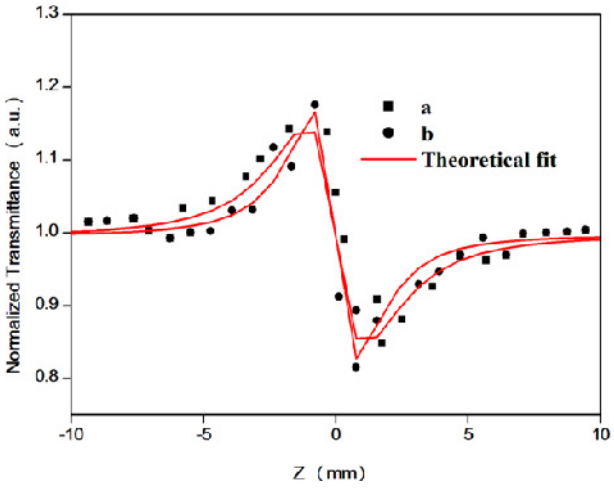

Fig. 5.11: Closed aperture z-scan traces of (a) P(EDOT-TH) and (b) P(EDOT-MeTH) at 112 µJ.

The values obtained for non-linear absorption coefficient (β, m/W), the non-linear refraction coefficient (n_2, esu) and the third-order non-linear susceptibility ($\chi^{(3)}$, esu) are given in Table 5.4. The β value of P(EDOT-TH) and P(EDOT-MeTH) is obtained to be 3.11×10^{-10} and 3.19×10^{-10} m/W, respectively. Furthermore, the $\chi^{(3)}$ value is found to be 1.27×10^{-11} and 1.48×10^{-11} esu, respectively. Copolymers showed strong non-linear absorption

and non-linear refraction coefficient due to donor-π-acceptor scheme. In D-π-A copolymers, non-linearity originates due to the intramolecular charge transfer from donor to acceptor unit and delocalization of π electrons.

Table 5.4: Calculated values of non-linear absorption, non-linear refraction, and non-linear susceptibility of P(EDOT-TH) and P(EDOT-MeTH) at 112 μJ intensity.

Copolymer	β (m/W)	n_2 (esu)	Im $\chi^{(3)}$ (esu)	Re $\chi^{(3)}$ (esu)	$\chi^{(3)}$ (esu)
P(EDOT-TH)	3.11×10^{-10}	-0.70×10^{-10}	0.07×10^{-10}	-1.07×10^{-11}	1.27×10^{-11}
P(EDOT-MeTH)	3.19×10^{-10}	-0.85×10^{-10}	0.07×10^{-10}	-1.31×10^{-11}	1.48×10^{-11}

5.2.9. Optical power limiting

To probe the optical limiting behaviour of EDOT/thiophene copolymers, the non-linear transmission is measured as a function of input fluence under OA z-scan configuration at 532 nm. Optical limiter can be used as chopper for high energy inputs, i.e., once the input fluence exceeds optical limiting threshold it becomes opaque. Therefore it could be developed as devices which can protect human eye and high sensitive instruments from laser induced damages. Optical limiting property has different origins such as two photon absorption (TPA), free carrier absorption, RSA, self-focusing, self-defocusing or induced scattering. The optical limiting performance of copolymers exhibiting RSA behaviour is revealed in Fig. 5.12. The approximate fluence at which the normalized transmission begins to deviate from linearity is called optical limiting threshold and it is obtained to be 0.45 GW/cm^2 for both copolymers.

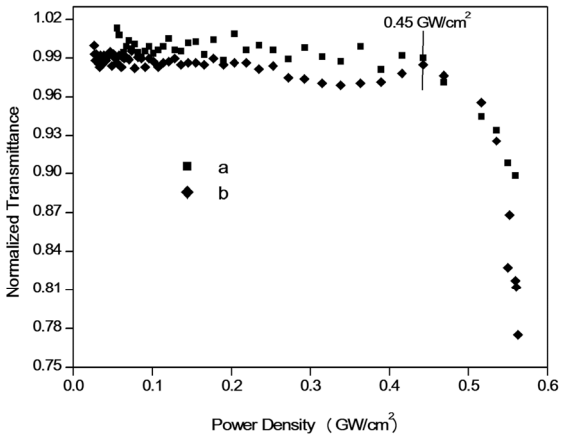

Fig. 5.12: Optical limiting curves of (a) P(EDOT-TH) and (b) P(EDOT-MeTH).

5.3. Experimental

5.3.1. Materials

3,4-Ethylenedioxythiophene (EDOT, Aldrich, 98 %), tetrabutylammonium bromide (TBAB, Avra Synthesis Pvt. Ltd., 98%), sodium acetate (anhydrous) (Spectrochem Pvt. Ltd.), palladium (II) acetate ($Pd(OAc)_2$, Aldrich, 99.98 %), tetrabutylammonium hexafluorophosphate (Bu_4NPF_6, Aldrich, >99 %), 2,5-dibromothiophene (Aldrich, 95%) and 2,5-dibromo-3-methylthiophene (Aldrich, 97 %) were used as received. Acetonitrile HPLC grade (CH_3CN, Aldrich), dimethyl acetamide (anhydrous) (DMAc, Spectrochem Pvt. Ltd.), chloroform ($CHCl_3$, Spectrochem Pvt. Ltd.), dicholoromethane (CH_2Cl_2, Spectrochem Pvt. Ltd.), tetrahydrofuran HPLC grade (THF, Spectrochem Pvt. Ltd.), n-hexane (Spectrochem Pvt. Ltd.) and methanol (anhydrous) (MeOH, Spectrochem Pvt. Ltd.) were dried and distilled when necessary according to the standard procedures.

5.3.2. Computation methods

Theoretical calculations were done using computational methods, which has been described in section 2.3.4.

5.3.3. Polymer Synthesis

5.3.3.1. *Synthesis of P(EDOT-TH) (4)*

To a stirred solution of EDOT (1) (0.024 g, 0.17 mmol) in 10 mL DMAc was added TBAB (0.055 g, 0.17 mmol) and sodium acetate (0.055 g, 0.68 mmol). The reaction mixture was stirred at room temperature for 30 min followed by addition of 2,5-dibromothiophene (2) (0.04 g, 0.17 mmol) and 10 % palladium acetate. The reaction mixture was stirred at 90 ^{o}C for 48 h. The reaction mixture was cooled to room temperature and poured in to methanol (20 mL). The precipitate was filtered and washed with methanol. The polymer was purified by soxhlet extraction using hexane and methanol for 24 h. The residue was dissolved in minimum amount of $CHCl_3$ and precipitated using methanol and dried under vacuum. A yield of 62 % was observed.

5.3.3.2. *Synthesis of P(EDOT-MeTH) (5)*

To a stirred solution of EDOT (1) (0.024 g, 0.17 mmol) in 10 mL DMAc was added TBAB (0.055 g, 0.17 mmol) and sodium acetate (0.055 g, 0.68 mmol). The reaction mixture was stirred at room temperature for 30 min followed by addition of 2,5-dibromo-3-methylthiophene (3) (0.05 g, 0.17 mmol) and 10 % palladium acetate. The reaction mixture was stirred at 90 ^{o}C for 48 h. The reaction mixture was cooled to room temperature and poured in to methanol (20 mL). The precipitate was filtered and washed with methanol. The polymer was purified by soxhlet extraction using

hexane and methanol for 24 h. The residue was dissolved in minimum amount of $CHCl_3$ and precipitated using methanol and dried under vacuum. A yield of 65 % was observed.

5.3.4. Instrumentation

Copolymers were characterized by analytical and spectral methods which have been described in section 2.3.3.

5.3.5. NLO Measurements

NLO properties were determined by methods which have been described in section 2.3.6.

5.4. Conclusion

The synthesis and characterizations of copolymers containing EDOT and thiophene units via the direct arylation method is reported. Their electronic properties were investigated by DFT calculation at B3LYP/6-31G level. The addition of EDOT to the PTH backbone causes fine tuning of HOMO and LUMO energy levels. Also, the introduction of EDOT units into the PTH conjugated backbone facilitated the broadening of absorption spectrum in the polymer. Moreover, optical and electrochemical results show that the copolymers have low band gap as compared to polythiophene. This can be attributed to the rigid and planar molecular geometry induced in the conjugated backbone by the incorporation of EDOT units. The copolymers exhibit large refractive index coefficient and the third-order non-linear susceptibility at 532 nm. Both the copolymers showed optical limiting threshold of 0.45 GW/cm^2, which confirms the suitability in optical limiting devices. This indicates that these polymers can be used in non-linear optical devices.

References

[1] P. Dutta, H. Park, W. -H. Lee, I. N. Kang, S. -H. Lee, *Polym. Chem.,* 2014, 5, 132.

[2] Q. Hou, J. Liu, T. Jia, S. Luo, G. Shi, *J. Appl. Polym. Sci.*, 2013, 130**,** 3276.

[3] W. Zhuang, M. Bolognesi, M. Seri, P. Henriksson, D. Gedefaw, R. Kroon, M. Jarvid, A. Lundin, E. Wang, M. Muccini, M. R. Andersson, *Macromolecules*, 2013, 46, 8488.

[4] E. Zhou, J. Cong, K. Hashimoto, K. Tajima, *Macromolecules*, 2013, 46**,** 763.

[5] Q. Huang, G. A. Evmenenko, P. Dutta, P. Lee, N. R. Armstrong, T. J. Marks, *J. Am. Chem. Soc.*, 2005, 127, 10227.

[6] P. M. Beaujuge, J. R. Reynolds, *Chem. Rev.*, 2010, 110, 268.

[7] P. Shi, C. M. Amb, A. L. Dyer, J. R. Reynolds, *J. Am. Chem. Soc.*, 2012, 4, 6512.

[8] E. Kaya, A. Balan, D. Baran, A. Cirpan, *Organic Electronics*, 2011, 12, 202.

[9] L. C. Pekel, B. Karabay, A. Cihaner, *J. Electroanal. Chem.*, 2014, 730, 26.

[10] M. P. Algi, S. Tirkes, S. Ertan, E. G. C. Ergun, A. Cihaner, F. Algi, *Electrochim. Acta*, 2013, 109, 766.

[11] M. P. Algi, Z. Öztaş, S. Tirkes, A. Cihane, F. Algi, *Organic electronics*, 2013, 14, 1094.

[12] K. M. de Silva, E. Hwang, W. K. Serem, F. R. Fronczek, J. C. Garno, E. E. Nesterov, *Applied Materials and Interfaces*, 2012, 4, 5430.

[13] B. D. Martin, G. A. Justin, M. H. Moore, J. Naciri, T. Mazure, B. J. Melde, R. M. Stroud, B. Ratna, *Adv. Funct. Mater.*, 2012, 22, 3116.

[14] L. Miozzo, N. Battaglini, D. Braga, L. Kergoat, C. Suspene, A. Yassar, *J. Polym. Sci., Part A: Polym. Chem.*, 2012, 50, 534.

[15] S. Sun, L. R. Dalton, Introduction to Organic Electronic and Optoelectronic Materials and Devices, CRC Press, Taylor & Francis Group, Boca Raton, FL, 2008.

[16] L. V. Interrante, M. J. Hampden-Smith, Chemistry of Advanced Materials, An Overview, Wiley-VCH, New York, 1998.

[17] W. Denk, J. H. Strickler, W. W. Webb, *Science*, 1990, 248, 73.

[18] C. C. Corredor, Z. -L. Huang, K. D. Belfield, A. R. Morales, M. V. Bondar, *Chem. Mater.*, 2007, 19, 5165.

[19] L. D. Zarzar, B. S. Swartzentruber, J. C. Harper, D. R. Dunphy, C. J. Brinker, J. Aizenberg, B. Kaehr, *J. Am. Chem. Soc.*, 2012, 134, 4007.

[20] B. H. Cumpston, S. P. Ananthavel, S. Barlow, D. L. Dyer, J. E. Ehrlich, L. L. Erskine, A. A. Heikal, S. M. Kuebler, I. Y. S. Lee, D. McCord-Maughon, J. Qin, H. Rockel, M. Rumi, X. -L. Wu, S. R. Marder, J. W. Perry, *Nature*, 1991, 398, 51.

[21] C. Tang, Q. Zheng H. Zhu, L. Wang, S. -C. Chen, E. Ma, X. Chen, *J. Mater. Chem. C*, 2013, 1, 1771.

[22] J. M. Hales, S. Zheng, S. Barlow, S. R. Marder, J. W. Perry, *J. Am. Chem. Soc.*, 2006, 128, 11362.

[23] R. Zieba, C. Desroches, F. Chaput, M. Carlsson, B. Eliasson, C. Lopes, M. Lindgren, S. Parola, *Adv. Funct. Mater.*, 2009, 19, 235.

[24] T. C. Lin, Y. F. Chen, C. -L. Hu, C. -S. Hsu, *J. Mater. Chem.*, 2009, 19, 7075.

[25] T. -C. Lin, G. S. He, P. N. Prasad, L. -S. Tan, *J. Mater. Chem.*, 2004, 14, 982.

[26] P. N. Prasad, D. J. Williams, Introduction to nonlinear optical effects in molecules and polymers, Wiley, New York, 1992.

[27] H. S. Nalwa, S. Miyata, Nonlinear optics of organic molecules and polymers, CRC Press, USA, 1997.

[28] B. A. Reinhardt, L. L. Brott, S. J. Clarson, A. G. Dillard, J. C. Bhatt, R. Kannan, L. Yuan, G. S. He, P. N. Prasad, *Chem. Mater.*, 1998, 10, 1863.

[29] M. Albota, D. Beljonne, J. -L. Brebas, J. E. Ehrlich, J. -Y. Fu, A. A. Heikal, S. E. Hess, T. Kogej, M. D. Levin, R. S. Marder, D. McCord-Maughon, J. W. Perry, H. Rockel, M. Rumi, G. Subramaniam, W. W. Webb, X. -L. Wu, C. Xu, *Science*, 1998, 281, 1653.

[30] R. G. Parr, W. Yang, Density-Functional Theory of Atoms and Molecules, Oxford University Press, New York, 1989.

[31] A. D. Becke, Density-functional thermochemistry, III. The role of exact exchange, The Journal of Chemical Physics, 1993, 98**,** 5648

[32] C. Lee, W. Yang, R. G. Parr, *Phys. Rev. B*, 1998, 37, 785.

[33] K. Burke, J. P. Perdew, Y. Wang, J. F. Dobson, G. Vignale, M. P. Das, Electronic Density Functional Theory: Recent Progress and New Directions, Plenum Press, New York, 1998.

[34] Gaussian 09, Revision B02, M. J. Frisch, G. W. Trucks, H. B. Schlegel, G. E. Scuseria, M. A. Robb, J. R. Cheeseman, G. Scalmani, V. Barone, B. Mennucci, G. A. Petersson, H. Nakatsuji, M. Caricato, X. Li, H. P. Hratchian, A. F. Izmaylov, J. Bloino, G. Zheng, J. L. Sonnenberg, M. Hada, M. Ehara, K. Toyota, R. Fukuda, J. Hasegawa, M. Ishida, T. Nakajima, Y. Honda, O. Kitao, H. Nakai, T. Vreven, J. A. Montgomery Jr., J. E. Peralta, F. Ogliaro, M. Bearpark, J. J. Heyd, E. Brothers, K. N. Kudin, V. N. Staroverov, R. Kobayashi, J. Normand, K. Raghavachari, A. Rendell, J. C. Burant, S. S. Iyengar, J. Tomasi, M. Cossi, N. Rega, N. J. Millam, M. Klene, J. E. Knox, J. B. Cross, V. Bakken, C. Adamo, J. Jaramillo, R. Gomperts, R. E. Stratmann, O. Yazyev, A. J. Austin, R. Cammi, C. Pomelli, J. W. Ochterski, R. L. Martin, K. Morokuma, V. G. Zakrzewski, G. A. Voth, P. Salvador, J. J. Dannenberg, S. Dapprich, A. D. Daniels, Ö. Farkas, J. B. Foresman, J. V. Ortiz, J. Cioslowski, D. J. Fox, Gaussian, Inc., Wallingford CT, 2009.

[35] M. Yildirim, I. Kaya, A. Aydin, *React. Funct. Polym.*, 2013, 73, 1167.

[36] T. -C. Chung, J. H. Kaufman, A. J. Heeger, F. Wudl, *Phys. Rev. B*, 1984, 30, 702.

[37] A. O. Patil, A. J. Heeger, F. Wudl, *Chem. Rev.*, 1988, 88, 183.

[38] W. -L. Yu, H. Meng, J. Pei, W. Huang, *J. Am. Chem. Soc.*, 1998, 120, 11808.

[39] M. Sheik–Bahae, A. A. Said, T. -H. Wei, D. J. Hagan, E. W. VanStryland, *IEEE Journal of Quantum Electronics*, 1990, 26, 760.

.....ꕥ.....

Chapter 6

Novel Soluble Phenothiazine-Triazine Copolymer: Synthesis and Third-order Non-linear Optical Properties

Abstract

Novel soluble conjugated phenothiazine-N-piperidine substituted triazine copolymer, (P(PH-TZ)) has been designed and synthesized via Suzuki coupling reaction. The electronic properties of the copolymer were investigated by employing density functional theory (DFT) in the periodic boundary condition (PBC) formalism at HSE06 and B3LYP level of theory. The copolymer showed good solubility in common organic solvents like chloroform, tetrahydrofuran and chlorobenzene. Polymer showed broad absorption spectrum with wavelength maximum at 395 nm with optical band gap of 2.5 and 2.3 eV in THF solution and as thin film, respectively. The theoretically calculated values were in good agreement with experimental results. In thin film, the energy gap tends to narrow and the absorption and emission peaks are red shifted to longer wavelengths due to the increase in planarity of the copolymer in thin film. The copolymer, P(PH-TZ) showed third-order non-linear optical susceptibility and optical limiting threshold of 1.27×10^{-11} esu and 0.22 GW/cm^2, respectively.

6.1. Introduction

Organic π conjugated structures with 1,3,5-triazine as the core unit have received significant attention due to their promising applications in liquid crystalline materials,[1,2] magnetic materials,[3] solar cells[4-6] and light emitting diodes (LEDs).[7-9] Owing to their high thermal stability, polymers containing 1,3,5-triazine unit are widely used in industry. Recently, some new polymers bearing 1,3,5-triazine units have been reported.[8-11] The 1,3, 5-triazine unit possesses high electron affinity,[12] structural symmetry, high thermal, mechanical and oxidative resistance.[13-17] Unfortunately, these features also lead to low solubility and processability. Insertion of phenothiazine unit with bulky alkyl substituent imparts flexibility to this copolymer. The 1,3,5-triazine unit in the polymer backbone favoured the better electron injection and transportation in devices.[7,8]

Phenothiazines are a class of electron rich tricyclic nitrogen-sulphur heterocycle compound with low oxidation potential, high luminescence and photoconductivity. They are widely used as dyes, antioxidants, pharmaceuticals etc.[18,19] These molecules are potential candidates for applications in LEDs,[20-22] photovoltaic devices[23-26] and organic field effect transistors.[27,28] The π conjugated organic compounds have emerged as promising candidates due to their fast response time, large third-order susceptibility and processability.[29,30] The NLO properties of organic molecules can be tuned by adopting suitable synthetic strategies, such as donor–π–acceptor (D–π–A), donor–π–donor (D–π–D), donor–acceptor–donor (D–A–D), and acceptor–donor–acceptor (A–D–A).[31,32] Here, we are mainly interested in the alternating donor-acceptor copolymer since their optoelectronic properties

can be tuned by efficient intramolecular charge transfer. The strong donor-acceptor intramolecular interaction and delocalized π-electron system yields NLO properties in π conjugated organic compounds. This in turn intrigued our research interest in the third-order NLO behaviour of D-π-A type copolymer, P(PH-TZ). In this paper, we discuss the electronic structure, synthesis, optical and electrochemical properties of phenothiazine-triazine copolymer and have demonstrated the applicability of the polymer as active material in optical limiting devices.

6.2. Results and discussion

6.2.1. Theoretical calculation

All the DFT[33] calculations were carried with Gaussian 09[34] program. The monomer geometries were optimized by B3LYP/6-31G method.

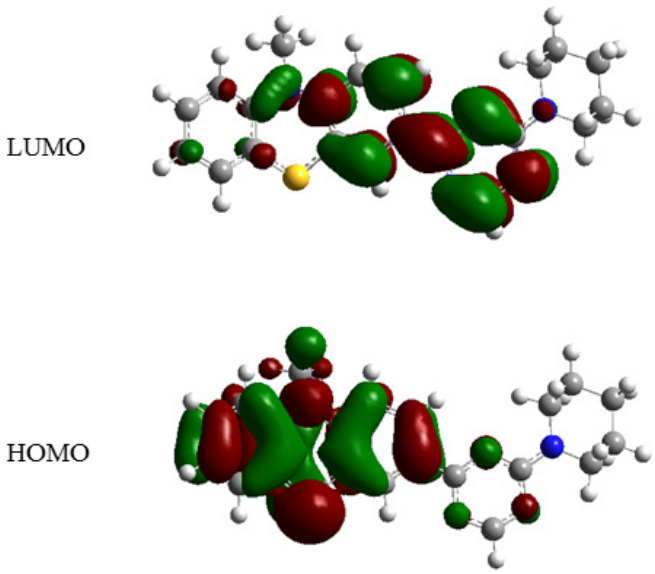

Fig. 6.1: Frontier molecular orbital distribution of monomeric unit of P(PH-TZ) by B3LYP/6-31G method.

Fig. 6.1 shows the frontier molecular orbitals of monomeric unit, PH-TZ. It reveals that the HOMO (highest occupied molecular orbital) level of PH-TZ was located on phenothiazine unit and LUMO (lowest unoccupied molecular orbital) level was located on triazine moieties. This large degree of polarization might be responsible for the small band gap value for P(PH-TZ) compared to homopolymer, poly(phenothiazine) (P(PH)).

The electronic properties of the P(PH) and P(PH-TZ) were studied by PBC calculation at two different energy levels (B3LYP[35-37]/6-31G and HSE06[38,39]/6-31G) and the band structure obtained by HSE06/6-31G level have been plotted in Fig. 6.2. Table 6.1 lists the calculated theoretical HOMO-LUMO energy levels and band gaps of the homopolymer, (P(PH)) and copolymer, P(PH-TZ).

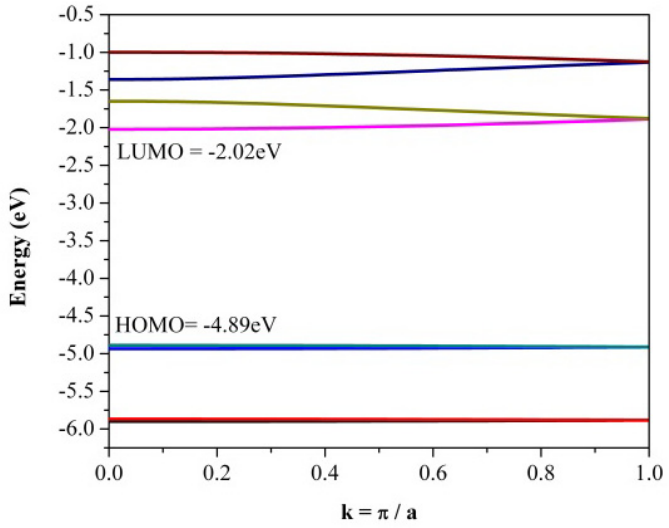

Fig. 6.2: Band structure of P(PH-TZ) by HSE06/6-31G method.

Comparing the band structure of P(PH-TZ) with band structure of P(PH), it could be seen that energy of HOMO level of P(PH) was lowered

by a factor of 0.13 eV while LUMO level was lowered by a factor of 0.61 eV and we get P(PH-TZ) with a reduced band gap of 2.87 eV. The lower band gap of P(PH-TZ) compared to that of P(PH), indicated a significant effect of intramolecular charge transfer between the phenothiazine and triazine moieties.

Table 6.1: Computational data of P(PH) and P(PH-TZ) with DFT/B3LYP/6-31G and DFT/HSE06/6-31G methods.

Polymer	HOMO (eV)	LUMO (eV)	E_g (eV)
P(PH)	-4.76	-1.41	3.35
P(PH-TZ)[a]	-5.02	-1.75	3.27
P(PH-TZ)[b]	-4.89	-2.02	2.87

[a]Obtained by the DFT/B3LYP/6-31G method, [b]Obtained by the DFT/HSE06/6-31G method.

6.2.2. Synthesis and Characterization

The synthetic procedures towards the synthesis of monomers and copolymer are outlined in Schemes 1 and 2. Scheme 1 summarizes the synthesis of key monomers. The monomer 2-(N-piperidine)-4,6-dichloro-s-triazine (3) was synthesized from cyanuric chloride (1) and piperidine (2) in acetone according to standard procedure.[40] The monomer, 10-octyl-3,7-bis(4,4,5,5-tetramethyldioxaborolan-2-yl)-phenothiazine (7) was synthesized in three steps starting from the phenothiazine (4). Firstly, 10-octylphenothiazine (5) was synthesized by the alkylation of phenothiazine (4) using 1-bromooctane and KOH. 3,7-Dibromo-10-(octyl)-phenothiazine (6) was prepared by brominating the 10-octylphenothiazine in CH_2Cl_2. To obtain 10-octyl-3,7-bis(4,4,5,5-tetramethyldioxaborolan-2-yl)-phenothiazine (7), 3,7-dibromo-10-(octyl)-phenothiazine (6) was stirred with n-butyl lithium followed by 2-isopropoxy-4,4,5,5,-tetramethyl-1,3,2-dioxaborolane in THF at -78 ^oC according to standard procedure.[41]

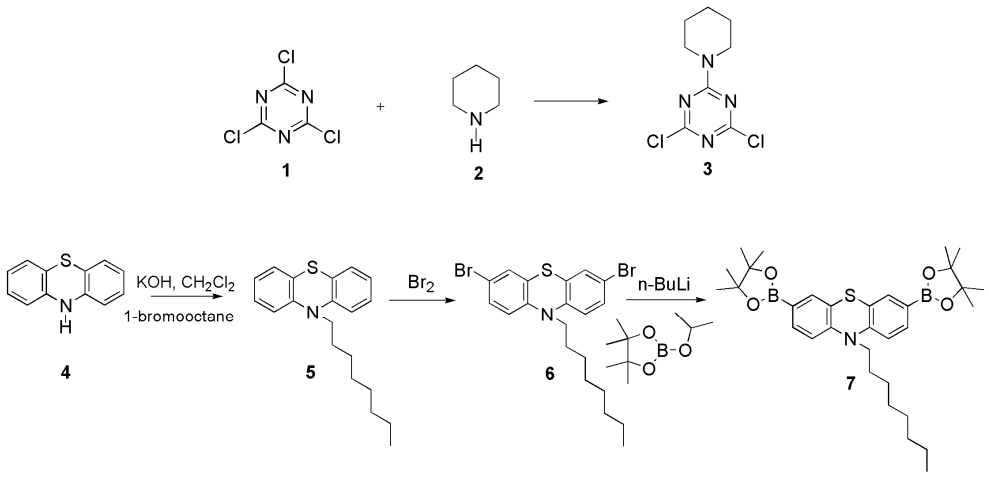

Scheme 1: Synthesis of monomers.

The conjugated polymer derived from phenothiazine and triazine was synthesized by palladium (0) catalysed Suzuki coupling reaction with an equivalent ratio of diboronyl phenothiazine monomer (7) and 2-(N-piperidine)-4,6-dichloro-s-triazine monomer (3) using freshly prepared palladium triphenylphosphene as the catalyst. The copolymer was purified by washing with methanol and hexane in a soxhlet apparatus to remove the oligomers and catalyst residues and was dried under reduced pressure. After purification, the polymer was obtained in good yield (60 %).

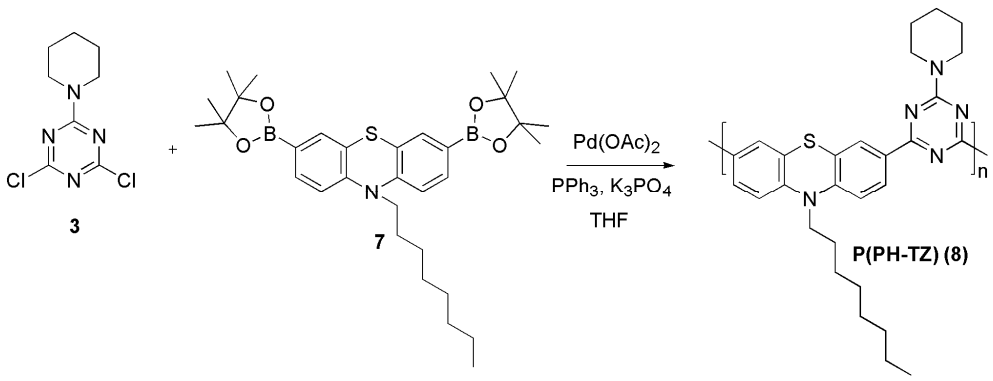

Scheme 2: Synthesis of copolymer, P(PH-TZ).

The copolymer was readily soluble in common organic solvents, such as THF, chloroform, dichloromethane and chlorobenzene. The molecular weight of polymer was determined by gel permeation chromatography in THF referring to polystyrene standards. GPC analysis showed that copolymer had number average molecular weight (Mn) of 3580, weight average molecular weight (Mw) of 4928 and polydispersity index (PDI) of 1.66.

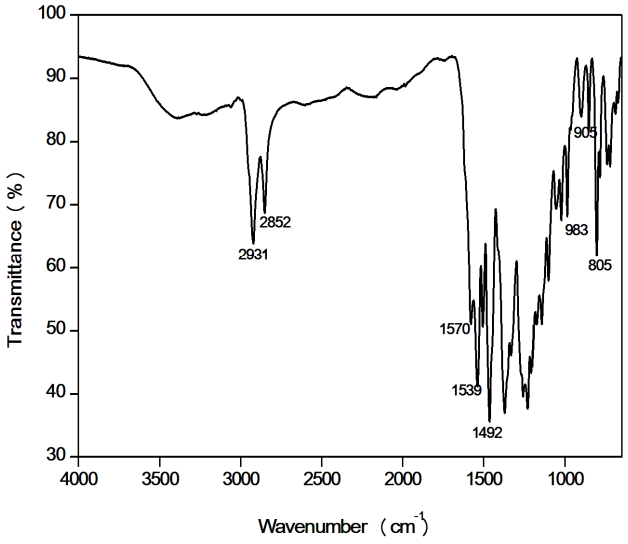

Fig. 6.3: FT-IR spectrum of P(PH-TZ).

The molecular structure of the copolymer was verified by FT-IR, ^{1}H NMR and XPS analysis. A representative FT-IR spectrum of triazine copolymer is shown in Fig. 6.3, where the bands at 805 and 1492 cm^{-1} are attributed to the out of plane vibrations of 1,3,5-triazine ring.[40] The intense bands at 1570 and 1539 cm^{-1} are attributed to the aromatic C=C stretching of phenothiazine moiety. The aliphatic C-H stretching vibration appeared at 2931 and 2852 cm^{-1} is an indication of alkylated phenothiazine moiety. The

copolymer also exhibited two bands at 905 and 983 cm^{-1} due to C-C deformation of piperidine ring. FT-IR results clearly indicated that copolymerization was successfully achieved.

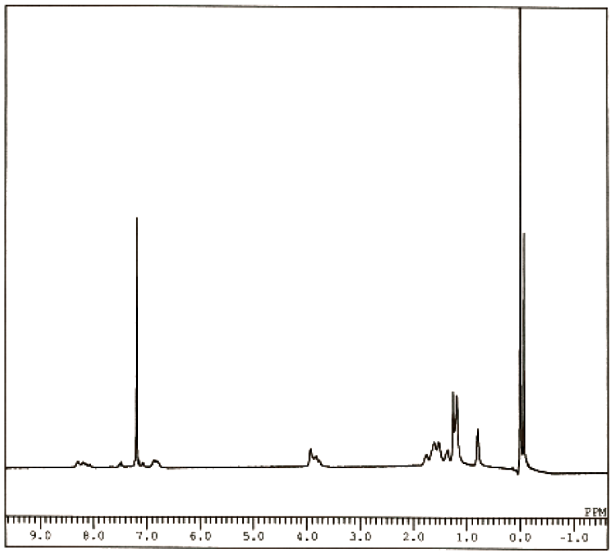

Fig. 6.4: ^{1} H NMR spectrum of P(PH-TZ).

The ^{1}H NMR spectrum of P(PH-TZ) copolymer is depicted in Fig. 6.4. The ^{1}H NMR spectrum showed multiplets at δ 0.65-1.9 ppm due to alkyl protons of phenothiazine and piperidine units and the characteristic signal of CH_2 segments attached to the nitrogen atoms of phenothiazine and piperidine units was observed as multiplet at δ 3.8 ppm. The peaks corresponding to aromatic protons of phenothiazine units were observed at δ 6.8-7.5 ppm as multiplets.

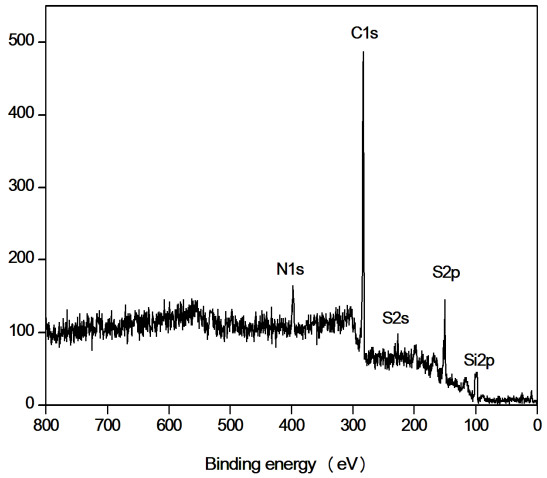

Fig. 6.5: XPS survey scan of P(PH-TZ) showing the presence of N1s, C1s, S2s, S2p and Si2p peaks.

Fig. 6.5 represents the XPS survey scan of the copolymer, P(PH-TZ) which showed the presence of C, N, S as the characteristic elements of the comonomers. In XPS spectrum, the signals related to C1s are observed at 282 eV, which is mainly due to aromatic carbons of the polymeric conjugated backbone.[42] The N1s signal appear at 396 eV and is attributed to the presence of C-N bonding.[43] The 2s and 2p core levels of S atom show signals at 228 and 160 eV, respectively, which reveals that monomeric units containing phenothiazine rings are present in the copolymer, as expected. The FT-IR, ^{1}H NMR and XPS spectra of P(PH-TZ) are consistent with the chemical structure.

6.2.3. Photophysical properties

The photophysical characteristics of copolymer were investigated by both UV-Visible absorption (Fig. 6.6) and photoluminescence (PL) (Fig. 6.7) spectra in dilute THF solution and as thin film. As shown in Fig. 6.6, copolymer exhibited two distinct peaks and one of the peak appeared at

304 nm which is assigned to the π-π* transition and the other peak at longer wavelength at 395 nm, with tailing of absorption to around 496 nm can be attributed to the intramolecular charge transfer between the donor and acceptor unit. In thin film, copolymer exhibited two absorption bands at 294 and 410 nm, which are assigned to the π-π* transition and intramolecular charge-transfer, respectively. The thin film absorption pattern of P(PH-TZ) is nearly identical to the dilute solution spectrum, with red shifted absorption maximum of 425 nm.

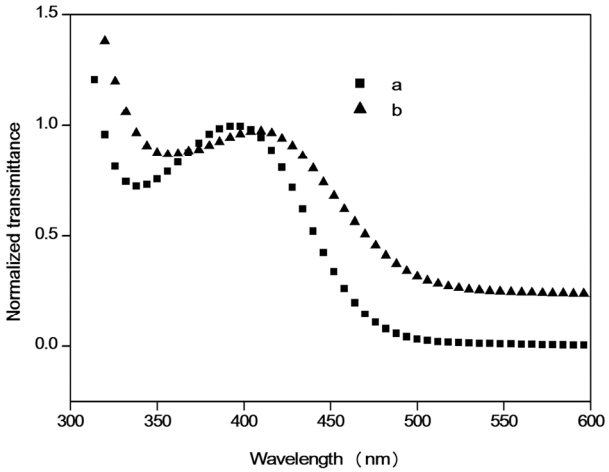

Fig. 6.6: UV-Visible spectra of copolymer, P(PH-TZ) in (a) THF solution and (b) as thin film.

The optical band gap of P(PH-TZ) was calculated to be 2.5 eV, from the cut-off wavelength of optical absorption in THF solution. Optical band gap derived from the absorption edge of the polymer film was 2.3 eV, differed 0.2 eV, from the solution band gap. As expected, the copolymer has lower band gap than the conjugated homopolymer, poly(phenothiazine) (2.76 eV)[41] due to better charge transfer between the units. Even if the optical band gap of copolymer showed good agreement with the theoretical

prediction (DFT/HSE06), some deviations still exists. This could be due to negligence of solid-state effects (polarization effects and intermolecular forces) and environmental effects in theoretical prediction.[44,45]

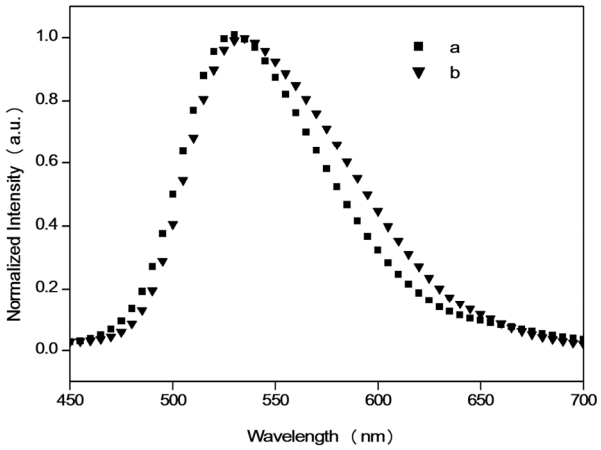

Fig. 6.7: PL spectra of copolymer, P(PH-TZ) in (a) THF solution and (b) as thin film.

The PL emission maximum of P(PH-TZ) in THF solution and film are observed at 529 and 535 nm, respectively (Fig. 6.7). The absorption and emission peaks of P(PH-TZ) film show red shift in wavelength maximum compared to those obtained in the solution, which is caused by intermolecular interaction in thin film. Here, the copolymer emits in the green region, whereas its homopolymer emits in blue region (486 nm).[41] The observed Stokes shift according to poly(phenothiazine) emission suggests that there is an intramolecular charge transfer between the phenothiazine and neighbouring triazine units.

6.2.4. Thermal properties

The thermal stability of copolymer was investigated by TGA and DSC under nitrogen atmosphere. The TG thermogram is depicted in Fig. 6.8. The

thermogram of the copolymer revealed that 5 W% loss was observed at 201 ^{o}C, which is an indication of moderate thermal stability. The thermal induced phase transition behaviour of copolymer was investigated with DSC under nitrogen atmosphere. The insert picture in Fig. 6.8 shows the DSC trace of the copolymer, P(PH-TZ). As for DSC trace, the copolymer exhibited no obvious phase transition until 250 ^{o}C, which is sufficient for device applications. The lower thermal stability of P(PH-TZ) in comparison with P(PH) (320 ^{o}C)[41] could be due to the presence of piperidine units, which are highly prone to degradation.

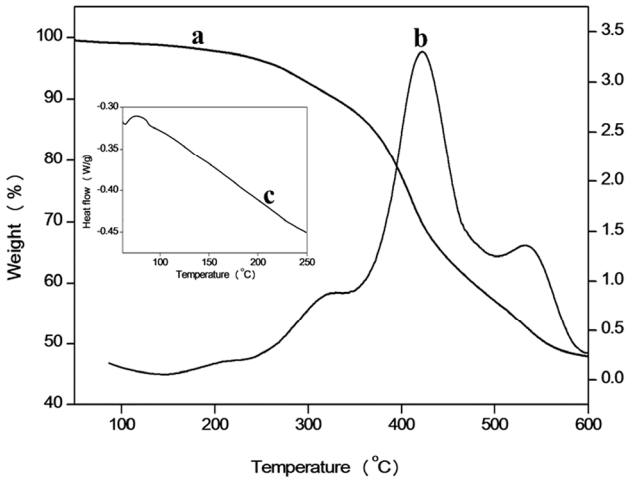

Fig. 6.8: TG (a), DTG (b) and DSC (c) curves of copolymer, P(PH-TZ).

6.2.5. Electrochemical characterization

Electrochemical investigations of the copolymer were performed by cyclic voltammetry (CV) and differential pulse voltammetry (DPV). To determine the HOMO and LUMO energy levels of the polymer, CV and DPV were carried out in thin polymer film which was coated on Pt electrode using 0.1M Bu_4NPF_6 electrolyte in acetonitrile. The HOMO and LUMO

energies of the polymer were calculated from the onset values of the first oxidation and reduction peaks of CV and DPV using Bredas equation.[46] The onset of oxidation occurs at 0.82 and 0.69 V in CV and DPV corresponding to HOMO energies of -5.22 and -5.09 eV, respectively. Similarly, onset of reduction occurs at -1.61 and -1.41V corresponding to LUMO energies of -2.99 and -2.79 eV for CV and DPV, respectively. The electronic properties of the copolymer are summarized in Table 6.2. Hence the electrochemical band of P(PH-TZ) was obtained to be 2.43 and 2.1 eV from CV and DPV, respectively. The band gap obtained from DPV is found to be smaller than CV values, because of reduced back current and sharper onset. The HOMO level of P(PH) was reported to be -5.0 eV.[41] It is clear that the HOMO level of copolymer was lowered by 0.22 eV. This indicates that triazine unit is a strong electron acceptor due to the presence of more number of nitrogen atoms.

Table 6.2: Redox properties of copolymer, P(PH-TZ).

Polymer	HOMO (eV)	LUMO (eV)	E_g (eV)
P(PH)[a]	-5.0		
P(PH-TZ)[b]	-5.22	-2.99	2.43
P(PH-TZ)[c]	-5.09	-2.79	2.10

[a]Reproduced from ref. 41, [b]Obtained by CV, [c]Obtained from DPV.

6.2.6. Non-linear optical (NLO) properties

The measurement of third-order NLO properties of copolymer, P(PH-TZ) was performed with the z-scan technique at 532 nm by the reported method.[47] The open-aperture (OA) z-scan signal in dilute $CHCl_3$ is shown in Fig. 6.9.

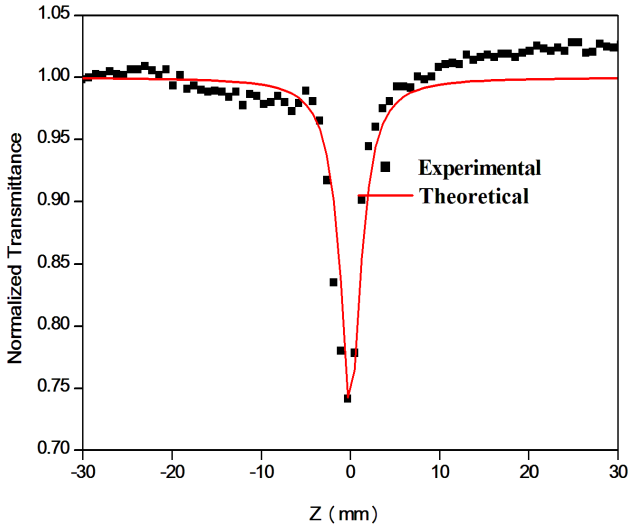

Fig. 6.9: Open aperture z-scan trace of P(PH-TZ).

The normalized transmittance valley of light at the focus suggests that the copolymer is reverse saturation absorber (RSA) with positive NLO absorption coefficient. The non-linear optical absorption coefficient, β is obtained by fitting the experimental data using equation (1)[47] (equation (3), given in section 2.2.7). The imaginary part of the third-order susceptibility ($\mathrm{Im}\,\chi^{(3)}$) of P(PH-TZ) is determined by equation (2)[47] (equation (4), given in section 2.2.7). To determine the sign and magnitude of non-linear refraction, closed aperture (CA) z-scan[47] was performed by placing an aperture in front of the detector. The non-linear refraction data can be obtained from the ratio of the closed aperture transmittance divided by the open aperture transmittance. The peak to valley configuration of the trace indicates that the refractive index change of copolymer is negative, signifying self-defocusing effect of copolymer, P(PH-TZ) shown in Fig. 6.10.

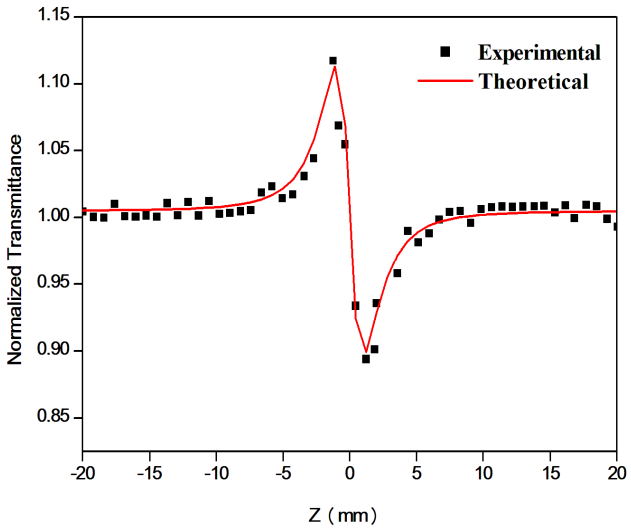

Fig. 6.10: Closed aperture z-scan trace of P(PH-TZ).

The normalized transmittance, T(z) for NLR is given by relation (3)[47] (equation (5), given in section 2.2.7). The effective non-linear refractive index (n_2), the real parts of $\chi^{(3)}$ ($\mathrm{Re}\,\chi^{(3)}$) and third-order non-linear susceptibility ($\chi^{(3)}$) of P(PH-TZ) copolymer are calculated by following the equations (4)-(6)[47] (equations (6)-(8), given in section 2.2.7). The calculated non-linear optical parameters have been compared with reported values in Table 6.3. Non-linearity originated in the copolymer, P(PH-TZ) is due to strong delocalization of π-electrons. The polymer investigated here is designed based on the donor–π–acceptor scheme. As evident from Table 6.3, the copolymer synthesized showed large optical non-linearity than the reported ones.

Table 6.3: Calculated values of non-linear absorption, non-linear refraction and non-linear susceptibility of copolymer, P(PH-TZ).

Copolymer	B (m/W)	n_2 (esu)	Re $\chi^{(3)}$ (esu)	Im $\chi^{(3)}$ (esu)	$\chi^{(3)}$ (esu)
P(PH-TZ)	3.75×10^{-10}	-0.58×10^{-10}	0.09×10^{-10}	0.09×10^{-10}	1.27×10^{-11}
P3[a]					1.57×10^{-12}
P2[b]	9.4×10^{-11}				2.7×10^{-11}
TPD-PFE[c]					5.7×10^{-14}
HMePc[d]	5.7×10^{-12}		3.6×10^{-13}	1.9×10^{-13}	4.07×10^{-13}

[a]Reproduced from ref. 48, [b]Reproduced from ref. 49, [c]Reproduced from ref. 50, [d]Reproduced from ref. 51.

6.2.7. Optical limiting property

An optical power limiter is a device which has very high transmission for weak optical signals, but becomes opaque for intense optical signals.[52] The optical power limiting property is mainly due to non-linear absorption property of a molecule. The optical power limiting behaviour of the polymer obtained from the OA z-scan curve is shown in Fig. 6.11.

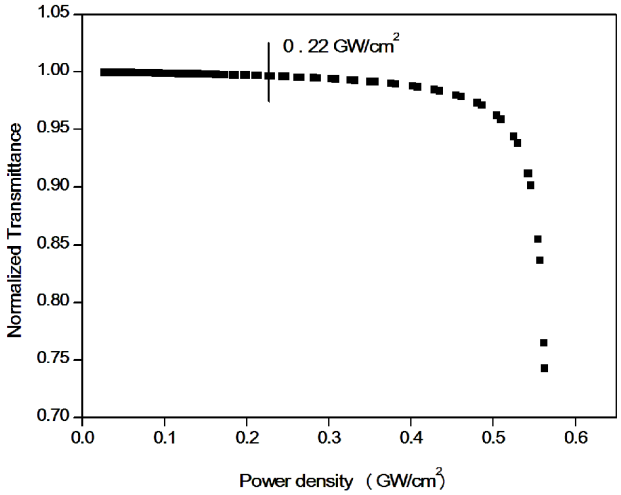

Fig. 6.11: Optical limiting curve of P(PH-TZ).

The optical limiting threshold will determine the ability of the limiter. The lower the limiting threshold value, the better is the optical limiter. Optical limiting threshold of the copolymer, P(PH-TZ) is obtained to be 0.22 GW/cm^2.

6.3. Experimental

6.3.1. Materials

Phenothiazine (Aldrich, >98 %), cyanuric chloride (2,4,6-trichloro-1,3,5-triazine, Aldrich, 99 %), 1-bromooctane (Aldrich, 99 %), piperidine (Aldrich, 99 %), sodium bicarbonate (Aldrich, 99.5 %), palladium (II) acetate ($Pd(OAc)_2$, Aldrich, 99.98 %), triphenyl phosphine (PPh_3, Aldrich, 99 %), potassium phosphate (K_3PO_4, Aldrich, >98%), tetrabutylammonium hexafluorophosphate (Bu_4NPF_6, Aldrich, >99 %), bromine (Merck), diethyl ether (Spectrochem Pvt. Ltd.), magnesium sulphate (anhydrous) ($MgSO_4$, Spectrochem Pvt. Ltd.), n-butyl lithium (Aldrich, ~1.6M in hexane), 2-isopropoxy-4,4,5,5-tetramethyl -1,3,2-dioxaborolane (Aldrich, 97 %), and potassium hydroxide (Spectrochem Pvt. Ltd.) were used as received. Acetonitrile HPLC grade (CH_3CN, Aldrich), dimethyl acetamide (anhydrous) (DMAc, Spectrochem Pvt. Ltd.), chloroform ($CHCl_3$, Spectrochem Pvt. Ltd.), dichloromethane (CH_2Cl_2, Spectrochem Pvt. Ltd.), tetrahydrofuran HPLC grade (THF, Spectrochem Pvt. Ltd.), n-hexane (Spectrochem Pvt. Ltd.), acetone (Spectrochem Pvt. Ltd.), dimethyl sulphoxide (DMSO, Spectrochem Pvt. Ltd.) and methanol (anhydrous) (MeOH, Spectrochem Pvt. Ltd.) were dried and distilled when necessary according to the standard procedures.

6.3.2. Computation methods

Theoretical calculations were done using computational methods, which have been described in section 2.3.4.

6.3.3. Chemical procedures

6.3.3.1. *2-(N-piperidine)-4,6-dichloro-s-triazine[40] (3):*

A solution of cyanuric chloride (1) (9.22 g, 0.05 mol) in 30 mL acetone was added with stirring to a cold solution (0±5 ^{o}C) of sodium bicarbonate (5.3 g) in 50 mL of distilled water, in a two necked flask. This resulted in the formation of slurry of cyanuric chloride. A solution of piperidine (2) (4.3 mL, 0.05 mol) in 5 mL of acetone was added to the cold slurry of cyanuric chloride. The reaction mixture was stirred for 2 h at 0±5 ^{o}C. The white product was filtered, dried and recrystallized from ethanol.

Yield	:	80 %
M. P.	:	86 ^{o}C.
^{1}H NMR 400MHz, $CDCl_3$)	:	δ 1.6-1.9 (m, 6H), 3.7-3.9 (m, 4H).

6.3.3.2. *10-Octylphenothiazine[41]* (5):

A mixture of phenothiazine (4) (5 g, 25 mmol), KOH (10.0 g, 250 mmol), and DMSO (100 mL) were placed in a 250 mL two-necked flask. The reaction mixture was stirred for 30 min and octyl bromide (3.8 mL, 22.5 mmol) was added drop wise to the reaction mixture in 20 min, and this mixture was stirred for 24 h at room temperature. The reaction mixture was poured into water, extracted with CH_2Cl_2, and dried with $MgSO_4$. The resulting liquid was purified by column chromatography using hexane as eluent which gave colourless liquid.

Yield	:	93 %
^{1}H NMR 400 MHz, $CDCl_3$)	:	δ 0.87 (t, J=6.8 Hz, 3H), 1.24-1.43 (m, 10H), 1.77 (m, 2H), 3.80-3.84 (t, J=7.2 Hz, 2H), 6.83-6.91 (m, 4H), 7.11-7.15 (m, 4H).

6.3.3.3. *3,7-Dibromo-10-(octyl)-phenothiazine[41] (6):*

10-Octylphenothiazine (5) (7.5 g, 0.024 mol) was dissolved in 50 mL of CH_2Cl_2, and bromine (8.0 g, 0.05 mol) was injected into the solution using a syringe and stirred for 4 h at room temperature. Dilute aqueous NaOH (20 mL) was added to the reaction mixture and kept for 30 min. The reaction mixture was extracted with CH_2Cl_2 and brine. The concentrated crude product was purified using column chromatography using hexane as the eluent which gave yellow oil.

Yield : 79 %

^{1}H NMR (400 MHz, $CDCl_3$) : δ 0.86 (t, J=6.4 Hz, 3H), 1.14-1.51 (m, 10 H), 1.74 (m, 2H), 3.72 (t, J=7.2 Hz, 2H), 6.66 (d, J=8.4 Hz, 2H), 7.18–7.20 (dd, J1=8 Hz, J2=2.4 Hz, 2H), 7.24 (d, J=8 Hz, 2H).

6.3.3.4. *10-octyl-3,7-bis(4,4,5,5-tetramethyldioxaborolan-2-yl)-10Hphenothiazine[41] (7):*

To a solution of 3,7-dibromo-10-(octyl)-phenothiazine (6) (2 g, 4.262 mmol) in THF (35 mL) at -78 ^oC, n-butyl lithium (1.6 M in hexane) (5.59 mL, 8.95 mmol) was added. The reaction mixture was stirred at -78 ^oC, warmed to 0 ^oC for 20 min and then cooled again to -78 ^oC for 20 min. 2-Isopropoxy-4,4,5,5,-tetramethyl-1,3,2-dioxaborolane (1.86 g,10 mmol) was added to the reaction mixture and warmed to room temperature and stirred for 24 h. The reaction mixture was poured into water and organic layer was extracted with ether and brine. The residue was purified by

several reprecipitation from methanol/acetone mixture to provide the product as a slight yellow solid.

Yield	:	51 %
M. P.	:	87 ^{o}C
^{1}H NMR (400 MHz, $CDCl_3$)	:	δ 0.78 (t, J=6.3 Hz, 3 H), 1.49-1.71 (m,34 H), 2.4 (m, 2 H),3.75 (t, J=7.2 Hz 2 H), 6.71 (m, 2 H), 7.48 (m, 2 H), 7.4 (m, 2H).

6.3.3.5. *Synthesis of P(PH-TZ)(8):*

Suzuki polycondensation reaction was used to synthesize phenothiazine-triazine copolymer, P(PH-TZ) (8). Dry THF (20 mL) was added to a flask charged with 10 mol% palladium acetate (0.0036 g, 0.016 mmol) and 20 mol% PPh_3 (0.0086 g, 0.032 mmol) and stirred for 30 min. To the reaction mixture of 2-(N-piperidine)-4,6-dichloro-s-triazine (3) (0.038 g, 0.164 mmol) and 10-octyl-3,7-bis(4,4,5,5-tetramethyldioxaborolan-2-yl)-phenothiazine (7) (0.1 g, 0.18 mmol), K_3PO_4 (2 equ. 0.07 g) was added and stirred at 80-90 ^{o}C for 72 hours. Copolymer was precipitated from the reaction mixture by adding large amount of methanol. Repeated purification by soxhlet extraction was performed using methanol and hexane to remove oligomers and dried under reduced pressure. The polymer was obtained as yellowish green powder with 60 % of yield.

^{1}H NMR (400 MHz, $CDCl_3$)	:	δ 0.65-1.9 (m, 21H), 3.8 (m, 6 H), 6.8-7.5 (m, 6 H).

6.3.4. Instrumentation

Copolymer, P(PH-TZ) was characterized by analytical and spectral methods which have been described in section 2.3.3.

6.3.5. NLO Measurements

NLO properties were determined by methods which have been described in section 2.3.6.

6.4. Conclusions

In conclusion, we have developed a new soluble conjugated copolymer of phenothiazine and triazine via standard Suzuki coupling reaction. Structural characterization was performed by FT-IR, ^{1}H NMR and XPS. We have performed a theoretical investigation on the copolymer, P(PH-TZ) using density functional theory calculations at two different energy levels. The band gap obtained by DFT/HSE06 method reveals good agreement with the optical band gap. Compared to the homopolymer, copolymer exhibited decreased band gap value (2.5 eV) and red shifted emission. The third-order non-linear optical parameters were studied using z-scan technique. The z-scan results indicate that the polymer exhibits negative non-linear refractive index and positive non-linear absorption and it is calculated to be -0.58×10^{-10} esu and 3.75×10^{-10} m/W, respectively. The copolymer exhibits optical power limiting behaviour at 532 nm wavelength. Hence, the polymer investigated seem to be promising candidate for photonic and optoelectronic applications.

References

[1] C. -H. Lee, T. Yamamoto, *Tetrahedron Lett*., 2001, 42, 3993.

[2] R. Bai, S. Li, Y. Zou, C. Pan, *Liq. Cryst*., 2001, 28, 1873.

[3] S. Hayami, K. Inoue, *Chem. Lett*., 1999, 28, 545.

[4] Y. Zhou, L. Wang, J. Wang, J. Pei, Y. Cao, *Adv. Mater.,* 2008, 20, 3745.

[5] O. Alévêque, P. Leriche, N. Cocherel, P. Frère, A. Cravino, J. Roncali, *Sol. Energy Mater. Sol. Cells*, 2008, 92, 1170.

[6] S. -C. Yuan, Q. Sun, T. Lei, B. Du, Y. -F. Li, J. Pei, *Tetrahedron*, 2009, 65, 4165.

[7] R. Fink, C. Frenz, M. Thelakkat, H. -W. Schmidt, *Macromolecules*, 1997, 30, 8177.

[8] J. Pang, Y. Tao, S. Freiberg, X. -P. Yang, M. DIorio, S. Wang, *J. Mater. Chem.,* 2002, 12,206.

[9] P. Zhou, C. Zhong, X. Chen, J. Qin, I. Mariz, E. Maçôas, *Macromolecules*, 2014, 47, 6679.

[10] A. K. Sekizkardes, S. Altarawneh, Z. Kahveci, T. İslamoğlu, H. M. El-Kaderi, *Macromolecules*, 2014, 47, 8328.

[11] D. Saikia, C. -G. Wu, J. Fang, L. -D. Tsai, H. -M. Kao, *J. Power Sources*, 2014, 269, 651.

[12] F. Chérioux, P. Audebert, H. Maillotte, J. Zyss, *Chem. Commun*., 1999, 20, 2083.

[13] G. F. DAlelio, J. V. Crivello, R. K. Schoenig, T. F. Huemmer, *J. Macromol. Sci.* A1*,* 1967, 1161.

[14] G. F. DAlelio, W. F. Strazik, D. M. Feigl, R. K. Schoenig, *J. Macromol. Sci. Chem*., 1968, 2, 1457.

[15] G. F. DAlelio, R. K. Schoenig, *J. Macromol. Sci.: Rev. Macromol. Chem. C*, 1969, 3, 105.

[16] G. F. DAlelio, *Encyl. Polym. Sci. Technol.,* H. F. Mark, N. G. Gaylord, N. M. Bikales, eds., John Wiley, New York, 1969, 10, 659.

[17] P.W. Morgan, S. L. Kwolek, T. C. Pletcher, *Macromolecules*, 1987, 20, 729.

[18] C. Garcia, R. Oyola, L. E. Pinero, R. Arce, J. Silva, V. Sanchez, *J. Phys. Chem.*, 2005, 109, 3360.

[19] M. Hauck, J. Schonhaber, A. J. Zucchero, K. I. Hardcastle, T. J. J. Muller, U. H. F. Bunz, *J. Org. Chem.*, 2007, 72, 6714.

[20] S. A. Elkassih, P. Sista, H. D. Magurudeniya, A. Papadimitratos, A. A. Zakhidov, M. C. Biewer, M. C. Stefan, *Macromol. Chem. Phys.*, 2013, 214, 572.

[21] A. P. Kulkarni, X. Kong, S. A. Jenekhe, *Macromolecules*, 2006, 39, 8699.

[22] B. Kim, J. Lee, Y. Park, C. Lee, J. W. Park, *J. Nanosci. Nanotechno.*, 14, 2014, 6404.

[23] Q. Tan, X. Yang, M. Cheng, H. Wang, X. Wang, L. Sun, *J. Phys. Chem. C*, 2014, 118, 16851.

[24] J. -H. Huang, K. -C. Lee, *Appl. Mater. Interfaces*, 2014, 6, 7680.

[25] G. D. Sharma, M. A. Reddy, D. V. Ramana, M. Chandrasekharam, *RSC Adv.*, 2014, 4, 33279.

[26] W. Jang, F. Lyu, H. Park, Q. B. Meng, S. -H. Lee, Y. -S. Lee, *Chem. Phys. Lett.*, 2013, 584, 119.

[27] J. -H. Kim, Y. -H. Seo, W. -H. Lee, Y. Hong, S. K. Lee, W. -S. Shin, S. -J. Moon, I. -N. Kang, *Synth. Met.,* 2011, 161, 72.

[28] S. -K. Son, Y. -S. Choi, W. -H. Lee, Y. Hong, J. -R. Kim, W. -S. Shin, S. -J. Moon, D. -H. Hwang, I. -N. Kang, *J. Polym. Sci., Part A: Polym. Chem.*, 2010, 48, 635.

[29] P. N. Prasad, D. J. Williams, Introduction to nonlinear optical effects in molecules and polymers, Wiley, New York, 1992.

[30] H. S. Nalwa, S. Miyata, Nonlinear optics of organic molecules and polymers, CRC Press, Boca Raton, Florida, 1996.

[31] B. A. Reinhardt, L. L. Brott, S. J. Clarson, A. G. Dillard, J. C. Bhatt, R. Kannan, L. Yuan, G. S. He, P. N. Prasad, *Chem. Mater*., 1998, 10, 1863.

[32] M. Albota, D. Beljonne, J. L. Brebas, J. E. Ehrlich, J. Y. Fu, A. A. Heikal, S. E. Hess, J. T. Koge, M. D. Levin, R. S. Marder, D. M. Maughon, J. W. Perry, H. Rockel, M. Rumi, G. Subramaniam, W. W. Watt, X. L. Wu, C. Xu, *Science*, 1998, 281, 1653.

[33] R. G. Parr, W. Yang, Density-Functional Theory of Atoms and Molecules, Oxford University Press, New York, 1989.

[34] Gaussian 09, Revision B02, M. J. Frisch, G. W. Trucks, H. B. Schlegel, G. E. Scuseria, M. A. Robb, J. R. Cheeseman, G. Scalmani, V. Barone, B. Mennucci, G. A. Petersson, H. Nakatsuji, M. Caricato, X. Li, H. P. Hratchian, A. F. Izmaylov, J. Bloino, G. Zheng, J. L. Sonnenberg, M. Hada, M. Ehara, K. Toyota, R. Fukuda, J. Hasegawa, M. Ishida, T. Nakajima, Y. Honda, O. Kitao, H. Nakai, T. Vreven, Jr. J. A. Montgomery, J. E. Peralta, F. Ogliaro, M. Bearpark, J. J. Heyd, E. Brothers, K. N. Kudin, V. N. Staroverov, R. Kobayashi, J. Normand, K. Raghavachari, A. Rendell, J. C. Burant, S. S. Iyengar, J. Tomasi, M. Cossi, N. Rega, N. J. Millam, M. Klene, J. E. Knox, J. B. Cross, V. Bakken, C. Adamo, J. Jaramillo, R. Gomperts, R. E. Stratmann, O. Yazyev, A. J. Austin, R. Cammi, C. Pomelli, J. W. Ochterski, R. L. Martin, K. Morokuma, V. G. Zakrzewski, G. A. Voth, P. Salvador, J. J. Dannenberg, S. Dapprich, A. D. Daniels, Ö. Farkas, J. B. Foresman, J. V. Ortiz, J. Cioslowski, D. J. Fox, Gaussian, Inc., Wallingford CT, 2009.

[35] A. D. Becke, *J. Chem. Phys.,* 1993, 98, 5648.

[36] C. Lee, W. Yang, R. G. Parr, *Phys. Rev. B*., 1994, 37, 785.

[37] K. Burke, J. P. Perdew, Y. Wang, J. F. Dobson, G. Vignale, M. P. Das, Electronic Density Functional Theory: Recent Progress and New Directions, Plenum Press, New York, 1998.

[38] J. Heyd, G. E. Scuseria, M. Ernzerhof, *J. Chem. Phys*., 2003, 118, 8207.

[39] A. V. Krukau, O. A. Vydrov, A. F. Izmaylov, G. E. Scuseria, *J. Chem. Phys*., 2006, 125, 224106.

[40] P. M. Patel, S. K. Patel, K. C. Patel, *Eur. Polym. J.*, 2000, 36, 861.

[41] X. Kong, A. P. Kulkarni, S. A. Jenekhe, *Macromolecules*, 2003, 36, 8992.

[42] I. Venditti, I. Fratoddi, C. Palazzesi, P. Prosposito, M. Casalboni, C. Cametti, C. Battocchio, G. Polzonetti, M. V. Russo, *J. Colloid. Interf. Sci.,* 2010, 348, 424.

[43] A. S. Sarac, S. A. M. Tofail, M. Serantoni, J. Henry, V. J. Cunnane, J. B. McMonagle, *Appl. Surf. Sci*., 2004, 222, 148.

[44] P. Puschning, C. Ambrosch-Draxl, G. Heimel, E. Zojer, R. Resel, G. Leising, M. Kriechbaum, W. Graupner, *Synth. Met*., 2001, 116, 327.

[45] V. J. Eaton, D. J. Steele, *Chem Soc; Faraday Trans*, 1973, 2, 1601.

[46] J. L. Bredas, R. Silbey, D. X. Boudreux, R. R. Chance, *J. Am. Chem. Soc*., 1983, 105, 6555.

[47] M. S. -Bahae, A. A. Said, T. -H. Wei, D. J**.** Hagan, E. W. VanStryland, *IEEE Journal of Quantum Electronics*, 1990, 26, 760.

[48] P. K. Hegde, A. V. Adhikari, M. G. Manjunatha, C. S. S. Sandeep, R. Philip, *J. Appl. Polym. Sci.,* 2010, 117, 2641.

[49] M. S. Sunitha, A. V. Adhikari, K. A. Vishnumurthy, K. Safakath, R. Philip, *Int. J. Polymer. Mater.*, 2012, 61,483.

[50] X. Zhan, Y. Liu, D. Zhu, W. Huang, Q. Gong, *Chem. Mater.,* 2001, 13, 1540.

[51] X. Chen, J. Zhang, W. Wei, Z. Jiang, Y. Zhang, *Eur. Polym. J*., 2014, 53, 58.

[52] G. S. He, G. C. Xu, P. N. Prasad, B. A. Reinhardt, J. C. Bhatt, A. G. Dillard, *Opt. Lett.*, 1995, 20, 35.

.....ooo.....

Chapter 7

Summary and Outlook

The main focus of the present study was to develop ideal low band gap D-A copolymers for photoconducting and non-linear optical applications. This chapter summarizes the overall research work done. Designed copolymers were synthesized via direct arylation or Suzuki coupling reactions. Copolymers were characterized by theoretical and experimental methods. The suitability of these copolymers in photoconducting and optical limiting devices has been investigated. Major achievements of the present work and scope for future work are also outlined here.

7.1. Summary of the work

Conjugated polymers with alternating electron donor and electron acceptor units along their conjugated backbone (D-A copolymers) have recently received significant attention because of their potential applications in transistors, photovoltaic devices, light emitting diodes (LEDs), photorefractive devices and in non-linear optical devices. The intramolecular charge transfer between donor and acceptor units is responsible for lowering of band gap and hence low energy optical transitions. Π conjugated polymers have several inherent advantages over the traditional inorganic systems such as low cost, high optical contrast and stability, processability, low dielectric constant, etc. One of the major challenges in device applications has been

the development of suitable material that simultaneously possesses suitable HOMO-LUMO energy levels and processability. In the present thesis, the aim was to develop polymers which are suitable for use in both photoconducting and non-linear optical devices. So an attempt was made to develop D-A low band gap copolymers. To identify the suitability of the polymer, density functional theory methods were adopted to design D-A copolymers. D-A copolymer systems offered a very simple alternative as tunability of properties can be achieved easily by varying the donor-acceptor combinations through the conjugated backbone.

In the present thesis, we have designed '9' D-A copolymers composed of 3,4-ethylenedioxythiophene (EDOT), phenothiazine as donor units and fluorene, 2,1,3-benzothiadiazole, 2,1,3-benzoselenadiazole, quinoxaline, triazine, thiophene as the acceptor units for photoconducting and non-linear optical applications by employing density functional theory in the periodic boundary condition formalism. A DFT calculation prior to synthesis is an economic way to screen out the unsuitable materials before synthesis. The electronic properties such as HOMO-LUMO energy levels and band gaps were calculated by DFT/PBC methods. To account the reliability of the theoretical calculations with experimental results, DFT calculations at different energy levels (HSE06/6-31G, B3LYP/6-31G and LSDA/6-31G) were carried out.

In this work, EDOT based eight D-A copolymers were synthesized successfully via a simple and facile route, direct arylation reaction and piperidine substituted phenothiazine-triazine copolymer was synthesized via standard Suzuki coupling reaction. Copolymers were characterized by analytical and spectral methods. All the polymers are readily soluble in THF,

chlorobenzene and dichlorobenzene. This gives the processability in device applications. Optical and electrochemical band gaps were determined by UV-Visible spectroscopy and cyclic voltammetry. The theoretical values along with the experimental band gaps are given in the Table 7.1. Theoretically calculated values are in good agreement with the experimental values.

Table 7.1: Theoretical and experimental band gap of copolymers.

No.	Copolymer	DFT/PBC Band gap, eV	Optical Band gap, eV (In soln)	Optical Band gap, eV (As film)	Electrochemical band gap, eV
1	P(EDOT-FL)	2.28	2.29	2.12	2.29
2	P(EDOT-BTZ)	1.26	1.7	1.04	1.06
3	P(EDOT-BTSe)	1.25	1.61	1.04	1.03
4	P(EDOT-ACEQX)	1.81	1.80	1.71	1.05
5	P(EDOT-BZQX)	1.76	1.75	1.53	1.0
6	P(EDOT-PHQX)	1.63	1.66	1.58	0.99
7	P(EDOT-TH)	1.74	2.10	1.82	1.42
8	P(EDOT-MeTH)	1.72	2.06	1.82	1.40
9	P(PH-TZ)	2.87	2.5	2.3	2. 1

Photocurrent measurements of P(EDOT-FL) were done in the sandwich cell configuration as blend with $PC_{61}BM$ (1:1). A low band gap copolymer system designed to be photorefractive have been prepared and the photoconductive properties have been characterized at different wavelengths, intensities and electric fields. Photoluminescence quenching and moderate photoconductive sensitivity (7.6×10^{-10} $ScmW^{-1}$) of P(EDOT-FL) confirmed the suitability of the copolymer for fabricating photoconductive devices. The third-order non-linear optical (NLO) properties of copolymers were investigated by z-scan technique. All the copolymers showed negative non-linear refraction and switch over from RSA (reverse saturation absorption) to SA (saturable absorption) behaviour were observed as the sample changed from the solution

to the thin film. The non-linear absorption coefficient (β), the non-linear refraction coefficient (n_2), the third-order non-linear susceptibility ($\chi^{(3)}$) and the optical limiting threshold of the polymer were calculated using the procedure reported in literature and tabulated in Table 7.2.

Table 7.2: Values of non-linear optical coefficients and optical limiting thresholds of copolymers.

No.	Copolymer	Non-linear absorption coefficient (β, m/W)	Non-linear refraction coefficient (n_2, esu)	Third-order non-linear susceptibility ($\chi^{(3)}$, esu)	Optical limiting threshold (GW/cm^2)
1	P(EDOT-FL)	3.19×10^{-10}	-0.68×10^{-10}	1.25×10^{-11}	0.47
2	P(EDOT-BTZ)	0.8×10^{-10}	-0.46×10^{-10}	0.74×10^{-11}	0.25
3	P(EDOT-BTSe)	2.08×10^{-10}	-1.29×10^{-10}	2.04×10^{-11}	0.34
4	P(EDOT-ACEQX)	1.58×10^{-10}	-0.47×10^{-10}	0.82×10^{-11}	0.41
5	P(EDOT-BZQX)	2.4×10^{-10}	-0.95×10^{-10}	1.46×10^{-11}	0.35
6	P(EDOT-PHQX)	2.54×10^{-10}	-0.64×10^{-10}	1.17×10^{-11}	0.41
7	P(EDOT-TH)	3.11×10^{-10}	-0.70×10^{-10}	1.27×10^{-11}	0.45
8	P(EDOT-MeTH)	3.19×10^{-10}	-0.85×10^{-10}	1.48×10^{-11}	0.45
9	P(PH-TZ)	3.75×10^{-10}	-0.58×10^{-10}	1.27×10^{-11}	0.22

All the copolymers showed strong non-linear optical absorption and refraction coefficient due to donor-π-acceptor scheme. In D-A copolymers, non-linearity originates due to the intramolecular charge transfer from donor to acceptor units and delocalization of π electrons. The non-linear refractive indices of copolymers were found to be negative and it was in the order of 10^{-10} esu. Non-linear absorption coefficient (m/W) and third-order non-linear susceptibility (esu) of copolymers are in the order of 10^{-10} and 10^{-11}, respectively. The tabulated results suggest that the copolymers investigated in the present study have a good non-linear optical response and are comparable to or even better than the D-A copolymers reported in the

literature and hence could be chosen as ideal candidates with potential applications for non-linear optics. The results also show that the structures of the polymers have great impact on NLO properties. Copolymers studied here exhibits good optical limiting property at 532 nm wavelength due to two-photon absorption (TPA) process. The results revealed that the two copolymers, (P(EDOT-BTSe) and P(PH-TZ)) exhibited strong two-photon absorption and superior optical power limiting properties, which are much better than that of others.

Importance of the present work is that copolymers were synthesized via a new method, which is more simple and economic than the conventional synthesis methods like Suzuki, Stille and Kumada coupling. The main advantage is that these polymers may find applications in holography because of the inherent photoconductivity and non-linearity due to the donor-acceptor scheme. The study was a success in the sense that the aim was achieved along with some results which may find applications in other areas like solar cells and LEDs also.

7.2. Major achievements

- Designed and synthesized '9' copolymers for photoconductive and NLO applications.
- Photoconductive devices were fabricated using P(EDOT-FL) with device structure of ITO/(PEDOT-FL):$PC_{61}BM$/Ag.
- P(EDOT-FL) showed good photoconductivity at 488 nm.
- All the copolymers showed third-order NLO properties.

- The copolymers exhibited good optical power limiting behaviour at 532 nm.
- The copolymers investigated seem to be promising candidates for future photonic applications.

7.3. Future Outlook

P(EDOT-FL)/$PC_{61}BM$ blend films showed photoconductivity per unit light intensity in the order of 10^{-10} $ScmW^{-1}$ which is higher than conducting polymers used for photorefractivity. Hence, the suitability of P(EDOT-FL):$PC_{61}BM$ blend films as a photorefractive material for hologram recording is to be investigated. Out of the polymers synthesized, only one polymer was used to study photoconductivity to measure the suitability in photorefractive devices. Other polymers could be subjected to more detailed studies to explore the suitability of these copolymers in photoconducting device applications. To be photorefractive, polymer should have both photoconducting and non-linear optical (second-order NLO) properties simultaneously. Second-order NLO properties of these copolymers is to be investigated. A number of copolymers investigated in the present study have wide applications in solar cells, light emitting diodes and electrochromic devices. This leads to the possibility of copolymers in these frontier areas also.

Publications

1) Theoretical and Experimental Investigations on the Photoconductivity and Non-linear Optical properties of Donor-Acceptor π Conjugated Copolymer, Poly(2,5-(3,4-ethylenedioxythiophene)-alt-2,7-(9,9-dioctylfluorene)), **Sona Narayanan**, Anshad Abbas, Sreejesh Poikavila Raghunathan, Krishnapillai Sreekumar, Cheranellore Sudha Kartha, Rani Joseph, **RSC Advances, 2015, 5, 8657, DOI: 10.1039/c4ra13024c.**

2) Third-order nonlinear optical properties of 3,4-ethylenedioxythiophene copolymers with chalcogenadiazole acceptors, **Sona Narayanan**, Sreejesh Poikavila Raghunathan, Aby Cheruvathoor Poulose, Sebastian Mathew, Krishnapillai Sreekumar, Cheranellore Sudha Kartha, Rani Joseph, **New Journal of Chemistry, 2015, DOI: 10.1039/c4nj01899k.**

3) Synthesis and third-order nonlinear optical properties of low band gap 3,4-ethylenedioxythiophene–quinoxaline copolymers, **Sona Narayanan**, Sreejesh Poikavila Raghunathan, Sebastian Mathew, M.V. Mahesh Kumar, Anshad Abbas, Krishnapillai Sreekumar, Cheranellore Sudha Kartha, Rani Joseph, European Polymer Journal, 2015, 64, 157–169, http://dx.doi.org/10.1016/j.eurpolymj.2015.01.002.

4) Third-order Non-linear Optical properties of EDOT-thiophene Copolymers, **Sona Narayanan**, Sreejesh Poikavila Raghunathan, Sebastian Mathew, Krishnapillai Sreekumar, Cheranellore Sudha Kartha, Rani Joseph, **Polymer International.** (Under Review)

5) Novel Soluble Phenothiazine-triazine Copolymer: Synthesis and Third-order Non-linear Optical Properties, **Sona Narayanan**, Sreejesh Poikavila Raghunathan, Sebastian Mathew, Krishnapillai Sreekumar, Cheranellore Sudha Kartha, Rani Joseph, under preparation.

Publications in Conferences

1) Synthesis and Photoconductivity studies of low band gap copolymer P(EDOT-FL) sensitized with PCBM, **Sona Narayanan**, A. Anshad, Sreejesh P. R., C. Sudha Kartha, K. Sreekumar, Rani Joseph, Proceeding of national seminar on 'Current trends in Chemistry', **ISBN No: 978-81-927942-4-2**. (Best Poster Award)

2) Large Third-order Nonlinearity of π-conjugated EDOT-fluorene Donor-Acceptor Copolymer, **Sona Narayanan**, Sreejesh P. Raghunathan, Sebastian Mathew, Anshad Abbas, Cheranellore Sudha Kartha, Krishnapillai Sreekumar, Rani Joseph**,** Proceeding of 13th Prof. K. V. Thomas endowment National seminar on 'New Frontiers in Chemical Research', **ISBN: 978-81-930558-0-9**, Page No. 101-104.

3) Photoconductivity studies on newly developed low band gap copolymer P(EDOT-fluorene) sensitized with PCBM, A. Anshad, **Sona Narayanan**, Jisha J. Pillai, C. Sudha Kartha, Rani Joseph, K. Sreekumar, National laser Symposium, Department of Atomic and Molecular Physics, MIT, Manipal University, January 8-11, 2014.

4) Theoretical and Experimental Investigations on the Electronic Properties of EDOT-chalcogenadiazole Donor-Acceptor Copolymers, **Sona Narayanan**, Sreejesh Poikavila Raghunathan, A. Abbas, Krishnapillai Sreekumar, Cheranellore Sudha Kartha, Rani Joseph, National Seminar on 'Stimulating Concepts in Green Chemistry', Sponsored by UGC, P.G. & Research department of chemistry, Sree Narayanan Mangalam College, Maliyankara, 13 &14 November, 2014. (Best Poster Award)

5) Investigation on the Third-order Nonlinear and Optical Power Limiting Properties of EDOT-Chalcogenadiazole D-A Copolymers, **Sona Narayanan**, Sreejesh P. Raghunathan, Sebastian Mathew, Cheranellore Sudha Kartha, Krishnapillai Sreekumar, Rani Joseph, National Seminar on 'Frontiers in Polymer science and Rubber Technology' FPSRT-2014, St. Pauls college, Trikakkara, 4th and 5th December 2014. (Best Poster Award)

Abbreviations

A	Acceptor
ACEQX	7,10-Diaza-8,9-benzofluoranthene
A-D-A	Acceptor-Donor-Acceptor
Bu_4NPF_6	Tetrabutylammonium hexafluorophosphate
B3LYP	Becke, three parameter, Lee-Yang-Parr
BTZ	2,1,3-Benzothiadiazole
BTSe	2,1,3-Benzoselenadiazole
BZQX	2,3-Diphenyl quinoxaline
BLA	Bond length alteration
BG, E_g	Band gap
CT	Charge-transfer
C_{60}	Fullerene
C-C	Carbon-Carbon
CV	Cyclic Voltammetry
D-A	Donor-Acceptor
DTG	Differential Thermogravimetry
DSC	Differential Scanning Calorimetry
DPV	Differential Pulse Voltammetry
DC	Direct Current
d8-THF	Deuterated tetrahydrofuran
DANS	4-N,N-dimethylamino-4'-nitrostilbene
DMSO	Dimethyl sulphoxide
DCM	Dicholoromethane
DFT	Density functional theory
D-A-D	Donor-Acceptor-Donor
D-π-D	Donor-π-Donor
D-π-A	Donor-π-Acceptor
EDOT	3,4-Ethylenedioxythiophene
E_g^{opt}	Optical band gap
E_g	Band gap
EA	Electron affinity

EDOT-ACEQX	(3,4-Ethylenedioxythiophene)-(7,10-diaza-8,9-benzofluoranthene)
EDOT-BZQX	(3,4-Ethylenedioxythiophene)-(2,3-diphenyl-quinoxaline)
EDOT-PHQX	(3,4-Ethylenedioxythiophene)-(1,2-3,4-dibenzophenazine)
EO	Electro-optic
e	Electronic charge
E	Electric field applied
FL	Fluorene
FT-IR	Fourier Transform Infra-Red
GPC	Gel Permeation Chromatography
Grad	Gradient
GRIM	Grignard metathesis
G	Rate at which carriers are photogenerated
HOMO	Highest occupied molecular orbital
HSE06	Heyd-Scuseria-Ernzerhof
HPLC	High Performance Liquid Chromatography
h	Hour
^{1}H NMR	^{1}H Nuclear magnetic resonance
ICT	Intermolecular charge transfer
ITO	Indium tin oxide
I_D	Steady state current values, prior to illumination
I_L	Steady state current values, after illumination
I_{ph}	Photosensitivity
i_{ph}	Photocurrent
I_0	Irradiance at focus.
Im $\chi^{(3)}$	Imaginary part of the third-order susceptibility
IP	Ionization potential
Is	Saturation intensity
Int	Intermolecular interactions
k	Wave vector
LUMO	Lowest unoccupied molecular orbital
L_{eff}	Effective thickness with linear absorption coefficient

LSDA	Local Spin Density Approximation
LEDs	Light emitting diodes
Mn	Number average molecular weight
Mw	Weight average molecular weight
M. P.	Melting point
MeTH	3-methyl thiophene
NLO	Non-linear optical
n_0	Linear refractive index of the polymer solution
NLR	Non-linear refraction
n_2	Non-linear refractive index
Nd:YAG	Neodymium-doped yttrium aluminium garnet
OPV	Organic photovoltaic
OA	Open-aperture
OFETs	Organic field-effect transistors
P(EDOT-FL)	Poly(2,5-(3,4-ethylenedioxythiophene)-alt-2,7-(9,9-dioctylfluorene))
$PC_{61}BM$	[6,6]-Phenyl C_{61} butyric acid methyl ester
$PC_{71}BM$	[6,6]-Phenyl C_{71}-butyric acid methyl ester
PFs	Polyfluorenes
PLED	Polymer light-emitting diodes
PBC	Periodic boundary condition
P(FL)	Poly(dioctyl fluorene)
PDI	Poly dispersity index
PL	Photoluminescence spectrum
P	Laser power
PVK	Poly(vinyl carbazole)
PEDOT	Poly(3,4-ethylenedioxythiophene)
P(EDOT-BTSe)	Poly(3,4-ethylenedioxythiophene-alt-2,1,3-benzoselenadiazole)
P(EDOT-BTZ)	Poly(3,4-ethylenedioxythiophene-alt-2,1,3-benzothiadiazole)
P(EDOT-ACEQX)	Poly(3,4-ethylenedioxythiophene-alt- 7,10-diaza-8,9-benzofluoranthene)
P(EDOT-BZQX)	Poly(3,4-ehylenedioxythiophene-alt-2,3-diphenyl-quinoxaline)

P(EDOT-PHQX)	Poly(3,4-ethylenedioxythiophene-alt-1,2-3,4-dibenzophenazine)
PHQX	1,2-3,4-dibenzophenazine
P(EDOT-ACEQX-EDOT)	Poly(3,4-ethylenedioxythiophene-co-acenaphthylene quinoxaline-co-3,4-ethylenedioxythiophene)
P(EDOT-BZQX-EDOT)	Poly(3,4-ethylenedioxythiophene-co-2,3-diphenylquinoxaline-co- 3,4-ehylenedioxythiophene)
p	Polymer
P(EDOT-TH)	Poly(3,4-ethylenedioxythiophene-alt-thiophene)
P(EDOT-MeTH)	Poly(3,4-ethylenedioxythiophene-alt-(3-methyl)-thiophene)
PTH	Poly(thiophene)
PMeTH	Poly(3-methyl thiophene)
P(PH-TZ)	poly(N-octylphenothiazine-alt-2-(N-piperidine)-s-triazine)
PH-TZ	N-octylphenothiazine-2-(N-piperidine)-s-triazine
P(PH)	Poly(phenothiazine)
PQ	Poly(fluorene-co-quinoxaline)
PSC	Polymer solar cell
ProDOT	3,4-Propylenedioxythiophene
P_0	Light power density
q_0	Fitting parameter
RSA	Reverse saturation absorber
Re $\chi^{(3)}$	Real parts of $\chi^{(3)}$
SA	Saturation absorber
SWV	Square Wave Voltammetry
SCE	Standard calomel electrode
std	Standard
Sub	Substituents
SHG	Second harmonic generation
TCNQ	7,7,8,8-Tetracyanoquinodimethane
TG	Thermogravimetry
T_g	Glass transition temperature
TPA	Two photon absorption
TBAB	Tetrabutyl ammoniumbromide

THF	Tetrahydrofuran
T(z)	Normalized transmittance
TH	Thiophene
TNT	Trinitrotoluene
TOF	Time of flight
T	Temperature
UV–Visible	Ultraviolet-Visible
V	Applied voltage.
x	z/z_0
XPS	X-ray Photoelectron Spectroscopy
z	Position of sample
σ/I	Photoconductivity per unit light intensity
σ	Photoconductivity
β	Non-linear absorption coefficient
α	Linear absorption coefficient
ω	Angular frequency of radiation used
Φ_0	On-axis non-linear phase shift
$\chi^{(3)}$	Third-order non-linear susceptibility
γ	Molecular cubic hyperpolarizability
λ	Wavelength
Φ	Quantum yield
λ_{max}	Wavelength maximum
3D	Three dimensional
Δ	Chemical shift in ppm
Θ	Dihedral angle
μ	Field dependence of mobility
τ	Recombination time
α	Polarizability
β	First hyperpolarizability
γ	Second hyperpolarizability
μi	Dipole moment

.....ꕥ.....